9th International Symposium on Materials for Energy Storage and Conversion

01-04 September 2025, Kocaeli, Türkiye

Book of Abstracts/Proceedings

book of abstracts/proceedings
ISBN 978-625-00-6333-0

mesc-is.org

mESC-IS 2025

The Ninth International Symposium on Materials for Energy Storage and Conversion

Edited by
R. Gültekin Akay and Tayfur Öztürk

01-04 September 2025
Kocaeli, Türkiye

ISBN 978-625-00-6333-0

Participants in - mESC-IS 2025

Preface

The 9th International Symposium on Materials for Energy Storage and Conversion (mESC-IS 2025) took place from September 01-04, 2025, at the Kocaeli Congress Center. As an annual gathering, this meeting has once again proven its strategic importance as a premier forum bringing together global scientists, researchers, and industry professionals to discuss the latest developments and future strategies for materials of energy storage and conversion technologies. The mESC-IS symposium series had humble beginnings in Ankara in 2015 and has quickly gained a respectable place in the international scientific community. Over the years, our symposium has significantly expanded its geographical reach, welcoming participants from Europe, the Caucasus, the Middle East, the Mediterranean basin, and Africa. It has also become a platform for global dialogue with researchers from North America and the broader Eurasian geography, including India, China, Korea, and Japan. This global dialogue fosters a rich exchange of ideas by bringing together diverse research priorities, thereby creating a truly global innovation ecosystem. Building upon this deep-rooted history, this year's symposium has carried its thematic focus even further by embracing new research areas that respond to the dynamic nature of the field while preserving its traditional themes.

While continuing its tradition of addressing the most critical issues in energy storage and conversion, mESC-IS 2025 has dynamically expanded its scope to reflect new research horizons. This adaptability in keeping pace with scientific progress and opening space for emerging disciplines ensures that the symposium maintains its relevance and value for the scientific community. Our program this year was structured around four main activity areas that constitute the pillars of the field and cover the latest developments: batteries and supercapacitors, renewable hydrogen and hydrogen production, fuel and electrolytic cells, and hydrogen for energy storage and conversion. A significant innovation this year was the "Spin-Off Poster and Exhibition Session." This special session was designed to bridge the gap between academic research and commercial application, offering start-ups, university spin-offs, and entrepreneurial teams the opportunity to showcase their prototypes, products, and technology-driven solutions directly and to meet with potential investors and industry leaders. This enriched thematic structure set the stage for the high-quality academic work presented throughout the symposium and summarized in this book.

The academic richness and scientific depth of the symposium were evident at every stage of the program. The true value of the event comes from the high-quality contributions presented in various formats, such as plenary speeches, parallel sessions, and poster presentations. Collectively, these presentations offer a comprehensive snapshot of the current state of the field of materials for energy storage and conversion. In this ninth symposium, a total of 90 presentations were successfully delivered, comprising 15 plenary, 6 parallel, and 37 poster sessions. Our symposium's commitment to the dissemination of knowledge is not limited to presentations. Contributions presented in the symposium will be available as book of abstracts/proceedings in mESC-IS web site. Distinguished papers selected by our publication committee will also be published in leading journals of the field, including the International Journal of Hydrogen Energy, Materials Research Bulletin, and the Turkish Journal of Chemistry, following a rigorous peer-review process. These publication opportunities ensure that the valuable research shared at the symposium reaches a wider audience and makes lasting contributions to the field. Ensuring the dissemination of current research is only half of our mission; investing in the cultivation of the next generation of scientists who will build upon these findings is equally vital.

One of the core missions of our symposium is to support and encourage the young talent that will shape the future of the field. The integration of students and early-career researchers into the scientific community is vital for the long-term health, dynamism, and innovation of our field. Accordingly, various platforms have been established for young researchers. Foremost among these is the four-day "mESC-School" held immediately prior to the symposium. This intensive summer school plays a complementary role by offering

participants overviews on selected topics, future perspectives, and hands-on experience in material/electrochemical characterization techniques.

The poster session, one of the central and most dynamic components of the symposium, provided a vibrant environment where early-career researchers presented their work and engaged in productive one-on-one discussions with experienced members of the community. Following evaluations by session chairs and senior members of mESC-IS community, "Best Poster/Young Researcher" awards were presented to **Ilgar Ayyubov**, **Zhansaya Bakthytzanova, Tuana Bal , Mukhammed Kenzhebek**, and **Hakan Yüce**, We congradulate them all for their success.

Planning and successfully executing an international symposium of this scale would not have been possible without the dedicated efforts and support of numerous individuals and institutions. We would like to express our sincere thanks to everyone who contributed to the realization of mESC-IS 2025. We gratefully acknowledge the support of **TÜBİTAK** through the program **BİDEB 2223-B**. We also extend our deepest gratitude to our host, **Kocaeli University**, as well as to **Boğaziçi University, ENDAM, Gebze Technical University, Koç University, Middle East Technical University, Sabancı University.** The symposium was held in **Kocaeli Congress Center** for which we express our gratitude to **Kocaeli Metropolitan Municipality.** As a host institution**,** the generous support of Tüpraş is gratefully acknowledged**.** Referans Kimya was with us, as always from the beginning of mESC-IS series of symposia.

Finally, we thank all session chairs, authors, and participants for their esteemed contributions that ensured the scientific quality and success of our event. Together, we have created a productive environment for information exchange in the field of energy storage and conversion. We hope to meet again at future symposiums.

Ramiz Gültekin AKAY
mESC-IS 2025 Chair

.

COMMITTEES- mESC-IS

International Steering Committee

Tayfur Öztürk(chair), Middle East Technical University, Ankara
Hatem Akbulut, Sakarya University, Sakarya
Akif Aliyev, Azerbaijan National Academy of Sciences, Baku
M. Kadri Aydinol, Middle East Technical University, Ankara
Branimir Banov, Inst of Electrochemistry & Energy Systems, IEES-BAS, Sofia
Elena Carcadea, National Centre for Hydrogen & Fuel Cell, Valcea
Rezan Demir-Cakan , Gebze Technical University, Kocaeli
Selmiye Alkan Gürsel, Sabanci University, İstanbul
Gulfeza Kardaş, Cukurova University, Adana
Aliya Mukanova, Nazarbayev University, Astana
Jasmina Grbovic-Novakovic, Vinca Institute of Nuclear Sciences, Belgrade
Dragana Jugovic, Inst Tech Sci SASA, Belgrade
Saban Patat, Erciyes University, Kayseri
Olim Ruzimuradov, Turin Polytechnic University in Tashkent
Dilgam Taghiyev, Azerbaijan National Academy of Sciences, Baku
Grigor Tatishvili, Agladze Institute of Inorganic Chemistry and Electrochemistry, Tbilisi
Andras Tompos, Institute of Materials and Environmental Chemistry, Budapest
Ivan Tolj, University of Split, Split
Servet Turan, Eskisehir Technical University, Eskisehir
Mustafa Urgen, Istanbul Technical University, Istanbul
Ayse Bayarakceken Yurtcan, Ataturk University, Erzurum

Organizing Committee

Ramiz Gültekin Akay (Chair) -Kocaeli University, İzmit
Bilge Saruhan Brings -German Aerospace Center
Dilgam Tagiyev – Institute of Catalysis and Inorganic Chemistry, Baku
Cigdem Toparli –Middle East Technical University
Jasmina Grbovic Novakovic– Vinča Institute of Nuclear Science, Belgrade
Neslihan Yuca-Istanbul Technical University
Sarp Kaya, Koç University
Selmiye Alkan Gürsel, Sabancı University
Rezan Demir-Cakan, Gebze technical University
Damla Eroğlu Pala, Boğaziçi University

Scientific Committee

José Ramón Ares, Universidad Autónoma de Madrid, Madrid
Francois Beguin, Poznan University of Technology, Poznan
Fermin Cuevas, ICMPE/CNRS, Paris
Duncan Paul Fagg,University of Aveiro, Aveiro
Hiroshi Inoue, Osaka Prefecture University, Osaka
Semen N. Klyamkin, Moscow State University, Moscow
Sergey Mitrokhin Moscow State University, Moscow
Amelia Montone, ENEA, Rome
Dag Noreus, Stockholm University, Stockholm
Luca Pasquini,University of Bologna,Bologna
Saim Ozkar, Middle East Technical University, Ankara
H. Emrah Unalan, Middle East Technical University, Ankara
Rachid Yazami, Nanyang Technological University, Singapore
Volodymyr Yartys,IFE, Kjeller
Suha Yazıcı Istanbul Technical University , Istanbul

Regional Committee

R. Gültekin Akay, Kocaeli University, Kocaeli
Sedat AKKURT, Izmir Institute of Technology, İzmir
Serdar Altın, Inonu University, Malatya
Mustafa Anık, Osmangazi University, Eskisehir
Yilser Devrim, Atılım University, Ankara
Bahadır Keskin, Yıldız Technical University, Istanbul
Sarp Kaya, Koc University, Istanbul
Damla Eroğlu Pala, Bogazici University
Bora Timurkutluk, Nigde Omer Halisdemir University, Nigde
Burak Ulgut, Bilkent University
Ece Unur Yilmaz, Bursa Technical University

Local Organizing Committee

Ayşe Aytaç-Kocaeli University
Cenk Çelik-Kocaeli University
Müslüm Arıcı-Kocaeli University
Efgan Kibar-Kocaeli University
Mehmet Kodal-Kocaeli University
Ziya Gürün – Kocaeli University
Orhan Özcan-Kocaeli University
Ali Hassen Ali-Kocaeli University
Akbar Khoshnoudi-Kocaeli University
Necla Altın-Kocaeli University
Şeyma Yalçınkaya-Kocaeli University
Tuncay Kadıoğlu-Kocaeli University

Advisory Board

Ali Ata, Gebze Technical University, Kocaeli
Hüseyin Devrim, Teksis Ltd Sti, Ankara
İbrahim Dincer, University of Ontario Institute of Technology, Oshawa
İnci Eroglu, Middle East Technical Univerity, Ankara
Y. Eren Kalay, Middle East Technical University
Volkan Karahan, Yiğit Aku AS, Ankara
İbrahim Pamuk, : Lentatek, Ankara
Rasit Turan, Middle East Technical University, Ankara
Ziya Gürün, Kocaeli University,

mESC-IS 2025
9th Int. Symp on Materials for Energy Storage and Conversion
Kocaeli Congress Center , 01-04 September 2025

	Monday, 01 September 2025
	Kocaeli Congress Center
	Registration 8:30 -18:30
	Introductory Session Karamürsel Alp Hall
09:30 10:00	Ramiz Gültekin Akay Tayfur Öztürk Nuh Zafer Cantürk
	Chair: **Tayfur Öztürk** **Opening Session** Karamürsel Alp Hall
10:00 10:30	NiMH batteries will outperform Li batteries by utilizing H2 and O2 gas reactions combined with an α/ϒ- Ni(OH)/NiOOH-electrode 250 **Dag Noreus**
10:30 11:00	Enhancing the utilization efficacy of noble metal(0) nanocatalysts in hydrogen generation from the hydrolysis of ammonia borane 206 **Saim Ozkar**
11:00 11:30	Addressing Materials Challenges for Fuel Cells and Electrolyzer Technologies: Membrane and Catalyst Innovations 50 **Selmiye Alkan Gürsel**
11:30-11:50	Tea Break

	Chair: **Çiğdem Toparlı** Karamürsel Alp Hall Parallel Session-I	Chair: **Meltem Yıldız** Selim Sırrı Paşa Hall Parallel Session -II
11:50 12:15	Influence of Charge–Discharge Ratios on EDLC Performance Using Plasticized 2-HEC/B_2CaO_4 Electrolytes 56 **Siti Rohana Majid** and Ranaa M. Almarshedy	La(OH)3 and La2O3 Nanowires as Efficient Catalysts for Hydrogen Production via Sodium Borohydride Metanolysis 98 **Emel Engintep**e, Sibel Duman and Ayşe Nilgün Akın
12:15 12:35	Effect of Metal–Organic Framework (MOF) Additives on LMFP Cathode Performance in Lithium-Ion Batteries 67 **İlayda Kunan** and Umut Savacı	Syngas production via optimized oxidative reforming of model biogas 100 **Orhan Özcan**, Merve Doğan Özcan and Ayşe Nilgün Akın
12:35 12:55	Electrochemical Performance of Deep Discharged $Li_4Ti_5O_{12}$ Anode Material for Lithium-Ion Batteries 101 Halil Şahan, **Yusuf Taş** and Şaban Patat	Igneous Rocks in the Methanolysis of Sodium Borohydride 104 Aslıhan Erdoğan, Beray Alyakut, Derya Yıldız, Özgür Karaoğlu, Hüseyin Sendir, Emre Kırhan and **Hilal Demir Kivrak**
12:55 - 14:50	Lunch Break (Palmiye Restaurant, SEKA Park)	

	Chair:**Burak Aktekin** Karamürsel Alp Hall Parallel Session -III	Chair:**Fatih Pişkin** Selim Sırrı Paşa Hall Parallel Session -IV
14:50 15:15	Microwave-assisted synthesis of SnS and SnS/MWCNT anodes for sodiumion batteries 20 **Mehbare Dogrusoz**, Ali Ş. Ahsen and Rezan Demir-Cakan	Photochemical properties of cobalt phthalocyanine pigment for the of solar cells 21 **Khayit Turaev,** Sherzod Kasimov, Dilmurod Shukurov, Panji Tojiyev, Olim Ruzimuradov

15:15 15:35	Gel Polymer Electrolyte for Flexible Lithium-ion Batteries for Wearable Applications 86 **Baidaa Alkhateab** and Serap Hayat Soytas	Synthesis of reduced graphene oxide using copper (I) oxide nanoparticles 75 **Makhfuza Jumayeva**, Rustam Khasanov, Olim Ruzimuradov and Shavkat Mamatkulov
15:35 15:55	Developing High-Performance Anode Composites for Sodium-Ion Batteries from Hard Carbon and Graphene Mixtures 90 **Bongani Hadebe**	Electrochemical Properties of Ag and Ni Coated TiO2 Nanotubes 60 **Dilshod Boyqobilov**, F.Nurullayev, X.Musayev Olim Ruzimuradov
15:55 16:15	Tea break	

	Monday, 01 September 2025
	Chairs: **Saim Özkar** Joint Session-II Karamürsel Alp Hall
16:15 16:45	Unraveling the Impact of Charge Carrier Trapping on Photoelectrode Performance 120 **Sarp Kaya**
16:45 17:15	Development of palladium based alloys for hydrogen separation membranes 121 **Fatih Pişkin**

	Tuesday, 02 September 2025
	Chair: **Selmiye Alkan Gürsel** Joint Session-III Karamürsel Alp Hall
09:00 09:30	From Sulfur to Selenium: Bridging Concepts in Lithium Battery Design 202 **Rezan Demir-Cakan**
09:30 10:00	A novel electrochemical approach for quantitative characterization of side reactions on lithium metal anodes: CTTA 200 **Burak Aktekin**
10:00 10:30	EIS and NMR Characterization of Storage & Degradation Mechanisms in Sodium Batteries 209 **Mohammed Ahmed Zabara**
10:30-11:50	Tea Break

	Chair:**Muhammed Ahmed Zabara** Parallel Session -III Karamürsel Alp Hall	Chair: **Aligül Büyükaksoy** Parallel Session -IV Selim Sırrı Paşa Hall
10:50 11:15	Mill scale-derived hematite as a low-cost supercapacitor electrode material 110 Ozan Aydin, Metin Gençten, **Burak Birol**	Microwave Assisted Synthesis of Graphene Supported PtCo Alloys as Efficient Cathode Electrocatalysts for PEM Fuel Cells 107 **Çiğdem Karadağ**
11:15 11:35	Re-synthesis of Nickel Manganese Cobalt Oxide Cathode Material from Black Mass Waste via Hydrometallurgical Processes 112 **Berk Çoban**, Burak Birol, Ozan Aydın and Metin Gençten	Fabrication and Characterization of SPEEK Proton Exchange Membranes (PEM)for Fuel Cells by Electro-spinning and Solution Casting Methods 55 **Akbar Khoshnoud**i, Sema Samatya Yılmaz, Ramiz Gültekin Akay and Ayşe Aytaç
11:35 11:55	Metal Recovery from Spent NMC811 Li-Ion Batteries Using Perchloric Acid 102 **Tuğçe Günşen** and Meltem Yıldız	Directions for Solving Design and Long-Term Operation Problems of Solid Oxide Fuel Cell Installations 69 Ramiz Hasanov, **Riad Naghiyev** and Saida Musevi

	Tuesday, 02 September 2025

13: 15- 15:45 Lunch break (Foyer) and Poster Session

	Poster Session Chairs**: Çiğdem Toparlı, Burak Aktekin and Berke Pişkin, Serap Hayat Soytaş** Foyer
Tuesday, 02 September 13:15-15:40 Poster Session	g-C3N4-based Z-Scheme Ternary Heterostructures for Photocatalytic Hydrogen Production 3 Mehmet Poyraz and **Fatih Pişkin**
	Effect of HNT surface modification on photocatalytic hydrogen production of HNT/g-C3N4 6 Mehmet Poyraz and **Fatih Pişkin**
	LSMA-LCMF Dual Perovskite Oxides for Hydrogen Production 5 Seyfettin Berk Şanlı, Gülhan Çakmak, Fatih Pişkin and **Berke Pişkin**
	The influence of the composition of Ni-P thin films on their electrocatalytic properties. 8 Aygun Zeynalova , Ulviyya Gurbanova, Natavan Soltanova, Ruhangiz Huseynova, Akif Aliyev and Dilgam Tagiyev
	Subproducts of Ammonia Borane in First Step Release with Principal Components Analysis 24 **Roberto Hinojosa,** E.V. Mejía-Uriarte and R.Y. Sato-Berrú
	Development of a CrMnFeCoNi/NF electrocatalyst for enhanced hydrogen production 26 Mariya Pecherskaya, F. Hoshimov, D. Akhmedova, Kh. Butanov, O. Ruzimuradov and Sh. Mamatkulov
	Zn Doped Silicon Oxycarbide (SiOC) as Efficient Catalysts for Vinylation of Aromatic Carboxylic Acids 48 Askar Parmanov , Suvankul Nurmanov, Wilamowska Monika, Dilshod Boykobilov and Olim Ruzimuradov
	. Applıcatıon of the Digital Vısualızatıon Method in the Reactıon of Producing Hydrogen From Hydrides by Hydrolysis 52 Chimnaz Shabanova, Mirsalim Asadov and Dilqam Tagiyev
	MXene based electrodes for efficient water splitting 53 Javlonbek Mamanazirov**,** Shavkat Mamatkulov, Olim Ruzimuradov
	Synthesis of Metal/C electrocatalysts for seawater electrolysis 123 **Dzhamal Uzun**, Ognian Dimitrov, Mariela Dimitrova, Adriana Gigova and Ivelina Tsacheva
	Design of Co/BaTiO3@Vulcan XC-72 R with application in electrolysis of seawater 124 **Ivelina Tsacheva**, Mihaela Aleksandrova, Vladimir Petkov, Mariela Dimitrova, Adriana Gigova , Ognian Dimitrov , Shaban Uzun and Dzhamal Uzun
	Enhanced Electrochemically Active Surface Area of CoFeNi-MF/NF Electrocatalyst for Efficient HER and OER in Alkaline Medium 62 Farhodjon Hoshimov, Khakimjan Butanov, Shavkat Mamatkulov and Olim Ruzimuradov Farhodjon Hoshimov, Khakimjan Butanov, Shavkat Mamatkulov and Olim Ruzimuradov
	Obtaining Bi2O3 via electrochemical method for Solar to Hydrogen processes 17 **Vusala Majidzade**, Sevinj Javadova, Samira Jafarova, Nazakat Aliyeva Mammadova and Akif Aliyev
	Hydrogen Production from Sodium Borohydride Using La_2O_3 Nanoparticles: A Promising Catalytic Approach 99 **Emel Engintep**e, Sibel Duman and Ayşe Nilgün Akın
	Investigation of the Effect of Air Flow Rate on PEM Fuel Cell Performance and Comparison with an Alternative Membrane Prepared with Hygroscopic Additive to Reduce Drying Effect 42 **Zeynep Dere** and Ramiz Gültekin AKAY
	Improving Zinc Anode Stability and Efficiency in Alkaline Rechargeable Batteries 127 **Beyzanur Acar**, A. Engin Serin and A. Gul Ozturk, Ozgur Darıcıoglu and Tayfur Ozturk
	Graphene derived materials as carbon component of composite supported platinum catalyst for polymer electrolyte membrane fuel cells (PEMFCs) 74 **Ilgar Ayyubov**, Emília Tálas, Irina Borbáth, Zoltán Pászti, László Trif, Ágnes Szegedi, Tamás Szabó, Erzsébet Dodony and András Tompos
	3D-structured nanoporous SnO2 thin-film anodes for lithium-ion microbatteries 54 **Yerkem Kanatbekkyzy,** Yessimzhan Raiymbekov, Zhumabay Bakenov and Aliya Mukanova

Tuesday, 02 September 13:15-15:40 Poster Session	Design and Development of 3D Zn/ZnO-C Architectures for Advanced Battery Electrodes 45 **Yerzhigit Serik**, Moldir Arkharbekova, Aliya Mukanova and Arailym Nurpeissova
	Study of LATP ceramics for subsequent fabrication of thin film electrolytes 58 **Ayazhan Bekmakhanova**, Zhansaya Bakhytzhanova, Mukagali Yegamkulov, Zhumabay Bakenov and Aliya Mukanova
	Engineering artificial solid electrolyte interface via carbon coating and VC additive for SnO2 thin-film lithium-ion anodes 59 **Zhansaya Bakhytzhanova**, Ayazhan Bekmakhanova, Mukagali Yegamkulov, Zhumabay Bakenov and Aliya Mukanova
	Exploring TiV-based alloys as potential anode materials for high-capacity NiMH batteries 126 **Hakan Yüce** , Berke Pişkin, Fatih Pişkin and Gülhan Çakmak
	From Waste to Resource: Engineering End-of-Life Graphite Anodes for Solid-State Hydrogen Storage 7 **Mukhammed Kenzhebek**, Fayil Sultanov and Almagul Mentbaeyva
	Preparation and Characterization of Fish Scale-Based Carbon Nanosheets for Bromine Redox Reactions in Flow Battery Systems 84 Bilge Bilgin Fıçıcılar, Pınar Aydın, Koray Korkmaz and Berker Fıçıclar
	A Comparative Study of A-site Deficient and Heterostructured $La_{0.6}Ca_{0.4}CoO_3$ Electrodes for Durable SOFCs 78 **Hatice Demirbas**, Onur Alp Aksan, Seda Kol and Mehmet Sezer
	MgO-Doped CaO-Stabilized Zirconia: A Promising Earth-Abundant Electrolyte for Next-Generation Solid Oxide Cells 79 **Canan Ekinci**, Mehmet Sezer, Aligül Büyükaksoy
	Enhancing the Long-Term Stability of La0.6Ca0.4CoO3 Cathodes for Solid Oxide Fuel Cells via Surface Modification with Constituent Cation Oxides 80 **Süleyman Enes Acar**, Onur Alp Aksan, Seda Kol and Mehmet Sezer
	Lowering the Supply Risk of Raw Electrolyte Materials by Developing Ca and Mn Co-doped ZrO2 Electrolytes for Solid Oxide Fuel Cells 82 **Tuana Bal** , Mehmet Sezer and Aligül Büyükaksoy
	Development of a flexible lithium-ion battery and integration of a triboelectric nanogenerator for self-charging energy systems 92 **Kaan Yapıcı**, Baidaa Alkhateab, Serap Hayat Soytaş
	Polyacrylic Acid-Based Gel Polymer Electrolyte Coated Ni/NiO Foam Anode for Enhanced Lithium-Ion Battery Performance 46 **Moldir Arkharbekova**, Yerzhigit Serik, Aliya Mukanova and Arailym Nurpeissova
	Upcycling High-Density Polyethylene into Carbon Anode Materials for Sustainable Energy Storage Systems 122 **Kuanysh Kurtibay** and Arailym Nurpeissova
	PET-Derived Nitrogen-Doped Hard Carbon as a Sustainable Anode for Sodium-Ion Batteries 106 **Aizhuz Sarsengaliyeva** and Arailym Nupeissova
	Sustainable Carbon Anode Materials Derived from Polypropylene via Eco-Friendly Pretreatment and Carbonization 105 **Yryszhan Tashenova** and Arailym Nurpeissova
	Synthesis and characterization a novel polythiourethanes as candidate materials for supercapacitor applications 108 Laya Zarei-Gharehbaba, **Reza Najjar** and Pariya YardaniSefidi
	Poly(4-vinylpyridine)/NiCo2S4/polyaniline nanocomposites as supercapacitor electrode materials in alkaline media 114 Mohyaddin Gholizadeh Ghaleh-Aziz, **Reza Najja**r and Mir Ghasem Hosseini
	Fe2O3 based supercapacitors derived from electric arc furnace dust 109 **Ozan Aydin**, Koray B. Donmez, Metin Gencten and Burak Birol
	Recovery of Nickel-Based Materials from Ni-Ti Alloys for Application as Electrode Materials in Supercapacitors 111 **Berk Çoban**, Mert Zoraga, Burak Birol and Metin Gençten
	Electrochemical Characterization of Cobalt Hydroxide Based Materials 97 **Caner Korkmaz**, Berk Çoban, Ayşe Hacınecipoğlu and Metin Gençten
5:45 – 16:00	Tea break

	Tuesday, 02 September 2025
	Chair: **Dag Noreus** Joint Session-IV Karamürsel Alp Hall
16:0016:30	Design of TiFe-based alloys via substitutional elements for tailored equilibrium pressure and easy activation 119 **Mohammad Faisal**,
16:30 17:00	Synergistic Dual Doping of Graphene Oxide: A New Route to High-Capacity Anodes for Sodium-Ion Batteries 118 **Metin Gencten**
17:00 17:30	Nanoscale Electrodes for Solid Oxide Cells: Fabrication, Microstructure and Stability 201 **Aligül Büyükaksoy**

	Wednesday, 03 September 2025	
	Chair:**Apurba Ray** Parallel Session -VII Karamürsel Alp Hall	Chair: **Çiğdem Karadağ** Parallel Session -VIII Selim Sırrı Paşa Hall
09:00 09:25	Suppressing Dendrite Formation in Zinc–Air Batteries via Bi_2O_3-Modified Zinc Powder Anodes with Bio-Derived Binders 115 **Tuncay Erdil** and Cigdem Toparli	Dynamic Analysis of Vanadium Redox Flow Cell System Integrated Into Solar Power Plant in Türkiye 19 **Batuhan Laçinkaya,** Mert Taş and Gülşah Elden
09:25 09:45	Dual Bi/Cu Pre-Intercalation Strategy for High-Performance δ-MnO_2 Cathodes in Zinc-ion Batteries 1 **Engin Serin** and Tayfur Ozturk	Parametric Study and Microstructural Characterization of YSZ Electrolytes for Reversible Solid Oxide Cells 25 Ahmed Emin Kilic, Meryem Sena Akkus, Selahattin Celik, Cihangir Duran and Erol Arcaklioglu
09:45 10:05	Suppressing Hydrogen Evolution in Iron Anodes for Alkaline Rechargeable Batteries 2 **Beyzanur Acar,** A. Engin Serin, Ozgur Darıcıoglu and Tayfur Ozturk	An Investigation into the Phase Formation, Ionic Conductivity, Surface Oxygen Exchange, and Long-Term Stability of Sr-Doped versus Undoped $LaFeO_3$ Composites with Gadolinium-Doped Ceria 77 **Mehmet Sezer**, Hayri Sezer, Ali Şems Ahsen and Aligül Büyükaksoy
10:05-10:30	Tea Break	

	Chair: **Reza Najjar** Parallel Session IX Karamürsel Alp Hall	Chair :**Metin Gençten** Parallel Session X Selim Sırrı Paşa Hall
10:50 11:15	Ionic liquid integrated high-voltage polymer gel electrolyte to improve the capacitance and cyclic stability of supercapacitors 89 **Apurba Ray** and Bilge Saruhan	High Proton-Conducting Electrospun Sulfonated-Silica-Based Composite Membranes for PEM Fuel Cell Applications 95 **Naeimeh Rajabalizadej Mojarrad**, Selmiye Alkan Gürsel Alp Yürüm and Begüm Yarar Kaplan
11:15 11:35	Synthesis and characterization of poly(ethylene thiosuccinate) (PETS) with succinic anhydride and 1,2-ethanedithiol monomers as supercapacitor electrode materials 113 Laya Zarei-Gharehbaba, **Reza Najjar** and Mir Ghasem Hosseini	Synthesis, Characterization and Ion conductivity Analysis of Pyridine, Meta, and ParaPolybenzimidazole based Membranes for High-Temperature PEM Fuel Cells 43 **Ali Hassen Ali** and Ramiz Gültekin Akay
11:35 11:55	Laser-Induced Surface Patterning of Zinc Anodes for Dendrite Control in Zn–Air Batteries 116 **Çağla Özgür** and Çiğdem Toparlı	Effect of Aluminium Oxide on the Conductivity and Performance of Lanthanum Ferrite Perovskite Anode for Fuel Cells 94 **Amjad Ali**, Sadaf Abid, Bilal Mazhar and Rizwan Raza
11:55 - 14:00	Lunch Break (Palmiye Restaurant, SEKA park)	
	Chair: **Ramiz Gültekin Akay** Joint Session-IV **Spin-off Poster and Exhibit session** Foyer	
14:00 14:15	Nushaba Kazimova Anadolu Plazma Teknoloji Enerji Merkezi	
14:15 14:30	Kaan Yapıcı Beespenser Teknoloji Anonim Şirketi	

	Wednesday, 03 September 2025
	Chairs:**Sarp Kaya** Joint Session-VI Karamürsel Alp Hall
14:30 15:00	Machine Learning for Sustainable Energy Materials and Technologies 208 **Ramazan Yıldırım**
15:00 15:30	2D MBenes for Energy Storage and Conversion Technology 49 **Muslum Demir**
15:30 -15:50	Tea break

15:30 20:00	Social Program
20:00 23:45	Symposium Dinner

	Thursday 04 September 2025	
	Chair: **Mohammed Faisal** Karamürsel Alp Hall Parallel Session: XI	Chair: **Ramazan Yıldırım** Selim Sırrı Paşa Hall Parallel Session XII
09:00 09:25	MOF-Derived Dual-Activity Oxygen Catalysts Empowering Next-Generation Renewable-Energy Storage 117 **Uygar Geyikçi** Hüseyin İnan Cihan and Çiğdem Toparlı	Development of MoS_2/ZIF-67 Hybrid Catalysts for Enhanced Cathodic Performance 23 Yaren Erdağ Maden, Ali Furkan Albora, **Murat Efgan Kibar**, Şahika Sena Bayazit, Özge Kerkez Kuyumcu
09:25 09:45	Chia Seeds-Based Gel Electrolyte for Sustainable and Stable Zinc Ion Batteries 83 **Gulsah Yaman Uzunoglu**	Advancements in Direct Liquid Fuel Cells: A Comparative Study of Methanol, Ethanol, and Glycerol 91 **Moussa Djibrine Ali** and Ramiz Gültekin AKAY
09:45 10:05	Electrochemical Evaluation of Lead Electrodes in Polyaniline-Doped Fumed Silica Gel Electrolytes 41 **Ziyad Mira**, Irem Cemre Türü and Metin Gençten	Development of Biodegradable Membranes Functionalized with Reduced Graphene Oxide Reinforcement for Microbial Fuel Cell Applications 81 **Necla Altın** and Ayşe Aytaç
10:05 10:25	Development of LSC Cathodes for Intermediate-Temperature SOFCs via Spray Pyrolysis 4 **Hakan Yüce** and Gülhan Çakmak	A New Perspective on the Liquid-Vapor, Liquid-Solid, and Solid-Vapor Critical Points of Hydrogen 61 Beycan Ibrahimoglu and **Nushaba Kazimova**
10:25 - 10:40	Tea Break	

	Thursday, 04 September 2025
	Chair **Rezan Demir-Çakan** Joint Session-VII Karamürsel Alp Salonu
10:40 11:10	Hydrogen Processing of Ti6Al4V tuırnings for fabrication of fine powders for additive Manufacturing 128 **Tayfur Öztürk**
11:10 11:30	Performance and Evaluation of Synthesized Polybenzimidazole/Functionalized Boron Nitride Composite Membranes for High-Temperature PEM Fuel Cell Test System 85 **Ramiz Gultekin Akay**

Thursday, 04 September 2025

	Final Session Chair: **Ramiz Gültekin Akay** Karamürsel Alp Hall
12:00 12:20	Presentations regarding upcoming events
	Poster/Young Researchers Awards

TABLE OF CONTENTS

GENERAL/OVERVIEWS

BATTERIES

SUPERCAPACITORS

RENEWABLE HYDROGEN AND HYDROGEN PRODUCTION

HYDROGEN STORAGE AND SEPARATION

FUEL CELLS AND ELECTROLYSERS

GENERAL/OVERVIEWS

A novel electrochemical approach for quantitative characterization of side reactions on lithium metal anodes: CTTA

Burak Aktekin
Institute of Physical Chemistry & Center for Materials Research, Justus-Liebig-Universität Giessen, Germany

Lithium-ion batteries (LiBs) have become a critical component of countless devices we use in our daily life, and they are predicted to play a pivotal role in electrification of transport (and grid energy storage) in the near future. In order to enable a widespread energy transition, the development of advanced battery technologies is crucial. Ideally, electrode materials should have high specific charge capacities, enable high cell voltages and allow fast charge and discharge kinetics. In this sense, the most promising anode active material would be lithium metal since it has a specific charge capacity of 3860 mAh g−1 and operates at the lowest electrode potential possible (i.e., 0 V vs. Li+/Li, or –3.04 V vs. the standard hydrogen electrode). All-solid-state batteries (ASSBs) are quite promising to enable the use of lithium metal anodes due to their projected safety characteristics (e.g., non-flammable components, mechanical rigidity, very high transference numbers). Unfortunately, most solid electrolytes have a narrow electrochemical stability window (ESW) and thus are subject to parasitic side reactions with lithium metal resulting in accelerated cell failure. It is essential to understand the chemical and quantitative nature of such reactions (and their kinetics) to design better performing battery systems. In this talk, it will be presented how the use of electrochemical methods (such as the novel CTTA method) and advanced analytical characterization methods (e.g., XPS, ToF-SIMS, FIB-SEM, operando HAXPES, etc.) can be used to obtain fundamental understanding of degradation reactions occurring at the interface between lithium metal and solid electrolyte in all-solid state batteries (with a particular focus on argyrodite-type sulfide-based solid electrolytes).

Burak Aktekin received his BSc (2010) and MSc (2013) in Metallurgical and Materials Engineering Department in Middle East Technical University. He then joined Uppsala University for his doctoral studies where he worked on the high voltage spinel type positive electrodes for LiBs. Having obtained his PhD in late 2019 and following a brief postdoctoral period at Uppsala University, Dr. Aktekin joined J. Janek's research group at the Institute of Physical Chemistry, Justus Liebig University Giessen. His current research activities focus on understanding interfacial side reactions in all-solid-state batteries using electrochemical methods as well as a range of analytical tools available in house or in synchrotron facilities

EIS and NMR Characterization of Storage & Degradation Mechanisms in Sodium Batteries

Mohammed A. Zabara, Jeongjae Lee, Christopher A. O'Keefe, Svetlana Menkin, Clare P. Grey
Yusuf Hamied Department of Chemistry, University of Cambridge
Lensfield Road, Cambridge, CB2 1EW

Sodium batteries have emerged as a leading candidate to reduce dependence on lithium-based systems for sustainable energy storage. Their development in multiple configurations—such as metal oxide cathodes with hard carbon anodes, as well as anode-free architectures—has attracted growing interest due to sodium's abundance and cost advantages. Despite these benefits, large-scale commercialization remains constrained by limited specific capacity and poor cycle life. Overcoming these barriers requires a mechanistic understanding of sodium storage dynamics and the physicochemical origins of electrode degradation. Integrating electrochemical characterization with advanced structural probes is therefore essential for revealing the processes that govern performance.

In this work, we employ a combined electrochemical impedance spectroscopy (EIS) and ^{23}Na solid-state nuclear magnetic resonance (NMR) spectroscopy methodology to investigate sodium storage behavior and degradation pathways in sodium batteries. EIS enables quantification of interfacial resistances and charge-transfer kinetics [1], exemplified in Figure 1(a) for a representative hard carbon anode. Complementarily, NMR provides atomic-scale insights into the local coordination environments of sodium ions, as illustrated in Figure 1(b) for distinct sodium species in hard carbon [2].

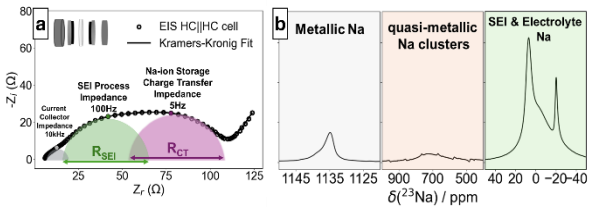

Figure 1. a) Nyquist plot of EIS response of hard carbon symmetric cell demonstrating SEI and charge transfer response, b) Solid state NMR spectra of different Na local environments in hard carbon.

We systematically examine the influence of electrolyte composition, electrode material, and state of charge on storage mechanisms and degradation pathways. EIS measurements performed under varying conditions—including temperature, cell geometry, and state of charge—enable precise evaluation of charge transfer processes and interfacial phenomena. Local structural changes during electrochemical cycling are monitored using a combination of in situ and ex situ NMR spectroscopy. Our results reveal critical correlations between structural evolution and electrochemical performance, providing design principles for improved material architectures.

In addition, we investigate interfacial behavior and plating/stripping characteristics of metallic sodium electrodes in anode-free cell configurations. Figure 2 presents the impedance response of a Cu||Na cell in different electrolyte environments. A two-order-of-magnitude decrease in impedance is observed when transitioning from carbonate-based to ether-based electrolytes, indicating the high reactivity of sodium and the associated formation of thick, heterogeneous SEI in carbonate systems. Ether-based electrolytes demonstrate better compatibility with sodium anodes, highlighting their potential for enabling stable and efficient Na anode-free designs.

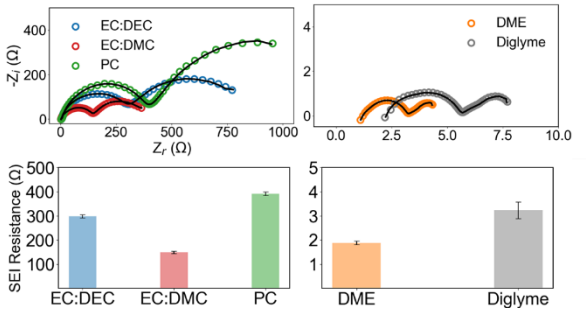

Figure 2. Nyquist plot of EIS response and fitted SEI resistance values of Na||Cu cell at different electrolyte enviorenments

These insights inform the design of optimized materials and cell architectures capable of delivering both high capacity and extended cycle life in sodium batteries.

Acknowledgment
MAZ thanks the Faraday institute/Nexgenna for the funding to perfrom this work.

References

[1] M. A. Zabara et al. Electrochimica Acta, 485, (2024), 144080
[2] J. M. Stratford et al. J. Am. Chem. Soc., 143, 35, (2021) 14274–14286

Mohammed Ahmed Zabara is a Research Associate in the Department of Chemistry at the University of Cambridge. He earned his BSc and MSc degrees from the Middle East Technical University and holds a PhD in electrochemistry from Bilkent University, where he specialized in applying Electrochemical Impedance Spectroscopy to study energy storage systems. Following his doctorate, he conducted research at Sabanci University, investigating the electrochemistry of metal oxides for energy storage applications. His current work focuses on elucidating electrochemical mechanisms in emerging battery chemistries. He was recently awarded a Marie Skłodowska-Curie Postdoctoral Fellowship to investigate degradation mechanisms in hard carbon anodes for sodium batteries.

Presentating author: Mohammed Ahmed Zabara, e-mail: mz527@cam.ac.uk

From Sulfur to Selenium: Bridging Concepts in Lithium Battery Design

Rezan Demir-Cakan
Department of Chemical Engineering, Gebze technical University

To satisfy the growing energy demands of modern applications, research efforts have traditionally centered around sulfur-based battery chemistries, owing to sulfur's high theoretical energy density and cost-effectiveness. Despite these advantages, the commercialization of Li–S batteries has been limited by persistent challenges such as drastic volumetric expansion during cycling, poor electrical and ionic conductivities of sulfur and its discharge products, and the sluggish redox kinetics of intermediate polysulfides. These limitations often result in poor cycling stability, irreversible loss of active material, and the formation of passivating layers that hinder performance.

In recent years, lithium–selenium batteries have gained attention as a promising alternative among chalcogen-based systems. Selenium offers a higher volumetric capacity and much better intrinsic conductivity compared to sulfur. Nevertheless, Li–Se batteries still face critical hurdles, particularly large volume fluctuations during charge and discharge, as well as uncontrolled accumulation of Li 2 Se on the electrode surface. Building on the knowledge gained from Li–S battery research, our work focuses on addressing these challenges by studying the reversible conversion reactions and tackling capacity loss caused by imperfect re-oxidation of Li_2Se. In this presentation, we will first review the progress made with sulfur-based batteries, then explore strategies to enhance the performance of Li–Se systems. Special attention will be given to the use of electrocatalysts that improve Li 2 Se conversion and increase active material utilization.

Rezan Demir-Cakan received her Ph.D. degree in 2009 from the Max Planck Institute of Colloids and Interfaces. Between 2009 and 2012, she conducted postdoctoral research in the group of Prof. Jean-Marie Tarascon, where she focused on rechargeable lithium batteries, particularly lithium–sulfur systems. She is currently a Professor in the Department of Chemical Engineering at Gebze Technical University. Her research activities center on the design and synthesis of nanostructured energy materials for advanced battery systems, with particular emphasis on sodium-ion, lithium–sulfur, and aqueous electrolyte zinc-ion batteries. Rezan Demir-Cakan has been the recipient of several prestigious awards, including the French Embassy Research Fellowship (2018, 2023), the Turkish Academy of Sciences Outstanding Young Scientist Award (TÜBA-GEBİP, 2018), the L'Oréal–UNESCO "For Women in Science" Award (2016), the Science Academy's Young Scientist Award (BAGEP, 2015), the IMLB Young Researcher Award (2012), and the Japan Carbon Award (2008). Since 2014, she has served as an expert evaluator for energy-related calls within EU-funded programs (H2020, Horizon Europe), and she currently coordinates the EU-funded project TwinBat.

NiMH batteries will outperform Li batteries by utilizing H_2 and O_2 gas reactions combined with an α/ϒ- Ni(OH)/NiOOH-electrode

Dag Noréus[1] and Weikang Hu[2]

[1]Department of Chemistry, Stockholm University, SE-106 91 Stockholm, Sweden

[2] Chilwee Power Co., Ltd., Changxing 313100, Zhejiang, China

Rechargeable electrochemical cells and the resulting batteries are complicated and development is slow as rechargeable batteries form chaotic systems as they undergo charge-discharge cycling. All reactions (including parasitic side reactions) occurring in both electrodes must be as reversible as possible, else the battery will derail upon cycling. Although several thousand of redox reactions have been characterized and described in various tables and chemical textbooks very few redox reactions have been realized in rechargeable batteries. Lead acid-, NiCd-, NiMH- and Li-ion batteries are still the dominating rechargeable battery chemistries.

Nickel-hydrogen batteries (NiH_2) combine a nickel hydroxide electrode with a hydrogen electrode. They have the longest cycle life of all batteries and are used in space application. In a NiMH battery a metal hydride is both a hydrogen electrode and a solid-state hydrogen storage leading to a significantly better volumetric capacity.

The charge carrier hydrogen is shuttled between the electrodes by water molecules during charge and discharge. The NiMH battery can also be charged and discharge by gaseous additions of H_2 and O_2 respectively.[1] These gaseous additions can be used to mitigate performance deterioration by electrolyte dry out by replenishing the amount of water in the electrolyte and also rebalance the electrode capacities. [2] This mitigates pressure, build ups during overcharge and overdischarge states that in practical battery packs can be difficult to avoid. Improved understanding of the reaction kinetics at the metal hydride surfaces have thus led to NiMH-batteries with the largest capacity-throughput of all present battery chemistries. (Capacity-throughput = cycle life*cell capacity) as the gas additions will significantly increase the cycle life. The cell capacity, however, remains the same.

From these findings we could also collude that the MH-alloy powder in spent NiMH batteries can be used to make new batteries if the corroded surface is cleaned from $Mm(OH)_3$ corrosion products. This cleaning can be made by a simple grinding process where the $Mm(OH)_3$ corrosion products are washed away. NiMH cells made by using such treated and reconditioned MH-powders showed superior reaction kinetics as well as longer life time as the reconditioned powder are already activated and covered by an active as well as protective surface.[3,4]

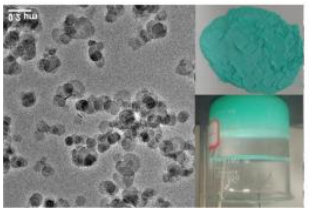

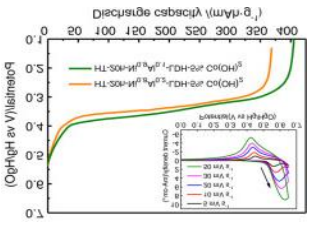

A way to increase the cell capacity is to utilize the α/γ $Ni(OH)_2$ /Ni(III)OOH redox couple for the Ni-electrode. Commercial Ni-electrodes presently use the β/$Ni(II)(OH)_2$ + OH^- ↔

Al stabilized Ni-hydroxide Al. stabilized Ni-electrode

β/Ni(III)OOH + H_2O + e^- redox reaction. This corresponds to a capacity of 289 mAh/gram.[5]

An interesting aspect of the nickel oxidation state in the α/γ $Ni(OH)_2$ /Ni(III)OOH redox couple can possibly reach 3.67 upon charging. This would correspond to a capacity increase to 482 mAh/gram. If this can be implemented as a stable redox couple NiMH batteries will reach the capacity of Li-ion batteries.

The α/γ $Ni(OH)_2$ /$Ni(3.67?)OOH_{0.33?}$ redox couple is possible to stabilize via intercalation of anions such as OH^-, $NO3^-$, CO_3^{2-} as well as cations Al^{3+}, Co^{2+}, Fe^{3+}.[6]

The problem with a Ni-electrode based on the α/γ redox couple is that has been shown to be unstable and reverts back to the β/β redox couple. This makes it difficult to build battery packs as the cells in the pack can get different capacities in the battery string. Work is underway to address these issues.

[1] Ye, Z.; Noréus, D. Oxygen and hydrogen gas recombination in NiMH cell, *Journal of Power Sources*, **2012**, 208, 232–236

[2] Shen, Y.; Noréus, D.; Starborg, S. Increasing NiMH battery cycle life with oxygen. *Int. J. Hydrog. Energy* **2018**, 43C 18626–18631.

[3] Shen, Y.; Peng, F.S.; Kontos, S.; Noréus, D. Improved NiMH performance by a surface treatment that creates magnetic Ni-clusters. *Int. J. Hydrog. Energy* **2016**, 41, 9933–9938.

[4] Shen, Y.; Svensson-Grape, E.; Noréus, D.; Widenkvist, E.; Starborg, S. Upcycling of Spent NiMH Battery Material-Reconditioned Battery Alloys Show Faster Activation and Reaction Kinetics than Pristine Alloys. *Molecules* **2020**, 25, 2338.

[5] Zhou, F.; Wu, M.; Hu, W-K; Jiang, Z-G.; Noréus, D. Alpha nickel hydroxide electrodes improve aqueous rechargeable batteries capacity, *Materials Research Bulletin*, **2024**, **179**, 112967-

[6] Lskavian, D. N.; Diakonov, A.K.; Sinitsyn P.A.; Kokin, A. A.; Levin E.E.; Nikitina V.A. Quantifying polarization losses in undoped and Co-doped $Ni(OH)_2$ electrodeposits. *Electrochimica Acta*, **2026**, 545, 147736-48.

Dag Noréus is a professor in the Department of Materials and Environmental Chemistry at Stockholm University. He earned his PhD degree in reactor physics in 1982 at the Royal Institute of Technology, Stockholm, Sweden, and completed his postdoc at Daimler-Benz, Metal Hydride Laboratory, Stuttgart, Germany, in 1983. Noréus became a researcher in 1984 and a professor in 2000 in the Department of Structural Chemistry, Stockholm University. His research interests include x-ray diffraction, elastic and inelastic neutron scattering, and electrochemistry focusing on the understanding of metal-hydrogen interaction in metal hydrides and electrodes. http://www.h2fc-fair.com/hm14/exhibitors/nilar.html dag.noreus@su.se

Ionic liquid integrated high-voltage polymer gel electrolyte to improve the capacitance and cyclic stability of supercapacitors

Apurba Ray, and Bilge Saruhan
German Aerospace Center (DLR), Institute for Frontier Materials on Earth and in Space, 51147 Cologne, Germany

With the rapidly increasing demand for the most promising electrical energy storage devices, supercapacitors (SCs) have attracted widespread interest due to their high capacity, specific power density and long cyclic performance. To date, symmetric electrodes made of various types of porous carbons such as activated carbon (AC), carbon nanofibers, carbon nanotubes (CNT), and graphene/reduced graphene oxide (rGO) are commonly used for commercial electrical double layer capacitors (EDLCs) or supercapacitors [1]. Electrolytes also play an important role for supercapacitor devices through their physical, thermal and electrochemical properties. Because of high ionic conductivity, simple processing, low cost and good interfacial (electrode/electrolyte) properties of aqueous electrolytes and organic liquid-based electrolytes have been widely used for SCs. However, lower voltage windows, lower cycle life, corrosion, leakage problem, flammability and safety issues limit their commercialization [2].

To address the above-mentioned issues, ionic liquids (ILs) integrated solid/semi-solid polymer electrolytes have attracted wide interest as an alternative electrolyte in electrochemical energy storage due to their wide potential windows (≥3V), high ionic conductivity ($10^{-4}\Omega^{-1}cm^{-1}$), leakage free, low flammability, good thermal stability, flexibility, tunable chemical functionalities and self-healing capabilities [3,4]. Significant efforts have also been devoted to integrating various ionic liquids (ILs) into solid/semi-solid polymer electrolytes for emerging SCs. In this work, 1-Ethyl-3-Methylimidazolium bis(trifluoromethylsulfonyl)imide [EMIM][TFSI] ionic liquid embedded in Polypropylene Carbonate (PPC) and Polycarbonate (PC) based polymer gel electrolyte has been developed by entrapping the IL in the polymer network for activated carbon (AC) electrode-based pouch cell SC and laser induced graphene (LIG) electrode micro-supercapacitors (MSCs) applications. The electrochemical performance of this [EMIM][TFSI]/ PPC/PC polymer gel electrolyte has been evaluated by cyclic voltammetry (CV), galvanostatic charge-discharge (GCD) (Figure 1a), electrochemical impedance spectroscopy (EIS) and long cycle charge-discharge (CCD) analysis. Relying on the combined effect of IL, this novel semi-solid electrolyte improves the capacitance (0.94 mF/cm^2 @ 2V),

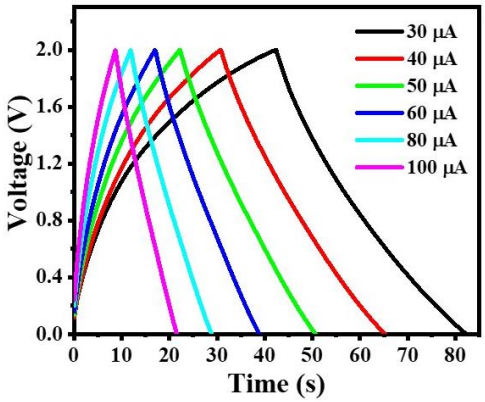

Figure 1. Galvanostatic charge-discharge (GCD) curves of [EMIM][TFSI] /PPC/PC polymer electrolyte integrated–laser induced graphene (LIG) electrode micro-supercapacitor (MSC).

electrode/electrolyte interface compatibility, voltage windows (≥2.0V), ionic conductivity and long cycle stability (≥ 50000 cycles) making it a potential electrolyte for next-generation supercapacitors.

Acknowledgment
The authors A. Ray and B. Saruhan would like to acknowledge GRAPHERGIA (grant agreement No. 101120832), supported by the European Union's Horizon Europe research and innovation programme, for financial support.

References

[1] W. Wu, S. Dong, X. Zhang, J. Hao, Chemical Engineering Journal 446 (2022) 137328.

[2] S. Pan, M. Yao, J. Zhang, B. Li, C. Xing, X. Song, P. Su and H. Zhang, Frontiers in Chemistry 8 (2020) 261.

[3] B. Saruhan and A. Ray, Materials Research Bulletin 180 (2024), 113052.

[4] W. Chen, Z. Xing, Y. Wei, X. Zhang, Q. Zhang, Polymer 268 (2023) 125727.

Dr. Apurba Ray is currently working as a Research Scientist at the Institute for Frontier Materials on Earth and in Space, German Aerospace Center (DLR) in Cologne. He accomplished his PhD in Jadavpur University, India in 2019 in the field of high-power supercapacitors. Afterwards, he was selected for the DLR-DAAD Post-doctoral Research Fellow in Germany. To date, he has published more than 45 research papers in various international journals. He was awarded the INSPIRE Scholarship in 2008 from the Department of Science and Technology (DST) and Senior Research Fellowship in 2018 from Council of Scientific and Industrial Research (CSIR), Govt. Of India.

Presentating author: Apurba Ray, e-mail: Apurba.Ray@dlr.de tel: +492203 601-4575

Unraveling the Impact of Charge Carrier Trapping on Photoelectrode Performance

Sarp Kaya
Department of Chemistry, Koç University

Photoelectrochemical water splitting is a promising approach for converting solar energy into chemical energy stored in molecular hydrogen and oxygen. However, the efficiency of this process strongly depends on the properties of the photoelectrode materials. Metal oxide semiconductors are commonly employed as photoelectrodes, but their poor charge transport properties and limited surface catalytic activity can significantly constrain overall performance. In particular, charged defect sites, both in the bulk and on the surface of oxide semiconductors, can trap charge carriers and slow down interfacial kinetics. In this talk, I will present the time-evolution of interfacial charge trapping and transfer processes in $BiVO_4$ photoanodes and $CuBi_2O_4$ photocathodes.

Sarp Kaya received his PhD in Physical Chemistry in 2007 after completing his studies on ultrathin metal oxide layers at Fritz Haber Institute of the Max Plank Society and Humboldt University. During his post-doctoral studies at Stanford University (2007-2010) and following research activities as a scientist at SLAC National Accelerator Laboratory (2010-2014) and Joint Center of Artificial Photosynthesis (JCAP) (2011-2014) he heavily utilized synchrotron radiation for investigations on gas-solid and liquid-solid interfaces. He has joined the Department of Chemistry, Koç University in 2013. He has also been co-director of Koç University Tüpraş Energy Center (KUTEM) since 2019.

Enhancing the utilization efficacy of noble metal(0) nanocatalysts in hydrogen generation from the hydrolysis of ammonia borane

Saim Özkar
Department of Chemistry, Middle East Technical University, 06800 Ankara, Turkey.

The growing concern on global warming [1] and the increasing worry on the depletion of fossil energy reserves [2] appeal the replacing fossil fuels with the renewable energy sources for a sustainable energy policy in the future [3]. As environmentally benign energy carrier hydrogen will play key role in such a transition on the way towards a sustainable green future [4,5]. Main hindrances in using H_2 as green energy vector are essentially resulting from the difficulties in its safe and efficient storage [6]. New materials have been persistently developed for storing hydrogen safely and efficiently [7,8,9]. One of the promising candidates for storing hydrogen safely and efficiently is ammonia borane (H_3NBH_3, AB) [10]. Its hydrolysis is the best way of releasing hydrogen gas (Equation 1) [11].

$$H_3NBH_3(aq) + 2H_2O(l) \rightarrow NH_4^+(aq) + BO_2^-(aq) + 3H_2(g) \qquad (1)$$

However, this reaction takes place at appreciable rate under ambient conditions only in the presence of suitable catalysts [12]. Transition metal nanoparticles are known to be efficient catalysts in hydrogen generation from the hydrolysis of AB [13]. The noble metals such as platinum [14], rhodium [15], palladium [16] or ruthenium [17] show much higher catalytic activity than the non-noble metals in this reaction. However, precious metals have very high price which prevents their employment in this dehydrogenation reaction. Furthermore, the principles of green chemistry require the amount of non-reagent metal to be minimized [18]. Therefore, it is mandatory to keep the metal content of catalyst as low as possible to increase the utilization efficacy of the metal catalyst. Using a minimum catalyst to substrate ratio is another target for developing efficient catalyst. Here, an obvious challenge is to develop nanocatalysts of noble metals which have outstanding catalytic activity, long lifetime and exceptionally high reusability for the complete release of 3 equivalent H_2 per mole of ammonia borane under ambient conditions. The existing literature will be reviewed to find out all the available methods to increase catalytic efficiency of noble metal nanocatalysts in hydrogen generation from the hydrolysis of AB.

Although colloidal nanoparticles of noble metals can provide high catalytic activity, they are unstable against agglomeration. Supporting nanoparticles on the surface of carbonaceous materials with large surface area such as activated carbon, graphene, nitrogen-doped graphene, carbon nanotubes can provide some escalation in catalytic activity [19]. Since the noble metals are not tightly bound to the surface of carbonaceous materials, they undergo leaching during the catalysis and have short life and low reusability. The use of oxide supports for the noble metal(0) nanoparticles escalate their catalytic activity in the hydrolysis of AB. Particularly, the reducible oxides such as titania, ceria, tungsten(VI) oxide, cobalt(II,III) oxide provide high activity and long lifetime for the supported rhodium(0) [20], ruthenium(0) [17], palladium(0) [21] and platinum(0) [22] nanoparticles. Using the magnetic powders as support for noble metal(0) nanoparticles makes them magnetically separable provided that nanoparticles are tightly bound on the surface of magnetic powder. Thus, magnetically isolable ruthenium(0) [23], palladium(0) [24], rhodium(0) [20] and platinum(0) [25] nanocatalysts have outstanding catalytic activity, long lifetime and exceptionally high reusability in hydrogen generation from the from the hydrolysis of AB at room temperature.

[1] B. Demirel, N. Bicakcioglu et al. Int. J. Global Warming 18 (2019) 385.
[2] P. Nejat, F. Jomehzadeh, et al. Renewable Sustainable Energy Rev 2015, 43, 843-862.
[3] T.R. Anderson, E. Hawkins, P.D. Jones. Endeavour, 40 (2016) 178.
[4] T. Uyar, D. Besikci. Int. J. Hydrogen Energy, 42 (2017) 2453−2456.
[5] M. R. Usman. Renew Sustain Energy Rev. 167 (2022) 112743.
[6] D. Zivar, S. Kumar, J. Foroozesh. Int J Hydrogen Energy 2021, 46, 23436-23462.
[7] E. Boateng, A. Chen. Materials today Adv. 2020, 6, 100022.
[8] N. A. Ali, N. A. Sazelee, M. Ismail. Int. J. Hydrogen Energy 46 (2021) 31674.
[9] T. He, P. Pachfule, H. Wu, Q. Xu, P. Chen. Nat. Rev. Mater. 1 (2016) 1.
[10] U. B. Demirci. Int. J. Hydrogen Energy 42 (2017) 9978.
[11] M. Chandra, Q. Xu. J. Power Sources 156 (2006) 190.
[12] M. Zahmakıran, S. Özkar. Topics in Catal., 56 (2013) 1171.
[13] S. Akbayrak, S. Özkar, Int. J. Hydrogen Energy 43 (2018) 18592.
[14] S. Özkar. Int. J. Energy Res., 46 (2022) 22089.
[15] S. Özkar. Int. J. Hydrogen Energy, 54 (2024) 54, 327.
[16] L. Zhang, et al. J. Zhu. Nano Research 15 (2022) 3034.
[17] S. Akbayrak, Y. Tonbul, S. Özkar. Turk. J. Chem. 47 (2023) 1224.
[18] M. Poliakoff, J. M. Fitzpatrick,et al. Science 2002, 297, 807-810.
[19] S. Akbayrak, S.Özkar, ACS Appl.Mater. Interfaces 4 (2012) 6302.
[20] Y. Tonbul, S. Akbayrak, S. Özkar, ACS Sustainable Chem. Eng. 8 (2020) 4216.
[21] S. Akbayrak, S. Özkar, J. Colloid Interface Sci. 626 (2022) 752.
[22] S. Akbayrak, S. Özkar. ACS Appl. Mater. Interfaces 13 (2021) 34341
[23] S. Akbayrak, G. Çakmak, T. Öztürk, S. Özkar, Int. J. Hydrogen Energy 46 (2021) 13548.
[24] S. Akbayrak, G. Çakmak, T. Öztürk, S. Özkar. J. Alloys Compounds, (2024) 175199.
[25] S. Akbayrak, S. Özkar, J. Colloid Interface Sci. 596 (2021) 100.

Dr. Özkar graduated from Technical University of Istanbul in 1972, received Ph.D. in inorganic chemistry at Technical University of Munich in 1976 and joined Middle East Technical University in 1979. He spent one year at Max Planck Institute in Mülheim a.d. Ruhr, Germany in 1986, 2 years at University of Toronto in 1988-1990, and now 5 total years at Colorado State University since 2000. He was awarded Science Prize by the Scientific and Technological Research Council of Turkey in 1996 and has been member of Turkish Academy of Sciences since 1996. His research interests: metal nanoparticles, catalysis, mechanism, kinetics, synthesis and hydrogen.

Saim Özkar, e-mail: sozkar@metu.edu.tr tel: +90 538 826 8560

Addressing Materials Challenges for Fuel Cells and Electrolyzer Technologies: Membrane and Catalyst Innovations

Selmiye Alkan Gürsel[1,2], Naeimeh Mojarrad Rajabalizadeh[2], Cem Meriç[1], Hediyeh Nobar Malekzadsani[2], Navid Haghmoradi[1], Sina Abdolhosseinzadeh[1], Bilal Iskandarani[1], Bahadır Patır[1], Hamza Arslan[1], Büşra Çetiner[1], Begüm Yarar Kaplan[2], Alp Yürüm[1,2], Aidan Ladewig[3], Foysal Neerob Ahmed[3], Stoyan Bliznakov[3], Ugur Pasaogullari[3]

[1] Sabanci University, Faculty of Engineering and Natural Sciences, 34956, Istanbul, Turkey

[2] Sabanci University SUNUM Nanotechnology Research Center, 34956, Istanbul, Turkey

[3] University of Connecticut, School of Mechanical, Aerospace, and Manufacturing Engineering, 191 Auditorium Rd. U-3139, Storrs, CT 06269, USA

The transition to sustainable hydrogen economies faces fundamental materials limitations across the polymer electrolyte membrane (PEM) electrolyzer and fuel cell value chain. Despite enabling carbon-free power generation through fuel cells, green hydrogen production via electrolysis and its conversion in fuel cells remain constrained by performance limitations, efficiency losses, and durability challenges. Other key challenges include reliance on perfluorosulfonic acid membranes with high cost, and hydration-dependent performance; gas crossover phenomena compromising efficiency and safety; catalyst systems dominated by platinum-group metals (PGMs), notably Pt cathodes for oxygen reduction reaction (ORR) in fuel cells and Ir anodes for oxygen evolution reaction (OER) in acidic electrolyzers in which scarcity and high cost.

To address membrane limitations, our group focuses on alternative and cost-effective solutions [1,2]. We develop ion-conducting membranes via radiation-*induced graft polymerization* of vinyl monomers onto various base polymers. These radiation-grafted membranes offer distinct advantages including utilization of commercial base polymers, precise control, spatially resolved functionalization and intrinsic avoidance of solution-processing steps. Our group utilizes *electrospinning* as well to fabricate composite and hybrid membranes. These approaches enable membranes with tunable ion exchange capacity, water uptake and ionic conductivity. We achieved the development of new generation asymmetric membranes and bipolar membranes as well. Moreover, for PEM electrolyzers, we embedded recombination catalysts within thin membranes mitigate hydrogen crossover, eliminating auxiliary layers while maintaining efficiency.

Our complementary catalyst innovations target PGM reduction and activity enhancement to reduce cost and enhance performance [3-6]. For ORR in fuel cells, Pt nanoparticles (2–3 nm) on functionalized graphene supports (nanoplatelets, rGO, hybrids) reduce Pt consumption while enhancing activity. These catalysts are synthesized by impregnation-reduction, microwave-assisted deposition, photocatalytic deposition, and electrophoretic deposition.

Moreover, we develop transition metal-doped iridium oxide catalysts (Mn, Ni, Ti) for acidic OER in PEM electrolyzers. Our work engineers Mn-, Ni-, and Co doped IrO_2 systems via sol-gel synthesis, where dopant integration induces significant electronic modulation that optimizes reaction energetics. This reduces OER activation barriers, enhances exothermic behavior, and improves catalytic efficiency. Specifically, Mn-doped variants achieve substantial reductions in noble metal loading while delivering significantly lower overpotentials compared to pure IrO_2, attributed to Mn redox cycling facilitating lattice-oxygen-mediated pathways. To further boost stability, we leverage anodized TiO_2 nanotube arrays on titanium mesh substrates, providing high-surface-area supports that enhance catalyst anchoring and mitigate dissolution through synergistic charge transfer. These advances enable high-performance, durable electrodes with reduced precious metal reliance, and advancing scalable hydrogen technologies toward commercial viability.

In this presentation, we contextualize these material innovations within global efforts to overcome fuel cell and electrolyzer limitations. We highlight key projects including *Graphene Flagship*, *HYSouthMarmara Hydrogen Shore* (Turkiye's first hydrogen valley initiative) and other projects.

References

[1] M. M. Nasef, S. Alkan Gürsel, D. Karabelli, O. Güven, Progress in Polymer Science 63, 1 (2016).
[2] N. R. Mojarrad, S. Sadeghi, B. Yarar Kaplan, S. Alkan Gürsel, E. Güler, ACS Appl. Energy Mat. 3, 532 (2020).
[3] S. Abdolhosseinzadeh, S. Sadighikia, S. Alkan Gürsel, ACS Sustainable Chem. Eng. 6, 3773 (2018).
[4] E. Quesnel, F. Roux, F. Emieux, P. Faucherand, E. Kymakis, G. Volonakis, F. Giustino, B. Martín-García, I. Moreels, S. Alkan Gürsel, et al., 2D Mater. 2, 030204 (2015).
[5] B. Yarar Kaplan, A. C. Kırlıoğlu, M. Alinezhadfar, M. A. Zabara, N. R. Mojarrad, B. Iskandarani, A. Yürüm, C. S. Ozkan, M. Ozkan, S. Alkan Gürsel, Chem Catal. 3(5), 100601 (2023)
[6] M. A. Zabara, B. Ölmez, M. Buldu-Akturk, B. Y. Kaplan, A. C. Kırlıoğlu, S. Alkan Gürsel, M. Ozkan, C. S. Ozkan, A. Yürüm, Glob. Chall. 8(8), 2470088 (2024)

Acknowledgments

This work was supported by several grants: the Scientific and Technological Research Council of Türkiye (TÜBİTAK) under Grant Number 123N418, within the framework of the M-ERA.NET program and European Union's Horizon 2020 research and innovation programme under grant agreement No 696656 (Graphene Flagship). The authors also acknowledge the support of the Sabancı University–University of Connecticut collaboration.

Prof. Dr. Selmiye Alkan Gürsel is Faculty Member at Faculty of Engineering and Natural Sciences, Sabanci University. Her scientific activities have included PEM &AEM fuel cells (electrodes, catalysts, membranes & electrochemical characterization), hydrogen & electrolysis technologies, lithium-ion & lithium-sulfur batteries, polymer electrolyte membranes, graphene, radiation-induced grafting, and conducting polymers.

Selmiye Alkan Gürsel, e-mail: selmiye@sabanciuniv.edu tel: +90 216 483 95 73

Nanoscale Electrodes for Solid Oxide Cells: Fabrication, Microstructure and Stability

Aligül Büyükaksoy
Gebze Technbical University

Solid oxide cells (SOCs) are high-temperature (600-800 °C) electrochemical devices that can both convert electricity and water to hydrogen and oxygen hydrogen and vice versa – a trait that can address the intermittency problem of renewables. The combination of these two technologies can address the carbon emission issues we are facing today. SOCs are associated with challenges, including insufficient electrochemical performance and degradation of microstructures and materials chemistries upon long-term exposure to operating conditions. For example, SOC electrodes fabricated by conventional powder-based methods are short of electrochemically active electrocatalyst-ionic conductor-gas triple phase boundaries (TPBs), their electrocatalysts undergo agglomeration and diminish TPBs, and Sr segregates to the surfaces of (La, Sr)(Co/Fe/Mn)O 3 -type perovskite oxygen electrocatalysts to finally deactivate them. Changing the electrode fabrication approach from a powder sintering-based route into a liquid precursor-based one generates several opportunities to address these challenges. First, it enables the fabrication of nanoscale composites from a single precursor, to form electrocatalyst and ionic conductor phases via self-assembly, which yields extremely long TPBs. Second, the layer-by layer nature of this approach enables the application of multiple interlayers, which can be tailored to mechanically constrain electrocatalyst agglomeration, reverse the concentration gradients to avoid cation segregation or generate desired interfaces for synergistic other synergistic effects, thereby addressing many challenges SOCs are facing. In this talk, microstructure – electrochemical performance relationships in nanoscalecomposite SOC electrodes will be elaborated. Impact of the introduction of multiplenanolayers on the structural and chemical stability of electrodes is discussed.

Aligul Buyukaksoy Aligül Büyükaksoy obtained his BS and MSc degrees in Materials Science and Engineering from Gebze Technical University (then, Gebze Institute of Technology) in 2007 and 2009, respectively. He completed his PhD work in 2013, at Missouri University of Science and Technology in the same field. Through Eyes High and Calgary Innovates – Technology Futures fellowships, he then worked under the supervision of Prof. Viola Birss at the University of Calgary for two years. In 2016, he joined the Materials Science and Engineering department, at Gebze Technical University as an assistant professor and got promoted to associate professor position in 2021. His research interests include solid oxide cells, defect chemistry, solid state electrochemistry, electroceramics and ceramic fabrication techniques.

Machine Learning for Sustainable Energy Materials and Technologies

Ramazan Yıldırm

Department of Chemical Engineering, Boğaziçi University, İstanbul

As a major enabler for most of human activities from food and fresh water production to transportation, telecommunication and healthcare, the energy is a critical ingredient for a sustainable future. While UN Sustainable Development Goal 7 (SDG 7) directly aims to "ensure access to affordable, reliable, sustainable and modern energy for all", most of 169 targets stated under the all of 17 SDGs are also involved with energy production or utilization. Machine learning (ML), as another enabler technology of recent years, has been employed in most of the activities in SDGs as well as the implementation projects and programs to attain SDGs through data collection, monitoring and analysis. ML also frequently used in sustainable energy production and storage technologies including the search and design of new materials. In this presentation, the potential roles of ML for the sustainable energy future, will be discussed. First, the basic principles and more recent developments will be summarized Then the use of ML in energy production and storage will be discussed in detailed examples together with a perspective on the challenges and opportunities for the future.

Ramazan Yıldırım is a professor of Chemical Engineering at Boğaziçi University. He received his B.Sc from Ege University and his MS is from Boğaziçi University. Then, he moved to University of California, Los Angeles where he received his Ph.D. After his Ph.D., he had worked as quality and management consultant for about five years before he joined Boğaziçi University Chemical Engineering Department in 2001 as a full time professor. His research focuses on catalysis and photocatalysis, machine learning analysis of energy conversion technologies (e.g. catalytic hydrogen production and purification, water splitting, photocatalytic CO2 reduction, biofuel production and solar cells) and energy storage systems.

2D MBenes for Energy Storage and Conversion Technology

Muslum DEMIR
Department of Chemical Engineering, Bogazici University, Istanbul 34342, Türkiye
TUBITAK Marmara Research Center, Material Institute, Gebze 41470, Türkiye

The growing demand for sustainable and high-performance energy technologies has accelerated interest in two-dimensional (2D) materials. Among them, transition metal borides—MBenes—represent a promising class due to their high electrical conductivity, mechanical robustness, and tunable surface chemistry. As boron-containing analogs of MXenes, MBenes offer distinct advantages for energy storage and conversion applications.

This talk presents recent progress in MBene synthesis, functionalization, and application in supercapacitors, batteries, and electrocatalytic systems such as HER, OER, and ORR. We explore how boron-metal bonding, layer structure, and surface modifications influence electrochemical performance. Advances in molten salt synthesis and hybrid nanocomposite design have led to MBenes with excellent pseudocapacitive behavior, fast charge–discharge rates, and high energy density.

By bridging fundamental materials chemistry with practical device engineering, this presentation aims to shed light on the transformative potential of 2D MBenes in advancing sustainable energy conversion and storage technologies.

Müslüm Demir is a materials scientist specializing in energy storage, 2D nanomaterials, and CO_2 capture technologies. With over 100 peer-reviewed publications and extensive experience in academic and industrial research, he has made significant contributions to the development of MXenes, MBenes, and porous carbon-based hybrid materials for supercapacitors, batteries, and electrocatalysis. He is currently associate professor at Boğaziçi University and a senior researcher at TÜBİTAK-MAM.

Presentating author: Name Surname, e-mail: tel:

BATTERIES

Synergistic Dual Doping of Graphene Oxide: A New Route to High-Capacity Anodes for Sodium-Ion Batteries

MohammedMustafa Almarzoge[1], Metin Gencten[1]*, Gamzenur Ozsin[2]

[1] Yildiz Technical University, Faculty of Chemical and Metallurgical Engineering, Department of Metallurgy and Materials Engineering, 34210 Istanbul, Turkey

[2] Bilecik Şeyh Edebali University, Faculty of Engineering, Department of Chemical Engineering, 11230, Bilecik, Turkey

Sodium-ion batteries (NIBs) have emerged as promising alternatives to lithium-ion batteries (LIBs) for large-scale energy storage systems, owing to the abundance, low cost, and geographic availability of sodium [1]. Despite these advantages, the relatively large ionic radius of Na^+ and its weak interaction with the graphite lattice hinder its intercalation, rendering conventional graphite anodes nearly inactive in NIB systems. This fundamental limitation is primarily due to the insufficient interlayer spacing in graphite, which fails to accommodate Na^+ ions effectively. To address this challenge, various carbonaceous materials—such as amorphous carbon, hard carbon, and doped graphene derivatives—have been explored [2]. These materials possess high electronic conductivity, tunable pore structures, and chemical stability, making them suitable hosts for sodium storage. Among them, heteroatom-doped graphene-based materials have shown considerable potential due to their enhanced Na^+ adsorption sites, expanded interlayer distances, and defect-rich structures that facilitate ion transport [3,4]. Dual doping, in particular, has gained attention as a strategy to synergistically tailor the electronic structure and surface chemistry of graphene. Nitrogen atoms can introduce active sites and improve electronic conductivity, while sulfur doping can enlarge the interlayer spacing and enhance Na^+ binding through polar interactions. Together, these dopants can promote reversible sodium storage by stabilizing intermediate states and reducing energy barriers for ion insertion and extraction. Additionally, the choice of electrolyte plays a critical role in enabling effective Na^+ intercalation. Ether-based electrolytes such as diglyme have been reported to facilitate the co-intercalation of solvated Na^+ ions into carbon matrices, a process not feasible with conventional carbonate-based systems. This co-intercalation mechanism can mitigate structural degradation and improve the long-term stability of the anode.

In this study, we investigate nitrogen-sulfur dual-doped graphene oxide (N-S-GO) as a standalone anode material for NIBs, in combination with an ether-based (diglyme) electrolyte. Without requiring additional conductive additives or composite components, N-S-GO exhibits stable cycling performance, enhanced sodium-ion diffusion, and improved reversibility. The structural advantages provided by dual doping, combined with the favorable ion transport properties of the ether-based electrolyte, make this approach a promising candidate for future sodium-ion battery technologies. To the best of our knowledge, this is the first report demonstrating the direct use of N-S dual-doped graphene oxide with an ether-based electrolyte system for sodium-ion batteries. This work contributes to the development of high-performance, scalable, and cost-effective anode materials for next-generation energy storage systems.

Acknowledgment

This work was supported by Yıldız Technical University under grant numbers FCD-2024-6420. M. Gençten gratefully acknowledges TÜBA for the Outstanding Young Scientists Award (GEBİP).

References

[1] Hasa, I., Hassoun, J., & Passerini, S. (2017). Nano Research, 10(12), 3942-3969.

[2] Kim, H., Kim, H., Ding, Z., Lee, M. H., Lim, K., Yoon, G., & Kang, K. (2016). Advanced Energy Materials, 6(19), 1600943..

[3]Almarzoge, M., Gencten, M., & Ozsin, G. (2024). ECS Journal of Solid State Science and Technology, 13(7), 071001.

[4]Almarzoge, M., Gencten, M., & Ozsin, G. (2025). ChemElectroChem, 12(4), e202400564.

Dr. Metin GENÇTEN earned his master's and doctoral degrees from the same university in 2013 and 2017, respectively. He began his academic career as a research assistant in 2010 and has worked at Anadolu University and Ordu University. In 2018, he joined Yıldız Technical University as an Assistant Professor and became an Associate Professor in 2019. He leads the Gençten Research Group and conducts research at the Advanced Materials Technologies Laboratory for Energy Storage Systems (ENDEP-LAB), focusing on energy storage systems such as Li/Na-ion batteries, supercapacitors, lead-acid batteries, and redox flow batteries, as well as advanced material technologies such as 2D materials and conducting polymers, and the recycling of industrial and battery waste.

Presentating author: Metin Gencten, **e-mail:** mgencten27@gmail.com

Microwave-assisted synthesis of SnS and SnS/MWCNT anodes for sodium-ion batteries

Mehbare Dogrusoz[1,3], Ali Ş. Ahsen [2] and Rezan Demir-Cakan [3]

[1] Maritime Higher Vocational School, Piri Reis University, İSTANBUL, TÜRKİYE

[2] Department of Physics, Gebze Technical University, KOCAELİ, TÜRKİYE

[3] Department of Chemical Engineering, Gebze Technical University, KOCAELİ, TÜRKİYE

Sodium ion battery system is based on the migration of sodium ions through the electrolyte between the anode and cathode structures. This mechanism is analogues to that of a lithium ion battery system due to the similar physical and chemical properties of lithium and sodium metal as is well- known. Sodium ion battery system stands out because of the abundance and parallely cost advantage of sodium. Hence, the availability of various battery systems will be able to support the utilisation of renewable energy as well as powering mobile systems, including electric vehicles [1].

Several anode candidates have been studied in order to develop the sodium ion battery system with the highest accessible energy density. The following criteria are significant for designing anode materials: i) cheap and abundant starting materials; ii) lower redox potentials and stable working potentials; iii) high sodium storage capability; iv) high initial coulombic efficiency. Consequently, the hard carbon anode is the most powerful anode candidate for commercial SIBs due to its low redox potentials, high sodium storage capacity, and stable cycle life [2]. However, despite the intense study of hard carbon anodes, their theoretical capacity is around 300 mAh·g^{-1} and their initial coulombic efficiency ranges from 20–90% [3]. To overcome these challenges, other candidates have also been investigated. Among these, tin (Sn) and tin disulphide (SnS) have a relatively high specific capacity against sodium metal (Sn: 847 mAh·g^{-1}, SnS: 1022 mAh·g^{-1}) [4, 5]. Despite their high theoretical capacity, pulverisation occurs during the charge/discharge process due to volume expansion.

Herein, SnS and SnS/MWCNT anodes were synthesised via a microwave-assisted method in a short time of around 45 minutes. The influence of the microwave reaction time and the amount of MWCNTs added on the electrochemical performance of SnS and SnS/MWCNT anode samples for sodium ion batteries was investigated. Based on the test results, reaction durations of 15, 30 and 45 minutes were investigated and 45 minutes was determined to be sufficient for the intended outcome. Following this finding, the amount of MWCNTs was optimised. The results were evaluated in terms of reaction time, capacity retention and initial coulombic efficiency values. **Figure 1** depicts the discharge capacity results for all samples.

Looking at the galvanostatic charge/discharge test results, SnS-1 and SnS-2 samples which are synthesized by 15 min and 30 min., respectively, showed poor cycling performance and the capacity decreased rapidly. SnS-3 sample provided the more stable cycling performance and its capacity was 200 mAh·g^{-1} at 100th cycle.

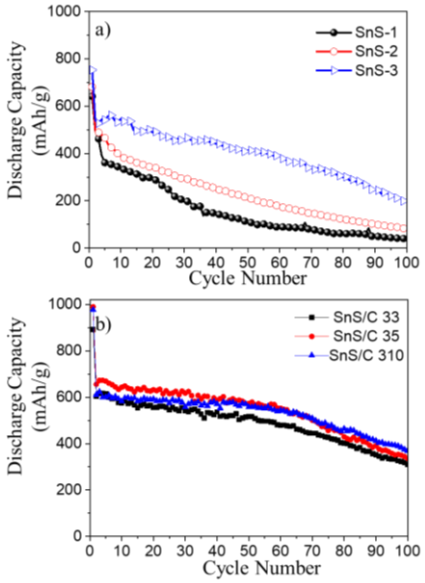

Figure 1. Discharge capacity comparison of the a) SnS-1 (15min), SnS-2 (30 min), SnS-3 (45 min), b) SnS/C 33 (3mg MWCNT addition), SnS/C 35 (5mg MWCNT addition), SnS/C 310 (10 mg MWCNT addition) at 36 mA·g^{-1} current density. Electrolyte: 1M $NaClO_4$ in PC- 5% FEC, Binder : Na-alginate.

To improve the capacity, MWCNT was added by certain amount varying with 3 mg, 5mg and 10mg to SnS-3 sample. MWCNT addition enhanced the obtained capacity due to the inreased electrical conductivity and surface area. Although the SnS/C-310 sample exhibited the highest capacity, its intial colombic efficiency was relatively low at 57 % . Thus, taking into consideration of initial colombic efficiency, the SnS/C-35 sample, with a values of 60 %, was regarded as the best performing sample overall.

References

[1] P. Phogat, S. Dey, M. Wan, Materials Science and Engineering: B, 312(2025).

[2] J. Cui, P. Su, W. Li, X. Wang,Y. Zhang, Z. Xiao, Q. An and Z. Chen, Advanced Energy Materials, 15(2025).

[3] H. Wang., H. Niu, K. Shu, L. Sun, Y. Wang, Y. Du, Y. Han,C. Yang, Y-M. Kang, Journal of Materials Science and Technology, 209 (2025).

[4] J.Song, X. Zu, W. Jian, Y. Sun, W. Zhang, X. Qiu, Chemical Engineering Science, 300(2024).

[5] R. F. Shahzad, S. Rasul, M. Mamlouk, I. Brewis, R.A. Shakoor, A.W. Zia, Small Structures, 6(2025).

Mehbare DOGRUSOZ is asistant proffesor in Maritime Higher Vacational School in Piri Reis University, Turkey. She received her BSc degree chemical engineering in Hacettepe University and MSc in Materials Science and Engineering in Gebze Technical University . She did her Ph.D. degree on metal sulphide anodes for sodium ion batteries under the supervision of Proffesor Rezan DEMIR-CAKAN.

Presentating author: Mehbare DOGRUSOZ, e-mail:mdogrusoz@pirireis.edu.tr

PET-derived nitrogen-doped hard carbon as a sustainable anode for sodium-ion batteries

Aizhuz Sarsengaliyeva[1], Arailym Nurpeissova[1,2*]
[1]Institute of Batteries LLP, 53 Kabanbay Batyr Ave., Astana, Kazakhstan
[2]National Laboratory Astana, 53 Kabanbay Batyr Ave., Astana, Kazakhstan
*arailym.nurpeissova@nu.edu.kz

The growing demand for energy storage and the rising cost and limited availability of lithium have prompted the exploration of alternative battery technologies. Sodium-ion batteries (SIBs) have emerged as a promising substitute due to sodium's natural abundance, low cost, and similar chemical properties to lithium [1]. Concurrently, the global plastic crisis driven by rapidly growing polyethylene terephthalate (PET) production and consumption calls for sustainable recycling strategies. Recent studies suggest that recycled PET can serve as a viable precursor for carbon materials in SIB anodes, offering high structural stability, conductivity, and surface area [2]. However, challenges remain in optimizing synthesis processes and ensuring the long-term electrochemical performance of such materials, necessitating further innovation in material design and processing.

In this study, nitrogen-doped hard carbon (N-HC) was synthesized via direct pyrolysis of PET waste in the presence of a nitrogen source, aiming to introduce structural defects and heteroatom functionalities to enhance sodium storage capability. The resulting carbon was thoroughly characterized using Fourier-transform infrared spectroscopy (FTIR), thermogravimetric analysis (TGA), X-ray diffraction (XRD), Raman spectroscopy and scanning electron microscopy (SEM) to investigate its structural and morphological features.

Electrochemical performance was evaluated through galvanostatic charge–discharge tests and cyclic voltammetry (CV). The nitrogen doping was found to significantly improve electrical conductivity, provide additional active sites, and enhance sodium-ion intercalation behavior compared to non-doped carbon materials.

Acknowledgment
This study was funded by the Science Committee of the Ministry of Science and Higher Education of the Republic of Kazakhstan (grant No. BR24992766, grant No. AP23483880).

References

[1] Kim, S. W., Seo, D. H., Ma, X., Ceder, G., & Kang, K. (2012). Electrode materials for rechargeable sodium-ion batteries: potential alternatives to current lithium-ion batteries. *Advanced Energy Materials*, *2*(7), 710-721.
[2] Puravankara, S. (2023). Utilization of PET derived hard carbon as a battery-type, higher plateau capacity anode for sodium-ion and potassium-ion batteries. *Journal of Electroanalytical Chemistry*, *946*, 117731.

Presenting author: Aizhuz Sarsengaliyeva, e-mail: saizhuzzaa@gmail.com tel: 8(705)395-73-50

Electrochemical Performance of Deep Discharged $Li_4Ti_5O_{12}$ Anode Material for Lithium-Ion Batteries

Halil Şahan[1,2], Yusuf Taş[3], Emirhan Selçuk[1,2] and Şaban Patat[1,2]

[1] Erciyes University, Faculty of Science, Deparment of Chemistry, Kayseri, Türkiye

[2]Erciyes University, Nanotechnology Application and Research Center (ERNAM), Kayseri, Türkiye

[3] ASPİLSAN Energy, Battery Cell and Battery Systems Production Facility, Kayseri, Türk

Lithium titanate ($Li_4Ti_5O_{12}$, LTO) is considered a promising anode material for next-generation lithium-ion batteries due to its excellent thermal stability, long cycle life, and intrinsic safety [1]. Its "zero-strain" property during Li^+ intercalation/deintercalation minimizes volume change and ensures outstanding structural stability [2]. The relatively high voltage plateau (~1.55 V vs. Li/Li^+) suppresses lithium dendrite formation, providing superior safety compared with graphite anodes [3]. The spinel structure of LTO offers abundant Li-ion sites, allowing a theoretical capacity of 293 mAh g^{-1} when Ti^{4+} is fully reduced to Ti^{3+} under deep-discharge conditions near 0 V [4]. However, most studies have examined the 1.0–3.0 V range, with limited attention to performance below 1.0 V [4]. To improve conductivity and Li^+ diffusivity, doping at Ti or Li sites and *in situ* or *ex situ* carbon coating are effective strategies that enhance electrochemical performance and rate capability [5].

In the present work, we investigate the electrochemical behavior of Na- and Yb-co-doped, carbon-coated LTO anodes under deep-discharge conditions at room temperature. Pristine $Li_4Ti_5O_{12}$ (LTO) and $Li_{3.98}Na_{0.02}Ti_{4.98}Yb_{0.02}O_{12}$ (LTO–Na–Yb), along with their carbon-coated derivatives (LTO@C and LTO–Na–Yb@C), were synthesized via a conventional solid-state reaction method. The carbon-coated variants were further prepared through an *ex situ* pyrolysis process using organic carbon precursors. Galvanostatic charge–discharge tests were conducted within the potential range of 3.0–0.01 V at current densities of 30, 300, and 500 mA g^{-1}, respectively. Structural, morphological, and electrochemical properties were comprehensively characterized using X-ray diffraction (XRD), field-emission scanning electron microscopy (FESEM), galvanostatic cycling, cyclic voltammetry (CV), and electrochemical impedance spectroscopy (EIS).

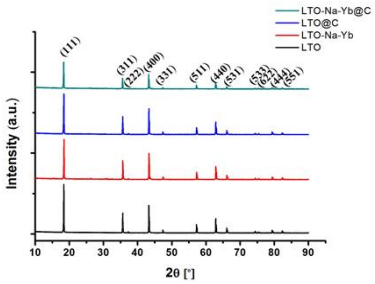

Fig.1. XRD patterns of the pristine LTO and LTO-Na-Yb, LTO@C, LTO-Na-Yb@C.

The phase purity was analyzed by XRD (PANalytical Empyrean, Cu–Kα, 2θ = 10–90°). As shown in Fig. 1, both LTO and doped-coated anodes exhibit diffraction peaks consistent with the cubic spinel structure (JCPDS No. 72-0426). All diffraction peaks correspond to pure cubic LTO, and the refined lattice parameter of pristine LTO and LTO–Na–Yb materials were determined as 8.357 Å and 8.359 Å, respectively.

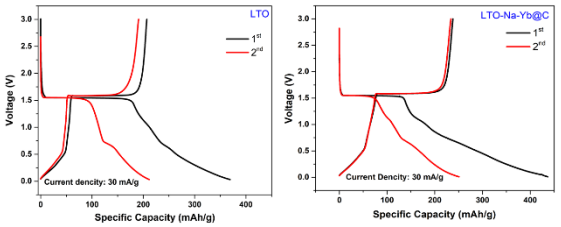

Fig 2. The charge-discharge profiles of LTO and LTO-Na-Yb@C anodes at 30 mA/g in the range of 0.02–3 V (vs. Li/Li^+)

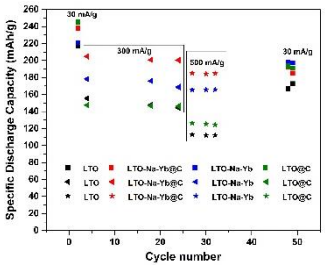

Fig. 3. Rate capabilities of LTO and LTO-Na-Yb, LTO@C, LTO-Na-Yb@C anode materials

As can be seen in Figs. 2 and 3, among all the as-prepared composite anodes, LTO–Na–Yb@C delivers the highest initial discharge capacity across various current densities. Furthermore, it exhibits superior rate capability compared with pristine LTO, LTO–Na–Yb, and LTO@C at 30, 300, and 500 mA /g.

Acknowledgements

The authors thank the Erciyes University Scientific Research Projects Unit for financial support and ASPİLSAN Energy for their support.

References

[1] J.-M. Tarascon, M. Armand, *Nature* **414** (6861), 359–367 (2001).
[2] X. Su, et al., *RSC Advances* **6** (109), 107355–107363 (2016).
[3] J.E. Hong, K.S. Kim, H.J. Jeon, K.S. Ryu, *J. Electrochem. Sci. Technol.* **1** (1), 72–75 (2021).
[4] C. Han, et al., *ACS Appl. Mater. Interfaces* **8**, 18788–18796 (2016).
[5] B.V. Babu, et al., *Results Phys.* **9**, 28

Dr.Yusuf TAŞ is Experienced Electrical and Electronics Engineer with nearly a decade of expertise in the rechargeable battery and machinery industries. Recognized for consistently delivering high-impact results and driving innovation across complex projects. Specialized in lithium-ion and sodium-ion cell technologies, battery testing protocols, quality control systems, and performance optimization of electrochemical storage solutions.
Corresponding author: Yusuf Taş , e-mail:yusuf.tas@aspilsan.com tel:+90 505 151 38 76

3D-structured nanoporous SnO_2 thin-film anodes for lithium-ion microbatteries

Yerkem Kanatbekkyzy[1], Yessimzhan Raiymbekov[1,2], Zhumabay Bakenov[1,2], Aliya Mukanova[1,2]
[1]National Laboratory Astana, Nazarbayev University, 53 Kabanbay Batyr Ave., Astana, 010000, Kazakhstan
[2] Institute of Batteries, Kabanbay Batyr Ave. 53, Astana, 010000, Kazakhstan
*aliya.mukanova@nu.edu.kz

The growing demand for compact energy storage in micro- and nanoscale devices requires high-capacity anodes with outstanding cycling stability. Traditional thin-film SnO_2 anodes suffer from rapid capacity fade due to large volume changes during cycling, limiting their long-term reliability.

In this work, we present a novel three-dimensional (3D) SnO_2 anode architecture, fabricated using self-assembled polystyrene (PS) microspheres as a sacrificial template. This bottom-up method allows precise control over pore size and distribution, resulting in a uniform, interconnected porous network unattainable by conventional deposition techniques. SnO_2 thin films were deposited by RF magnetron sputtering, followed by thermal annealing to remove the PS template.

Electrochemical evaluation revealed that the 3D-structured anodes deliver significantly enhanced performance compared to planar counterparts. At a current density of 0.5C, the electrodes retained a capacity of ~600 mAh g^{-1} after 400 cycles, demonstrating excellent stability and improved Li^+ transport due to the porous architecture.

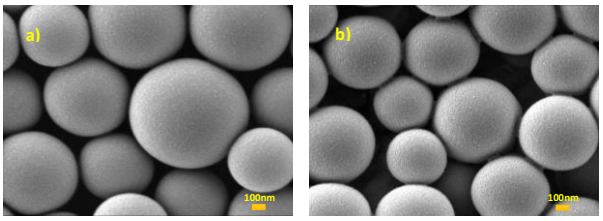

Fig. 1. SEM images of 3D nanoporous SnO_2 (100 nm): (a) As-prepared with PS template (b) After 620°C/N_2 annealing, showing enhanced crystallinity and intact porous structure.

Comprehensive materials characterization and electrochemical results will be presented and discussed at the conference.

The proposed 3D SnO_2 architecture offers a promising pathway toward high-performance lithium-ion microbatteries for wearable electronics and IoT devices, where compactness and durability are essential.

Acknowledgments
This research was funded by the research project AP19680567 “Advanced nanocomposite 3D thin film electrodes for lithium-ion batteries” from the Ministry of Science and Higher Education of the Republic of Kazakhstan.

Presenting author: Yerkem Kanatbekkyzy e-mail: erkem.kanatbekkyzy@nu.edu.kz tel: +77075969472

Study of LATP ceramics for subsequent fabrication of thin film electrolytes

Ayazhan Bekmakhanova[1, 2], Zhansaya Bakhytzhanova[1, 2], Mukagali Yegamkulov[1, 4], Zhumabay Bakenov[1, 3, 4], Aliya Mukanova[1, 3, 4*]

[1]National Laboratory Astana, Nazarbayev University, Kabanbay Batyr Ave. 53, Astana 010000, Kazakhstan

[2]Department of Chemistry, Faculty of Nature Sciences, L.N. Gumilyov Eurasian National University, Kazhymukan str. 13, Astana 010000, Kazakhstan

[3]Department of Chemical and Materials Engineering, School of Engineering and Digital Sciences, Nazarbayev University, Kabanbay Batyr Ave. 53, Astana 010000, Kazakhstan

[4]Institute of Batteries LLC, Kabanbay Batyr Ave. 53, Astana 010000, Kazakhstan

*aliya.mukanova@nu.edu.kz

In recent years, solid lithium-ion batteries (SLIBs) have attracted increased interest due to their safety, high energy efficiency, and wide range of applications, from portable electronics to electric vehicles. One of the key components of such batteries is a solid electrolyte, which provides reliable and stable conductivity of lithium ions, as well as stability at the interface with the electrodes [1].

Among the many solid electrolytes studied, special attention is paid to materials with a NASICON-like structure, in particular lithium-aluminum-titanium-phosphate (LATP) compounds. These materials have a number of valuable characteristics, including high ionic conductivity, chemical inertness, and thermal stability, which makes them promising for use in modern SLIBs [2–3].

This study investigates the influence of different lithium concentrations in LATP on its structural and electrochemical properties, synthesized using the molten flux method.

To evaluate the ionic conductivity and study the effect of composition on the transport properties of LATP, studies were carried out using the electrochemical impedance spectroscopy (EIS) method. Measurements were performed in the frequency range from 1 MHz to 1 Hz with an amplitude of 0.01 V at temperatures of 25°C and 85°C for samples with different lithium content ($Li_{1.3}$, $Li_{1.4}$, $Li_{1.5}$).

X-ray diffraction (XRD) analysis confirmed the formation of the main phase LATP in all the studied samples. However, with increasing lithium content, the formation of secondary phases ($Li_4P_2O_7$, TiP_2O_7, $AlPO_4$), was observed, which can potentially reduce the ionic conductivity of the material. These structural changes are shown in **Figure 1.**

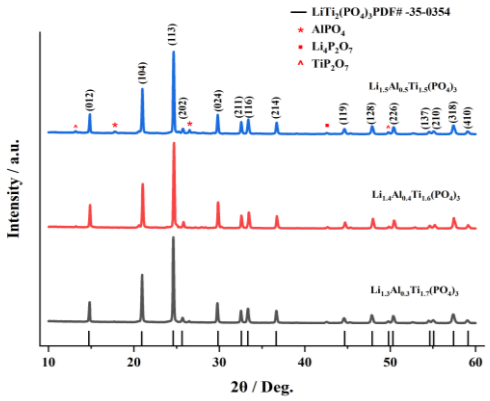

Figure 1. XRD patterns of LATP

Extensive characterization of the materials and corresponding electrochemical performance will be presented and discussed at the conference.

In a broader sense, precise selection of the composition of ceramic electrolytes is important to ensure stable ionic conductivity and can be further used to obtain thin-film electrolyte for microbatteries.

Acknowledgment

This research was funded by the research project AP19680567 "Advanced nanocomposite 3D thin film electrodes for lithium-ion batteries" from the Ministry of Science and Higher Education of the Republic of Kazakhstan.

References

[1] Hou, M., et al. *Nanotechnology*, 31, 132003 (2020). https://doi.org/10.1088/1361-6528/ab5be7

[2] Kundu, S., Kraytsberg, A., & Ein-Eli, Y. *Journal of Solid State Electrochemistry*, 26, 180–1838 (2022). https://doi.org/10.1007/s10008-022-05206-x

[3] Waetzig, K., et al. *Journal of Alloys and Compounds*, 818, 153237 (2020). https://doi.org/10.1016/j.jallcom.2019.153237

Ayazhan Bekmakhanova is a Master's student at L.N. Gumilyov Eurasian National University, having completed her Bachelor's degree there in 2024. She conducts her research at the National Laboratory Astana, Nazarbayev University. Her research focuses on the study of thin-film electrolytes for solid-state batteries, with an emphasis on enhancing ionic conductivity.

Ayazhan Bekmakhanova, e-mail: ayazhan.bekmakhanova@nu.edu.kz tel: +7 771 451 45 05

Polyacrylic Acid-Based Gel Polymer Electrolyte Coated Ni/NiO Foam Anode for Enhanced Lithium-Ion Battery Performance

Moldir Arkharbekova [1,3], Yerzhigit Serik [1,3] , Aliya Mukanova [1,2] and Arailym Nurpeissova [1,2*]

[1] Laboratory of Energy Storage Systems, National Laboratory Astana, Astana 010000, Kazakhstan

[2] Institute of Batteries, Kabanbay Batyr Ave. 53, Astana, 010000, Kazakhstan

[3] L.N. Gumilyov Eurasian National University, Astana 010008, Kazakhstan

* arailym.nurpeissova@nu.edu.kz

Lithium-ion batteries (LIBs) are among the most widely used energy storage technologies, powering portable electronics, electric vehicles, and renewable energy systems due to their high energy density, long cycle life, and reliable performance. However, their further development is often hindered by challenges such as structural degradation of electrode materials, limited ion transport in conventional two-dimensional architectures, and unstable electrode–electrolyte interfaces, all of which contribute to capacity fading and reduced cycling stability [1].

Lithium-ion batteries with traditional flat, two-dimensional architectures face inherent limitations in achieving high energy output per unit area and in utilizing internal volume efficiently. The planar configuration of these electrodes restricts the loading of active material and extends the pathways for both lithium-ion and electron transport. Consequently, such structural constraints negatively impact electrochemical performance, leading to slower charge–discharge rates and reduced overall energy storage capacity.

A promising strategy to address the limitations of conventional battery designs is the development of three-dimensional (3D) electrode architectures. These advanced structures provide a larger surface area, enable greater loading of active materials, and reduce the diffusion paths for both ions and electrons. As a result, they facilitate faster electrochemical processes and significantly improve energy storage capability. Incorporating 3D frameworks into LIBs holds great potential for building compact, high-performance systems that meet the demands of modern, energy-intensive technologies [2].

Nickel foams are highly promising 3D electrode architectures for lithium-ion batteries due to their dual role as conductive current collectors and mechanically stable frameworks. Their porous, interconnected structure offers large surface area, uniform active material distribution, and efficient electron transport, while the open-cell design improves electrolyte infiltration and ion diffusion. With excellent chemical stability, catalytic activity, and mechanical resilience, Ni foams support high mass loading without structural failure, resulting in enhanced capacity, faster charge/discharge rates, and improved cycling stability, making them ideal candidates for advanced LIB anodes.

Ni/NiO foam is a promising anode material for lithium-ion batteries due to its high surface area, conductivity, and porous 3D framework, but its practical performance is limited by severe volume fluctuations during lithiation/delithiation and unstable electrode–electrolyte interfaces, which lead to capacity fading and poor cycling stability. To overcome these challenges, a polyacrylic acid (PAA)-based gel polymer electrolyte (GPE) coating can be employed, providing a flexible and adhesive layer that buffers mechanical stress, improves interfacial contact, and enhances electrode wettability. The gel structure of PAA accommodates liquid electrolyte, offering efficient lithium-ion conduction while simultaneously stabilizing the solid–electrolyte interphase and suppressing side reactions. As a result, the incorporation of PAA-based GPE with Ni/NiO foam electrodes significantly improves reversible capacity, rate capability, and long-term cycling performance, making this hybrid system a promising candidate for next-generation lithium-ion batteries.

In this work, a Ni/NiO foam-based anode was coated with polyacrylic acid (PAA) to address the challenges of volume expansion and unstable electrode–electrolyte interfaces. The PAA-based gel polymer electrolyte not only enhanced mechanical stability and ionic conductivity but also improved interfacial contact, resulting in higher reversible capacity, superior rate performance, and prolonged cycling stability. This strategy demonstrates the effectiveness of polymer-assisted interface engineering for advancing Ni/NiO foam electrodes in next-generation lithium-ion batteries.

Acknowledgments

This research is funded by the Science Committee of the Ministry of Science and Higher Education of the Republic of Kazakhstan (Grant No. AP19578472)

References

[1] Y. Wang, X. Zhang, K. Li, G. Zhao, and Z. Chen, “Perspectives and challenges for future lithium-ion battery control and management,” Oct. 01, 2023, *Elsevier B.V.* doi: 10.1016/j.etran.2023.100260.

[2] T. S. Arthur *et al.*, “Three-dimensional electrodes and battery architectures,” *MRS Bull*, vol. 36, no. 7, pp. 523–531, Jul. 2011, doi: 10.1557/mrs.2011.156.

Arkharbekova Moldir is a master's student and young researcher. She earned her bachelor's degree in organic chemistry at Eurasian National University, where she is currently pursuing her master's degree. She works as a research assistant on a project “Electrophoretic deposition of composite multilayer gel-polymer electrolyte for 3D lithium-ion batteries” at the National Laborotory Astana.

Presenting author: Moldir Arkharbekova; e-mail: moldir.arkharbekova@nu.edu.kz tel: +77076104229

Upcycling High-Density Polyethylene into Carbon Anode Materials for Sustainable Energy Storage Systems

Kuanysh Kurtibay[1,2], Arailym Nurpeissova[1,3]
[1]Institute of Batteries LLP, 53 Kabanbay Batyr Ave., Astana, Kazakhstan
[2]L. N. Gumilyov Eurasian National University, 2 Satbayev St., Astana, Kazakhstan
[3]National Laboratory Astana, 53 Kabanbay Batyr Ave., Astana, Kazakhstan

In the context of sustainable development and the transition toward a circular economy, the conversion of polymer waste into high–value-added materials for energy storage systems represents a significant scientific and technological challenge [1]. This study investigates the transformation of high-density polyethylene (HDPE) into carbon anode materials for lithium-ion batteries (LIBs) through a multistep process comprising sulfonation (crosslinking), preliminary carbonization at 350 °C, and final carbonization at temperatures ranging from 600 to 1300 °C.

Treatment with concentrated sulfuric acid (98%) initiates a sulfonation reaction accompanied by the substitution of hydrogen atoms with sulfonic groups (–SO_3H). Owing to its pronounced dehydrating and acidic properties, sulfuric acid promotes the formation of a dense crosslinked polymer network [2]. Crosslinking of HDPE at 170 °C for 6 h results in a mass increase of 2.7%, indicating a relatively limited degree of chemical modification, attributed to the high crystallinity of the material, which hinders deep acid diffusion. Following sulfonation, the polymer turns black while retaining its shape, but macrocracks appear on its surface.

Final carbonization in an argon atmosphere, after intermediate heating at 350 °C, improves the properties of the resulting carbon—specifically, increasing the specific surface area and porosity, and potentially facilitating heteroatom incorporation. Scanning electron microscopy revealed that with increasing carbonization temperature, the morphology evolves from dense agglomerates with limited porosity (600 °C) to highly porous nanoparticle-based structures (700–900 °C), and subsequently to more ordered, densely packed graphite-like spheres (1100–1300 °C). X-ray diffraction (XRD) patterns display broad (002) and (100) peaks characteristic of turbostratic carbon, with the interlayer spacing (d_{002}) decreasing as the temperature rises, indicating an increase in the degree of layer ordering. Raman spectroscopy further shows that the G-band shifts toward higher frequencies with increasing temperature, providing additional evidence of enhanced structural ordering.

These structural improvements lead to superior electrochemical performance of the anode materials, particularly in terms of specific capacity and cycling stability [3]. The effectiveness of the proposed method is confirmed through comprehensive physicochemical characterization and electrochemical testing, including cyclic voltammetry, galvanostatic charge–discharge cycling, and performance evaluation.

Acknowledgements
This research was supported by the targeted research program BR24992766, “Development of methods and technologies for environmentally friendly ‘green’ processing of polymer waste for energy storage”, funded by the Science Committee of the Ministry of Science and Higher Education of the Republic of Kazakhstan.

References

[1] Balu, R., Dutta, N. K., & Roy Choudhury, N. (2022). Plastic waste upcycling: A sustainable solution for waste management, product development, and the circular economy. Polymers, 14(22), 4788.
[2] Polgar, L. M., Cerpentier, R. R. J., Vermeij, G. H., Picchioni, F., & van Duin, M. (2016). Influence of the chemical structure of crosslinking agents on properties of thermally reversible networks. Pure and Applied Chemistry, 88, 1103–1116.
[3] Qin, C., Feng, T., Li, G., & Wang, K. (2025). Pre-carbonization and Mg powder-induced synergistic optimization: Enhancing the pore structure of coffee grounds-derived hard carbon to improve sodium storage performance. Journal of Power Sources, 630, 236093.

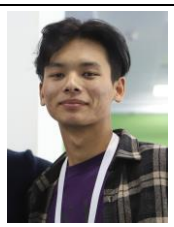

Kuanysh Kurtibay works at the Institute of Batteries and is pursuing a Master’s degree at L. N. Gumilyov Eurasian National University. His research interests include the recycling of plastic waste, the production of carbon materials for energy storage systems, and the development of sustainable technologies within the framework of the circular economy concept.

Kuanysh Kurtibay, e-mail: kurtibayqb@gmail.com, tel.: +7 707 216 7404

Sustainable carbon anode materials derived from polypropylene via eco-friendly pretreatment and carbonization

Yryszhan Tashenova[1], Arailym Nurpeissova[1,2*]
[1]Institute of Batteries LLP, 53 Kabanbay Batyr Ave., Astana, Kazakhstan
[2]National Laboratory Astana, 53 Kabanbay Batyr Ave., Astana, Kazakhstan
*arailym.nurpeissova@nu.edu.kz, iriszhan9696@gmail.com

Waste polypropylene (PP) poses significant environmental challenges due to its non-degradability and common disposal methods such as incineration or landfilling [1]. Converting PP into carbon materials for lithium-ion battery (LIB) anodes offers a sustainable alternative [2] but typically involves harsh chemical treatments to improve thermal stability and carbon yield. This study introduces a novel, eco-friendly method that utilizes a bio-derived additive—composed of chitosan, montmorillonite, and sodium phytate—to enhance the thermal resistance of PP during carbonization. The additive, incorporated at 5 wt% through ball milling, effectively suppresses PP decomposition above 400 °C and increases residual carbon retention. The resulting carbon materials were characterized by Fourier-transform infrared spectroscopy (FTIR), thermogravimetric analysis (TGA), X-ray diffraction (XRD), Raman spectroscopy, scanning electron microscopy (SEM), and transmission electron microscopy (TEM) to investigate their structural and morphological features. Electrochemical performance was evaluated using galvanostatic charge–discharge, cyclic voltammetry, and electrochemical impedance spectroscopy, demonstrating the material's potential as a viable anode in LIBs. These findings highlight a promising pathway for sustainable plastic waste valorization through green chemistry and energy storage innovation.

Keywords: Waste polypropylene, lithium-ion batteries, anode material, upcycling, plastic recycling, sustainable energy storage, carbonization.

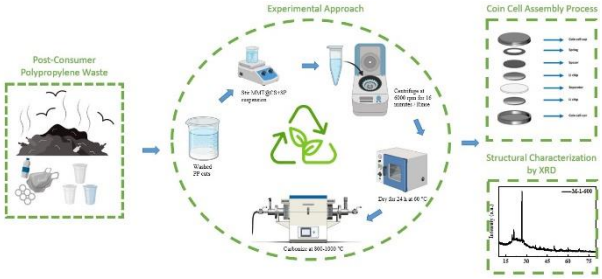

Figure 1. A schematic representation of the eco-friendly upcycling process that converts polypropylene (PP) waste into carbon anode material for lithium-ion batteries.

Acknowledgment
This study was funded by the Science Committee of the Ministry of Science and Higher Education of the Republic of Kazakhstan (grant No. BR24992766, grant No. AP23483880).

References

[1] Lee, G., Lee, M. E., Kim, S. S., Joh, H. I., & Lee, S. (2022). Efficient upcycling of polypropylene-based waste disposable masks into hard carbons for anodes in sodium ion batteries. Journal of Industrial and Engineering Chemistry, 105, 268-277.
[2] Chae, W., Song, S., Kim, M., Kim, H., Jeon, H., Lee, H., & Earmme, T. (2025). Transformation of waste polypropylene disposable masks into advanced anode materials for high-performance Lithium-ion batteries. Journal of Industrial and Engineering Chemistry, 146, 349-356.

Presenting author: Yryszhan Tashenova; e-mail: iriszhan9696@gmail.com tel:+77058418829

Study of LATP ceramics for subsequent fabrication of thin film electrolytes

Ayazhan Bekmakhanova[1, 2], Zhansaya Bakhytzhanova[1, 2], Mukagali Yegamkulov[1, 4], Zhumabay Bakenov[1, 3, 4], Aliya Mukanova[1, 3, 4*]

[1]National Laboratory Astana, Nazarbayev University, Kabanbay Batyr Ave. 53, Astana 010000, Kazakhstan

[2]Department of Chemistry, Faculty of Nature Sciences, L.N. Gumilyov Eurasian National University, Kazhymukan str. 13, Astana 010000, Kazakhstan

[3]Department of Chemical and Materials Engineering, School of Engineering and Digital Sciences, Nazarbayev University, Kabanbay Batyr Ave. 53, Astana 010000, Kazakhstan

[4]Institute of Batteries LLC, Kabanbay Batyr Ave. 53, Astana 010000, Kazakhstan

*aliya.mukanova@nu.edu.kz

In recent years, solid lithium-ion batteries (SLIBs) have attracted increased interest due to their safety, high energy efficiency, and wide range of applications, from portable electronics to electric vehicles. One of the key components of such batteries is a solid electrolyte, which provides reliable and stable conductivity of lithium ions, as well as stability at the interface with the electrodes [1].

Among the many solid electrolytes studied, special attention is paid to materials with a NASICON-like structure, in particular lithium-aluminum-titanium-phosphate (LATP) compounds. These materials have a number of valuable characteristics, including high ionic conductivity, chemical inertness, and thermal stability, which makes them promising for use in modern SLIBs [2–3].

This study investigates the influence of different lithium concentrations in LATP on its structural and electrochemical properties, synthesized using the molten flux method.

To evaluate the ionic conductivity and study the effect of composition on the transport properties of LATP, studies were carried out using the electrochemical impedance spectroscopy (EIS) method. Measurements were performed in the frequency range from 1 MHz to 1 Hz with an amplitude of 0.01 V at temperatures of 25°C and 85°C for samples with different lithium content ($Li_{1.3}$, $Li_{1.4}$, $Li_{1.5}$).

X-ray diffraction (XRD) analysis confirmed the formation of the main phase LATP in all the studied samples. However, with increasing lithium content, the formation of secondary phases ($Li_4P_2O_7$, TiP_2O_7, $AlPO_4$), was observed, which can potentially reduce the ionic conductivity of the material. These structural changes are shown in **Figure 1.**

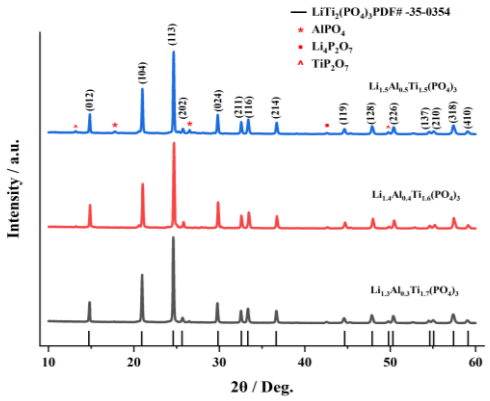

Figure 1. XRD patterns of LATP

Extensive characterization of the materials and corresponding electrochemical performance will be presented and discussed at the conference.

In a broader sense, precise selection of the composition of ceramic electrolytes is important to ensure stable ionic conductivity and can be further used to obtain thin-film electrolyte for microbatteries.

Acknowledgment

This research was funded by the research project AP19680567 "Advanced nanocomposite 3D thin film electrodes for lithium-ion batteries" from the Ministry of Science and Higher Education of the Republic of Kazakhstan.

References

[1] Hou, M., et al. *Nanotechnology*, 31, 132003 (2020). https://doi.org/10.1088/1361-6528/ab5be7

[2] Kundu, S., Kraytsberg, A., & Ein-Eli, Y. *Journal of Solid State Electrochemistry*, 26, 180–1838 (2022). https://doi.org/10.1007/s10008-022-05206-x

[3] Waetzig, K., et al. *Journal of Alloys and Compounds*, 818, 153237 (2020). https://doi.org/10.1016/j.jallcom.2019.153237

Ayazhan Bekmakhanova is a Master's student at L.N. Gumilyov Eurasian National University, having completed her Bachelor's degree there in 2024. She conducts her research at the National Laboratory Astana, Nazarbayev University. Her research focuses on the study of thin-film electrolytes for solid-state batteries, with an emphasis on enhancing ionic conductivity.

Ayazhan Bekmakhanova, e-mail: ayazhan.bekmakhanova@nu.edu.kz tel: +7 771 451 45 05

Design and Development of 3D Zn/ZnO-C Architectures for Advanced Battery Electrodes

Yerzhigit Serik [1,3], Moldir Arkharbekova [1,3], Aliya Mukanova [1,2] and Arailym Nurpeissova [1,2*]

[1] Laboratory of Energy Storage Systems, National Laboratory Astana, Astana 010000, Kazakhstan

[2] Institute of Batteries, Kabanbay Batyr Ave. 53, Astana, 010000, Kazakhstan

[3] L.N. Gumilyov Eurasian National University, Astana 010008, Kazakhstan

* arailym.nurpeissova@nu.edu.kz

Lithium-ion batteries (LIBs), recognized as one of the most advanced rechargeable power sources, have garnered considerable interest over the past few decades. Today, they are the primary energy solution for portable electronic devices, including smartphones and laptops. Since their commercial debut around twenty years ago, LIBs have played a pivotal role in powering the personal digital electronics revolution. [1].

A major drawback of traditional two-dimensional (2D) LIBs is their limited areal energy density and poor space utilization, primarily due to their flat electrode design. This planar structure restricts the amount of active material that can be incorporated and extends the pathways for ion and electron transport, ultimately leading to lower electrochemical efficiency and slower charge/discharge capabilities.

To address these limitations, the advancement of three-dimensional (3D) structured electrodes has gained attention as an effective strategy. The 3D architecture provides a larger surface area, greater active material loading, and reduced diffusion distances, which collectively enhance rate capability and overall energy storage performance. Integrating 3D designs into LIB systems holds significant potential for the development of next-generation, high-performance energy storage solutions tailored for compact and high-demand applications. [2].

Metal foam-based 3D architectures present notable benefits as current collectors and structural frameworks in LIB electrodes. Their porous, interconnected networks offer a high surface area that promotes uniform active material distribution and efficient electron transport. The open-cell design enables effective electrolyte infiltration, minimizing ion diffusion resistance and enhancing electrochemical kinetics. Metals like zinc and nickel, commonly used in such foams, provide excellent mechanical strength and electrical conductivity, supporting high active material loading without compromising structural stability. Altogether, these features contribute to enhanced areal capacity, improved rate performance, and greater cycling stability in advanced battery systems.

To mitigate the volume expansion typically seen in metal oxide-based electrodes during repeated lithiation and delithiation, a promising approach involves polymer coating followed by carbonization. Applying a polymer layer such as polyethylene oxide (PEO) creates a conformal coating that serves as a mechanical buffer, helping to absorb stress and prevent particle fracture. When this polymer is carbonized under an inert atmosphere, it transforms into a conductive carbon shell that enhances electrical conductivity and reinforces the structural stability of the electrode. This carbon layer not only maintains the integrity of the active material throughout cycling but also boosts electrochemical performance by accelerating charge transfer and reducing capacity degradation.

The primary objective of this study was to enhance the electrochemical performance of pure Zn/ZnO foam through the carbonization of a polymer coating. SEM-EDS analysis confirmed that the carbon formed a uniform layer on the ZnO surface. In addition, electrochemical tests demonstrated that the specific capacity of the polymer-coated Zn/ZnO foam remained around 260 mAh/g after 100 cycles, compared to approximately 100 mAh/g for the uncoated foam. The carbon layer contributed to performance improvement by increasing electronic conductivity and shielding the ZnO surface from mechanical degradation throughout the cycling process.

Acknowledgments

This research is funded by the Science Committee of the Ministry of Science and Higher Education of the Republic of Kazakhstan (Grant No. AP19578472)

References

1. Yoshio M., Brodd R. J., Kozawa A. Lithium-ion batteries. – New York : Springer, 2009. – T. 1. – C. 2-3.
2. Zhang T., Ran F. Design strategies of 3D carbon-based electrodes for charge/ion transport in lithium ion battery and sodium ion battery //Advanced Functional Materials. – 2021. – T. 31. – №. 17. – C. 2010041.

Yerzhigit Serik is a master's student and emerging researcher. He completed his bachelor's degree in materials science at Eurasian National University and is currently continuing his master's studies there. He is involved as a research assistant in the project “Electrophoretic Deposition of Composite Multilayer Gel-Polymer Electrolyte for 3D Lithium-Ion Batteries” at the National Laboratory Astana.

Presenting author: Yerzhigit Serik; e-mail: yerzhigit.serik@nu.edu.kz tel: +77751631752

Effect of Metal–Organic Framework (MOF) Additives on LMFP Cathode Performance in Lithium-Ion Batteries

İlayda Kunan[1], Umut Savacı[1]

[1]Eskişehir Technical University, Department of Materials Science and Engineering, Eskişehir, Türkiye

Lithium-ion batteries have become an indispensable component of modern energy storage systems, but cathode materials often limit their performance, especially in terms of energy density and cycle stability. $LiFe_{0.3}Mn_{0.7}PO_4$ (LMFP) is a promising olivine-type phosphate cathode with increased voltage (4.1 V), thermal stability, and cost-effective synthesis compared to $LiFePO_4$. However, its intrinsically low electrical conductivity and lithium-ion diffusion coefficients pose serious limitations for high-current applications. In the literature, various methods such as carbon coating and doping were applied to improve the performance of LMFP cathodes. In recent years, the incorporation of metal-organic framework (MOF) particles into cathode materials has attracted considerable research interest due to their potential to enhance electrochemical performance due to their Li-ion conducting nano porous structure. In the literature, it was shown that the performance of $LiFePO_4$ was successfully improved by the incorporation of MOF particles [1].

In this study, we introduce Zeolitic Imidazolate (ZIF-8) MOF nano particles with varying concentrations as a surface addition to LMFP to improve charge transport through the electrode interface. ZIF-8 was synthesized as a surface dopant on LMFP and tested for the effect of doping concentrations on electrochemical performance at different weight ratios (1%, 3%, 5%, 7%, 10%). The cathode slurries were prepared in 8:1:1 LMFP: carbon black (C45): PVDF binder (N-methyl-2pyrrolidone), then coated with aluminum foil, and dried. The electrodes were assembled into a coin cell with a lithium metal as a counter electrode, and a Celgard separator with EC:DMC electrolyte. The cells have been fully tested in electrochemical tests, including electrochemical impedance spectroscopy (EIS), rate capability, and cycle stability of 100 cycles in conditions of C/10 and 1C. Electrochemical analyses showed that the addition of MOF particles to the LMFP cathode reduces the surface resistance depending on its ratio. EIS results showed that 5% of ZIF-8 doping yielded the lowest surface resistance in **Fig. 1 (a)**, which confirmed effective surface changes and improved charge transfer. Rate discharge capacity tests showed that small amounts of additives successfully improved the discharge capacity while high MOF concentration reduces the discharge capacity dramatically as shown in **Fig. 1(b)**.

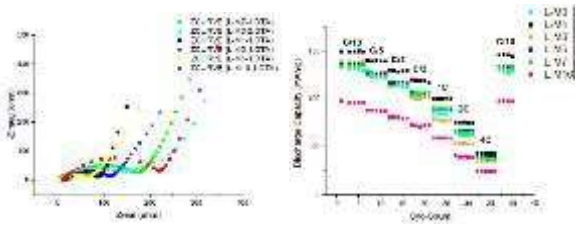

(a) **(b)**

Figure 1. (a) Nyquist plots and **(b)** rate discharge capacity profiles at C-rates of C/10 to 4C of the undoped LMFP cathode and ZIF-8 doped cathodes.

Additionally, the 1% doped sample showed superior cycle stability over 100 cycles, surpassing both the undoped electrodes and the strongest doped electrodes. On the other hand, 10% doping caused significant degradation, probably due to excessive MOF coverage, which blocks the pathway of lithium ions and obscures conductive carbon additives. Surface characteristics by scanning electron microscopy (SEM) confirmed the coatings of MOF particles at surface LMFP particles as well as agglomerations at high MOF ratios. The X-ray diffraction (XRD) patterns showed the presence of ZIF-8 particles.

In this presentation, the effects of ZIF-8 additives on the microstructure and electrochemical performance of LMFP cathodes will be discussed, focusing particularly on how surface saturation and pore blocking at high MOF concentrations can counteract the gains in conductivity.

Acknowledgments

The authors would like to thank Prof. Dr. Ünal Şen for providing ZIF-8 MOF particles.

References

[1] P. Mathur, J-Y. Shih, Y-JJ . Li , T-F. Hung, B. Thirumalraj, S.K. Ramaraj, R. Jose, C. Karuppiah, C-C. Yang, Batteries. 2023; 9(3):182.

A researcher in Materials Science and Engineering from Eskişehir Technical University. She has successfully completed her Bachelor's thesis on **MOF-modified phosphate cathodes** for lithium-ion batteries under the supervision of Dr. Umut Savacı. She is currently advancing this research into a peer-reviewed scientific publication. Her academic focus is centered on electrode materials and surface engineering for advanced energy storage systems.

Electrochemical Characterization of Cobalt Hydroxide Based Materials

Caner KORKMAZ [1], Berk ÇOBAN [1], Ayşe HACINECİPOĞLU [1] and Metin GENÇTEN [1]
[1]Yıldız Technical University, Metallurgical and Materials Engineering Department, 34220,İstanbul,Turkey

The increasing environmental damage caused by fossil fuel consumption has prompted significant research into alternative and more environmentally friendly energy storage systems. Among these, supercapacitors have attracted considerable attention due to their high power density and specific capacitance. The choice of electrode material plays a critical role in determining the electrochemical performance of supercapacitors [1]. Commonly used electrode materials include carbon-based materials, conductive polymers, and various metal oxides. Among the metal oxides, ruthenium oxide exhibits superior electrochemical properties; however, its high cost and toxicity associated with production limit its widespread application [2]. In this regard, cobalt-based materials, particularly cobalt oxide and cobalt hydroxide, emerge as promising alternatives due to their specific capacitance values that are comparable to those of ruthenium oxide.

In this study, to address the aforementioned limitation, cobalt oxide and cobalt hydroxide materials with a nanoflower-like morphology were synthesized via an electrodeposition method using cobalt nitrate and potassium chloride as precursor components. The electrodeposition process, monitored using cyclic voltammetry, is illustrated in Figure 1.

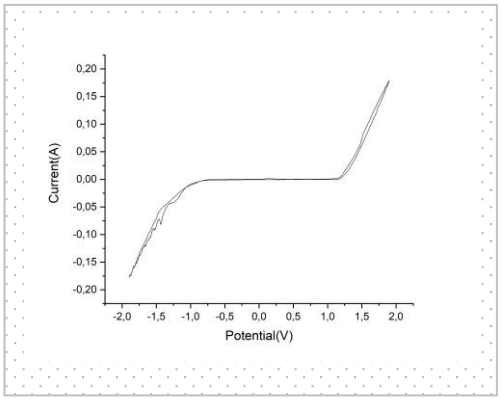

Figure 1: Cyclic voltammogram of Pt electrode in the cobalt nitrate solution in the potential range of -1.8 V to 1.6 V vs. Ag/AgCl (in 3 M KCl)

Comprehensive characterization was performed through XRD, SEM, XPS, and BET analyses, all of which confirmed the desirable morphological and structural features of the synthesized materials. Figure 2 shows the SEM picture of synthesized cobalt hydroxide. Nonetheless, a major drawback of cobalt-based materials is that their morphological characteristics—illustrated in Figure 2—typically require complex synthesis methods to be effectively controlled [3]. Additionally, electrochemical performance was evaluated using cyclic voltammetry (CV), electrochemical impedance spectroscopy (EIS), and galvanostatic charge-discharge (GCD) tests, yielding promising results. Due to their high capacity and specific capacitance over extended cycling, cobalt oxide materials with a nanoflower-like structure are considered strong candidates for next-generation supercapacitor electrode materials.

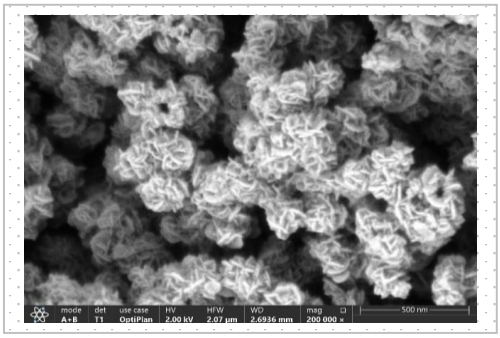

Figure 2: FESEM Analysis of Cobalt Hydroxide at 200,000× Magnification

Acknowledgment
M. Gençten thanks to the Outstanding Young Scientist Award (GEBİP) program of the Turkish Academy of Sciences (TÜBA).

References

[1] O. Aydın, K. B.Dönmez, M. Gencten, Birol, B. *J Mater Sci Mater Electron*, *36*(7) (2025) 428
[2] B. O. Park, C. D. Lokhande, H. S. Park, K. D. Jung, O. S. Joo J. Power Sources *134*(1) (2004) 1677-1682
[3] S. Yasa, B. Birol, K. B. Donmez, M. Gencten J. Energy Storage *81* (2024) 110291

I am Caner Korkmaz, a research assistant in the Department of Metallurgical and Materials Engineering at Yıldız Technical University. I hold a B.Sc. degree in Metallurgical and Materials Engineering from Middle East Technical University (METU), graduated in 2022. My research focuses on energy storage devices, particularly supercapacitor electrode materials. I am committed to advancing my expertise and contributing to developments in this field.
Presentating author: Caner KORKMAZ, e-mail:canerkorkmaz150@gmail.com tel: +90 552 495 45 61

Exploring TiV-Based Alloys as Potential Anode Materials for High-Capacity Ni-MH Batteries

Hakan Yüce , Berke Pişkin, Fatih Pişkin and Gülhan Çakmak
Energy Materials Laboratory, Dept. of Metallurgical and Materials Engineering,
Muğla Sıtkı Koçman University
*Corresponding author e-mail: gulhancakmak@mu.edu.tr

The growing demand for efficient and sustainable energy storage systems has increased interest in advanced electrode materials for rechargeable batteries. Nickel-metal hydride (Ni-MH) batteries remain attractive due to their favorable energy density, long cycle life, and lower environmental impact compared to other chemistries [1].Recently, TiV-based multicomponent alloys have drawn attention as potential anode materials for Ni-MH batteries. These alloys tend to form body-centered cubic (BCC) structures, which provide abundant interstitial sites and efficient hydrogen diffusion pathways, enhancing storage capacity and kinetics. In addition, alloying elements such as Ti, V, Zr, and Nb improve mechanical stability and corrosion resistance, both of which are critical for long-term performance..

This study focuses on the synthesis of TiV-based multicomponent alloys via arc melting and the investigation of their structural, morphological, and electrochemical properties, with particular emphasis on BCC phase stabilization and hydrogen storage behavior. Specifically, Ti-V-La-Ni-x (x = Fe, Zr, Mn) alloys are developed, where each alloying element is introduced to optimize mechanical stability, electrochemical capacity, and reaction kinetics for improved Ni-MH battery performance..

Figure 1. Arc Melter System

High-purity metal powders will be pelleted in stoichiometric ratios determined beforehand. The pellet will be melted multiple times using a turbomolecular vacuum arc melting device until a homogeneous alloy is obtained. The resulting alloy will then be ground to 45 microns using a ball mill. After pulverization, crystal structure analysis will be conducted with X-ray diffraction (XRD). The microstructure will be examined using a field emission scanning electron microscope (FE-SEM) with an acceleration voltage of 15 kV.

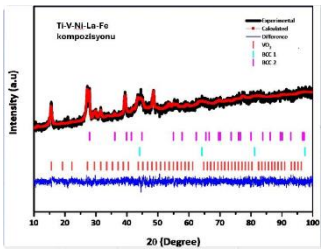

Figure 1. T-V-Ni-La-Fe XRD

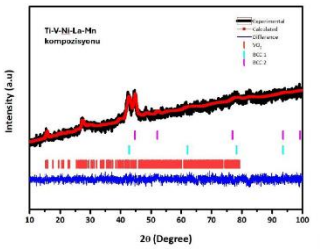

Figure 3. T-V-Ni-La-Mn XRD

Negative electrodes for electrochemical testing will be prepared by mixing 0.25 g of the alloy powder with 0.75 g of high-purity nickel powder (99.999%). The electrolyte solution will be 6 M KOH, while NiOOH/$Ni(OH)_2$ and Hg/HgO will be used as the positive and reference electrodes, respectively. Electrochemical properties will be measured using a Bio-Logic SP-300 electrochemical workstation. Experimental studies on TiV-based multicomponent alloys are still ongoing, with the primary objective of synthesizing alloys exhibiting a BCC crystal structure through arc melting. The results revealed the formation of a dual-phase BCC structure. The formation of such a structure is considered an important finding, since the presence of even a single BCC phase is regarded as sufficient for achieving favorable hydrogen storage characteristics.

Following synthesis, comprehensive characterizations will be conducted, including XRD for phase analysis and FE-SEM for microstructural examination, while electrochemical tests will be performed to evaluate hydrogen storage behavior and assess their potential as anode materials in Ni-MH batteries. The main goal of this study is to obtain high discharge capacity and stable electrochemical performance. The findings are expected to contribute to the design of durable, high-performance electrode materials for future energy storage applications.

Acknowledgment

This work was supported by TUBITAK (The Scientific and Technological Research Council of Turkey) with project Number 121N774, which the authors gratefully acknowledge.

Hakan Yüce is currently a Master's student in Metallurgical and Materials Engineering at Muğla Sıtkı Koçman University. He is working at the Energy Materials Laboratory, and his research areas include Energy Storage Materials, Ni-MH Batteries, High Entropy Alloys, and Solid Oxide Fuel Cell cathode materials.

Presenting author: Hakan Yüce, e-mail: hakanyuce2@posta.mu.edu.tr tel: +90 531 526 4175

Dual Bi/Cu Pre-Intercalation Strategy for High-Performance δ-MnO_2 Cathodes in Zinc-Ion Batteries

A. Engin Serin[1,2*] and Tayfur OZTURK1,[2]

[1]Department of Matallurgical and Materials Engineering METU, Ankara
[2]ENDAM, Center for Energy Materials and Storage Devices , METU, Ankara

Abstract: The MnO_2 polymorph of birnessite considered as a promising and attractive cathode material for Zn-ion batteries. However, its rate performance and capacity contribution hindered by slow reaction kinetics, low conductivity and poor structural stability. Herein, multi-ion doping strategy conducted by facile co-precipitation route which can eliminate addressed issues. Phase analysis showed that produced powders are δ-MnO_2. Dopant elements are incorporated by using $Cu(SO)_4.H_2O$, Na_2SO_4 and $Bi_5O(OH)_9(NO_3)_4$ as a dopant precusors. The chemically synthesized powders as produced are used as active cathode material displayed a substantial capacity of 349 mAh/g at 0.1 C-rate which can be a competitive cathode material for developing high performance rechargeable Zn-MnO_2 batteries.

1.Introduction

Zn-MnO_2 batteries have attracted considerable attention due to their low cost as both Zn and Mn are quite abundant in earth crust. Moreover, it has high working potential and in terms of energy density with zinc delivering 820 mAh/g and MnO_2 with two electron exchange delivering 616 mAh/g is quite exceptional [1]. The need for low-cost batteries in grid scale energy storage motivated interest in these batteries and means are sought to improve their rechargeability [2]. The primary alkaline Zn-MnO_2 batteries have been widely used to power most handheld devices. However, the advancement of rechargeable aqueous Zn-MnO_2 batteries were hindered by their inferior cycling properties in alkaline electrolyte owing to the formation of irreversible by-products at neither the cathode ($Mn(OH)_2$, etc.) nor anode (ZnO, $Zn(OH)_2$, etc.)[3]. The first report of mildly acidic Zn/MnO_2 battery were made by Yamamoto and Shoji in 1986 with some success [4]. Pan et al. [2016] compared the cyclability of aqueous alkaline (KOH) and mildly acidic ($ZnSO_4$+$MnSO_4$) electrolyte and claimed that mildly acidic electrolyte showed better performance, lower polarization and stable behavior compared to alkaline counterparts. They also found that Zn anode in alkaline media permanently transformed to ZnO after few cycles, meanwhile, Zn in mildly acidic media survived over 400 hours without oxidation [5]. Therefore, the focus on Zn/MnO_2 batteries has shifted to mildly acidic or neutral aqueous electrolyte. Another efforts to improve rechargeability, mainly focus on finding the suitable polymorph of cathode active material for Zn-ion batteries. There are many reports about H^+/Zn^{+2} ion insertion/extraction kinetics for different types of MnO_2 polymorphs such as α-MnO_2, β-MnO_2, γ-MnO_2, δ-MnO_2 and etc. [6]. Among them, δ-MnO_2 has a layered structure which is considered to be more suitable for ion ingress/egress rather than the tunnel allotropes [7]. However, almost all types of MnO_2 polymorphs undergo structural collapse and dissolution of Mn ions. Moreover, low conductivity and high charge transfer resistance of MnO_2, restricting the rate capability and rechargeability [8-9]. Ion doping strategy is an effective way to hinder the structural breakdown of MnO_2 and enhancing the charge transfer kinetics of the cathode [10]. Thus, ion pre-intercalation mostly conducted by simple hydrothermal method in the literature. For example, Xia et. al. modified the cathode by molybdenum doping, the capacity has reached 652 mAh/g at 0.2 A/g, higher than theoretical capacity of MnO_2 [11]. In another study, Sun et. al. doped the δ-MnO_2 with Bi-Cu dual ion pre-intercalation strategy by hydrothermal method, delivering a capacity of 412.3 mAh/g at 0.1 A/g [12]. Dual ion doping strategy enhanced the structural stability, increased the intrinsic conductivity of the host material, also decreased the Zn^{+2}

Engin Serin graduated from the Department of Materials Science Engineering in Gebze Technical University in 2022. He is now a graduate student in the same department and materials engineer at Innovascope Materials Technologies. His research interest covers the development of positive and negative electrodes in Zn/MnO_2 rechargable batteries.

*Corresponding author: A. Engin Serin, e-mail: engin.serin@metu.edu.tr tel: +90 531 741 87 74

ion diffusion barrier. However, hydrothermal method requires high temperature and pressure environment, there is an urgent need for alternative production routes for low cost production alternatives. Yang et. al. synthesized Co-doped δ-MnO_2 by co-precipitation route at room temperature, the total specific capacity has reached 408.9 mAh/g at a current denstiy of 0.1 A/g [13]. It is clear from the above that the potential of doped-MnO_2 as cathode material can be improved quite substantially by systematic alteration of its chemistry. We therefore undertaken a program of study where MnO_2 was modified by multi-ion doping operations, namely bismuth, copper and a sodium as a source via co-precipitation synthesis.

2. Experimental

The spherical δ-MnO_2 nanosheet structures were obtained through a simple chemical co-precipitation method described by Zhang et. al. with small modifications [14]. In a three-necked flask, $KMnO_4$ (2.016 g), $MnSO_4 \cdot H_2O$ (0.654 g), and deionized water (100 mL) were added and continuously and mechanically stirred for 1 h. Then, 2.5 mL of concentrated sulfuric acid was gradually added, and the mixture was stirred for another hour. The mixture was heated to 80 °C in a water bath and vigorously stirred for an additional 1 h until the reaction was completed. The resulting solution was filtered and washed with deionized water until the pH of the filtrate reached 7, followed by drying the filter cake in an oven at 80 °C for 24 h. For doped particles, same procedure was conducted with addition of precursors of $Cu(SO)_4.H_2O$ and $Bi_5O(OH)_9(NO_3)_4$. In addition, Na ions are intercalated into the electrolyte via Na_2SO_4 as a source. Having doped the active materials, the cathode slurry was prepared by mixing the active ingredients with ketjen black and binder of selected proportions in DI water-ethanol (60:40) solution. First, the binder (dispersion PTFE) was dissolved in the solution for 15 mins and then ketjen black was added and mixed for 30 mins. Finally, active material was added and mixed for 60 minutes. All mixing were carried out using magnetic stirrer. Ni foam was used as the current collector. The slurry was coated onto Ni foams by dipping it into the solution. Then nickel foam was dried overnight in an oven at 60°C. Before and after coating, the foam was weighed (Sartorius CPA225D-0.01 mg sensitivity) from which the quantity of the cathode was determined. Ni foam loaded with cathode material was then pressed under 20 MPa to increase the compaction of the whole assembly.

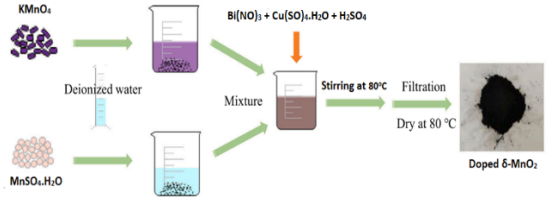

Fig. 1. Schematic illustration of co-precipitation technique to obtain doped δ-MnO_2.

2.3. Electrochemical tests

Cell used for electrochemical characterization was of Swagelok type(shown in Fig. 2). Conventionally prepared MnO_2 based cathodes were loaded on Ni foams of 12.7 mm in diameter. Anode was Zn foil 300 µm thick (99.8 % pure). Separator was Freudenberg FS 2226. Electrolyte was 2M $ZnSO_4$+0.1M $MnSO_4$ and desired amount of Na_2SO_4 in DI water. Current collectors in the Swagelok cell were 12.9 mm diameter stainless steel rods. The Cell had a spring between the anode and the stainless-steel current collector which presses the cell assembly against the current collector on the cathode side. Spring was made of 1 mm stainless steel wire wound to a diameter of 12.4 mm with the length of 10.5 mm. Electrochemical measurements were made with BioLogic MPG2 multichannel battery testing system. Galvanostatic charge/discharge tests were conducted in the cut-off range of 0.8-1.9 V.

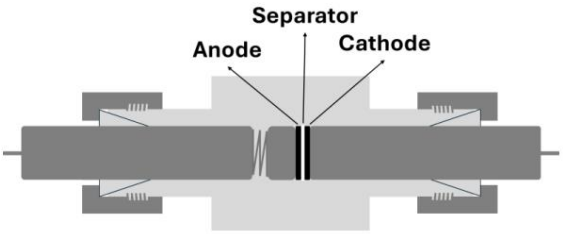

Fig. 3. Schematic representation of Swagelok cell for two electrode configuration.

3- Results and Discussion

3.1. Morphological and structural properties of synthesized powders

Particle morphology identified by scanning electron microscopy. On Figure 3(a), there are some agglomerations at low magnifications which are primarly composed of individual nanostructures. δ-MnO_2 particles formed relatively uniform sphere-like nanoflowers with an approximate diameter of 0.5 µm, composed primarily of nanosheets, shown in Figure 3(b). It is considered to be the spherical individual

nanostructures create electrochemically more active surface sites for rapid ion transport of H^+/Zn^{+2} diffusions.

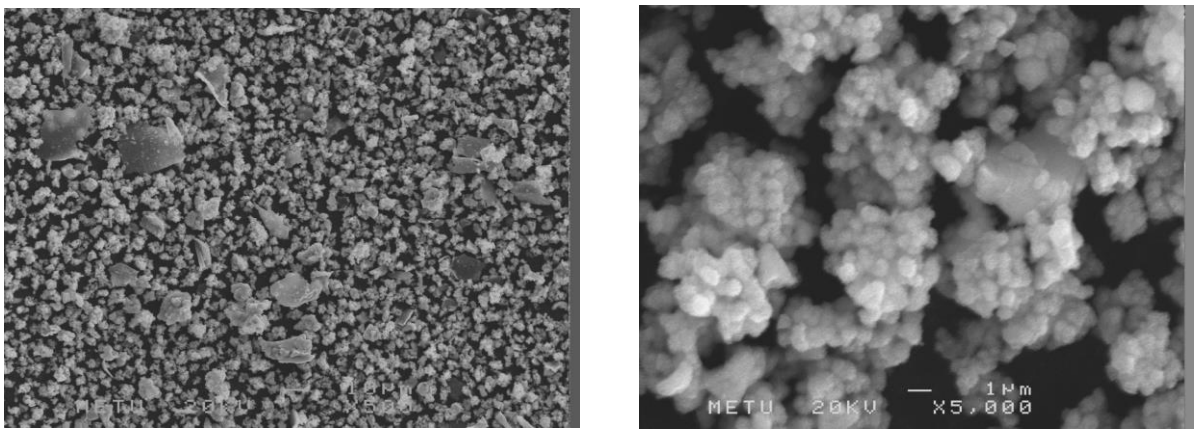

Figure 3. SEM images of synthesized δ-MnO_2 particles under (a) x500 and (b) x5000 magnifications

Table 1.

EDX results of doped MnO_2.

Element	Weight Conc. %	Atomic Conc. %
Mn	85.04	89.98
Cu	4.54	4.15
Bi	7.96	2.22
K	2.46	3.65

Energy dispersive X-ray analysis (EDX) carried out for elemental analysis. The EDX data provided in Table 1 indicates that corresponding stoichiometry is $K_{0.03}Bi_{0.02}Cu_{0.04}Mn_{0.90}O_x$. The layered-$MnO_2$ can accommodate K^+ ions inside the interlayers due to $KMnO_4$ is used as active material precursor. The results showed that Bi and Cu ions successfully doped with an amount of approximately 2.22 at. % and 4.15 at. %, respectively.

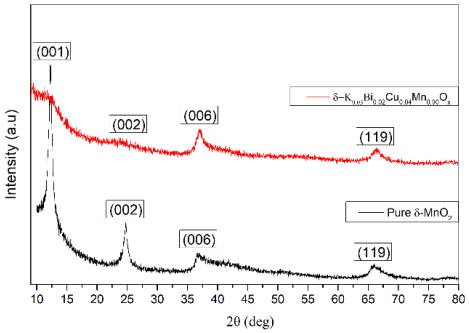

Figure 4. XRD patterns of co-precipitated bare and doped δ-MnO_2 nanoflowers.

On Figure 4, the diffraction peaks of doped and bare δ -MnO_2 peaks observed at 2θ = 12.3°, 24.9°, 37.1°, and 66,1° corresponded to crystal planes of (001), (002), (006), and (119), respectively, which are associated with two-dimensional layered birnessite. The weak intensity of (001) and (002) planes indicated a low degree of crystallinity for doped δ-MnO_2 which may facilitate the diffusion of ions [15].

3.2. Electrochemical characterizations

The cyclic voltammetry analysis of doped- δ-MnO_2 at different scan rates shown in Fig. 5(a). There were two cathodic peaks around at 1.31V and 1.18V, which corresponded to H^+/Zn^{+2} insertions and two anodic peaks around 1.6V and 1.69V at 0.1 mVs^{-1}. However, the two well defined voltage peaks(in both anodic/cathodic), although their prominence increases with increasing scan rate, have become broader and merged into one in each cycle. The total current density intensified and the peak voltages of both cathodic/anodic shifted.

Typically, the peak current (i) and scanning rate (υ) obey the following equation [16]: $i = a\upsilon^b$, where a and b are two constants. The b value determines whether the electrochemical process is ion diffusion or

capacitive controlled. The b value changes between 0.5 and 1.0. The electrochemical process is ion diffusion-controlled when the b value is close to 0.5, while capacitive behavior is highly dominant when the b value approaches 1.0. The b values of doped δ-MnO_2 cathode are 0.6868 (peak 1), 0.5193 (peak 2) and 0.4224 (peak 3), respectively.

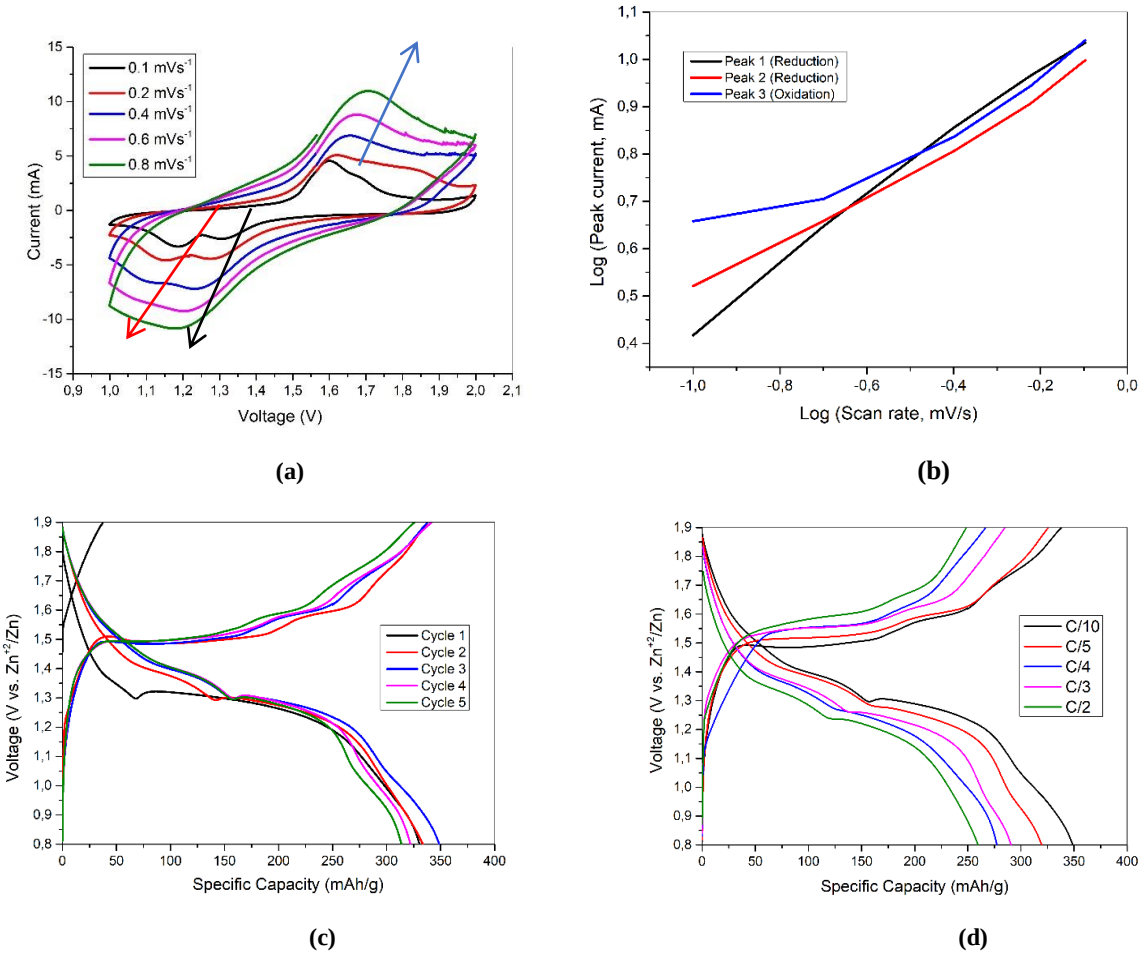

Figure 5. (a) Cyclic voltammogram of Bi/Cu co-doped δ-MnO_2 at a scan rates of (0.1, 0.2, 0.4, 0.6, 0.8) mVs^{-1}. (b) Plots of log (i) – log (υ) at the current peaks. (c) Galvanostatic charge-discharge profiles at 0.1 C-rate in initial five cycles. (d) Charge-discharge profiles of doped δ-MnO_2 under cycling rates from 0.1 to 0.5 C-rate.

Plot of log(peak current) versus log(scan rate) shown in Fig. 5(b). These values of b close to 0.5 indicate that electrochemical reaction is dominantly ion diffusion controlled.

Fig. 5(c) displays the galvanostatic electrochemical performance of doped δ-MnO_2 at 0.1 C-rate in the initial five cycles. The total capacity increases from 330.6 mAh/g to 336.6 mAh/g and 349 mAh/g in the first three cycle, then decreased to 322 mAh/g and 313 mAh/g, respectively. These results indicate that Bi-Cu co-intercalation strategy improve the charge storage behaviour of the cathode, achieving higher than the first electron capacity of (308 mAh/g for first electron exchange) MnO_2. The discharge curve consists of two distinct discharge plateus: an inclined plateu between 1.45-1.32 V caused by the H^+ insertion, almost flat plateu in the vicinity of 1.30 V attributed to the Zn^{+2} ion insertion, commonly reported in the literature [17].

The galvanostatic charge-discharge performance of doped δ-MnO_2 cathodes were carried out at varied cycling rates from 0.1 C-rate to 0.5 C-rate and shown in Fig.5 (d). As the discharge rate increases, the Zn^{+2} ion storage capability decreases, which may be due to the H^+ ions have high diffusion rates with smaller radius rather than Zn^{+2} ions, indicating the H^+ storage is more prominent at high discharge rates. The maximum

discharge capacities are as follows: 349 mAh/g at a 0.1 C-rate, 339 mAh/g at a 0.2 C-rate, 280 mAh/g at a 0.3 C-rate, 294 mAh/g at a 0.4 C-rate, and 259 mAh/g at a 0.5 C-rate, respectively.

4. Conclusion

In summary, the Bi-Cu co-doped δ-MnO_2 as the cathode was produced via facile one step co-precipitation route. It was found that the capacity significantly improved compared to the conventional cathodes, higher than the one electron exchange of Mn^{+4}/Mn^{+3} redox in MnO_2. Production of sub-micron size with homogenous spherical particle morphology provides shorter ion diffusion lenght and more active surface area between electrode and electrolyte that exhibiting better electrochemical kinetics. Besides, it is clear to note that pre-intercalation of Bi/Cu ions among the interplanar spacing, which could manipulate the interlayers of the host material, enhancing the structural stability and possibly preventing the spinel lattice transformation. The cathode exhibits a superior specific capacity of 349 mAh/g at 0.1 C-rate, surpassing the performance of alkaline counterparts reported in the literature.

Lastly, it may be worth pointing out that the intrinsic conductivity is probably increased, however detailed characterization of the pure and Bi/Cu modified cathode by comparative impedance spectroscopy is required for further investigation. Moreover, rate performance tests are required for cycling stability of the cathode. Therefore, our research opens a new path for low-cost production techniques to solve unsatisfied energy density and reaction kinetics of manganese based cathodes in aqueous rechargeable zinc-ion batteries.

References

[1]K. Kordesch, J. Gsellmann, M. Peri, K. Tomantschger, R. Chemelli, The rechargeability of manganese dioxide in alkaline electrolyte, Electrochim Acta 26 (1981) 1495–1504.

[2] M.B. Lim, T.N. Lambert, B.R. Chalamala, Rechargeable alkaline zinc–manganese oxide batteries for grid storage: Mechanisms, challenges and developments, Materials Science and Engineering R: Reports 143 (2021) 100593.

[3] Y. Wang et. al.Towards high-areal-capacity aqueous zinc–manganese batteries: promoting MnO2 dissolution by redox mediators.

[4] Shoji, T.; Hishinuma, M.; Yamamoto, T. Zinc-Manganese Dioxide Galvanic Cell Using Zinc Sulphate as Electrolyte. Rechargeability of the Cell. J. Appl. Electrochem. 1988, 18, 521–526.

[5] H. Pan, Y. Shao, P. Yan, Y. Cheng, K.S. Han, Z. Nie, C. Wang, J. Yang, X. Li, P. Bhattacharya, K.T. Mueller, J. Liu, Reversible aqueous zinc/manganese oxide energy storage from conversion reactions, Nat Energy 1 (2016) 1–7.

[6] X.Y. Gao, H.Z. Zhang, X.Q. Liu, X.H. Lu, Flexible Zn-ion batteries based on manganese oxides: progress and prospect, Carbon Energy 2 (2020) 387–407.

[7] N. Qiu, H. Chen, Z. Yang, S. Sun, Y. Wang, Electrochim. Acta 272 (2018) 154–160.

[8] Z.C. Zhang, W. Li, Y. Shen, R.X. Wang, H.M. Li, M. Zhou, W. Wang, K.L. Wang,K. Jiang, Issues and opportunities of manganese-based materials for enhanced Zn-ion storage performances, J. Energy Storage 45(2022) 103729.

[9] Q.H. Zhao, A.Y. Song, S.X. Ding, R.Z. Qin, Y.H. Cui, S.N. Li, F. Pan, Preintercalation strategy in manganese oxides for electrochemical energy storage: review and prospects, Adv. Mater. 32 (2020) 2002450.

[10] P. Hu, T. Zhu, X. Wang, X. Wei, M. Yan, J. Li, W. Luo, W. Yang, W. Zhang, L. Zhou, Z. Zhou and L. Mai, Nano Lett., (2018), 18, 1758–1763.

[11] X. Xia, Y. Zhao, Y. Zhao, M. Xu, W. Liu, X. Sun, Mo doping provokes two electron reaction in MnO2 with ultrahigh capacity for aqueous zinc ion batteries, Nano Res 16 (2023) 2511–2518.

[12] Y. Sun, S. Zhuang, Y. Ren, S. Jiang, X. Pan, G. Sun, B. Zhu, Y. Wen, X. Li, F. Tu, J. Guo, Promoting cycle stability and rate performance of birnessite-type MnO_2 cathode via copper and bismuth dual ions pre-intercalation for aqueous zinc-ion batteries, J. of Energy Storage 74 (2023) 109589.

[13] S. Yang, F. Li, P. Fu, C. Zhen, J. Wu, Y. Feng, H. Lu, Z. Sheng, Room temperature synthesis of the Co-doped δ-MnO2 cathode for high-performance zinc-ion batteries

[14] D. Zhang, J. Dai, J. Zhang, Y. Zhang, H. Liu, Y. Xu, J. Wu, P. Li, Preparation of Spherical δ−MnO2 Nanoflowers by One-Step Coprecipitation Method as Electrode Material for Supercapacitor, ACS Omega (2024), 9, 18032−18045.

[15] L.J. Yan, L.Y. Niu, C. Shen, Z.K. Zhang, J.H. Lin, F.Y. Shen, Y.Y. Gong, C. Li, X.J. Liu, S.Q. Xu, Modulating the electronic structure and pseudocapacitance of delta-MnO2 through transitional metal M (M = Fe, Co and Ni) doping, Electrochim. Acta306 (2019) 529–540.

[16] D. Chao, W. Zhou, C. Ye, Q. Zhang, Y. Chen, L. Gu, K. Davey, S.Z. Qiao, Anelectrolytic Zn-MnO(2) battery for high-voltage and scalable energy storage, Angew Chem. Int. Ed. Engl. 58 (2019) 7823–7828.

[17] H. Zhao, L. Wang, M. Li, Transition-metal ions intercalation chemistryenabled the manganese oxides based cathode with enhanced capacity and cycle life for high-performance aqueous zinc-ion batteries, RSC Adv,. (2024)

MOF-Derived Dual-Activity Oxygen Catalysts Empowering Next-Generation Renewable-Energy Storage

Uygar Geyikçi[1], Hüseyin İnan Cihan[1] and Çiğdem Toparlı[1]

[1] Department of Metallurgical And Materials Engineering Middle East Technical University, Ankara-Turkiye

The title of Escalating CO_2 emissions from continued fossil-fuel use intensify the urgency of shifting to renewable energy. Yet the intrinsic intermittency of solar and wind power demands large-capacity storage systems to smooth supply. Rechargeable zinc-air batteries (RZABs) are promising candidates, but their performance is limited by the sluggish four-electron oxygen evolution reaction (OER) [1,2]. Efficient, durable, and cost-effective bifunctional electrocatalysts are therefore essential. Conventional catalysts such as IrO_2 and RuO_2 offer acceptable overpotentials but are scarce, expensive, and degrade within only 2–4 h of operation[3].

Metal–organic frameworks (MOFs) provide a versatile platform for catalyst design. Constructed from metal nodes and organic linkers, MOFs form crystalline, highly porous networks with exceptionally large surface areas—traits that can be tuned for electrocatalysis. In this study, we rationally engineer MOFs to maximise catalytic activity and stability in alkaline media. Solvothermal, hydrothermal, and post-synthetic modification routes are employed to incorporate a range of metal, metal-oxide, and metal-hydroxide nodes into the frameworks.

The resulting materials are characterised by X-ray diffraction (XRD) for crystal structure, scanning electron microscopy (SEM) for morphology, and X-ray photoelectron spectroscopy (XPS) for electronic and chemical states. Electrochemical performance is then assessed in 1 M KOH using a rotating-disk three-electrode configuration (glassy-carbon working electrode coated with the MOF, platinum counter electrode, and Ag/AgCl reference electrode). We evaluate OER and oxygen reduction reaction (ORR) kinetics, electrochemical impedance spectroscopy (EIS) behaviour, and long-term durability. Finally, the MOF catalysts are integrated as air cathodes in rechargeable aqueous zinc-air batteries to gauge practical battery performance.

References

[1] Erdil, T., Lokcu, E., Yildiz, I., Okuyucu, C., Kalay, Y. E.,& Toparli, C. (2022). Facile Synthesis and Origin of Enhanced Electrochemical Oxygen Evolution Reaction Performance of 2H-Hexagonal Ba2CoMnO6− δ as a New Member in Double Perovskite Oxides. ACS omega, 7(48), 44147-44155.

[2] Zhou, C., Chen, X., Liu, S., Han, Y., Meng, H., Jiang, Q., ...& Zhang, R. (2022). Superdurable bifunctional oxygen electrocatalyst for high-performance zinc–air batteries.Journal of the American Chemical Society, 144(6), 2694-2704.

[3] Ozgur, C., Erdil, T., Geyikci, U., Okuyucu, C., Lokcu, E.,Kalay, Y. E., & Toparli, C. (2023). Engineering Oxygen Vacancies in (FeCrCoMnZn) 3O4-δ High Entropy Spinel Oxides Through Altering Fabrication Atmosphere for High-Performance Rechargeable Zinc-Air Batteries. Global Challenges, 2300199.

Uygar Geyikçi is a master student at Metallurgical and Materials Engineering Department of Middle East TechnicalUniversity. He is working on the bifunctional OER/ORR electocatalysts for rechargeable zinc-air batteries underthe supervision of Assist. Prof. Cigdem Toparli.

Presentating author: Uygar GEYİKÇİ , e-mail; uygargeyikci@metu.edu.tr tel: +905398404140

Chia Seeds-Based Gel Electrolyte for Sustainable and Stable Zinc Ion Batteries

Gulsah Yaman Uzunoglu[1]

[1] Department of Chemical Engineering, Istanbul Health and Technology University (ISTUN), Istanbul 34445, Türkiye

Aqueous zinc batteries represent a promising option for energy storage and conversion technologies in the "post-lithium" era, owing to their elevated energy density, enhanced safety, and affordability. Rechargeable aqueous zinc ion batteries (RZBs) are recognized as promising alternatives to lithium-ion batteries due to their cost-effectiveness, safe-and-sustainable-by-design, and scalability. Nonetheless, their performance is hindered by inadequate cyclability, which is attributed to dendrite formation and the hydrogen evolution reaction (HER) occurring at the zinc anode [1]. Such limitations demand the formulation of advanced electrolyte solutions to boost ZIB performance, concurrently prioritizing sustainability. The electrolyte is crucial in ZIBs, as it facilitates the ionic conductivity and ion transfer of the positive and negative electrodes. Natural materials and their derivatives, sourced from renewable and sustainable resources, may offer promising strategies to reduce both HER activity and dendrite formation [2]. Natural organic compounds, including proteins, amino acids, saccharides, and organic acids, have recently been demonstrated to influence the solvation structure of the electrolyte and to improve the electrode/electrolyte interface in ZIBs. These natural materials offer non-toxicity, excellent compatibility, biodegradability, and are abundant, aligning with the demand for safe-by-design, high-performance ZIBs. Chia seeds (CS) are a type of crop rich in protein, fatty acids, and carbohydrates. When these seeds are immersed in water, they generate a clear, adhesive gel that adheres to the seed coat [3].

In this work, a sustainable gel electrolyte derived from chia seeds containing 2M $ZnSO_4$ has been developed to improve the electrochemical stability of ZIBs. This electrolyte formulation aims to reduce the presence of free water molecules and alleviate the hydrogen evolution reaction (HER) as well as the formation of zinc dendrites. The results obtained indicate that the CS-based electrolyte significantly enhances the electrochemical stability and performance of ZIBs. The formulation of the CS-based electrolyte in symmetrical Zn‖Zn cells demonstrates an impressive cycle life of 800 hours at a current density of 1.0 mA cm^{-2} (1.0 mAh cm^{-2}), which significantly exceeds the longevity of traditional aqueous electrolytes used in ZIBs. Furthermore, the CS-based electrolyte, enriched with organic moiety, achieves a specific capacity of 250 mAh g^{-1} at 1.0 A g^{-1} for the V_2O_5 cathode in a fully assembled Zn‖V_2O_5 cell.

References

[1] X. Zhang, Y. Liu, S. Wang, J. Wang, F. Cheng, Y. Tong, L. Wei, Z. Fang, J. Mao, Energy Storage Materials 2024, 70, 103471; bZ. Zhang, Z. He, N. Wang, F. Wang, C. Du, J. Ruan, Q. Li, D. Sun, F. Fang, F. Wang, Advanced Functional Materials 2023, 33, 2214648.

[2] G. Yaman Uzunoglu, R. Yuksel, Small 2025, 21, 2411478.

[3] B. Kulczyński, J. Kobus-Cisowska, M. Taczanowski, D. Kmiecik, A. Gramza-Michałowska, Nutrients 2019, 11.

Gulsah Yaman Uzunoglu received her B.S. and M.S. degrees in Chemistry from Middle East Technical University, Ankara, Türkiye, in 2000 and 2002, respectively. She received her Ph.D. degree in Chemistry from the Ohio State University in 2008. She worked as a chief senior researcher for TUBİTAK National Metrology Institute (2008-2012) and TUBITAK Marmara Research Center Energy Institute (2016-2020). She is currently a faculty member in the Department of Chemical Engineering at Istanbul Health and Technology University. Her research interests are solid-state batteries, electrochemical energy storage, functional nanomaterials and sustainable materials.

Gulsah Yaman Uzunoglu, e-mail: gulsah.uzunoglu@istun.edu.tr tel: +90-530-760-0660

Suppressing Hydrogen Evolution in Iron Anodes for Alkaline Rechargeable Batteries

Beyzanur Acar[1], A. Engin Serin[2], Ozgur Darıcıoglu[2] and Tayfur Ozturk[2,3]

[1]Department of Chemical Engineering, Ankara University, Ankara, Türkiye
[2]Department of Metallurgical and Materials Engineering, Middle East Technical University, Ankara, Türkiye
[3]Innovascope Materials Technologies Ltd. Sti, Ankara, Türkiye

Iron as anode in Fe-Air or Fe-Ni batteries are gainig considerable attention due to their safety, affordability, nontoxicity, and high energy density. Iron is cheap, highly abundant and environmentally friendly, making it an attractive alternative to other battery chemistries. Additionally, iron does not form dendrites during cycling, enhancing both the safety and long-term stability of the battery. With a high theoretical capacity of 960 $mAhg^{-1}$, iron-based batteries hold significant potential for large-scale energy storage systems, offering a sustainable and cost-effective solution.[1] However, challenges such as passivation and hydrogen evolution reaction hinder their electrochemical performance. This study aims to develop solutions to overcome these challenges.

Passivation occurs when a non-conductive iron hydroxide layer forms on the surface of the iron anode, disrupting the contact between the anode and the electrolyte. We have used carbon coating as a way of providing solution for this passivation.

Hydrogen gas evolution is a parasitic reaction that occurs during charging when iron oxide converts back to iron, negatively impacting the battery's efficiency. We have used additives such as sulfur and bismuth additives (Bi_2S_3, FeS, and Bi_2O_3) so as to control hydrogen evolution for the sake of improved effciency.

Electrochemical tests were conducted in a Swagelok cell. The anode was prepared with 80 wt% active material as iron, 10 wt% carbon black, and 10 wt% PTFE. PTFE and 4 ml of ethanol/water mixture were stirred for 10-15 minutes, followed by the addition of carbon black and iron powder for 1 hour to form a slurry.Then, the slurry was applied onto Ni foam, dried at 60 °C overnight, and pressed at 20 MPa.

Commercial $Ni(OH)_2$ electrodes used as cathodes, and 6 M KOH was used as the electrolyte with a PP cloth separator.

For carbon coating, glucose is dissolved in ethanol, and 1 g of active material is added. After mixing for 1 hour and drying overnight at 60°C, the mixture is pyrolyzed in a tube furnace under nitrogen flow.

Further improvement, many concentrations and combinations of Bi_2S_3, FeS, and Bi_2O_3 were used as additive to suppress hydrogen evolution. Preliminary results indicate that 10 wt% FeS and 5 wt% Bi_2S_3 yield the best performance.

Recent studies have shown that with carbon coating and the addition of FeS and Bi_2S_3, the iron anode exhibits high capacity and improved stability.

The effect of these sulfide additives will be evaluated through a series of experiments, where they will be added to the anode and electrolyte both separately and together to see their effects on suppressing hydrogen evolution, and the carbon coating procedure will be optimized for improved performance.

Acknowledgment

We acknowledge to the Scientific and Technological Research Council of Turkey (TÜBİTAK) 2247-C Intern Researcher Scholarship Program (STAR) in conjuction with TEYDEB 7230112.

References

[1] He et al. Materials Today Advances 11 (2021) 100156.

Beyzanur Acar graduated from the Department of Chemical Engineering at Ankara University in 2024. She is now a TÜBİTAK project researcher in the Department of Metallurgical and Materials Engineering at Middle East Technical University. Her research interests include the development of iron anodes to enhance performance in alkaline rechargeable batteries.

Presentating author: Beyzanur Acar, e-mail: beyzacar29@gmail.com tel: +905426155296

Suppressing Dendrite Formation in Zinc–Air Batteries via Bi_2O_3-Modified Zinc Powder Anodes with Bio-Derived Binders

Tuncay Erdil[1] and Cigdem Toparli[1]

[1] Middle East Technical University, Faculty of Engineering, Department of Metallurgical and Materials Engineering, Ankara, Turkey

Aqueous rechargeable zinc–air batteries (AZABs) have gained significant attention as next-generation green energy storage systems owing to their high theoretical specific capacity (~820 mAh g^{-1}), large volumetric energy density, cost-effectiveness, and environmentally benign components. These features make them particularly attractive for grid-scale storage and portable electronic applications [1]. However, the widespread adoption of AZABs remains hindered by critical limitations associated with the zinc anode, such as hydrogen evolution reactions (HER), surface passivation due to the formation of insulating ZnO layers, morphological instability during cycling, and, most importantly, dendritic zinc growth that can lead to short circuits and rapid capacity fading.

To address these challenges, considerable research has focused on replacing zinc foil with zinc powder-based anodes, which offer several advantages. The high surface area of zinc powder reduces local current density, thereby suppressing dendrite formation and decreasing overpotentials. Moreover, powder-based electrodes enable better structural tunability and more uniform zinc utilization. However, simply using zinc powder is not sufficient. Additives that can improve charge transport, inhibit passivation, and regulate zinc deposition are crucial for achieving high performance and long-term reversibility [2-4].

In this study, we developed a tunable zinc powder anode incorporating functional additives and a bio-derived binder system aimed at enhancing the rechargeability and stability of AZABs. The anode composite consists of nanosized zinc powder as the active material, ZnO to assist in uniform zinc dissolution/deposition, Bi_2O_3 for dendrite suppression and passivation resistance, and carbon black to improve the electronic conductivity. A unique feature of this work is the use of natural gum as a green, cost-effective binder, replacing synthetic polymer matrices. This approach simplifies the electrode architecture and promotes sustainable materials design.

The composite mixture was homogenized and thermally treated at 200 °C before being coated onto a steel mesh current collector. Structural characterization was performed using X-ray diffraction (XRD) and scanning electron microscopy (SEM), while surface chemistry was examined through energy-dispersive X-ray spectroscopy (EDS), X-ray photoelectron spectroscopy (XPS), and Raman spectroscopy. These analyses confirmed the homogeneity of additive distribution and the morphological stability of the anode after cycling.

Electrochemical performance was evaluated in a custom-built zinc–air battery configuration employing a 6 M KOH electrolyte and a bifunctional high-entropy perovskite oxide catalyst supported on carbon cloth as the air cathode. Compared to zinc foil-based cells, the zinc powder anode demonstrated significantly higher gravimetric power density and specific capacity. Charge-discharge profiles at both low (1 mA cm^{-2}) and high (5 mA cm^{-2}) current densities revealed enhanced cycling stability and reduced polarization. SEM images of cycled anodes showed markedly lower dendritic features in the Bi_2O_3-modified samples, supporting the effectiveness of bismuth pathways in mitigating uneven zinc deposition.

These findings highlight a promising and scalable strategy for developing high-performance, environmentally friendly anodes for AZABs. Future work will focus on mechanistic studies of dendrite suppression, electrolyte optimization, and the integration of this system into flexible or hybrid battery architectures.

References

[1] Fu, Jing, et al. Advanced materials 29.7 (2017): 1604685.

[2]Parker, Joseph F., et al. ACS applied materials & interfaces 6.22 (2014): 19471-19476.

[3]Yang, Zefang, et al Angewandte Chemie 135.3 (2023): e202215306.

[4]He, Jian, et al. Chemical Engineering Journal 485 (2024): 149740.

Tuncay Erdil completed his bachelor's and master degree from Middle East Technical University at the Metallurgical and Materials Engineering Department. He is currently a PhD student and a research assistant in the same department working on developing bifunctional oxygen electrocatalysts in the Electrochemical Energy Materials Laboratory under the supervision of Dr.Cigdem Toparli.

Presentating author: Tuncay Erdil, e-mail: tunerdil@metu.edu.tr tel: (0312)2105829

Laser-Induced Surface Patterning of Zinc Anodes for Dendrite Control in Zn–Air Batteries

Cagla Ozgur[1] , and Cigdem Toparli[1]

[1] Department of Metallurgical And Materials Engineering Middle East Technical University, , Ankara-Turkiye

Climate change continues to pose a critical global threat, primarily driven by the extensive use of fossil fuels, while the world's energy demand increases steadily. Although renewable energy sources such as solar and wind provide promising alternatives, their intermittent nature necessitates the development of reliable and efficient energy storage technologies to ensure a stable energy supply. Among various energy storage options, metal-air batteries, particularly zinc-air batteries, have emerged as strong candidates due to their high specific energy, high volumetric energy density, environmental friendliness, and the abundance of zinc resources [1]. Despite these advantages, zinc-air batteries face significant challenges at the anode side, including zinc corrosion and hydrogen evolution [2]. These processes lead to the formation of electrochemically inactive products such as zinc oxide (ZnO), which reduces the active material utilization and overall battery performance. Furthermore, uneven zinc deposition during cycling results in dendritic growth, which can cause internal short circuits and compromise the long-term stability and safety of the battery.

In this study, we introduce a novel strategy to address these limitations by engineering the zinc anode surface using laser-patterned microstructures. By precisely altering the surface topology of zinc through laser processing, we aim to influence zinc nucleation behavior and guide uniform deposition, thereby suppressing dendritic growth. Various laser designs were applied and tested to determine the most effective surface configuration. The electrochemical performance of the laser-structured zinc anodes was evaluated using symmetric cell tests and cyclic charge-discharge cycling at a current density of 5 mA cm^{-2}. Post-cycling morphology was examined via SEM to assess the impact of surface patterning on dendrite suppression.

References

[1] K.W. Leong, Y. Wang, M. Ni, W. Pan, S. Luo, D.Y.C. Leung, Rechargeable Zn-air batteries: Recent trends and future perspectives, Renewable and Sustainable Energy Reviews 154 (2022) 111771. https://doi.org/10.1016/j.rser.2021.111771.

[2] J. Chang, G. Wang, Y. Yang, Recent Advances in Electrode Design for Rechargeable Zinc–Air Batteries, Small Science 1 (2021). https://doi.org/10.1002/smsc.202100044.

Cagla Ozgur is a PhD student and research assistant at Metallurgical and Materials Engineering Department of Middle East Technical University. She is working on the bifunctional OER/ORR electocatalysts, and the design of Zinc anodes for rechargeable zinc-air batteries under the supervision of Assist. Prof. Cigdem Toparli.

Presentating author: Cagla Ozgur, e-mail: caglaoz@metu.edu.tr tel: 0312 210 58 29

Improving Zinc Anode Stability and Efficiency in Alkaline Rechargeable Batteries

Beyzanur Acar[1], A. Engin Serin[2] and A. Gul Ozturk[3] , Ozgur Darıcıoglu[2], Tayfur Ozturk[2,3]

[1]Department of Chemical Engineering, Ankara University, Ankara, Türkiye
[2]Department of Metallurgical and Materials Engineering, Middle East Technical University, Ankara, Türkiye
[3]Innovascope Materials Technologies Ltd. Sti, Ankara, Türkiye

Zn-Ni and Zn-air rechargeable batteries are seen as promising candidates for next-generation energy storage, providing benefits including safety, abundant resources, environmental friendliness, low-cost, and sufficient energy density. Nevertheless, their practical application remains limited due to the instability of Zn anodes, where dendrite formation and hydrogen evolution reaction (HER) dramatically compromise cyclic stability and performance of battery. [1]

Zinc is highly susceptible to corrosion in alkaline electrolytes, leading to uneven surface morphology and the formation of insulating by-products such as ZnO and $Zn(OH)_2$. These passivation layers block active sites, lower Coulombic efficiency, and promote further surface degradation. Corrosion also drives inhomogeneous Zn dissolution and redeposition, which contributes to the shape change problem.

Non-uniform deposition during repeated Zn plating and stripping causes the creation of needle-like dendritic structures. These dendrites continue to grow and finally reach the cathode, resulting in internal short circuits, dead zinc formation, and sudden capacity drop.

The hydrogen evolution reaction takes place as an undesirable outcome of cycling, consuming electrolyte and generating gas bubbles. These bubbles block active sites, create internal pressure, and may cause swelling or bulging of cells. Local current density fluctuations resulting from gas evolution lead to non-uniform Zn deposition, accelerating dendritic growth and anode degradation.

Electrochemical tests were conducted in a Swagelok cell. The anode was prepared using 80 wt% arc-sprayed Zn/ZnO powder (Zn core with a thin ZnO shell) produced in the lab, 10 wt% carbon black, and 10 wt% PTFE. PTFE was first dispersed in 4 mL of an ethanol/water mixture and stirred for 10–15 min, followed by the addition of carbon black and Zn/ZnO powder, and mixed for 1 h to form a slurry. The slurry was applied onto Cu foam, dried at 60 °C overnight, and pressed at 20 MPa. Commercial $Ni(OH)_2$ electrodes were used as cathodes. The electrolyte was 6 M KOH saturated with 0.35 M ZnO, and a polypropylene (PP) cloth was used as the separator.

Bare Zn/ZnO anode showed poor performance with rapid capacity fading and high HER. To suppress HER, Bi_2O_3 was introduced as an additive. Adding 3 wt% Bi_2O_3 increased the capacity from 15 to 300 mAh/g and partly suppressed HER. Furthermore, adding 0.5 M LiOH into the electrolyte improved cycle life and stability, while providing better HER control.

For further improvement, carbon coating was applied. Glucose was dissolved in DI water and 1 g of active material was added. The mixture was stirred for 1 h, dried overnight at 60 °C, and then pyrolyzed in a tube furnace under nitrogen at 400 °C for 2 h with a heating rate of 3.33 °C/min. The obtained powder was cooled and used for electrode preparation.

Recent studies showed that carbon-coated Zn/ZnO anodes combined with these additives provide longer cycle life and higher capacity. As a result, HER was effectively suppressed and no significant capacity fading was observed up to the 50th cycle.

The ongoing study aims to achieve further improvements in both capacity and stability.

Acknowledgment

The support was provided by the Scientific and Technological Research Council of Turkey (TUBITAK) with a project number 123M130, which the authors gratefully acknowledge.

References

[1] F. Mo, N. He, L. Chen, M. Li, S. Yu, J. Zhang, W. Wang,J. Wei, Front. Chem., 9 (2022) 8226

Beyzanur Acar graduated from the Department of Chemical Engineering at Ankara University in 2024. She is now a TÜBİTAK project researcher in the Department of Metallurgical and Materials Engineering at Middle East Technical University. Her research interests include the development of iron and zinc anodes to enhance performance in alkaline rechargeable batteries.

Presentating author: Beyzanur Acar, e-mail: beyzacar29@gmail.com tel: +905426155296

Electrochemical Evaluation of Lead Electrodes in Polyaniline-Doped Fumed Silica Gel Electrolytes

Ziyad Mira[1], Irem Cemre Türü[2] and Metin Gençten[1]
[1]Metallurgy and Materials Engineering Department, Chemical Metallurgy Faculty, Yildiz Technical University, Istanbul, 34220
[2]Mechanical Engineering Department, Engineering Faculty, Adiyaman University, Adiyaman, 02040

The rapid advancement of technology increases energy demand, leading to natural resource depletion and environmental impact. Renewable energy offers an effective solution but suffers from intermittency issues, highlighting the need for energy storage systems. Valve-regulated lead-acid (VRLA) batteries are among the oldest, most cost-effective, maintenance-free, and recyclable storage options, widely used in emergency systems, telecommunications, and electric vehicles [1,2].

AGM (absorbed glass mat) and gel-type VRLA batteries use immobilized gel electrolytes, where a 3D network forms through the hydrolysis of fumed silica with sulfuric acid, creating a highly thixotropic gel with good capacity and high solution resistance [3].

Various additives have been developed to enhance gel resistance and charge transfer without compromising gel structure [4,5].

In this study, polyaniline (PANi) conductive polymer was incorporated as an additive in the preparation of gel electrolytes for VRLA batteries. PANi powder was synthesized through chemical oxidative polymerization in an aqueous solution, as illustrated in Fig. 1. Gel electrolyte were optimized using electrochemical analyses methode for charge-discharge test.

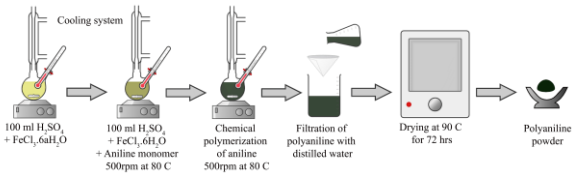

Fig.1. Synthesis of PANi conductive polymer

The produced polyaniline was characterized using BET, SEM, FTIR, and electrical conductivity measurements to assess its surface area, morphology, chemical structure, and conductive properties. All electrochemical analyses were carried out using a Gamry potentiostat (INTERFACE1010B) and a NEWARE 4000 multichannel device.

Electrochemical measurements, including cyclic voltammetry (CV), electrochemical impedance spectroscopy (EIS), and Tafel extrapolation, were conducted to evaluate the performance of lead electrodes in fumed silica-based gel electrolytes, both with and without polyaniline (PANi) incorporation. The observed redox peaks were attributed to the reversible electrochemical reactions involving the formation of lead sulfate from metallic lead and its subsequent reduction back to elemental lead. The results demonstrated that the inclusion of the conductive polymer polyaniline significantly enhanced the electrochemical activity and stability of the lead electrodes. Specifically, PANi contributed to improved charge transfer kinetics and reduced interfacial resistance, indicating its potential as an effective additive for improving the performance of gelled electrolytes in lead-based electrochemical systems.

Acknowledgment

This study was supported by The Scientific and Technological Research Council of Türkiye (TÜBİTAK) with project code 124M200. The authors would like to acknowledge that this work is submitted in partial fulfilment of the requirements for PhD degree at Yildiz Technical University, College of Chemical and Metallurgical Engineering, Department of Materials Engineering. Metin Gençten would like to thank TÜBA for the Outstanding Young Scientists Award (GEBIP).

References

[1] S. Sarmah, Lakhanlal, B.K. Kakati, D. Deka, Recent advancement in rechargeable battery technologies, Wiley Interdiscip. Rev. Energy Environ. 12 (2023). https://doi.org/10.1002/wene.461.

[2] J. Mitali, S. Dhinakaran, A.A. Mohamad, Energy storage systems: a review, Energy Storage Sav. 1 (2022) 166–216. https://doi.org/10.1016/j.enss.2022.07.002.

[3] P.T. Moseley, D.A.J. Rand, J. Garche, Lead–acid batteries for future automobiles, in: Lead-Acid Batter. Futur. Automob., Elsevier, 2017: pp. 601–618. https://doi.org/10.1016/B978-0-444-63700-0.00021-0.

[4] S. Yasa, O. Kumbasi, M.B. Arvas, M. Gencten, M. Sahin, Y. Sahin, S-Doped Graphene Oxide/N-Doped Graphene Oxide/PANI: A Triple Composite for High-Performance Supercapacitor Applications, ECS J. Solid State Sci. Technol. 12 (2023) 051002. https://doi.org/10.1149/2162-8777/acd3af.

[5] A. Mansuroglu, M. Gencten, M.B. Arvas, M. Sahin, Y. Sahin, Investigation the effects of chlorine doped graphene oxide as an electrolyte additive for gel type valve regulated lead acid batteries, J. Energy Storage 64 (2023) 107224. https://doi.org/10.1016/j.est.2023.107224.

Ziyad Mira is a Ph.D. candidate at the Graduate School of Science and Engineering, Department of Materials, Faculty of Chemical and Materials Engineering, Yildiz Technical University. He earned his B.Sc. from Babylon University in 2003 and completed his M.Sc. in 2017. His research focuses on developing novel additive materials for gel electrolytes in lead-acid batteries, with an emphasis on enhancing their performance as energy storage systems..

Ziyad Mira, e-mail: ziyadmira981@gmail.com tel: +90 (539) 548 86 89

From Waste to Resource: Engineering End-of-Life Graphite Anodes for Solid-State Hydrogen Storage

Mukhammed Kenzhebek[1], Fayil Sultanov[1]*, Almagul Mentbaeyva[1,2]

[1]National Laboratory Astana, Nazarbayev University, Astana, Kazakhstan;

[2]Department of Chemical and Materials Engineering, School of Engineering and Digital Sciences, Nazarbayev University, Astana, Kazakhstan

The rapid expansion of electric vehicles and portable electronics has driven a surge in lithium-ion battery (LIB) production, with global demand projected to surpass 1100 GWh by 2025. As these batteries reach end-of-life, they generate significant waste-particularly graphite anodes, which constitute 12-21 wt% of LIBs and represent up to 15% of their economic value, yet are largely overlooked in recycling streams [1]. This work explores an upcycling strategy that transforms spent graphite anodes into functional materials for hydrogen storage.

Graphite degrades during battery cycling due to lithium intercalation/deintercalation, increasing its interlayer spacing from 0.335 nm to over 0.370 nm and introducing defects such as cracking and SEI instability [2]. While detrimental for battery reuse, these structural changes enhance porosity and surface area-favorable for hydrogen adsorption, particularly via physisorption. Hydrogen uptake in carbon materials is strongly influenced by surface characteristics, with storage capacities reported up to 6.5 wt% for carbon nanofibers and 4.48 wt% for graphite [3]. Functionalization methods, including doping and composite formation, further improve performance [4].

In this study, we introduce a selective binder-removal process that preserves intercalated lithium ions to facilitate chemisorption-based hydrogen storage. Spent LIB cells were carefully disassembled, and binder removal was performed via two methods: deionized (DI) water washing and heat treatment at 550 °C. Thermogravimetric analysis (TGA) showed similar overall weight loss (Fig 1.), but heat treatment more effectively removed binders while retaining lithium-offering a dual advantage: organic removal without lithium loss, enabling both physisorption and chemisorption of hydrogen.

To enhance hydrogen uptake, the upcycled graphite anode is characterized by expanded interlayer distance (d-spacing), a result of lithium intercalation and structural distortion. This expanded spacing, combined with defect formation, promotes hydrogen sorption. Further modification through exfoliation increases specific surface area and porosity. Additionally, heteroatom doping and metal nanoparticle decoration tailor adsorption energy and introduce active sites, optimizing hydrogen storage behavior. These synergistic effects position spent graphite anodes as multifunctional, high-performance materials for solid-state hydrogen storage.

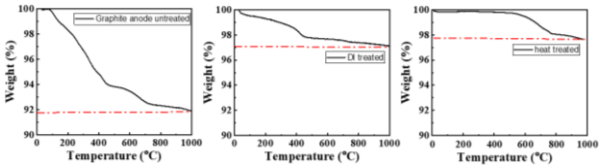

Figure 1. TGA curves of graphite samples.

Acknowledgment

This research was supported by the Collaborative Research Program (CRP) of Nazarbayev University under Grant No. [111024CRP2005].

References

[1] B. Niu, J. Xiao, Z. Xu, Advances and challenges in anode graphite recycling from spent lithium-ion batteries, J Hazard Mater 439 (2022). https://doi.org/10.1016/j.jhazmat.2022.129678.

[2] G. Wang, M. Yu, X. Feng, Carbon materials for ion-intercalation involved rechargeable battery technologies, Chem. Soc. Rev. 50 (2021) 2388–2443. https://doi.org/10.1039/D0CS00187B.

[3] M. Mohan, V.K. Sharma, E.A. Kumar, V. Gayathri, Hydrogen storage in carbon materials—A review, Energy Storage 1 (2019). https://doi.org/10.1002/est2.35.

[4] P. Murugan, R.D. Nagarajan, B.H. Shetty, M. Govindasamy, A.K. Sundramoorthy, Recent trends in the applications of thermally expanded graphite for energy storage and sensors - a review, Nanoscale Adv 3 (2021) 6294–6309. https://doi.org/10.1039/d1na00109d.

I, Mukhammed Kenzhebek, hold a Master's degree in Nuclear Physics from L.N. Gumilyov Eurasian National University (ENU), where I am currently pursuing a PhD in Nanomaterials and Nanotechnology. For the past three years, I have been working as a researcher at National Laboratory Astana (NLA), focusing on lithium-sulfur batteries and hydrogen storage materials.

Presenting author: Mukhammed Kenzhebek, email: mukhammed.kenzhebek@nu.edu.kz, tel: +7751218896

Re-synthesis of Nickel Manganese Cobalt Oxide Cathode Material from Black Mass Waste via Hydrometallurgical Processes

Berk Coban*, Burak Birol, Ozan Aydın and Metin Gençten

Yildiz Technical University, Istanbul,
Türkiye

For nearly two decades, lithium-ion batteries (LIBs) have been essential to our lives. They power electric vehicles (EVs), electronic devices like cellphones and smartwatches, and serve as energy storage for renewable sources, among many other daily applications. This is especially relevant given the increasing need for renewable energy, driven by the finite nature of fossil fuel resources and their negative environmental impact [1]. Consequently, the demand for EVs, as the most viable alternative to vehicles with internal combustion engines, continues to rise.

The primary limitation of LIBs is their cycle life, as a typical LIBs remains operational for approximately 5 to 10 years or 1000 charge-discharge cycles [2]. Given the projected increase in demand for LIBs by 2030, it is anticipated that 1.22 million tons of LIBs will have reached the end of their cycle life and become waste [2]. If these batteries are not recycled and end up in landfills, they risk contaminating both the soil and underground water. Additionally, leakage from the cell case due to corrosion or impact can lead to the release of toxic gases like hydrogen fluoride [3]. To prevent the aforementioned issues and address the depletion of elements in the Earth's crust used in LIBs, recycling these batteries is essential [4].

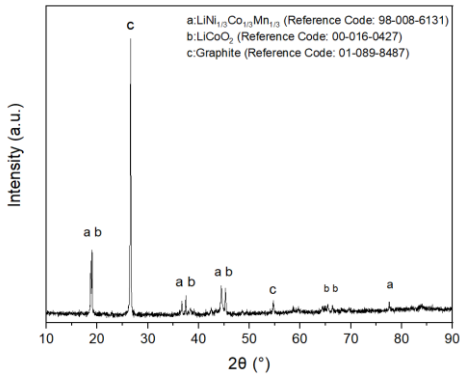

Figure 1. XRD analysis of the black mass

Black mass, a composite of LIB waste, was subjected to leaching using organic acids. After leaching, nickel, manganese, and cobalt ions were co-precipitated. The precipitate was then calcined to produce nickel manganese cobalt oxide (NMC) cathode material.

The black mass was studied using XRD analysis. Figure 1 shows XRD results, indicating the material contains graphite, NMC, and $LiCoO_2$ cathode material. In leaching processes, organic acids like citric acid, ascorbic acid, and acetic acid are used. Leaching parameters include a solid/liquid ratio of 50-250 g/L, acid concentration of 0.5-3 M, temperature range of 25-80°C, and time of 30-240 minutes. Each parameter is selected to improve leaching efficiency and achieve optimal dissolution rate. The Taguchi method was used to improve the process. After this, nickel, manganese, and cobalt ions were co-precipitated with oxalic acid. The precipitate was heated to get NMC cathode material.

Acknowledgment
This work was supported by the Yildiz Technical University under FBA-2024-6105 project code.

References

[1] Yasa S, Aydin O, Al-Bujasim M, Birol B and Gencten M 2023 Recycling valuable materials from the cathodes of spent lithium-ion batteries: A comprehensive review J Energy Storage 73 109073

[2] Wang Y, Shen K and Yuan C 2025 A Sustainable Direct Recycling Method for <scp>LMO</scp> / <scp>NMC</scp> Cathode Mixture from Retired Lithium-Ion Batteries in <scp>EV</scp> ENERGY & ENVIRONMENTAL MATERIALS 8

[3] Azimi G and Chan K H 2024 A review of contemporary and emerging recycling methods for lithium-ion batteries with a focus on NMC cathodes Resour Conserv Recycl 209 107825

[4] Ma X, Meng Z, Bellonia M V, Spangenberger J, Harper G, Gratz E, Olivetti E, Arsenault R and Wang Y 2025 The evolution of lithium-ion battery recycling Nature Reviews Clean Technology 1 75–94

Berk Çoban graduated with a B.Sc. degree in Metallurgical and Materials Engineering from Istanbul University-Cerrahpasa in 2021 and completed his M.Sc. at the same department in 2024. Since 2023, he has been working as a research assistant in the Department of Metallurgical and Materials Engineering at Yildiz Technical University, where he also started his Ph.D. studies in 2024. His research interests include hydrometallurgy, supercapacitors, and lithium-ion battery technologies.
Presentating author: Berk ÇOBAN, e-mail: berk.coban @yildiz.edu.tr tel: +90 531 294 20 75

Metal Recovery from Spent NMC811 Li-Ion Batteries Using Perchloric Acid

Tuğçe Selin Günşen[1] , Meltem Yıldız[1,2]
[1]Kocaeli University, Eng. Faculty, Department of Chemical Eng.,41380, Kocaeli, Turkey
[2]Alternative Fuels Research and Development Center, Kocaeli University, Kocaeli, Turkey

The acceleration of scientific and technological advancements has led to a global increase in energy demand. This rise has further exacerbated environmental and socio-economic challenges such as climate change, global warming, and energy supply security[1]. Lithium-ion batteries have emerged as a key energy storage technology across various applications, from portable electronic devices to electric vehicles, due to their high energy density, long cycle life, fast-charging capability, and wide operational temperature range[2,3].

Although the lifespan of electric vehicle batteries typically ranges from 8 to 10 years, it is of critical importance for Türkiye to establish a competitive position at the international level in battery recycling technologies. In this study, a widely adopted hydrometallurgical acid leaching process was employed to recover valuable metals from the cathode material of lithium-ion batteries. To date, both inorganic acids (such as hydrochloric, nitric, and sulfuric acids) and organic acids (such as lactic, malic, formic, and acetic acids) have been utilized in hydrometallurgical leaching processes. In contrast, this study introduces perchloric acid ($HClO_4$)—an acid not previously investigated for this purpose—as the leaching agent.

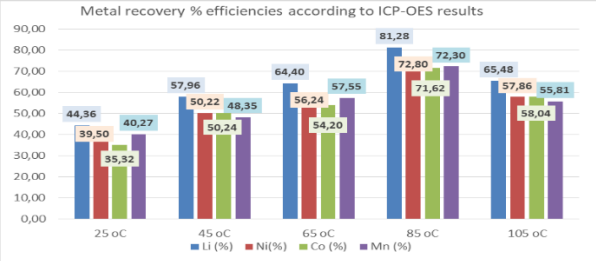

Fig.1 . Percentage recovery efficiencies of metals depending on leaching temperature

Based on previous studies involving perchloric acid leaching, the effects of temperature on the recovery efficiency of Li, Ni, Mn, and Co metals were investigated by keeping key parameters constant: acid concentration at 1.5 M, reaction time at 150 minutes, and solid-to-liquid ratio at 1:4. Experiments were conducted at temperatures of 25°C, 45°C, 65°C, 85°C, and 105°C. Following the hydrometallurgical acid leaching process, the leachate was analyzed using ICP-OES to determine the recovery percentages of Li, Ni, Mn, and Co. The calculated with ICP-OES metal recovery efficiencies are presented in Figure 1. The results indicated that the optimum operating temperature for the leaching process was 85°C. At this temperature, the metal recovery efficiencies were as follows: Li: 81.28%, Ni: 72.80%, Co: 71.62%, and Mn: 72.30%. Following the hydrometallurgical acid leaching process, cathode powder was synthesized from the leach solution using the sol-gel method in order to evaluate the effectiveness of the recovered material. The quality of the newly produced cathode powder was assessed through XRD and SEM characterizations.

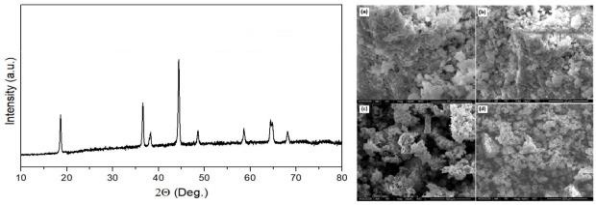

Fig.2 XRD and SEM analysis from perchloric acid leach solution via sol-gel method: (a) 10 µm, (b) 20 µm, (c) 100 µm, (d) 200 µm

SEM analysis revealed that the particles exhibited a compact and smooth surface, indicating homogeneous distribution in the sol-gel process and effective structural control during calcination. Particles appeared fused with more pronounced microstructural porosity. These pores likely enhance ionic conductivity and electrolyte penetration, providing the necessary porosity for ion transport in the electrode structure. XRD analysis shows medium-intensity peaks at $2\theta \approx 18°$, 37°, 44°, and 65°, corresponding to the (003), (101), (104), (018), and (110) planes, indicating a well-defined crystalline structure of the cathode sample. The most prominent peak at $2\theta \approx 44.5°–45°$ corresponds to the (104) plane, providing insights into the Li/Ni mixing within the cathode structure.

In conclusion, this study demonstrates that hydrometallurgical acid leaching using perchloric acid is an effective and successful approach for recycling used lithium-ion batteries. The results indicate that this method offers a promising strategy for metal recovery.

Acknowledgment

This work was supported by Kocaeli University General Scientific Research Projects (BAP) (Project No: FBA-2024-3560) in Turkey.

References

[1] Zhou, L et al. Journal of Energy Chemistry, 78, 104392. (2025).
[2] Wang, X. et al. Electrochimica Acta, 473.(2025).
[3] Kim, S. et al. Renewable and Sustainable Energy Reviews, 179.(2025).

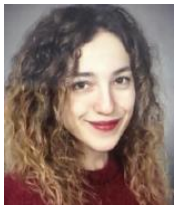

Tuğçe Selin Günşen graduated from İnönü University, Department of Chemical Engineering, in 2015 and completed her M.Sc. in Chemical Engineering at Kocaeli University in 2019. She is currently pursuing her Ph.D. in the same department, focusing on the recovery of valuable metals from spent NMC811 lithium-ion cells and their reuse in cathode production for new NMC811 cells. Most recently, she worked as an engineer at a lithium-ion battery manufacturing company for electric vehicles in Türkiye.
Tuğçe Selin Günşen, e-mail: tugce.gunsen@gmail.com Tel: +90 554 374 60 76

SUPERCAPACITORS

Influence of Charge–Discharge Ratios on EDLC Performance Using Plasticized 2-HEC/B_2CaO_4 Electrolytes

S. R. Majid[a,*] and Ranaa M. Almarshedy[a,b]

[a]Department of Physics, Faculty of Science, Universiti Malaya, 50603 Kuala Lumpur, Malaysia.
[b]Physics Department, College of Science, University of Ha'il, Ha'il, Saudi Arabia.

The development of efficient and environmentally friendly polymer electrolytes (PEs) is critical for advancing energy storage technologies such as electric double-layer capacitors (EDLCs). This study presents a systematic investigation of glycerol (GLY)-doped 2-hydroxyethyl cellulose (2-HEC) polymer electrolytes incorporating B_2CaO_4 as a calcium-based ionic dopant. The aim is to explore their structural, dielectric, ionic, and electrochemical properties for potential use in next-generation EDLCs. Polymer electrolyte films were synthesized by incorporating varying concentrations of glycerol (0-0.45 wt.%) into a 2-HEC matrix doped with 0.15 wt.% B_2CaO_4.

XRD patterns revealed reduced crystallinity with increasing glycerol content, confirming the plasticizing effect of glycerol that enhances the amorphous phase in the polymer matrix. FTIR peak deconvolution in the 700 to 1200 cm^{-1} and 1200 to 1750 cm^{-1} regions showed shifts in peaks corresponding to Ca-O-Ca and C-O-C vibrations, indicating complexation and strong interactions among GLY, B_2CaO_4, and the 2-HEC chains. These interactions improved chain flexibility and ion transport. The highest ionic conductivity of 5×10^{-5} $S \cdot cm^{-1}$ was recorded at 0.35 wt.% GLY, suggesting an optimal balance between polymer chain mobility and free volume. Temperature-dependent conductivity followed an Arrhenius trend, indicating thermally activated ion conduction.

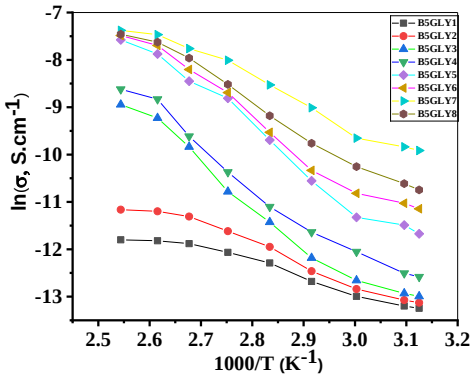

Fig. 1. Temperature-dependent ionic conductivity for GLY-doped 2-HEC-0.15 wt.% B_2CaO_4 polymer electrolytes

The B5GLY7 sample exhibited superior electrochemical performance, with specific capacitance values of 4.17 $F \cdot g^{-1}$ at 1.0 V and 7.22 $F \cdot g^{-1}$ at 1.5 V. It also maintained a wide electrochemical stability window from −2.25 V to +2.17 V. To improve capacitance under low initial values in symmetric conditions, a modified GCD approach was adopted using fixed charging (0.002 $A \cdot g^{-1}$) and decreasing discharge currents. This method significantly increased specific capacitance, reaching up to 149.86 $F \cdot g^{-1}$ at 1.5 V. The enhancement is attributed to the limited diffusion of Ca^{2+} ions in the polymer matrix, which is alleviated at lower discharge currents due to extended ion redistribution time. The B5GLY5 composition demonstrated robust stability with 90% capacitance retention after 1000 cycles at 1.0 V, confirming its potential for long-term EDLC applications.

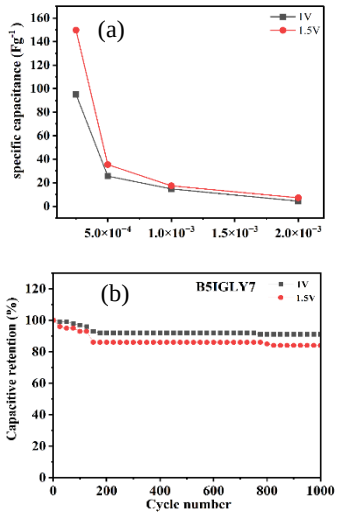

Fig. 2. (a) Specific capacitance vs. discharge current density at 1.0 V and 1.5 V for CN0.3IL5 PE; (b) Cycling stability over 1000 cycles at 1.0 V and 1.5 V with a charge-to-discharge ratio of 1:0.12.

Acknowledgment

We thank the Ministry of Higher Education Malaysia for supporting this research through the FRGS grant (FRGS/1/2024/STG05/UM/01/1) awarded to S. R. Majid.

References

[1] X. Fan et al. Chemical Reviews, 122 (2022) 17155-17239.

Siti Rohana Majid, from the Department of Physics at the University of Malaya, specializes in advanced materials and energy storage systems. She holds a BSc in Applied Physics (2001) and a PhD in Advanced Materials (2007). With an h-index of 47 and over 6,500 citations, her research has made significant contributions to the fields of electro-active ceramics, polymer electrolytes, and energy storage technologies.

https://umexpert.um.edu.my/shana
*e-mail: shana@um.edu.my

Mill scale-derived hematite as a low-cost supercapacitor electrode material

Ozan Aydin[1], Metin Gencten[1], Burak Birol[1]

[1] Yildiz Technical University, Faculty of Chemical and Metallurgical Engineering, Department of Metallurgy and Materials Engineering, 34210 Istanbul, Turkey

Energy has become an increasingly critical need in modern societies. Sectors such as industry, transportation, agriculture, and healthcare rely on a continuous power supply, making energy production and management a strategic priority. In this context, the efficient storage and reuse of energy through high-performance storage systems have gained great importance [1].

Due to the limitations of conventional storage systems like lithium-ion and lead-acid batteries, supercapacitors have attracted growing interest as next-generation electrochemical energy storage devices. Their key advantages include long cycle life (>1000 cycles), lightweight structure, fast charge-discharge capability, and reliable operation over a wide temperature range [2]. Transition metal oxides are commonly used as electrode materials in supercapacitors because their multiple oxidation states enable redox reactions that enhance specific capacitance and energy density [3]. However, their high production cost limits commercial use. Utilizing recycled waste-derived materials as electrodes offers a cost-effective and environmentally sustainable alternative [4,5].

Mill scale is a brittle layer of iron oxide formed on steel surfaces during high-temperature processes such as hot rolling or heat treatment. It mainly consists of FeO, Fe_3O_4, and Fe_2O_3, depending on the processing conditions [6]. Although often treated as waste, its high iron oxide content makes it a promising low-cost electrode material for energy storage applications.

In the present study, mill scale was subjected to chemical treatment using sulfuric acid (H_2SO_4) solutions to leach iron ions. The pH of the resulting solution was carefully adjusted to facilitate the precipitation of iron hydroxide. Subsequently, a thermal treatment was applied to convert the precipitate into hematite (Fe_2O_3). The structural and morphological properties of the synthesized Fe_2O_3 were characterized using X-ray diffraction (XRD) and scanning electron microscopy (SEM) analyses, which provided insights into its crystallographic phases and surface morphology, respectively. The obtained Fe_2O_3 was then utilized as an active electrode material in the fabrication of asymmetric coin-cell supercapacitors. The electrochemical performance of the assembled supercapacitors was systematically evaluated through a series of electrochemical techniques, including cyclic voltammetry (CV), electrochemical impedance spectroscopy (EIS), and galvanostatic charge-discharge (GCD) measurements. These analyses were employed to assess key performance metrics such as specific capacitance, charge-discharge capability, and the cycling stability of the Fe_2O_3-based supercapacitors.

Acknowledgment

This work has been supported by Yildiz Technical University Scientific Research Projects Coordination Unit under project number FBA -2025-7143. O. Aydin would like to express his gratitude for the support of the TÜBİTAK BİDEB-2211-A Program. Moreover, M. Gencten thanks to Turkish Academy of Sciences for Outstanding Young Scientists Awards (GEBİP).

References

[1] O.O. Yolcan, Innovation and Green Development 2 (2023) 100070

[2] J. Libich, J. Máca, J. Vondrák, O. Čech, M. Sedlaříková, J Energy Storage 17 (2018) 224–227

[3] S. Karthikeyan, B. Narenthiran, A. Sivanantham, L.D. Bhatlu, T. Maridurai, Mater Today Proc, (2020) 3984–3988.

[4] L. Ojeda, R. Mendoza, M. Vazquez-Lepe, K.P. Padmasree, V. Rodriguez-Gonzalez, G. Gonzalez-Contreras, J. Oliva, Ceram Int 48 (2022) 35495–35506.

[5] R. Mendoza-Jiménez, J. Oliva, A.I. Mtz-Enriquez, V. Rodriguez-Gonzalez, S. Diaz-Castañon, New J Chem 46 (2022).

[6] M.C. Bagatini, V. Zymla, E. Osório, A.C.F. Vilela, ISIJ International 51 (2011) 1072–1079.

Burak Birol received his B.Sc. (2004), M.Sc. (2007), and Ph.D. (2013) degrees in Metallurgical and Materials Engineering from Yildiz Technical University. He is currently an Associate Professor in the same department. His research interests include extractive metallurgy, recycling technologies, waste valorization, and energy storage systems.

Presentating author: Burak Birol, e-mail: burak.birol@gmail.com tel: +90 5356178166

Synthesis and characterization a novel polythiourethanes as candidate materials for supercapacitor applications

Laya Zarei-Gharehbaba[1,2], Reza Najjar[1*], Pariya YardaniSefidi[2]

[1]Polymer Research Laboratory, Faculty of Chemistry, University of Tabriz, Tabriz, Iran

[2]Electrochemistry Research Laboratory, Department of Physical Chemistry, Faculty of Chemistry, University of Tabriz, Tabriz, Iran.

Abstract

Sulfur-containing polymers are interesting materials for the next generation of functional materials. These polymers are mainly composed of aliphatic and aromatic copolymers with various functional groups such as phenyl, amine, and N-heterocycles. Polythiourethanes are polymers that contain sulfur and have not been extensively researched regarding their synthesis and applications. The use of various dithiols and diisocyanates is a common method for synthesizing these polymers in theory. In practical, there are certain limitations for synthesis, including the type of catalyst used, the catalyst's percentage, the suitable solubility of the isocyanate monomer, and the low efficiency of the reaction, which pose challenges in the synthesis of polythiourethanes. In this study, a new polythiourethane was synthesized using toluene diisocyanate and 1,2-ethane dithiol. FT-IR, ^{1}HNMR and EDAX analyses were used to confirm the synthesis. The melting point and glass transition temperature for the polymer were obtained 135 and 120 °C, respectively.The FE-SEM images revealed a sheet-like structure for the polymer. The supercapacitive behavior of the neat polymer and its nanocomposites will be investigated by electrochemical analyses of cyclic voltammetry (CV), charge/discharge (GCD) and electrochemical impedance (EIS).

1.Introduction

The incorporation of heteroatoms (such as S and N) into closed polymer structures, as functional groups, can give these materials special properties. These characteristics encompass enhanced thermal and mechanical properties, resulting in greater thermal stability of the polymer [1-3], improved metal adsorption capacity [4-6], self-healing or reprocessing abilities [86-91], as well as crystalline and optical attributes [7-8]. Polythiourethanes are widely recognized heteroatom-containing polymers characterized by the presence of sulfur (S) and nitrogen (N) atoms within their structure. In contrast to their oxygen analogues, polyurethanes, comprehensive research on the synthesis of polythiourethanes remains limited [9-10]. Polythiourethanes are used in optical materials, coatings, and medical technology due to their improved properties such as refractive index, adhesion strength, biocompatibility, and mechanical properties [9-11]. The facile addition of thiols to isocyanates for the synthesis of the thiourethane functional group was reported in 1960 by Dyer and co-workers [12] to produce alkyl thiourethane without side products. The efficiency and absence of by-products have been confirmed for both syntheses of small thiourethane and polythiurethane molecules [13-14]. The kinetics of the base-catalyzed reaction involving primary and secondary thiols with phenyl isocyanate suggest a rapid reaction, whereas the rate is significantly slower in the case of non-aromatic isocyanates. Despite the much higher efficiency of thiol-isocyanate reactions using mild catalysts at low concentrations compared to alcohol-isocyanate reactions, chemists' interest was minimal for almost half a century. Since the late 1980s, the use of amines as catalysts has led to the synthesis of a wide range of polythiourethanes by the reaction of dithiols and diisocyanates for applications as high-refractive index materials. This approach has continued to expand due to the successful industrial and commercial applications that have emerged for optical materials based on polythiourethane [15-16].

In this research, poly(ethylene 2,4-toluene dithiocarbamate) (PETDTC) was synthesized as a sulfur-containing polymer and its structure was investigated by various methods such as FT-IR and ^{1}HNMR and thermal analysis of the polymer by differential scanning calorimetry (DSC). The morphology of the synthesized polymer was investigated by FE-SEM images.

2.1 Materials Toluene diisocyanate, 1,2-ethanedithiol, triethylamine and acetone were purchased from Merck and used without any further purification.

2.2- . Preparation of poly(ethylene 2,4-toluene dithiocarbamate)(PETDTC)

To synthesize polythiourethane, toluene diisocyanate was stirred in acetone solvent until a clear solution was obtained. Then, the second monomer, ethane dithiol, was added to the solution in a molar ratio of 1 to 1 with the initial monomer. In this reaction, triethylamine was used as a catalyst. The reaction mixture was placed under argon gas for an appropriate time and under stirring conditions until the reaction was complete. The obtained precipitate was dried in a vacuum after washing several times at 60 ° C. The reaction yield was 54%.

3- Results and Discussions

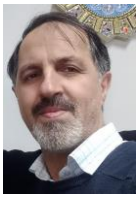

Dr. Reza Najjar, professor of chemistry currently working at the Faculty of Chemistry, University of Tabriz. Has has obtained PhD in polymer chemistry from Aachen University of Technology (RWTH-Aachen Germany) in June 2006, M. Sc., Chemistry, Sharif University of Technology, Tehran, Iran 1997, and B. Sc., Chemistry, University of Tabriz, Iran, 1994. His main research is focused on the preparation of new materials and investigation of their performance in various applications mainly related to the energy issues.

Reza Najjar, e-mail: najjar@tabriz.ac.ir T tel: +98-41-33393101, Cellphone: +98-912-0717158

PETDTC identification was done by FT-IR, ^{1}HNMR and DSC analysis. **Fig. 1** shows FT-IR analysis. The absorption band associated with the stretching vibrations of the aromatic -C-H bonds in the ring and the –N-H bond of the amide group appeared at 3070 and 3274 cm^{-1}, respectively, while the stretching vibrations of the aliphatic -C-H bonds were observed in the range of 2927-2954 cm^{-1}.The peaks associated with the stretching vibrations of the carbonyl group are noted at 1711 and 1643 cm^{-1}, respectively. The absorption bands resulting from the stretching vibrations of the -C=C- bonds related to the aromatic ring are found at 1598 and 1448 cm^{-1}, along with the bending vibration of the -N-H bonds at 1547 cm^{-1}. The peak corresponding to the stretching vibrations of the -S-H bond is detected in 2532 cm^{-1}. The peak observed at 1417 cm^{-1} is attributed to the -C-S- in the -S-CH2- group, while the absorption peak for the stretching vibrations of the -C-C- bond can be seen at 1218 cm^{-1}.

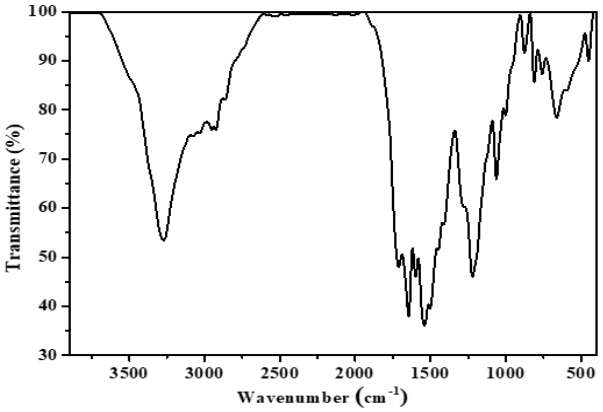

Fig. 1. The FTIR spectrum of PETDTC

According to the ^{1}HNMR spectrum in **Fig. 2.**, the peaks corresponding to the -S-H and -S-CH2- protons (f and e) appeared at 1.65 ppm, 2.89 ppm, and 2.96 ppm, respectively.

The peaks corresponding to the protons of the aromatic ring and the peak of the protons of the methyl group of the ring are visible at 7.26 ppm, 8.02 ppm, 6.91 ppm and 2.17 ppm, respectively. The proton of the amide group appears at 3.53 ppm. This spectrum was taken in CDCl3 solvent.

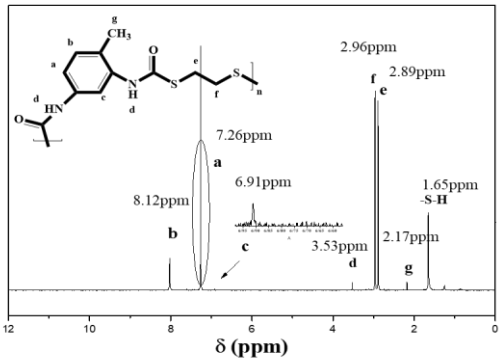

Fig. 2. 1H NMR spectrum of PETBTC polymer

The peaks corresponding to the protons of the aromatic ring and the peak of the protons of the methyl group of the ring are visible at 7.26 ppm, 8.02 ppm, 6.91 ppm and 2.17 ppm, respectively. The proton of the amide group appears at 3.53 ppm.

Fig. 3. illustrates the DSC analysis of PETDTC. The findings from this analysis are compiled in **Table 1**. The analysis was conducted at a scanning rate of 5 °C/min in a nitrogen environment.

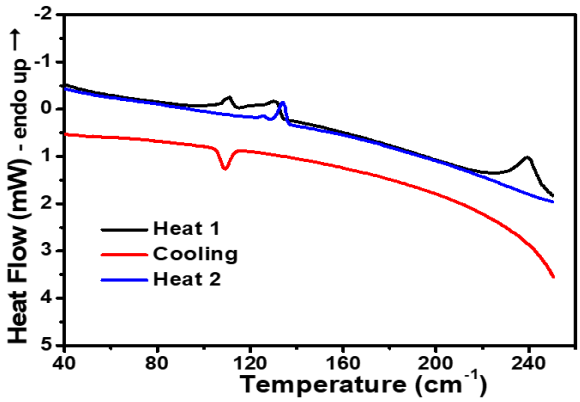

Fig. 3. DSC thermogram of PETDTC polymer

Table 1

Data extracted from DSC thermograms of PET DTC

T_m (°C)	Melting temperature	135
ΔH_m (J. g^{-1})	Enthalpy of melting	19.09
T_c (°C)	Crystallization temperature	100
ΔH_c (J. g^{-1})	Enthalpy of crystallization	-25.71
T_g (°C)	Glass transition temperature	120

According to the FE-SEM image (**Fig. 4**) at a scale of 1, 2 and 5 µm, the pristine PETDTC displays a nearly sheet-like configuration that is interconnected and shows a certain level of porosity.

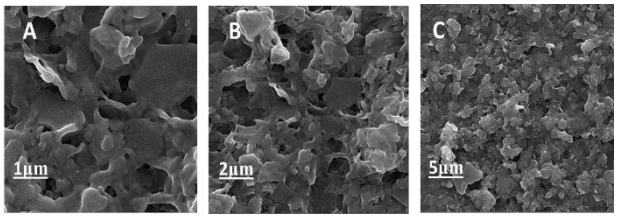

Fig. 4. FE-SEM image of PETDTC at the scale of 1, 2 and 5 µm.

The EDAX spectrum of the polymer is shown in **Fig. 5**. Based on the spectrum, the presence of C, O, N, and S atoms confirms the successful synthesis of the polymer.

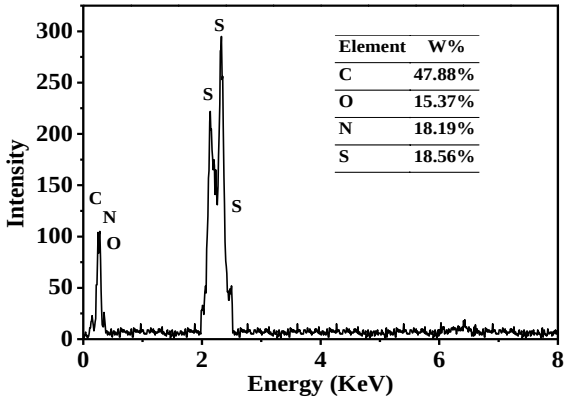

Fig. 5. EDAX spectrum of PETDTC

Electrochemical measurements

To prepare the sample for studying the supercapacitive behavior, first pure polythiourethane is completely dispersed in DMF solvent. Then, 6µl were placed on a glassy carbon electrode with a surface area of 0.1256 cm^2 as the working electrode. After evaporation of the solvent, their electrochemical behavior was carried out by cyclic voltammetry, charge/discharge and electrochemical impedance spectroscopy techniques in 0.5 M aqueous sodium sulfate electrolyte in a three-electrode system with a calomel electrode as the reference electrode and a 2*1cm^2 platinum sheet electrode as the auxiliary electrode. In the next step, Polymer nanocomposite was prepared with multi-walled carbon nanotubes in a ratio of 1 to 0.5 and the addition of 3% nickel cobalt hexacyanoferrate Ni_2CoHCF synthesized [17] nanoparticles and electrochemical analyses were performed under the same conditions as before.

Fig. 6A-6B. shows the CV curve of pure PETDTC.The quasi-rectangular shape of the graph shows the non-Faradic behavior of the electrode. In the presence of Ni_2CoHCF nanoparticles (**Fig. 6B**), the shape of the graphs of these electrodes is outside the ideal rectangular shape, and the oxidation and reduction peaks that appear are related to the $Fe^{II/III}$ redox reaction, which appears at a potential of 400 mV. The change in the shape of the graphs from rectangular indicates the Faradaic behavior of the electrodes. The charge and discharge diagrams are shown in **Fig. 6C-6D.** The shape of the curve for the neat polymer **Fig. 6C** is a symmetrical triangle, indicating the reversibility of the charging and discharging process.

For the electrodes containing nanoparticles (**Fig. 6D**), the shape of the curves is non-linear and due to the Faradaic behavior of Ni_2CoHCF, the curves do not follow the ideal linearity. The synergistic effect and interaction between the constituent materials creates a proper connection between the electrolyte ions and the electrode, increasing the charge and discharge time of PETDTC/MWCNT+3%Ni_2CoHCF composite. Electrochemical impedance spectroscopy (EIS) has been used to further investigate the electrodes. A critical factor influencing the analysis of electrode behavior, which can be investigated using electrochemical impedance spectroscopy, is the charge transfer resistance (R_{ct}). The Nyquist plots of the electrodes are shown in **Fig. 7** .

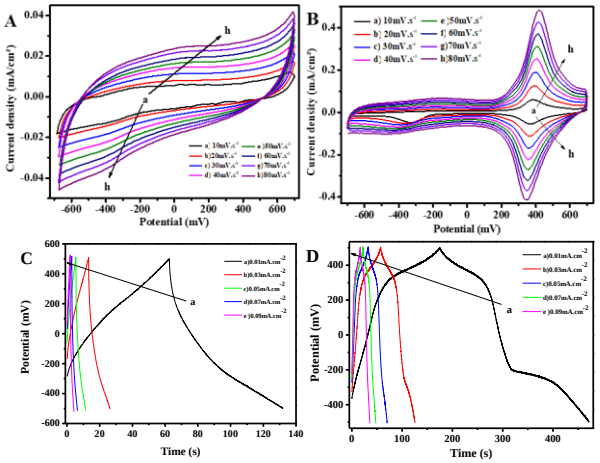

Fig. 6. CV curve of A) PETDTC B) PETDTC/MWCNT composite(1:0.5)+3% Ni_2CoHCF . Charge/discharge curve of C) PETDTC D) PETDTC/MWCNT composite(1:0.5)+3% Ni_2CoHCF .

The equivalent circuit in Figure where R1, CPE1, R2, and W1 are the solution resistance, the electric double layer constant phase element, the charge transfer resistance, and the Warburg element, respectively, aligns closely with the experimental data. In **Table 2** as the data show , the electrodes containing Ni_2CoHCF nanoparticles have much lower charge transfer resistance and the charge transfer resistance for these electrodes is also significantly lower than that of pure PETDTC. The low charge transfer and mass transfer resistance of these nanocomposites is due to the faradaic processes of the nanoparticles and the synergistic effect of the nanoparticles with MWCNT, which leads to increased ionic conductivity and CPE.

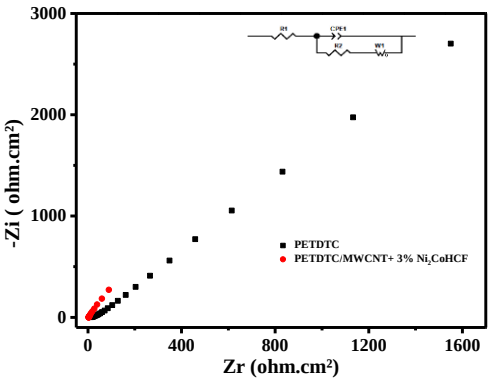

Fig. 7. Nyquist diagram of PETDTC and its composites as electrode material and equivalent circuit for fitting experimental impedance data of electrodes, Nyquist diagram of equivalent circuit for fitting experimental impedance data of various supercapacitor electrode made by various materials: □) PETDTC ○) PETDTC/MWCNT+3%Ni_2CoHCF.

Table 2
Equivalent circuit element values with experimental data of impedance diagrams obtained from **Fig. 7**

Electrode material	Values of equivalent circuit elements				
	R1 (Ω)	CPE-T ($\Omega^{-1}cm^{-2}s^{CPE-P}$)	CPE-P	R2 (Ωcm^2)	W-R ($\Omega s^{-0.5}$)
PETDTC	13.92	0.0004117	0.57	16.15	1577
PETDTC/MWCNT + 3% Ni_2CoHCF	4.11	0.0002199	0.93	3.62	72.36

4- Conclusions

In this work, poly(ethylene 2,4-toluene dithiocarbamate) was synthesized. Polymer identification was investigated by FT-IR and ^{1}HNMR. Based on the DSC analysis of polymer melting points was 135 °C. Also, the morphology of the polymer showed a sheet-like structure. The quasi-rectangular shape of the CV diagram and the symmetrical triangular shape in the charge-discharge analysis show non-Fardaic behavior for this polymer as an electrode. The use of Ni_2CoHCF cubic nanoparticles to prepare nanocomposites has changed the behavior of supercapacitor to Faradaic, and the morphology of these nanoparticles has caused the rapid migration of ions and increased the ionic conductivity.

Acknowledgement

The work was supported by The University of Tabriz which the Authors gratefully acknowledge.

References

[1] Mutlu, Hatice, Ezgi Berfin Ceper, Xiaohui Li, Jingmei Yang, Wenyuan Dong, Mehmet Murat Ozmen, and Patrick Theato, Sulfur chemistry in polymer and materials science. Macromolecular rapid communications, 2019. 40(1): p. 1800650.

[2] Ochiai, B. and T. Endo, Carbon dioxide and carbon disulfide as resources for functional polymers. Progress in Polymer Science, 2005. 30(2): p. 183-215.

[3] Sun, Ziyang, Huahua Huang, Le Li, Lixin Liu, and Yongming Chen, Polythioamides of high refractive index by direct polymerization of aliphatic primary diamines in the presence of elemental sulfur. Macromolecules, 2017. 50(21): p. 8505-8511.

[4] Bao, Junjie, Gaojian Shi, Can Tao, Chao Wang, Chen Zhu, Liang Cheng, Gang Qian, and Chunhua Chen, Polycarbonate-based polyurethane as a polymer electrolyte matrix for all-solid-state lithium batteries. Journal of Power Sources, 2018. 389: p. 84-92.

[5] Tian, T., R. Hu, and B.Z. Tang, Room temperature one-step conversion from elemental sulfur to functional polythioureas through catalyst-free multicomponent polymerizations. Journal of the American Chemical Society, 2018. 140(19): p. 6156-6163.

[6] Wu, Shuang, Ming Luo, Donald J. Darensbourg, and Xiaobing Zuo, Catalyst-free construction of versatile and functional CS2-based polythioureas: characteristics from self-healing to heavy metal absorption. Macromolecules, 2019. 52(22): p. 8596-8603.

[7] Chung, Woo Jin, Jared J. Griebel, Eui Tae Kim, Hyunsik Yoon, Adam G. Simmonds, Hyun Jun Ji, Philip T. Dirlam. Chung, Woo Jin, Jared J. Griebel, Eui Tae Kim, Hyunsik Yoon, Adam G. Simmonds, Hyun Jun Ji, Philip T. Dirlam, The use of elemental sulfur as an alternative feedstock for polymeric materials. Nature chemistry, 2013. 5(6): p. 518-524.

[8] Yue, Tian-Jun, Wei-Min Ren, Ye Liu, Zhao-Qian Wan, and Xiao-Bing Lu, Crystalline polythiocarbonate from stereoregular copolymerization of carbonyl sulfide and epichlorohydrin. Macromolecules, 2016. 49(8): p. 2971-2976.

[9] Podkościelny, W. and S. Szubińska, Linear polythioesters. XIII. Products of polycondensation of isomeric di (mercaptomethyl)–dimethylbenzenes with adipoyl and sebacoyl chlorides. Journal of applied polymer science, 1988. 35(1): p. 85-101.

[10] Suzuki, Akane, Daisuke Nagai, Bungo Ochiai, and Takeshi Endo, Facile synthesis and crosslinking reaction of trifunctional five-membered cyclic carbonate and dithiocarbonate. Journal of Polymer Science Part A: Polymer Chemistry, 2004. 42(23): p. 5983-5989.

[11] Li, Qin, Hui Zhou, Douglas A. Wicks, and Charles E. Hoyle, Thiourethane-based thiol-ene high Tg networks: Preparation, thermal, mechanical, and physical properties. Journal of Polymer Science Part A: Polymer Chemistry, 2007. 45(22): p. 5103-5111.

[12] Dyer, E., J.F. GLENN, and E.G. LENDRAT, The kinetics of the reactions of phenyl isocyanate with thiols1. The Journal of Organic Chemistry, 1961. 26(8): p. 2919-2925.

[13] Movassagh, B. and M. Soleiman-Beigi, Synthesis of thiocarbamates from thiols and isocyanates under catalyst- and solvent-free conditions. Monatshefte für Chemie-Chemical Monthly, 2008. 139: p. 137-140.

[14] Klemm, E. and C. Stöckl, Synthesis of SH-and NCO-terminated thiocarbamate prepolymers. Die Makromolekulare Chemie: Macromolecular Chemistry and Physics, 1991. 192(1): p. 153-158.

[15] Droger, N., O. Primel, and J.L. Halary, Characterization of the viscoelastic and mechanical properties of tightly cross-linked polythiourethane networks. Journal of applied polymer science, 2008. 107(1): p. 455-462.

[16] Nakayama, N. and T. Hayashi, Synthesis of novel UV-curable difunctional thiourethane methacrylate and studies on organic–inorganic nanocomposite hard coatings for high refractive index plastic lenses. Progress in Organic Coatings, 2008. 62(3): p. 274-284.

[17] Qiu, Y., Lin, Y., Yang, H., & Wang, L., Ni-doped cobalt hexacyanoferrate microcubes as battery-type electrodes for aqueous electrolyte-based electrochemical supercapacitors. Journal of Alloys and Compounds, 2019. 806: p. 1315-1322.

Poly(4-vinylpyridine)/$NiCo_2S_4$/polyaniline nanocomposites as supercapacitor electrode materials in alkaline media

Mohyaddin Gholizadeh Ghaleh-Aziz[1,2], Reza Najjar[1*], Mir Ghasem Hosseini[2]

[1]Polymer Research Laboratory, Faculty of Chemistry, University of Tabriz, Tabriz, Iran

[2]Electrochemistry Research Laboratory, Department of Physical Chemistry, Faculty of Chemistry, University of Tabriz, Tabriz, Iran.

Abstract

Nanocomposites composed of poly(4-vinylpyridine) (P4VPy), $NiCo_2S_4$ (NCS), and polyaniline (PAni) were synthesized and examined as promising electrode materials for supercapacitors. The hydrothermally prepared NCS formed a well-connected network structure, which contributed to an increased number of electroactive sites and improved charge transfer, leading to enhanced supercapacitor performance. The chemical characteristics of the nanocomposites were analyzed using FT-IR and EDX techniques, while their crystal structure and surface morphology were studied through XRD and FE-SEM, respectively. Electrochemical behavior was assessed using electrochemical impedance spectroscopy (EIS), galvanostatic charge–discharge (GCD), and cyclic voltammetry (CV). At a scan rate of 90 mV/s, the P4VPy/NCS/PAni nanocomposite demonstrated a specific capacitance of 347.3 F/g (from CV data). GCD analysis at a current density of 0.20 mA/g also showed that the nanocomposite had a capacitance of 95.82 F/g—nearly three times greater than that of pure P4VPy. This improvement is attributed to fast faradaic redox interactions between the conductive components and NCS, which created a strong synergistic effect, boosting energy storage capacity. These findings highlight the potential of heterogeneous nanomaterials in advancing energy storage technologies.

1.Introduction

Renewable energy sources require efficient electrical energy storage for use in everyday devices such as electric vehicles and smartphones [1, 2, 3]. Supercapacitors, compared to batteries, offer faster charge/discharge rates, flexibility, wide operating temperature, light weight, and simple maintenance [4, 5, 6]. Improving supercapacitor performance largely depends on developing high-performance electrode materials [7, 8, 9, 10]. Metal oxides (e.g., RuO_2, V_2O_5, MnO_2) [11] and mixed metal oxides have been widely studied for their fast redox reactions and multiple oxidation states [9, 12]. Recently, mixed metal sulfides like $NiCo_2S_4$ (NCS) have gained attention due to better electrochemical properties and conductivity [13]. Nanostructured metal sulfides show unique performances owing to their special crystal structures and rapid redox behavior. Conductive polymers such as polyaniline (PAni), with tunable conductivity and low cost, are promising for composite electrodes [14]. Their π-conjugated systems enhance charge transfer, especially when combined with metal oxides or sulfides [15]. Non-conductive polymers containing heteroatoms can also improve dispersion and conductivity of nanoparticles [16]. This study focuses on poly(4-vinylpyridine) (P4VPy), a polymer with nitrogen-containing side groups capable of coordinating with metal atoms, as a matrix to fabricate nanocomposites with NCS and PAni (P4VPy/NCS/PAni). The effect of incorporating hydrothermally synthesized NCS and PAni nanoparticles on supercapacitive performance is evaluated and compared to similar literature reports.

2.1 Materials

High purity grade nickel (II) nitrate ($Ni(NO_3)_2{\cdot}6H_2O$), cobalt (II) nitrate ($Co(NO_3)_2){\cdot}6H_2O$, potassium peroxydisulfate ($K_2S_2O_8$, KPS) and N-methylformamide (NMF) were obtained from Merck, Germany. Poly(2-vinylpyrrolidone) (P4VPy) and thioacetamide were from Sigma-Aldrich. Aniline (from Merck, Germany) was distillated under vacuum used as fresh for polymerization. Aniline was oxidatively polymerized by using KPS as oxidant/initiator in the hydrochloric acid (Merck) solution to obtain PAni. Urea was from Pardis Petrochemical Company, Iran. Deionized (DI) water was used in whole experiments.

2.2- Synthesis of $NiCo_2S_4$

Nickel cobalt sulfide ($NiCo_2S_4$, NCS) was prepared via a hydrothermal synthesis method. Initially, 1.454 g (5 mmol) of $Ni(NO_3)_2{\cdot}6H_2O$ and 2.91 g (16 mmol) of $Co(NO_3)_2{\cdot}6H_2O$ were dissolved in 30 ml of deionized (DI) water with magnetic stirring. Separately, a solution of 3 g (50 mmol) urea in 30 ml DI water was prepared and then added to the nickel and cobalt solution while stirring. Subsequently, 1.65 g (22 mmol) of thioacetamide was introduced to the mixture and stirred for 30 minutes. The resulting solution was transferred into an 80 ml Teflon-lined autoclave, which was sealed and heated in an oven at 180 °C for 12 hours to complete the reaction. After cooling to room temperature, the product was filtered using a Buchner funnel under vacuum, then washed with ethanol and DI water to remove residual reactants. The collected

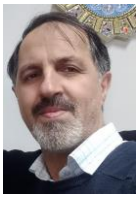

Dr. Reza Najjar, professor of chemistry currently working at the Faculty of Chemistry, University of Tabriz. Has has obtained PhD in polymer chemistry from Aachen University of Technology (RWTH-Aachen Germany) in June 2006, M. Sc., Chemistry, Sharif University of Technology, Tehran, Iran 1997, and B. Sc., Chemistry, University of Tabriz, Iran, 1994. His main research is focused on the preparation of new materials and investigation of their performance in various applications mainly related to the energy issues.

Reza Najjar, e-mail: najjar@tabriz.ac.ir T tel: +98-41-33393101, Cellphone: +98-912-0717158

precipitate was air-dried and further dried in a vacuum oven at 80 °C for 6 hours, yielding 1.32 g of product with an 86% yield.

2.3. Synthesis of P4VPy/NCS/PAni nanocomposite

Adequate amounts of the PAni, NCS and P4VPy were weighed into a mortar and mechanically blended to prepare a homogeneous P4VPy/NCS/PAni nanocomposites. The nanocomposites were then annealed at 80 °C for up to 25 h. The schematic representation of the detailed steps for preparation of the P4VPy/NCS/PAni nanocomposites are illustrated in Fig. 1. The relative weight ratios of P4VPy to NCS and PAni was varied and their effect on the performance of the nanocomposites was studied.

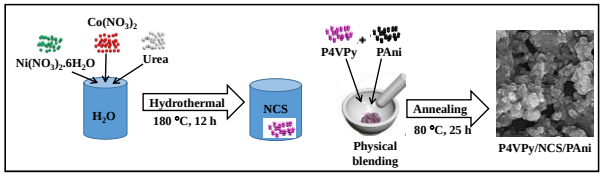

Fig. 1. the style to be used for graphs.

2.4. Characterizations

The SEM images and elemental analysis of the samples were obtained using a field emission scanning electron microscope (FE-SEM), specifically the Tescan MIRA3 FEG-SEM model from the Czech Republic, equipped with an energy dispersive X-ray spectroscopy (EDS) system. X-ray diffraction (XRD) patterns were recorded using a MAC Science M18XHFSRA instrument with CuKα radiation as the X-ray source. Fourier transform infrared (FT-IR) spectra were collected with a Perkin Elmer Spectrum One System spectrometer from the USA. The NCS samples underwent calcination in a tube furnace manufactured by Nabertherm, Germany.

2.5. Electrochemical measurements

An Origa Flex-OGF 01 A potentiostat-galvanostat electrochemical workstation (France), connected to a computer, was utilized to perform electrochemical measurements including electrochemical impedance spectroscopy (EIS), galvanostatic charge/discharge (GCD), and cyclic voltammetry (CV). The working electrode was prepared by coating the active electrode material onto a glassy carbon electrode. A platinum wire served as the counter electrode, and all measurements were conducted against an Ag/AgCl reference electrode. A 1 M H_2SO_4 solution was used as both the electrolyte and analysis medium. The active materials—P4VPy, P4VPy/NCS, and P4VPy/NCS/PAni—were each dispersed in N-methylformamide (NMF) and sonicated in an ultrasonic bath until a uniform slurry was formed. A suitable amount of this slurry was then evenly applied onto a cleaned glassy carbon electrode (0.4 cm diameter, approximately 0.126 cm² active area) to fabricate the working electrode, which was subsequently dried in an oven at 80 °C for around 4 hours.

The CV curves which were recorded at varying potential scan rates, and Eq. 1 were used to estimate the specific capacitance (C_{sp}) of the fabricated electrodes.

$$C_{sp} = \frac{1}{A \times v \times \Delta v} \int_{V_i}^{V_f} I dV \qquad \text{Eq. 1}$$

In Eq. 1, C_{sp} denotes the specific capacitance (F g^{-1}), I represents the current (A), A shows the active surface area of electrode (cm^2), $\boldsymbol{v}$ = scan rate (mV s^{-1}) and the observed potential window (V) is denoted with ΔV.

Also the GCD test results measured at varying constant current densities were utilized to estimate C_{sp} of electrodes by using Eq. 2.

$$C_{sp} = \frac{I \times \Delta t}{A \times \Delta v} \qquad \text{Eq. 2}$$

where I represents the constant current (A), Δt denotes discharging time (s), A is active area of electrode (cm^2), and ΔV represents the observed potential window (V).

3. Results and discussion

FT-IR spectra of P4VPy, P4VPy/NCS, and P4VPy/NCS/PAni are shown in Fig. 2. The addition of NCS nanoparticles to P4VPy introduces a strong absorption band around 664 cm^{-1}, related to NiS and CoS bonds. However, NCS nanoparticles do not cause disappearance or significant shifts in the polymer absorption bands, indicating no strong interactions between polymers and NCS. The main difference is the reduced relative intensity of polymer peaks due to the strong NCS bands.

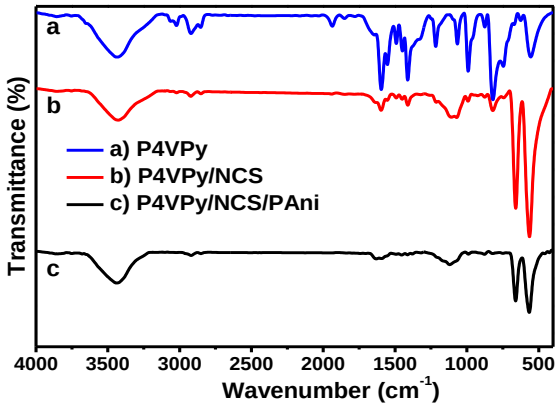

Fig. 2. The FT-IR spectra of: a) P4VPy, b) P4VPy/NCS and c) P4VPy/NCS/PAni samples measured as KBr disc.

The surface morphology of P4VPy/NCS/PAni sample was characterized via SEM micrographs and exhibited in Fig. 3. The SEM micrographs of the optimized P4VPy/NCS/PAni nanocomposite have revealed a very microporous structure for this sample.

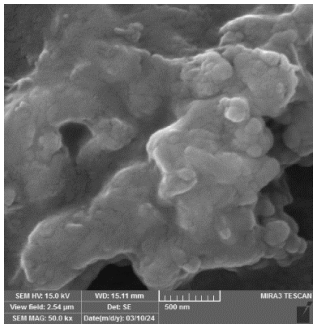

Fig. 3. SEM images of P4VPy/NCS/PAni nanocomposite with magnifications of 50 K.

The porous structure can significantly boost the specific capacitance (Csp) of the nanocomposite by enabling better electrolyte ion diffusion and providing a larger surface area for charge storage. EDX mapping (Fig. 4) confirmed uniform distribution of elements (C, N, O, Ni, Co, S) in the $NiCo_2S_4$ and P4VPy/NCS/PAni samples, indicating efficient mixing without noticeable agglomeration of NCS or PAni particles.

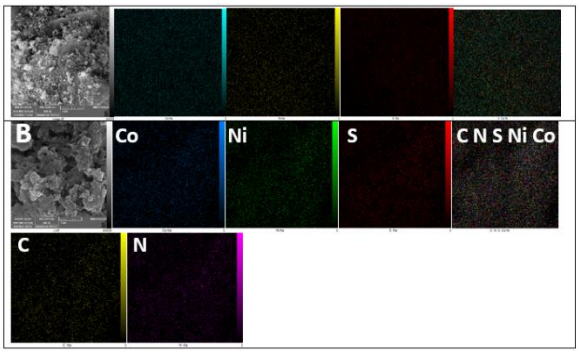

Fig. 4. The EDX mappings of the A) NiCo2S4 and B) P4VP/NCS/PAni nanocomposite samples.

The atomic ratio of Co to Ni in the P4VPy/NCS/PAni nanocomposite is 63.74% to 36.26%. Its flower-like morphology enhances charge transfer. The unique arrangement of benzene rings in PAni chains enables trapping of sulfide and oxide groups, leading to chain expansion and improved ion accessibility. Thus, PAni's structure promotes better interaction between electrolyte ions and active electrode sites compared to other electroactive materials.

3.2 Electrochemical investigations

CV curves of electrodes made with different materials were recorded between -0.4 V and 0.4 V at scan rates of 10, 30, 60, and 90 mV/s (Fig. 5). The curves show a quasi-rectangular, symmetrical shape, indicating fast, reversible Faradaic reactions and ideal capacitor behavior. Higher scan rates improve the rectangular shape, reflecting enhanced capacitive performance.

Table 1
The C_{sp} values calculated by using Eq. 1 from CV curves for electrodes prepared by using P4VPy, P4VPy/NCS and P4VPy/NCS/PAni at different potential scan rates in acidic media.

Electorde	C_s (F g^{-1}), Scan Rate (mV s^{-1})			
	10	30	60	90
P4VPy	184.08	132.44	107.28	94.53
$NiCo_2S_4$/P4VPy	350.39	240.03	192.38	172.24
PAni/$NiCo_2S_4$/P4VPy	482.22	362.20	295.24	261.76

3.3 GCD characteristics

The GCD performance of electrodes was evaluated at varying current densities (0.05–0.20 mA·cm^{-2}). As shown in Fig. 6, all electrodes demonstrated Faradaic behavior, with the P4VPy/NCS/PAni-based electrode exhibiting the longest discharge time. Specific capacitance (Csp) values, calculated from GCD data (Eq. 2, Table 2), decreased with increasing current density. At 0.20 mA·cm^{-2}, Csp values for P4VPy, P4VPy/NCS, and P4VPy/NCS/PAni were 18.33, 40.57, and 64.58 F·g^{-1}, respectively. The superior performance of P4VPy/NCS/PAni is attributed to its porous structure, which enhances ion diffusion and charge storage, as well as the synergistic effect of NCS and PAni that improves conductivity and promotes faster redox reactions.

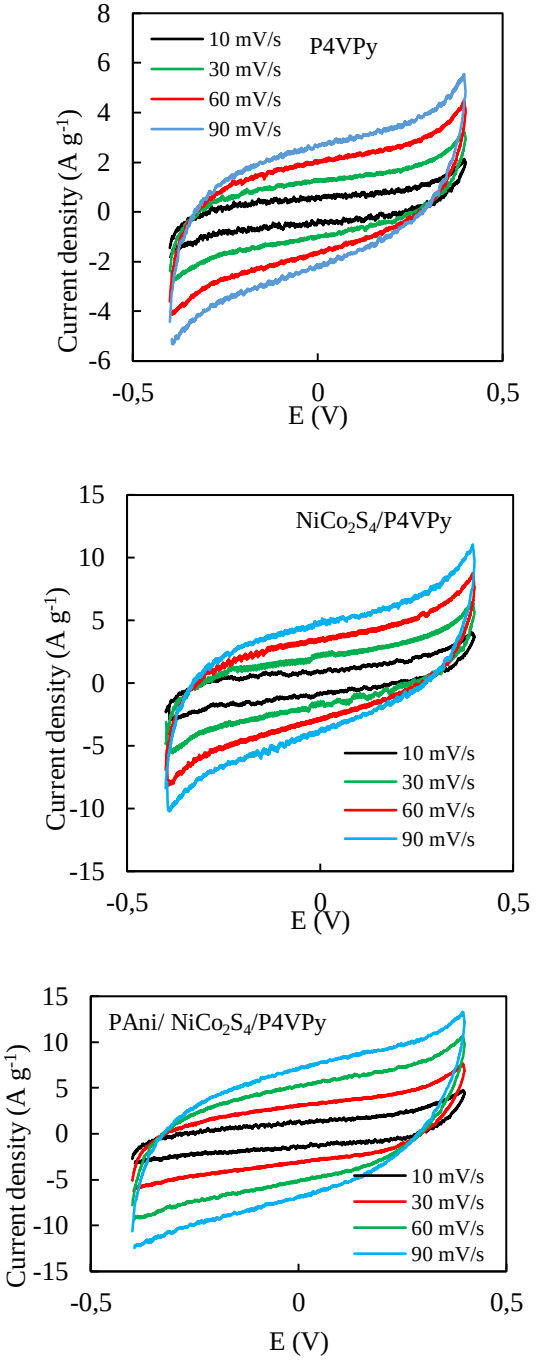

Fig. 5. CV curves for electrodes prepared by using A) P4VPy, B) P4VPy/NCS and C) P4VPy/NCS/PAni and measured at different potential scan rates in alkaline media.

Table 2
The C_{sp} values for electrodes prepared by using P4VPy, P4VPy/NCS, and P4VPy/NCS/PAni as electroactive materials, calculated via Eq. 2 and data extracted from GCD curves measured in different constant current densities in alkaline media.

. Electorde	C_s (F g^{-1}), Current (mA)			
	0.05	0.1	0.15	0.2
PVP	35.41	24.16	21.12	18.33
$NiCo_2S_4$/PVP	113.46	61.63	63.31	40.57
PA/ $NiCo_2S_4$/PVP	182.86	104.16	109.21	64.58

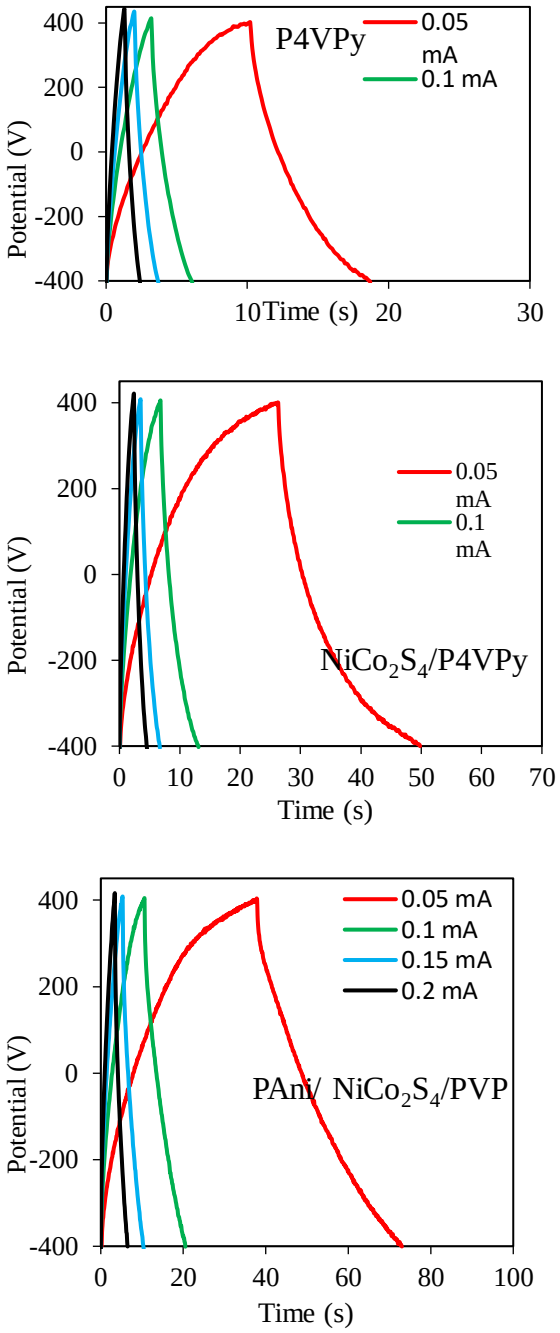

Fig. 6. GCD curves for A) P4VPy, B) P4VPy/NCS, C) P4VPy/NCS/PAni electrodes in different constant current densities in alkaline media

4- Conclusions

The PAni and NCS nanoparticles, synthesized via a simple hydrothermal method, were uniformly dispersed in the P4VPy matrix to form P4VPy/NCS/PAni nanocomposites. SEM and EDX analyses confirmed the homogeneous distribution of the mixed transition metal sulfide and conductive polymer nanoparticles. The synergistic effects of these components enhanced ionic conductivity by increasing the number of electroactive sites. This increase in active surface area provided additional pathways for efficient electron transfer and electrolyte ion diffusion, facilitating redox reactions. Ultimately, the optimized nanocomposite exhibited a maximum specific capacitance of 347.3 F/g at a scan rate of 90 mV/s and 95.82 F/g from GCD tests at 0.20 mA, demonstrating its potential as a high-performance electrode material for advanced supercapacitors.

Acknowledgement

The work was supported by the University of Tabriz which the Authors gratefully acknowledge.

References

[1] A. K. Das, S. Sahoo, P. Arunachalam, S. Zhang, and J.-J. Shim, *RSC Adv.*, 6 (2016) 107057–107064
[2] S. Prasad, D. Durairaj, M. AlSalhi, J. Theerthagiri, P. Arunachalam, and G. Durai, *Energies*, 11 (2018) 281
[3] R. R. Neiber *et al*, *J. Energy Storage*, P. Arunachalam, and G. Durai, *Energies*, 52 (2022) 104900
[4] M. D. Stoller, S. Park, Y. Zhu, J. An, and R. S. Ruoff, *Nano Lett*, 8 (2008) 3498–3502
[5] H. P. Wu *et al*, in *2010 8th International Vacuum Electron Sources Conference and Nanocarbon*, (2010) 465–466
[6] J. Theerthagiri *et al*, *J. Solid State Chem*, 267 (2018) 35–52
[7] S.-Y. Hsu, F.-H. Hsu, J.-L. Chen, Y.-S. Cheng, J.-M. Chen, and K.-T. Lu, *Mater. Chem*, 5 (2021) 4937–4949
[8] B. Gao *et al*, *J. Mater. Chem*, 7 (2009) 14–37
[9] M. Ahmad *et al*, *J. Power Sources*, 532 (2022) 231414
[10] B. Vedhanarayanan, K. C. S. Lakshmi, and T. W. Lin, *Batteries*, 9 (2023)
[11] M. G. Hosseini and E. Shahryari, *Ionics (Kiel)*, 25 (2019) 2383–2391
[12] N. Duraisamy *et al*, *J. Mater. Sci. Mater*, 30 (2019) 7435–7446
[13] V. Kumar and H. S. Panda, *Mater. Chem. Phys*, 272 (2021) 125042
[14] J. Park, S. Jo, N. Kitchamsetti, S. Zaman, and D. Kim, *J. Alloys Compd*, 926 (2022) 166815
[15] S. Bhadra and D. Khastgir, *Polym. Test*, 7 (2008) 851–857
[16] L. Zarei-Gharehbaba, R. Najjar, M. G. Hosseini, and P. YardaniSefidi, *Polym. Compos*, n/a (2024)

Fe_2O_3 based supercapacitors derived from electric arc furnace dust

Ozan Aydin[1], Koray B. Donmez[2], Metin Gencten[1], Burak Birol[1]

[1] Yildiz Technical University, Faculty of Chemical and Metallurgical Engineering, Department of Metallurgy and Materials Engineering, 34210 Istanbul, Turkey

[2] Sabanci University, Nanotechnology Research and Application Center, 34956, Istanbul, Turkey

The increasing global energy demand—driven by population growth, industrialization, and the shift toward sustainable technologies—has emphasized the need for energy storage systems that are both efficient and reliable [1]. In this regard, supercapacitors have attracted significant interest as next-generation energy storage devices due to their superior cycle life, low weight, high power density, and stable operation over a wide temperature range [2].

Transition metal oxides are among the most promising electrode materials for supercapacitors owing to their high specific capacitance and wide electrochemical windows. Their charge storage is primarily based on pseudocapacitive mechanisms involving fast and reversible redox reactions both on the surface and within the bulk of the material [3]. However, conventional synthesis methods for metal oxides often require high temperatures, controlled environments, or complex procedures, increasing energy use and production costs.

To address these challenges, the use of recycled waste-derived materials as electrodes has gained attention, offering both cost reduction and environmental benefits [4,5]. Electric arc furnace dust (EAFD), a byproduct of steelmaking, is rich in metal oxides formed by the condensation of volatilized metals in exhaust filters [6]. Its composition makes it a promising low-cost and energy-efficient raw material for the fabrication of metal oxide-based supercapacitor electrodes.

In the current study, EAFD was subjected to an acid leaching process using H_2SO_4 solutions to extract iron and other metal ions into solution. The resulting leach liquor was subsequently treated through a jarosite precipitation process to selectively remove iron in the form of jarosite. The obtained jarosite phase was then thermally decomposed via calcination to produce Fe_2O_3 particles. The structural and morphological properties of the synthesized Fe_2O_3 were thoroughly characterized by X-ray diffraction (XRD) to identify its crystalline phases, and by scanning electron microscopy (SEM) to examine its surface morphology and particle size distribution. The synthesized Fe_2O_3 was further utilized as an electrode material for the fabrication of asymmetric coin-cell supercapacitors. The electrochemical performance of the assembled devices was systematically evaluated using a combination of cyclic voltammetry (CV), electrochemical impedance spectroscopy (EIS), and galvanostatic charge-discharge (GCD) techniques. These electrochemical analyses provided insights into the specific capacitance, charge–discharge behavior, and cycling stability of the Fe_2O_3-based supercapacitors, highlighting the material's potential for use in energy storage applications.

Acknowledgment

This work has been supported by Scientific and Technological Research Council of Turkey (TÜBİTAK) under project number 123M490. O. Aydin would like to express his gratitude for the support of the TÜBİTAK BİDEB-2211-A Program. Moreover, M. Gencten thanks to Turkish Academy of Sciences for Outstanding Young Scientists Awards (GEBİP).

References

[1] G.G. Njema, R.B.O. Ouma, J.K. Kibet, Journal of Renewable Energy 2024 (2024) 1–35

[2] A. Aghmadi, O.A. Mohammed, Batteries 10 (2024) 141.

[3] P. Forouzandeh, V. Kumaravel, S.C. Pillai, Catalysts 10 (2020) 1–73

[4] M. Vijayakumar, A. Bharathi Sankar, D. Sri Rohita, T.N. Rao, M. Karthik, ACS Sustain Chem Eng 7 (2019) 17175–17185

[5] K. Adaikalam, A.M. Teli, K.P. Marimuthu, S. Ramesh, H. Lee, H.S. Kim, H.-S. Kim, Nanomaterials 14 (2024) 1129

[6] A.G. Guézennec, J.C. Huber, F. Patisson, P. Sessiecq, J.P. Birat, D. Ablitzer, Powder Technol, (2005) 2–11

Ozan Aydin was graduated from Gebze Technical University in 2019 and obtained his M.Sc degree from Yildiz Technical University Metallurgical and Materials Engineering Department in 2023. Currently, he is a Ph.D student, and works with the title of Research Assistant in the same department. His research interest covers hydrometallurgy, recycling, waste valorization and supercapacitors.

Presentating author: Ozan Aydin, e-mail: ozan.aydin@yildiz.edu.tr tel: +90 5349241272

Recovery of Nickel-Based Materials from Ni-Ti Alloys for Application as Electrode Materials in Supercapacitors

Berk Coban[1]*, Mert Zoraga[2], Burak Birol[1], Metin Gençten[1]

[1]Yildiz Technical University, Istanbul Türkiye
[2]Istanbul University-Cerrahpaşa, Istanbul, Türkiye

The demand for fossil fuels has led to several issues, including rising fuel costs, global warming, population growth, and geopolitical tensions [1-4]. Addressing these challenges requires enhancing alternative energy sources, such as renewable energy, and improving energy storage solutions. Supercapacitors have emerged as a significant alternative due to their high power densities and extended charge-discharge cycle lifespans [5].

Ni-Ti is extensively utilized in industry, yet there is no recycling process for products at the end of their life cycle due to the challenging conditions involved in manufacturing the alloy. Since Ni-Ti is frequently employed as a biomaterial, its production process is subject to stringent restrictions, as even minimal impurities can significantly degrade its properties [6].

In this study, an endodontic waste Ni-Ti rotary files were leached through a hydrometallurgical route to obtain the metallic values. The recovered values then were precipitated via pH adjustment and with the introduction of sulfur ions into the leach solution. From the precipitate an asymmetric type supercapacitor was produced successfully.

Waste Ni-Ti files underwent characterization using XRF analysis, with the findings presented in Table 1. The analysis revealed that the material primarily consists of nickel and titanium, with negligible impurities. Following characterization, the material was cut into small pieces and subjected to leaching in H_2SO_4. Various temperatures (55-85°C), solid-to-liquid ratios (1/10-1/50), and $H2SO_4$ concentrations (1-5 M) were tested to determine the optimal conditions. Once the material was successfully leached, the leach liquor was separated from the solid residue. By adjusting the pH of the leach liquor using a NaOH solution, the metallic values were precipitated individually. Nickel ions were precipitated at pH=5 in the presence of NaS_2. The precipitated material was then used to produce an asymmetric type supercapacitor, which was characterized through cyclic voltammetry (CV), galvanostatic charge-discharge and electrochemical impedance spectroscopy.

Table 1. XRF analysis of the Ni-Ti rotary files (wt%)

Ni	Ti	Zn	Fe	Au
56.62	43.19	0.13	0.05	0.01

Acknowledgment

This work was supported by the Yildiz Technical University under FBA-2025-7142 project code.

References

[1] P. Yang and W. Mai, Nano Energy, 8 (2014) 274-290.
[2] S. Kim, K. Kang, S. Kim and J. Jang, RSC adv., 4 (2014) 59310-59314.
[3] X. Li, W. Zhang, F. Gao and J. Fand, ACS Applied Materials & Interfaces, 6 (2014) 20569-20573.
[4] S. Xu, C. Hessel, H. Ren, R. Yu, Q. Jin, M. Yang, H. Zhao and D. Wang, Energy Environ. Sci., 7 (2014) 632-637.
[5] A. González, E. Goikolea, J. Barrena and R. Mysyk, Renewable and Sustainable Energy Reviews, 58 (2016) 1189-1206.
[6] A. Pelton, S. Russell and J. Dicello, The Journal of the Minerals 55 (2003) 33-37.

Berk Çoban graduated with a B.Sc. degree in Metallurgical and Materials Engineering from Istanbul University-Cerrahpasa in 2021 and completed his M.Sc. at the same department in 2024. Since 2023, he has been working as a research assistant in the Department of Metallurgical and Materials Engineering at Yildiz Technical University, where he also started his Ph.D. studies in 2024. His research interests include hydrometallurgy, supercapacitors, and lithium-ion battery technologies.
Presentating author: Berk ÇOBAN, e-mail: berk.coban @yildiz.edu.tr tel: +90 531 294 20 75

Synthesis and characterization of poly(ethylene thiosuccinate) (PETS) with succinic anhydride and 1,2-ethanedithiol monomers as supercapacitor electrode materials

Laya Zarei-Gharehbaba[1,2], Reza Najjar[1*], Mir Ghasem Hosseini[2]

[1]Polymer Research Laboratory, Faculty of Chemistry, University of Tabriz, Tabriz, Iran
[2]Electrochemistry Research Laboratory, Department of Physical Chemistry, Faculty of Chemistry, University of Tabriz, Tabriz, Iran.

Abstract

Sulfur, as a mineral element, plays an important role in the synthesis of organic compounds and polymer chemistry. Due to its reactivity, it produces a wide range of compounds with specific functional groups that have diverse physical and chemical properties. Polythioesters are a group of polymers with a sulfur-containing functional group that, unlike polyesters, has been less studied.
Polythioesters usually have high melting points and thermal stability, and low solubility in organic solvents.However, the reaction temperature, type of monomers, and polymerization methods affect the specific properties of the product. Various methods for synthesizing these polymers have been mentioned in the literature, but the use of succinic anhydride monomer has been investigated for the first time in this study for the synthesis of poly(ethylene thiosuccinate) (PETS) as polythioester in the presence of 1,2-ethanedithiol monomer without the presence of a catalyst. Identification of the polymer by FT-IR, ^{1}HNMR and EDAX analyses confirm its successful synthesis. Also, the melting point and glass transition temperature of the polymer by DSC analysis are 142 and 88, respectively. FE-SEM images show amorphous morphology for the polymer. Cyclic voltammetry (CV), galvanostatic charge-discharge (GCD), and electrochemical impedance spectroscopy (EIS) techniques were investigated for neat PETS and its nanocomposite with multi-walled carbon nanotubes and nickel(II) cobalt hexacyanoferrate (PETS/MWCNT + 5% Ni_2CoHCF).

1.Introduction

The thioester bond is a common functional group, especially in biological molecules, that has interesting properties and serves as a key component in biological systems. Unlike thioesters, esters are stabilized by resonance structures. The non-bonding pair of electrons on the oxygen atom attached to the carbonyl group resonates with the double bond electrons of the carbonyl group, forming a partial double bond that prevents rotation about the C-O single bond [1]. A similar resonance structure can be considered for thioesters, however, this resonance structure does not have much effect on the stability of thioesters because the overlap of the sulfur p3 orbitals with the carbon p2 orbitals is weak. Therefore, thioesters are very electrophilic and are more susceptible to attack by nucleophiles [2]. This makes them excellent acyl transfer agents, which nature has exploited. As acetyl-CoA acts as an acetylating reagent in the metabolism of cellular components such as peptides, fatty acids, terpenes, porphyrins, and lipids. In addition, the thiolate and thiol anions are good leaving groups due to their high polarizability and low degree of dipole [3]. The replacement of sulfur atoms with oxygen atoms in the polymer chain of polythioesters enhances their electrical, mechanical, optical, and thermal characteristics, in addition to their chemical resistance [4]. The chemical synthesis of polythioesters was first reported in 1951. However, the relatively complex and inefficient processes that require toxic and very expensive reagents are not suitable for commercialization [5]. In general, the synthesis of polythioesters is carried out by 1) addition polymerization of dithiol acids to non conjugatediolefins, 2) condensation reactions of dithiols with diacids or their derivatives such as diacid chlorides [6], 3) addition polymerization of bicyclic thioethers (e.g., tyranes) with active diacid derivatives [7], 4) ring-opening polymerization [8], and 5) microbial synthesis [9-11]. The first studies on the synthesis of polythioesters, carried out in the 1950s, were carried out using aliphatic dithiols and aliphatic or aromatic dichloroacids without solvent or with benzene solvent in the presence of pyridine. The low intrinsic viscosity of the obtained polymers indicates that only polymers with low molecular weight are synthesized. Polymerization using aromatic and aliphatic-aromatic dithiols carried out in the presence of NaOH as a hydrochloride acceptor gives high molecular weight polythioesters [12]. Ring-opening polymerization is another method for the synthesis of polythioesters, which uses specific monomers and was first performed in 1968 by Wise and Overberger [13-14]. The general reaction mechanism in this method is carried out in the presence of cationic and anionic initiators.
In this research, poly(ethylene thiosuccinate) (PETS) was synthesized with succinic anhydride and 1,2-ethanedithiol monomers and its structure was investigated by various methods such as FT-IR and ^{1}HNMR and thermal analysis of

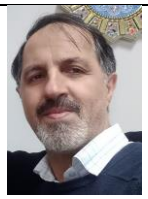

Dr. Reza Najjar, professor of chemistry currently working at the Faculty of Chemistry, University of Tabriz. Has has obtained PhD in polymer chemistry from Aachen University of Technology (RWTH-Aachen Germany) in June 2006, M. Sc., Chemistry, Sharif University of Technology, Tehran, Iran 1997, and B. Sc., Chemistry, University of Tabriz, Iran, 1994. His main research is focused on the preparation of new materials and investigation of their performance in various applications mainly related to the energy issues.

Reza Najjar, e-mail: najjar@tabriz.ac.ir T tel: +98-41-33393101, Cellphone: +98-912-0717158

the polymer by differential scanning calorimetry (DSC). Also, the morphology of the polymer was investigated by FE-SEM analysis.

2.1 Materials succinic anhydride, 1,2-ethanedithiol, triethylamine and N,N- dimethylformamide were purchased from Merck and used without any further purification.

2.2 . Preparation of poly(ethylene thiosuccinate) (PETS)

An appropriate molar amount of succinic anhydride was completely dissolved in dry DMF solvent. Then, 1,2-ethanedithiol was added to the reaction mixture at a molar ratio of 1:1 with succinic anhydride monomer and stirred under an argon atmosphere at room temperature. The reaction mixture was then heated to 80 °C in an oil bath under stirring and argon gas for 24 h until it turned from colorless to yellow. After that, the reaction temperature was increased to 100 °C and the reaction was continued for a certain period of time under the same previous conditions. Then a white precipitate was formed, which was separated by filtration and washed several times with distilled water, then dried in a vacuum oven at 60 °C for 12 hours. The reaction yield was 60%.

3- Results and Discussions

The FT-IR spectrum of PETS polymer is shown in **Fig. 1**. The absorption bands appearing in the range of 3031-2922 cm^{-1} are attributed to the stretching vibrations of aliphatic C-H bonds. The broad absorption band in the range of 2400 cm^{-1} to 3435 cm^{-1} is related to the stretching vibrations of the O-H bond in the possible carboxylic acid present in the polymer chain. The absorption bands due to the stretching vibrations of the S-H bonds remaining at the ends of the PETS chains are observed at 2552 cm^{-1} and 2680 cm^{-1}. The absorption band at 1687 cm^{-1} is assigned to the stretching vibrations of the C=O bonds in the thioester groups. The bands appearing at 1367 cm^{-1} and 1406 cm^{-1} are assigned to the bending vibrations of the C-S bonds in the –S-CH2- and –S-CO- groups. The stretching vibrations of the C-C bonds are observed at 1247-1128 cm^{-1}.

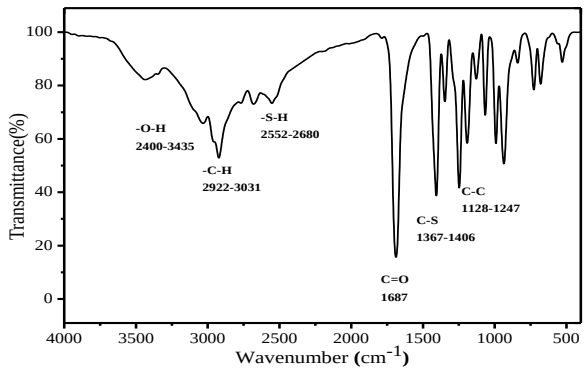

Fig. 1. The FTIR spectrum of PETS

Fig. 2. shows the ^{1}HNMR spectrum of the PETS polymer. This spectrum was taken in CDCl3 solvent. The triplet peak appearing at 2.2 ppm chemical shift is due to the protons of (a) -S- CH2- and the triplet peak at 1.5 ppm is due to the protons of (b) -CO-CH2- carbon. The peak corresponding to the -S-H proton appeared at 1.2 ppm. The peak at 7.25 ppm is related to the deuterated protons in chloroform. Due to the small number of acidic functional groups in the polymer, the probability of the appearance of the absorption peak corresponding to the acidic proton was very low and did not appear.

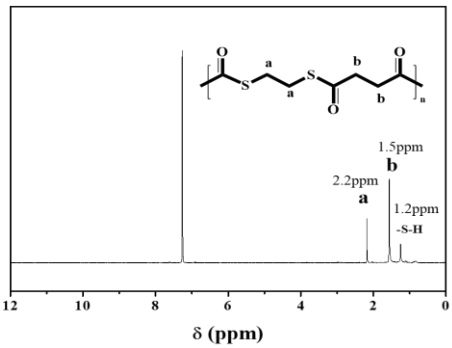

Fig. 2. 1H NMR spectrum of PETSpolymer

Differential scanning calorimetry (DSC) is a method for studying polymers in which important information about the glass transition temperature, melting point, and crystallization temperature is obtained by heating and cooling the material**. Fig. 3.** shows the graph of the DSC analysis of the PETS polymer. The results obtained are summarized in **Table 1**. The analysis was performed at a scan rate of 5 °C/min under a nitrogen atmosphere.

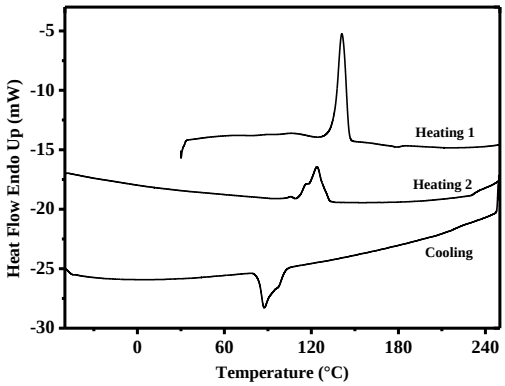

Fig. 3. DSC thermogram of PETS polymer

Table 1

Data extracted from DSC thermograms of PET DTC

T_m (°C)	Melting temperature	142
ΔH_m (J. g^{-1})	Enthalpy of melting	86
T_c (°C)	Crystallization temperature	87
ΔH_c (J. g^{-1})	Enthalpy of crystallization	-47
T_g (°C)	Glass transition temperature	88

Fig. 4. shows FE-SEM images of PETS polymer at 5 and 10 µm scales. The images show an amorphous structure and morphology without distinct particles for the polymer.

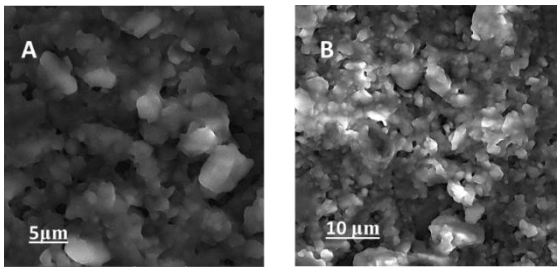

Fig. 4. FE-SEM image of PETS at the scale of 5 and 10 µm.

The EDAX spectrum of the polymer is shown in **Fig. 5**. According to the EDAX spectrum, the presence of C, O, and S atoms confirms the successful synthesis of the polymer.

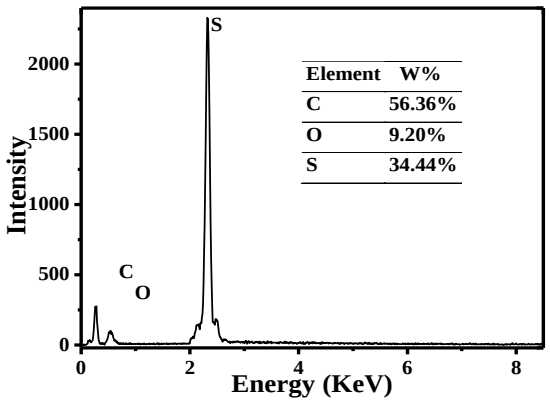

Fig. 5. EDAX spectrum of PETDTC

Electrochemical measurements

The electrochemical behavior of polymer nanocomposite with multiwall nanotubes at a ratio of 1:1 and the addition of 5% synthesized nickel(II)cobalt hexacyanoferrate Ni_2CoHCF [15] nanoparticles was investigated using cyclic voltammetry (CV), galvanostatic charge-discharge (GCD), and electrochemical impedance spectroscopy (EIS) techniques. Electrochemical behavior of nanocomposite in three-electrode system was used in 0.5 M sodium sulfate as electrolyte. Saturated calomel electrode (SCE) was used as reference electrode and a platinum sheet (1 cm × cm ^{2}) was used as auxiliary electrode. 10% Nafion solution in isopropanol was used as electrode material binder. Fully dispersed electrode material was coated on glassy carbon as working electrode with area of 0.1256 cm 2 in amount of 10 µl. After the solvent evaporated, electrochemical analyses were performed. **Fig. 6.** shows the CV curves of neat PETS polymer and its nanocomposite at different scan rates from 10-80 mV.s $^{-1}$. According to the curves, the current density increases with increasing scan rate and the shape of the curves does not change, indicating the good performance of these electrodes at high scan rates. The CV curve of the PETS in **Fig. 6A-6B** shows an ideal quasi-rectangular shape, which can be attributed to the non-Faradic charge storage mechanism at the interface between the electrode and the electrolyte. In the presence of Ni_2CoHCF nanoparticles (**Fig. 6B**), in addition to improving the current density, oxidation and reduction peaks related to the $Fe^{II/III}$ redox reaction appeared at a potential of near 400 mV. **Fig. 6C-6D** shows the charge-discharge curves of the electrodes at different current densities.

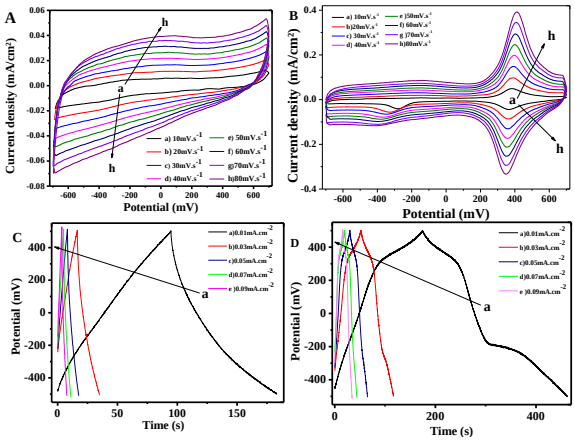

Fig. 6. CV curve of A) PETS B) PETS/MWCNT composite(1:1)+5% Ni_2CoHCF . Charge/discharge curve of D) PETS E) PETS/MWCNT composite(1:1)+5% Ni_2CoHCF .

The general shape of these graphs at different current densities confirms the good behavior of the supercapacitor material over a wide current range in sodium sulfate electrolyte. The charge-discharge curves for the PETS electrode are approximately symmetrical triangle-shaped, indicating the reversibility of the discharge process for the electrode. The nonlinear of the curve for the nanocomposite (**Fig. 6D**) is related to the Faradaic reactions of the Ni_2CoHCF nanoparticles. The long discharge time of the electrode with the nanocomposites compared to the neat polymer electrode indicates its high specific capacity, which is mainly due to the synergistic effects of the Ni_2CoHCF nanoparticles and the carbon nanotubes. Electrochemical impedance spectroscopy technique is used to study the capacitive behavior of electrodes. Charge transfer resistance (R_{ct}) is a parameter obtained by this method and its low value indicates easier charge transfer process in these electrodes. The Nyquist curves for the prepared electrodes are shown in **Fig. 7**. The equivalent circuit in **Fig. 7.** is in perfect agreement with the experimental impedance data. In this circuit, R_1, CPE1, R_2, and W1 are the solution resistance, the electric double layer constant phase element, the charge transfer resistance, and the Warburg element, respectively. The parameters of this equivalent circuit are shown in **Table 2**. According to the obtained data, the Faradaic reaction of Ni2CoHCF nanoparticles in the nanocomposite at the interface of the electrode and electrolyte increased the ionic conductivity and the amount of the CPE element increased, resulting in a decrease in the charge transfer resistance (R2).

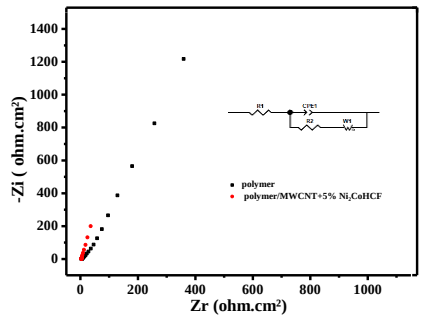

Fig. 5. Nyquist diagram of PETS and its composites as electrode material and equivalent circuit for fitting experimental impedance data of electrodes, Nyquist diagram of equivalent circuit for fitting experimental impedance data of various supercapacitor electrode made by various materials: □) PETS ○) PETS/MWCNT+5%Ni_2CoHCF.

Table 2
Equivalent circuit element values with experimental data of impedance diagrams obtained from **Fig. 7.**

Electrode material	Values of equivalent circuit elements				
	R1 (Ω)	CPE-T ($\Omega^{-1}cm^{-2}s^{CPE-P}$)	CPE-P	R2 (Ωcm^2)	W-R ($\Omega s^{-0.5}$)
PETS	0.93	0.001056	0.70	6.98	1269
PETS/MWCNT + 5% Ni_2CoHCF	3.31	0.008426	0.89	4.62	203

4- Conclusions

poly(ethylene thiosuccinate) (PETS) was synthesized with succinic anhydride and 1,2-ethanedithiol monomers and its structure was investigated by FT-IR and ^{1}HNMR. DSC analysis show a glass transition temperature of 88 °C for the polymer. Amorphous morphology is visible based on FE-SEM images for the synthesized polymer. Electrochemical analyses showed improved behavior for the nanocomposite. Also, the Faradaic behavior in the presence of nanoparticles was observed in CV and charge /discharge curves. The charge transfer resistance for the nanocomposite was lower than that of the neat polymer due to the synergistic effect of carbon nanotubes and nanoparticles.

Acknowledgement

The work was supported by The University of Tabriz which the Authors gratefully acknowledge.

References

[1] Marlier, John F., Emily J. Fogle, Richard L. Redman, Anthony D. Stillman, Matthew A. Denison, and Lori I. Robins, A mechanistic study of thioester hydrolysis with heavy atom kinetic isotope effects. The Journal of organic chemistry, 2015. 80(3): p. 1905-1908.

[2] Yang, W. and D.G. Drueckhammer, Understanding the relative acyl-transfer reactivity of oxoesters and thioesters: computational analysis of transition state delocalization effects. Journal of the American Chemical Society, 2001. 123(44): p. 11004-11009.

[3] Koval', I., Synthesis, structure, and physicochemical characteristics of thiols. Russian journal of organic chemistry, 2005. 41: p. 631-648.

[4] Yue, Tian-Jun, Ming-Chao Zhang, Ge-Ge Gu, Li-Yang Wang, Wei-Min Ren, and Xiao-Bing Lu, Precise synthesis of poly (thioester) s with diverse structures by copolymerization of cyclic thioanhydrides and episulfides mediated by organic ammonium salts. Angewandte Chemie, 2019. 131(2): p. 628-633.

[5] Andree Ben, C. and A. Steinbüchel, Recent developments in non-biodegradable biopolymers: Precursors, production processes, and future perspectives. Applied microbiology and biotechnology, 2019. 103(1): p. 143-157.

[6] You, Nam-Ho, Tomoya Higashihara, Suzuki Yasuo, Shinji Ando, and Mitsuru Ueda, Synthesis of sulfur-containing poly (thioester) s with high refractive indices and high Abbe numbers. Polymer Chemistry, 2010. 1(4): p. 480-484.

[7] Kameyama, A., Y. Kimura, and T. Nishikubo, New synthesis of poly (S-thioester) s by regioselective addition reaction of bis (thiirane) s with diacyl chlorides using quaternary onium salts. Macromolecules, 1997. 30(21): p. 6494-6497.

[8] Ura, Yasuyuki, Mohammad Al-Sayah, Javier Montenegro, John M. Beierle, Luke J. Leman, and M. Reza Ghadiri, Dynamic polythioesters via ring-opening polymerization of 1,4-thiazine-2,5-diones. Organic & biomolecular chemistry, 2009. 7(14): p. 2878-2884.

[9] Suzuki, M., K. Makimura, and S. i. Matsuoka, Thiol-Mediated Controlled Ring-Opening Polymerization of Cysteine-Derived β-Thiolactone and Unique Features of Product Polythioester. Biomacromolecules, 2016. 17(3): p. 1135-1141.

[10] Iwata, S., K. Toshima, and S. Matsumura, Enzyme-catalyzed preparation of aliphatic polyesters containing thioester linkages. Macromolecular rapid communications, 2003. 24(7): p. 467-471.

[11] Lütke-Eversloh, Tina, Andreas Fischer, Uwe Remminghorst, Jumpei Kawada, Robert H. Marchessault, Ansgar Bögershausen, Martin Kalwei, Biosynthesis of novel thermoplastic polythioesters by engineered Escherichia coli. Nature materials, 2002. 1(4): p. 236-240.

[12] Kultys, A., Sulfur-Containing Polymers. Encyclopedia of polymer science and technology, 2002.

[13] Overberger, C.G. and J.K. Weise, Anionic ring-opening polymerization of thiolactones. Journal of the American Chemical Society, 1968. 90(13): p. 3533-3537.

[14] Purohit, Vishal, Marlena Pieta, Joanna Pietrasik, and Christopher Plummer, Recent advances in the ring-opening polymerization of sulfur-containing monomers. Polymer Chemistry, 2022.

[15] Qiu, Y., Lin, Y., Yang, H., & Wang, L., Ni-doped cobalt hexacyanoferrate microcubes as battery-type electrodes for aqueous electrolyte-based electrochemical supercapacitors. Journal of Alloys and Compounds, 2019. 806: p. 1315-1322.

RENEWABLE HYDROGEN AND HYDROGEN PRODUCTION

g-C_3N_4-based Z-Scheme Ternary Heterostructures for Photocatalytic Hydrogen Production

Mehmet Poyraz[1,2] and Fatih Pişkin[2,3]

[1]Dept. of Mechanical Engineering, Muğla Sıtkı Koçman University, Muğla, Türkiye

[2]HyEn Materials Technologies Research Development and Consultancy Inc., Muğla, Türkiye

[3]Dept. of Metallurgical and Materials Engineering, Muğla Sıtkı Koçman University, Muğa Türkiye

Hydrogen is industrially produced by several methods such as natural gas reforming, coal gasification, and electrolysis of water [1]. Among them, natural gas reforming and coal gasification, causing fossil fuel-dependent hydrogen, are the current dominant production methods. Therefore, the utilization of production methods relying on renewable hydrogen sources is of great importance to achieve sustainable hydrogen production.

Photocatalytic hydrogen production is one of the promising methods since it only requires solar energy and water with the use of semi-conducting catalysts. However, the photocatalysts in question suffer from several problems such as chemical instability, low electron conductivity, covering a limited portion of the solar spectrum, electron-hole pair recombination, etc. [2]. These problems result in low quantum efficiencies in photocatalytic water splitting. That's why, there are some strategies to improve catalysts' efficiencies such as doping, surface decoration, and formation of heterojunctions (Type-I, Type-II, Type-III, or Z-Scheme) [3,4]. Among them, the Z-Scheme heterojunction strategy might be an effective way to suppress the electron-hole pairs recombination which has a critical role in the catalyst efficiency.

In the current work, dual Z-Scheme heterojunctions composed of g-C_3N_4, α-Fe_2O_3, and α-MnO_2 were systematically investigated to reveal their photocatalytic activity for hydrogen production. We performed a sequential synthesis for ternary heterostructure where α-Fe_2O_3 and α-MnO_2 were co-deposited onto g-C_3N_4 nanosheets.

Structural, chemical, optical, and morphological investigations were carried out to identify the ternary catalyst system. Following the material characterizations, 50 mg of g-C_3N_4, α-Fe_2O_3, and α-MnO_2 ternary heterostructure with a mole ratio of 5:1:1 was added into a 50 ml aqueous solution of 0.5 M Na_2S/Na_2SO_3 without the use of any noble metal. Photocatalytic water splitting tests were performed under UV (250-385 nm) and visible (385-740 nm) lights generated by Asahi Spectra MAX-350300W Xenon light source equipped with a mirror system to isolate the desired range of wavelengths. Gases released as a result of photocatalytic water splitting were analyzed and monitored by an online gas analyzer (Hiden Analytical QGA). Photocatalytic water splitting results indicated that the hydrogen production of the ternary heterostructure exceeds 500 μmol/g in an hour under UV light.

Acknowledgment

Authors gratefully acknowledge the financial support from the Scientific and Technological Research Council of Turkey Technology and Innovation Support Programs Directorate under the 1507 - TUBITAK SME R&D Start-up Support Program and project number 7240243.

References

[1] Nikolaidis P, Poullikkas A. A comparative overview of hydrogen production processes. Renew Sustain Energy Rev 2017;67:597–611. https://doi.org/10.1016/j.rser.2016.09.044.

[2] Low J, Yu J, Jaroniec M, Wageh S, Al-Ghamdi AA. Heterojunction Photocatalysts. Adv Mater 2017;29. https://doi.org/10.1002/adma.201601694.

[3] Tang Q, Meng X, Wang Z, Zhou J, Tang H. One-step electrospinning synthesis of TiO2/g-C3N4 nanofibers with enhanced photocatalytic properties. Appl Surf Sci 2018;430:253–62. https://doi.org/https://doi.org/10.1016/j.apsusc.2017.07.288.

[4] Fajrina N, Tahir M. A critical review in strategies to improve photocatalytic water splitting towards hydrogen production. Int J Hydrogen Energy 2019;44:540–77. https://doi.org/10.1016/j.ijhydene.2018.10.200.

Fatih Pişkin is an Assoc. Professor in Department of Metallurgical and Materials Engineering at Muğla Sıtkı Koçman University. He received his BSc degree from Anadolu University in 2009, MSc and PhD degrees from Middle East Technical University in 2013 and 2018, respectively.

Corresponding author: Fatih Pişkin, e-mail: fatihpiskin@mu.edu.tr tel: +90 252 211 20 56

Effect of HNT surface modification on photocatalytic hydrogen production of HNT/g-C_3N_4

Mehmet Poyraz[1,2] and Fatih Pişkin[2,3]

[1]Dept. of Mechanical Engineering, Muğla Sıtkı Koçman University, Muğla, Türkiye

[2]HyEn Materials Technologies Research Development and Consultancy Inc., Muğla, Türkiye

[3]Dept. of Metallurgical and Materials Engineering, Muğla Sıtkı Koçman University, Muğa Türkiye

Photocatalytic water splitting is a promising method enabling environmentally friendly hydrogen production. In recent years, a large number of materials such as TiO_2 [1], ZnO [2], CdS [3], g-C_3N_4 [4], and Fe_2O_3 [5] have been studied to develop an efficient photocatalyst for photocatalytic water splitting. Among them, metal-free g-C_3N_4 takes considerable attention due to its chemical stability, suitable band gap (2.7 eV) allowing absorption of visible light, tunable electronic properties, and low cost [6]. However, it suffers from photoinduced charge recombination, which leads to inefficient water splitting and hence hydrogen production [7]. There are, therefore some strategies such as doping and the formation of heterojunction to overcome charge recombination issues [8]. Another critical problem is the strong agglomeration of g-C_3N_4 catalysts causing a reduction in the effective surface area and hence photocatalytic activity. This is typically due to the utilization of high-temperature synthesis routes [6]. Employment of substrate material and synthesizing g-C_3N_4 on the substrate is one of the effective approaches to prevent agglomeration of g-C_3N_4 [9].

In the current work, halloysite nanotubes (HNT) were employed as a substrate material in order to reduce the g-C_3N_4 agglomeration and extend the effective surface area of g-C_3N_4, which leads to strengthening of the pathways of charge transfer and prolonging the lifetimes of photoexcited carriers. In the study, the HNT surface was also chemically modified using both acidic (H_2SO_4) and alkali (NaOH) solutions to create defects on the HNT surface and unzip the HNT spiral structure [10]. This approach also results in the formation of hydroxyl groups on the surface of HNTs, allowing for better dispersion of the HNT in water, and hence better dispersion of g-C_3N_4 photocatalysts.

g-C_3N_4 synthesized on the HNTs were chemically and structurally characterized. Following the material characterizations, g-C_3N_4/HNT photocatalysts were subjected to photocatalytic water splitting tests to identify the effect of HNT surface modification on the photocatalytic activity of g-C_3N_4 photocatalysts. Water splitting tests were performed under UV (250-385 nm) and visible (385-740 nm) lights generated by the Asahi Spectra MAX-350 300W Xenon light source. The gases produced as a result of photocatalytic water splitting were analyzed and monitored by an online gas analyzer (Hiden Analytical QGA).

Acknowledgment

Authors gratefully acknowledge the financial support from the Scientific and Technological Research Council of Turkey Technology and Innovation Support Programs Directorate under the 1507 - TUBITAK SME R&D Start-up Support Program and project number 7240243.

References

1. T. Gupta, Samriti, J. Cho, and J. Prakash, Mater. Today Chem. **20**, 100428 (2021).
2. S. Goktas and A. Goktas, J. Alloys Compd. **863**, 158734 (2021).
3. X. Ning and G. Lu, Nanoscale **12**, 1213 (2020).
4. A. Torres-Pinto, A. M. Díez, C. G. Silva, J. L. Faria, M. Á. Sanromán, A. M. T. Silva, and M. Pazos, Fuel **360**, 130575 (2024).
5. Y. Li, S. Zhu, Y. Liang, Z. Li, S. Wu, C. Chang, S. Luo, and Z. Cui, Mater. Des. **196**, 109191 (2020).
6. L. Ai, R. Shi, J. Yang, K. Zhang, T. Zhang, and S. Lu, Small **17**, 2007523 (2021).
7. N. Güy, Appl. Surf. Sci. **522**, 146442 (2020).
8. Y. Liu, J. Tian, L. Wei, Q. Wang, C. Wang, Z. Xing, X. Li, W. Yang, and C. Yang, Sep. Purif. Technol. **257**, 117976 (2021).
9. J. Li, M. Zhou, Z. Ye, H. Wang, C. Ma, P. Huo, and Y. Yan, RSC Adv. **5**, 91177 (2015).
10. A. Abotaleb, D. Al-Masri, A. Alkhateb, K. Mroue, A. Zekri, Y. Mashhour, and A. Sinopoli, RSC Adv. **14**, 4788 (2024).

Mehmet Poyraz is a Lecturer in Department of Mechanical Engineering at Muğla Sıtkı Koçman University. He received his BSc degree from Suleyman Demırel University in 2005, MSc and PhD degrees from Suleyman Demırel University in 2010 and 2019, respectively.

Corresponding author: Mehmet Poyraz, e-mail: mpoyraz@mu.edu.tr tel: +90 252 211 11 29

LSMA-LCMF Dual Perovskite Oxides for Hydrogen Production

Seyfettin Berk Şanlı[1,2], Gülhan Çakmak[1,2,3], Fatih Pişkin[1,2,3] and Berke Pişkin[1,2,3*]

[1]Mugla Sitki Kocman University, Engineering Faculty, Metallurgical and Materials Engineering Department, Mugla, Turkiye

[2]Energy Materials Laboratory, Mugla Sitki Kocman University, 48000, Mugla, Turkiye

[3]HyEn Materials Technologies Research Development and Consultancy Inc., Mugla, Turkiye

*Corresponding Author

Perovskite oxides are attracting attention as they can be used in thermochemical water splitting (TWS) reactions because they allow compositional diversity and provide higher structural stability. However, they need improvement in terms of structural stability, high reaction kinetics, and high stability during the thermal cycles [1].

For this purpose, it was aimed to improve the hydrogen production rate (>80%) with the existence of hetero-interfaces and preserve stability during the redox cycles. It is known that the hydrogen production capacity of perovskite oxides decreases dramatically (40%-80 %) in initial cycles [2].

In this study, $La_{0.6}Sr_{0.4}Mn_{0.6}Al_{0.4}O_3$-LSMA6464 perovskite oxide and $La_{1-x}Ca_xMn_yFe_{1-y}O_3$-LCMF (Ca=0.4-0.8, Al=0.4-0.8) families were selected for the dual-perovskites where LSMA6464 perovskite oxide is already one of the promising compositions for the TWS [3]. A total of 3 perovskite oxides, LCMF6482, LCMF6464, and LCMF6446, were selected from the LCMF family to create a hetero-interface. These compositions were then evaluated in thermochemical redox reactions (T_{red}=~1400 °C, T_{ox}=~800 °C). The H_2 production curves obtained from LSMA6464-LCMx compositions are given in Figure 1 and the calculated H_2 production rates and capacities are shown in Table 1.

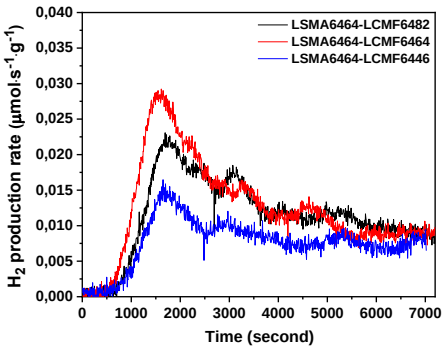

Figure 1. H_2 production curves obtained at 800 °C from dual perovskites of LCMF6482, LCMF6464, LCMF6446 with LSMA6464.

LSMA6464 has the highest hydrogen production with a first-cycle production value of 257.18 µmol/g. LCMF6482, LCMAF6464, and LCMF6446 had the hydrogen production rate with a value of 39.09 µmol/g, 37.21 µmol/g, and 59.51 µmol/g, respectively.

Table 1. H_2 production values obtained from compositions in the LSMA6464-LCMx oxide family in the water splitting test at 800 °C.

LSMA6464-LCMx	Highest H_2 production rate (µmol/g.s)	Time to reach the highest H_2 production (min)	Total H_2 production (µmol/g)
LSMA6464-LCMF6482	0.0232	28	83.92
LSMA6464-LCMF6464	0.0291	27	93.98
LSMA6464-LCMF6446	0.0164	27	53.49

Among the dual-perovskite, LSMA6464-LCM.F6464 was the composition with the highest hydrogen production, with a first cycle production value of 93.98 µmol/g. It was followed by LSMA6464-LCMF6482 and LSMA6464-LCMF6446 with 83.92 µmol/g and 53.49 µmol/g, respectively.

Although there was an improvement in the individual hydrogen production capacity of LCMF perovskite oxides, it was still insufficient to be able to use in TWS. The hydrogen production was not sufficient. Here, it can be commented that the hetero-interface approach has an effect on hydrogen production.

Acknowledgements

This work was supported by TUBITAK (The Scientific and Technological Research Council of Turkey) (Project Number 119M420), which the authors gratefully acknowledge.

References

[1] J.R. Scheffe, A. Steinfeld, Oxygen exchange materials for solar thermochemical splitting of H2O and CO2: a review, Mater Today, 17, 2014

[2] Abanades, Stéphane, Legal, A., Cordier, A., Peraudeau, G., Flamant, G., Julbe, A. 2010a. "Investigation of reactive cerium-based oxides for H2 production by thermochemical two-step water-splitting". Journal of Materials Science, *45*(15), 4163-4173.

[3] Şanlı SB, Pişkin B, Effect of B-site Al substitution on hydrogen production of La0.4Sr0.6Mn1-xAlx (x=0.4, 0.5 and 0.6) perovskite oxides, International Journal of Hydrogen Energy, 2022

Berke Pişkin is an Assoc. Prof. Dr. in the Department of Metallurgical and Materials Engineering at Muğla Sıtkı Koçman University. She earned a BS degree from Anadolu University in 2009, an MS degree from Middle East Techincal University in 2012, and a PhD degree from Middle East Techincal University in 2018.

Corresponding author: Berke Pişkin, e-mail: berkepiskin@mu.edu.tr tel: +90 534 424 20 45

Obtaining Bi_2O_3 via electrochemical method for Solar to Hydrogen processes

Vusala Majidzade, Sevinj Javadova, Samira Jafarova, Nazakat Aliyeva Mammadova and Akif Aliyev
Institute of Catalysis and Inorganic Chemistry Ministry of Science and Education of Azerbaijan Republic, Baku, Azerbaijan

In recent years, Bi-based catalysts have been studied many times due to their low cost, environmental friendliness, high electrochemical activity and high electrocatalytic efficiency for water splitting [1-2]. Bismuth (III) oxide is a semiconductor with excellent physical properties, especially optical and electrical properties, such as a wide energy gap, contributing to the very good photocatalytic properties, high refractive index and permittivity, very good photoconductivity and luminescence properties [6]. Bismuth oxide has six crystallographic structures, designated as α-Bi_2O_3 (monoclinic) [7], β-Bi_2O_3 (tetragonal) [8], δ-Bi_2O_3 (face-centered cubic) [9], γ-Bi_2O_3 (body-centered cubic) [10], ε-Bi_2O_3 (orthorhombic) [11], and ϕ-Bi_2O_3 (triclinic), respectively [12]. Bismuth-based mixed oxides exhibit predominantly n-type semiconductivity and therefore function as photoanodes in photoelectrochemical water splitting process. They exhibit low catalytic activity for oxygen evolution, resulting in hole accumulation at the electrode/electrolyte interface.

The aim of this work is to create corrosion-resistant semiconductor electrode materials that are sensitive to the visible region of the solar spectrum.

To obtain Bi_2O_3, metallic Bi was deposited on nickel electrodes by an electrochemical method. In this case, $Bi(NO_3)_3$ was used as a precursor and dissolved in ethylene glycol. The polarization curve of the process electroreduction bismuth ions shown Fig. 1.

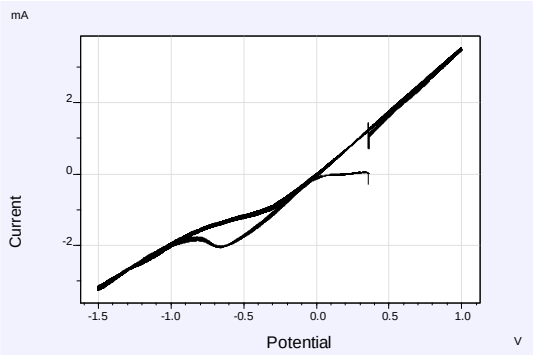

Fig.1. The polarization curve of the process electroreduction bismuth ions.

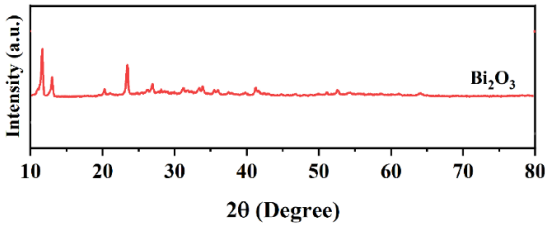

Fig. 2. Results of X-ray phase analysis for Bi_2O_3 obtaining via electrochemical method.

The electroreduction of bismuth ions occurs the potential range -0.25 - (-0.65) V. Starting from -0.25 V, to -0.65 V occurs electroreduction bismuth ions with this reaction:

$$Bi^{3+} + 3e = Bi^0$$

Further, with of the electrode surface passivation (here the electrode surface is completely covered with an bismuth film), the current spent on the process is stabilized. Starting from -0.85 V, with an increase in potential, there is also an increase in current.

After electrodeposition Bi thin films on the Ni electrode, they had been annealid at the 850^0C for obtaining Bi_2O_3. Getting of Bi_2O_3 had been comformed with X-ray analysis.

References

[1] Zhao, X., et al. Appl. Soft Comput., 24, 585–596 (2014)
[2] Syah, R., et al. Catalysts, 11(9), 1099 (2021)
[3] Sudrajat, H., et al. J. Mol. Liq., 242, 433–440 (2017)
[4] Zhang, L., et al. Appl. Catal. A, 308, 105-110 (2006)
[5] Liu, L. et al. Cryst. Eng. Comm, 13, 2529-2532 (2011)
[6] Gurunathan, K. Int. J. Hydrog. Energy, 29(9), 933-940 (2004)
[7] Gandhi, A.C. et al. Nanoscale, 12(47), 24119-24137 (2020)
[8] Aurivillius, B. et al. Nature, 155(3932), 305-306 (1945)
[9] Zhu, S. et al. J. Phys. Chem. C, 121(17) 9394-9401 (2017)
[10] Kodama, H. et al. J. Solid. State Chem., 67, 170-175 (1987)
[11] Cornei, N. et al. Inorg. Chem., 45, 4886-4888 (2006)
[12] Abu-Dief A.M. et al. Mater. Res. Express., 4(3) 035039 (2017)

Ph.D. Vusala Asim Majidzade is with the Institute of Catalysis and Inorganic Chemistry Ministry of Science and Education of the Azerbaijan Republic. Having graduated from Baku State University in 2000, Vusala Majidzade obtained her M.Sc in 2003 and Ph.D. in 2012. Her research interest covers obtaining semiconductor materials on based metal-chalcogenides for the conversion of Solar energy and electrocatalysts for water electrolyzing.

Vusala Majidzade, e-mail: vuska_80@mail.ru

Hydrogen Production from Sodium Borohydride Using Precipitated La_2O_3 Nanoparticles: A Promising Catalytic Approach

Emel Engintepe[1,2], Sibel Duman[3] and Ayşe Nilgün Akın[1,2]

[1]Kocaeli University, Department of Chemical Engineering, Kocaeli, 41380, Turkey
[2]AYARGEM, Alternative Fuels R&D Center, Kocaeli University, Kocaeli, 41380, Turkey
[3]Bingöl University, Department of Chemistry, Bingöl, 12000, Turkey

Hydrogen has emerged as a promising energy carrier due to its high energy density and environmentally friendly nature, making it a key component in the transition to sustainable energy systems. Among various hydrogen production methods, the methanolysis of sodium borohydride ($NaBH_4$) has attracted significant attention due to its ability to generate hydrogen efficiently under mild conditions. $NaBH_4$ is a well-known chemical hydrogen storage material with a high hydrogen content and stability, enabling hydrogen release through catalytic decomposition.

Recent studies have focused on developing efficient catalysts to enhance hydrogen production via $NaBH_4$ methanolysis. Various transition metal-based catalysts, including noble metals such as Pt, Ru, and Pd, have demonstrated high catalytic activity [1]. However, the high cost and scarcity of these metals have driven research toward alternative catalyst materials. Despite extensive research on $NaBH_4$ methanolysis, no studies in the literature have specifically investigated the catalytic behavior of La_2O_3. This study aims to address this gap by synthesizing and characterizing La_2O_3 nanoparticle catalyst for hydrogen production via $NaBH_4$ methanolysis.

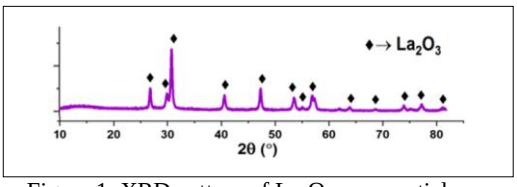

Figure 1. XRD pattern of La_2O_3 nanoparticle.

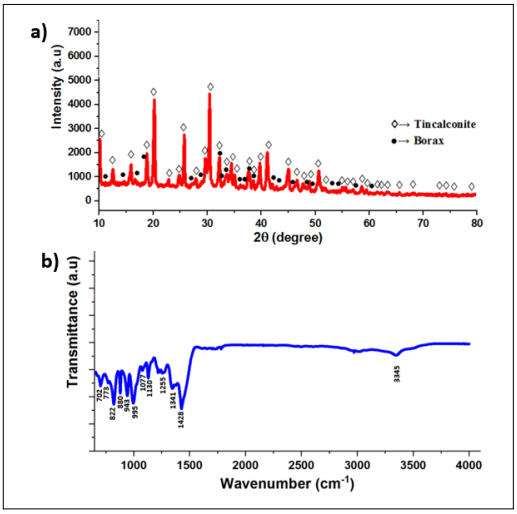

Figure 2. a) XRD b) FTIR spektrum of La_2O_3 catalysts after $NaBH_4$ methanolysis.

Figure 1 presents the XRD patterns of the synthesized La_2O_3 catalysts. In Figure 2, The XRD and FTIR spectra of La_2O_3 catalyst is given after the reaction. The several characteristic peaks, which are indicative of the borate species formed during the methanolysis reaction. The broad O–H band at 3345 cm^{-1} indicates hydroxyl groups and water, confirming the hydrated nature of the borates. Peaks at 1428 cm^{-1} and 1341 cm^{-1} are attributed to B–O^- and asymmetric borate ring stretching, while the 1200–800 cm^{-1} region reflects B–O stretches in tetra-coordinated B units. The band at 943 cm^{-1} suggests loose diborate rings, and peaks between 800–600 cm^{-1} correspond to B–O–B bending [2]. These spectral features, supported by XRD, confirm the formation of borax and tincalconite as reaction products.

The activation energy of the $NaBH_4$ methanolysis reaction was determined using the catalytic activity of La_2O_3 nanoparticle catalyst. To investigate the effect of temperature and to calculate kinetic parameters such as activation energy (Ea), activation enthalpy (ΔH), and activation entropy (ΔS), temperature-dependent experiments were conducted. In this context, methanolysis of 2.0 mmol $NaBH_4$ was carried out in the presence of 4.06 mM La_2O_3 nanoparticle catalyst within the temperature range of 20–40 °C.

This study is the first to explore the use of nanoparticle La_2O_3 catalysts for facilitating both the hydrolysis and methanolysis of $NaBH_4$ under controlled conditions at 25.0±0.1°C. It was found that $NaBH_4$ has much higher catalytic activity and stability in methanolysis than in its hydrolysis. The dependence of the rate of hydrogen production from $NaBH_4$ methanolysis on the amount of La_2O_3 was investigated by performing a series of catalytic reactions using different amounts of La_2O_3.

References

[1] Wang T., Jiang T., Zhang H., Zhao Y. 2022. Advances in catalysts for hydrogen production by methanolysis of sodium borohydride. International Journal of Hydrogen Energy 47:14589-14610.

[2] Hannauer, J., Demirci, U. B., Geantet, C., Herrmann, J. M., Miele, P. (2011). Enhanced hydrogen release by catalyzed hydrolysis of sodium borohydride–ammonia borane mixtures: a solution-state 11B NMR study. Physical Chemistry Chemical Physics, 13(9), 3809-381

Ph.D. Emel Engintepe is a researcher at Kocaeli University, Department of Chemical Engineering, and a member of the Alternative Fuels R&D Center (AYARGEM). Her academic work focuses on the development of nanowire-structured lanthanum-based catalysts for the oxidative coupling of methane (OCM). She has expertise in hydrothermal synthesis, material characterization, and catalytic applications for sustainable energy conversion.

Emel Engintepe, e-mail: emel.engintepe@kocaeli.edu.tr tel: +90 (538) 373 41 09

$La(OH)_3$ and La_2O_3 Nanowires as Efficient Catalysts for Hydrogen Production via Sodium Borohydride Metanolysis

Emel Engintepe[1,2], Sibel Duman[3] and Ayşe Nilgün Akın[1,2]

[1]Kocaeli University, Department of Chemical Engineering, Kocaeli, 41380, Turkey
[2]AYARGEM, Alternative Fuels R&D Center, Kocaeli University, Kocaeli, 41380, Turkey
[3]Bingöl University, Department of Chemistry, Bingöl, 12000, Turkey

Hydrogen is a clean energy carrier with high energy density, making it an attractive fuel option. Among various production methods, sodium borohydride ($NaBH_4$) methanolysis stands out for its safety, fast kinetics, and high hydrogen yield [1]. In this reaction, $NaBH_4$ reacts with methanol (CH_3OH) to produce hydrogen gas and sodium tetramethoxyborate ($NaB(OCH_3)_4$):

$$NaBH_4 + 4CH_3OH \rightarrow NaB(OCH_3)_4 + 4H_2 \qquad (1)$$

$NaBH_4$ is also non-toxic and non-flammable, enhancing its suitability for portable hydrogen systems. While many catalysts have been tested for this reaction, $La(OH)_3$ and La_2O_3 have not yet been studied. Given their catalytic potential, this work investigates hydrothermally synthesized $La(OH)_3$ and La_2O_3 nanowires as novel catalysts for $NaBH_4$ methanolysis, aiming to support sustainable hydrogen generation. The catalysts were characterized using XRD for phase identification, BET for surface area analysis, and FE-SEM for morphological examination. These techniques confirmed the structural and textural properties of the synthesized $La(OH)_3$ and La_2O_3 nanowire catalysts.

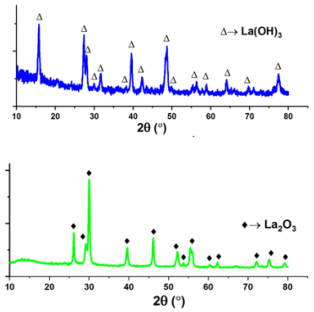

Figure 1. XRD patterns of $La(OH)_3$ and La_2O_3 nanowires.

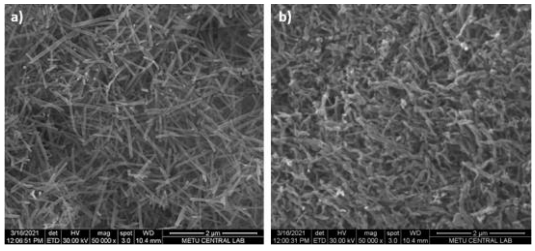

Figure 2. FE-SEM images of (a) $La(OH)_3$ (b) La_2O_3 nanowires.

Figure 1 demonstrates the formation of lanthanum oxides (La_2O_3) catalysts, while Figure 2 illustrate the FE-SEM images of the prepared $La(OH)_3$ and La_2O_3 nanowire catalysts. The specific surface area and total pore volume of the catalysts, as summarized in Table 1, show a significant decrease during the phase transformation from $La(OH)_3$ to La_2O_3.

Table 1. Specific surface area, and total pore volume.

Sample name	Specific surface area (m^2/g)	Total pore volume (cm^3/g)
$La(OH)_3$	35.4	0.190
La_2O_3	26.6	0.139

The experimental setup for $NaBH_4$ methanolysis and hydrogen gas measurement comprised a 50 mL jacketed reaction flask equipped with a Teflon-coated stir bar and placed on a magnetic stirrer. Temperature regulation was maintained by circulating water through the reactor jacket from a constant-temperature bath (PolyScience water bath). The evolved hydrogen gas was quantified using a graduated glass tube (50 cm in height, 2.5 cm in diameter) filled with water, which was connected to the reaction flask. Additionally, a thermocouple inserted into the reactor ensured precise temperature monitoring [2].

In this work, the catalytic performances of $La(OH)_3$ and La_2O_3 nanowires are systematically evaluated in terms of hydrogen yield, reaction kinetics, and stability under various operating conditions. The findings of this study provide valuable insights into the design of cost-effective and efficient catalysts for hydrogen generation, contributing to the advancement of clean energy technologies.

Acknowledgment
This work was supported by Kocaeli University Research Fund with Project Numbers: FAA-2025-4323.

References

[1] Taha T.A.M., Abouhaswa A.S., Mohamed W.S. 2025. Enhanced catalytic performance of magnetic zinc-doped cobalt ferrite nanoparticles. International Journal of Hydrogen Energy 112:133-143.
[2] Durap F., Zahmakiran M., Ozkar S. 2009. Water soluble laurate-stabilized rhodium(0) nanoclusters catalyst with unprecedented catalytic lifetime in the hydrolytic dehydrogenation of ammonia-borane. Applied Catalysis A: General 369: 53-59.

Ph.D. Emel Engintepe is a researcher at Kocaeli University, Department of Chemical Engineering, and a member of the Alternative Fuels R&D Center (AYARGEM). Her academic work focuses on the development of nanowire-structured lanthanum-based catalysts for the oxidative coupling of methane (OCM). She has expertise in hydrothermal synthesis, material characterization, and catalytic applications for sustainable energy conversion.
Emel Engintepe, e-mail: emel.engintepe@kocaeli.edu.tr tel: +90 (538) 373 41 09

Syngas production via optimized oxidative reforming of model biogas

Orhan Özcan [1,2], Merve Doğan Özcan [1] and Ayşe Nilgün Akın [1,2]
[1]Kocaeli University, Department of Chemical Engineering, 41001, Kocaeli, Türkiye
[2]AYARGEM, Alternative Fuels R&D Center, Kocaeli University, 41001, Kocaeli, Türkiye

Biogas, produced through the anaerobic digestion of organic matter, is gaining attention as a clean and renewable energy source. It primarily comprises methane (CH_4) and carbon dioxide (CO_2), with composition varying based on the feedstock [1]. Oxidative reforming (OR) of biogas has been widely studied as a method for hydrogen and syngas production. These processes are valuable not only for energy generation but also for reducing greenhouse gases, as both methane and carbon dioxide are consumed. A key advantage of oxidative reforming of biogas lies in the exothermic catalytic partial oxidation (CPO) of methane, which lowers energy requirements. When CPO is combined with the endothermic dry reforming (DR) process, a thermoneutral condition can be achieved by adjusting the $CH_4/CO_2/O_2$ ratios. Moreover, the presence of oxygen at high temperatures mitigates carbon deposition on catalyst surfaces, thereby enhancing long-term efficiency [2,3].

Catalysts are crucial in reforming reactions. While noble metals exhibit high activity, their high cost limits large-scale application. Nickel-based catalysts, when supported on metal oxides, provide a cost-effective alternative but suffer from deactivation [4]. To improve their stability, redox-active supports such as cerium oxide and hydrotalcite-derived mixed oxides are employed, offering enhanced performance across various reforming systems [5,6].

In this study, Mg-Al mixed oxide supports were synthesized from hydrotalcite via co-precipitation, followed by sequential impregnation with Ni and Ce. The resulting catalyst (10 wt% Ni and 5 wt% Ce on a Mg-Al (3:1) support) was evaluated for syngas production through oxidative reforming of model biogas. The effect of feed ratios (O_2/CH_4 and CO_2/CH_4) and reaction conditions (temperature and space velocity) on reactivity and product distribution were analyzed in relation to catalyst structure and texture.

Process parameters for the oxidative reforming of biogas were optimized using response surface methodology (RSM) with Design-Expert software. A total of 30 experimental runs were designed using a three-level approach and conducted in random order to evaluate the effects of independent variables on response outputs.

The effects of the independent variables (Table 1) was investigated within their respective operating ranges to identify optimal feed ratios and reaction conditions in the OR of biogas.

Table 1. Independent variables and responses studied in oxidative reforming of biogas.

Factors	Range	Responses
CO_2/CH_4	0.3-1	CH_4 conversion
O_2/CH_4	0-0.5	CO_2 conversion
Temperature (°C)	600-800	H_2/CO ratio
Space velocity ($mL/g_{cat}.h$)	45,000-90,000	H_2 yield

The results indicate that increasing CO_2/CH_4 and O_2/CH_4 ratios enhances CH_4 conversion and H_2 yield. However, higher O_2 levels reduce CO_2 conversion due to CH_4 combustion and CO oxidation. Temperature positively influences CH_4 and CO_2 conversions by promoting endothermic reactions such as dry reforming, but it lowers the H_2/CO ratio owing to the reverse water-gas shift reaction. Variations in space velocity exhibited minimal impact on reaction performance, suggesting that temperature and feed composition are the primary factors influencing reactivity.

References

[1] M. Doğan-Özcan, A.N. Akın Int. J Hydrogen Energy, 48 (2023) 22988

[2] C.S. Lau, A. Tsolakis, M.L. Wyszynski Int. J Hydrogen Energy, 36 (2011) 397

[3] U. Izquierdo, V.L. Barrio, N. Lago, J. Requies, J.F. Cambra, M.B. Guemez, P.L. Arias Int. J Hydrogen Energy, 37 (2012) 13829

[4] G. Jianzhong, H. Zhaoyin, G. Jing, Z. Xiaoming Fuel, 87 (2008) 1348–1354

[5] M. Doğan-Özcan, A.N. Akın Sustainable Chemistry and Pharmacy, 35 (2023) 101165

[6] N. Laosiripojana, S. Charojrochkul, P. Kim-Lohsoontorn, S. Assabumrungra Journal of Catalysis, 276 (2010) 6

Dr. Orhan Özcan is an Assistant Professor at the Department of Chemical Engineering, Kocaeli University. He received his B.Sc. degree from Kocaeli University in 2011, followed by an M.Sc. in 2014 and a Ph.D. in 2023. His research interests focus on hydrogen production through reforming technologies, thermodynamic and kinetic analysis, and the synthesis of heterogeneous catalysts.

Presentating author: Orhan Özcan, e-mail: orhan.ozcan@kocaeli.edu.tr tel: +90 262 303 3536

Subproducts of Ammonia Borane in First Step Release with Principal Components Analysis

Roberto Hinojosa[1], E.V. Mejía-Uriarte[2], R.Y. Sato-Berrú[2]
[1]Affiliation and address [1]Facultad de Ciencias, [2]Instituto de Ciencias Aplicadas y Tecnología
Universidad Nacional Autónoma de México,
Circuito Exterior S/N, Ciudad Universitaria, 04510, México City, México.

A material that receive a lot of attention due to his higt capacity to store hydrogen is ammonia borane (AB) with 19.6% wt. It is a white powder stable at room presure and temperature [1], making it easy to handle. Three steps are know in the release of hydrogen from ammonia borane as a temperature function. AB releases about 1mol of H_2 in each release step and loses approximately 6.5 wt% [3]. The first release step occurs around of 100 and 130 °C; hydrogen and a few gaseous residues are released such as diborane (B_2H_6), borazine ($B_3N_3H_6$), and NH_2BH_2 [2]. The second release step take place of 130 to 200 °C, release a little more than 1 mol of hydrogen for mol of AB, at this point, the main residue is borazine ($B_3N_3H_6$) and complex solid residues of type $[BNH_x]_n$ (with x less that 2) is also formed [3]. The last step occurs above 500 °C releasing residual hydrogen [4].

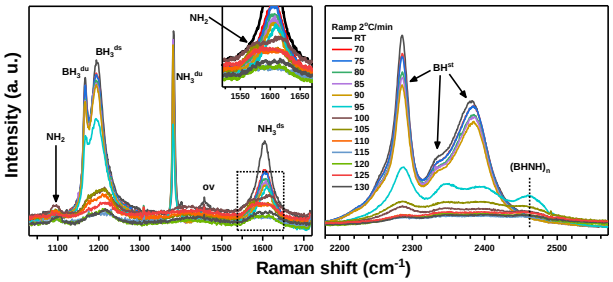

Figure 1. Raman spectra sequence to heating rate of 2 °C /min in regios corresponding to NH_3 and BH_3 (left) and BH (right). The appearance of bands related to subprodutc that have NH_2 and BHNH bonds is observed (du, umbrella, ds, scissors, and st,sthrech).

The firs step release was analyzed for Raman spectroscopy (Raman TriVista 557) in two spectral regions, that understand the vibrational modes du, ds and st, corresponding to bonds BH_3 and NH_3, and BH respectively. The first step release was analized in the range of 70-130°C, every 5°C for the four heating rates 1, 2(figure1), 10 and 30 °C /min. Data analysis was carried out on the MATLAB platform, based on a principal components analysis (PCA). The changes between the shapes of the Raman spectra were recorded in the PCAs with the highest percentage weight.as seen in figure 2.

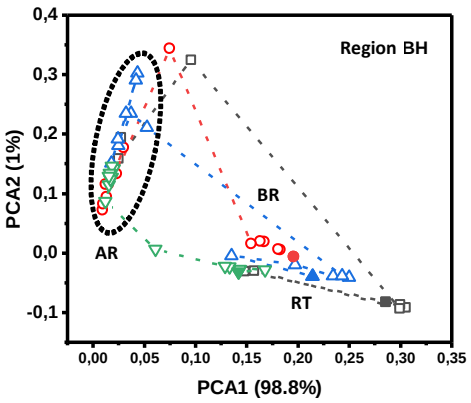

Figure 2. Principal Components Analysis of region corresponding to BH bonds, in the first release step, for the four heating rates(each pointrepresents a Raman spectrum). In this case the vibrational modes are represented in principal components PC1 and PC2. Points within the dotted ellipse indicate spectra after release (AR), and the points outside before release (BR), represent the Raman spectra obtained from room teperature (RT, full points) until the moments when the hydrogen release begins (95 °C).

The scattering of piont (spectra) in figure 2 are relationed with subproducts formation acording to PC1 that represente the aparence of new bands, in this case for compomts with NH2 and poliimonoboranes (BHNH)n. PC2 is related to the shifting of the bands. The scattering in general is related to a process of molecular rearrangement that can contribute to formation of subproducts.

Acknowledgment
The support from the School Sciences, Laboratory of Atomic and Molecular Physic (UNAM). PAPIIT projec IN108519, and PAPIME PE-107521, to University Laboratory for Spectroscopy Characterization (LUCE-ICAT-UNAM).

References

[1] Q. Wang et al. ACS Catal. 9, 1110-1119 (2019)
[2] . Petit J.F. Int. J Hydrog. Energy, 41:15462-15470 (2016)
[3] O.T. Summerscales et al. Dalton trans. 42, 10075-10084 (2013)
[4] S. Frueh et al. Inorg. Chem. 50(3), 783-792 (2011)

Ph.D. Roberto Hinojosa Nava is a member of Laboratory of Physic Atomic and Molecular, Physics Department of School Science of Universidad Nacional Autónoma de México (UNAM). Graduated from School Sciences UNAM in 2014 obtained her M.Sc in 2017, and Ph.D. in 2023. His work is about the synthesis of multiferroic materials on based of iron, and the study of ammonia borane for release of hydrogen.

Roberto Hinojosa Nava, e-mail: hinro36@ciencias,unam.mx tel: +52 (55) 36563401.

HYDROGEN STORAGE AND SEPARATION

Design of TiFe-based alloys via element substitution for tailored equilibrium pressure and easy activation

Mohammad Faisal[1, 2], June-Hyung Kim [2, 3], Young Whan Cho [2], Jae-il Jang [3], Jin-Yoo Suh [2], Jae-Hyeok Shim [2] and Young-Su Lee [2]

[1]Renewable and Sustainable Energy Research Center (RSERC), Technology Innovation Institute, Abu Dhabi, United Arab Emirates

[2]Center for Energy Materials Research, Korea Institute of Science and Technology, Seoul 02792, Korea

[3]Division of Materials Science and Engineering, Hanyang University, Seoul 04763, Korea

Titanium iron (TiFe) alloy is a room-temperature hydrogen-storage material, and it absorbs hydrogen via a two-step process to form TiFeH and then $TiFeH_2$. The effect of V addition in TiFe alloy was recently elucidated. The V substitution for Ti sublattice lowers P_2/P_1 ratio, where P_1 and P_2 are the equilibrium plateau pressure for TiFe/TiFeH and TiFeH/$TiFeH_2$, respectively, and thus restricts the two-step hydrogenation within a narrow pressure range. The focus of the present investigation was to optimize the V content such that maximum usable storage capacity can be achieved for the target pressure range: 1 MPa for absorption and 0.1 MPa for desorption. The effect of V substitution at selective Ti or Fe sublattices was closely analyzed, and the alloy composition $Ti_{46}Fe_{47.5}V_{6.5}$ displayed the best performance with ca. 1.5 wt.% of usable capacity within the target pressure range. At the same time, another issue in TiFe-based alloys, which is a difficulty in activation at room temperature, was solved by Ce addition. It was shown that 3 wt.% Ce dispersion in TiFe alloy imparted to it easy room-temperature (RT) activation properties.

Titanium iron (TiFe) alloy is a room-temperature hydrogen-storage material that absorbs hydrogen through a two-step process, forming TiFeH and $TiFeH_2$. Recent studies have shown that vanadium (V) substitution in TiFe alloy lowers the P2/P1 ratio (where P1 and P2 are equilibrium plateau pressures for TiFe/TiFeH and TiFeH/$TiFeH_2$, respectively), restricting hydrogenation within a narrow pressure range. This investigation aimed to optimize V content to achieve maximum usable storage capacity within the target pressure range of 1 MPa for absorption and 0.1 MPa for desorption. The $Ti_{46}Fe_{47.5}V_{6.5}$ alloy composition demonstrated the best performance, achieving approximately 1.5 wt.% usable capacity within the target pressure range. Additionally, the study addressed the challenge of room-temperature activation in TiFe-based alloys by adding 3 wt.% Ce, which facilitated easy activation.

The current investigation discusses the design and optimization of V-substituted TiFe-based alloys for hydrogen storage applications, focusing on achieving a target pressure range (0.1–1 MPa) and easy room-temperature activation. Key findings and methodologies include:

Optimal Composition: The alloy composition $Ti_{46}Fe_{47.5}V_{6.5}$ demonstrated the best performance, achieving a usable hydrogen-storage capacity of 1.5 wt.% within the target pressure range. V substitution at Fe sublattice lowered P2, while substitution at Ti sublattice raised P1, optimizing the pressure range.

Activation Improvement: Adding 3 wt.% Ce to TiFe alloys improved room-temperature activation and suppressed the formation of $Ti_4Fe_2O_{1-x}$ suboxide, ensuring better control of the TiFe phase composition.

Sample Preparation: Binary Ti-Fe and ternary Ti-Fe-V alloys with Ce addition were synthesized via arc melting and annealed at 1000°C. Structural analysis confirmed the presence of TiFe (B2 structure) as the main phase, along with Ce and CeO_2.

Hydrogen Sorption Testing: Pressure-composition isotherm (PCI) measurements showed that $Ti_{46}Fe_{47.5}V_{6.5}$ had closely positioned P1 and P2, forming a single plateau and maximizing usable capacity.

Conclusion: The study successfully designed a TiFe-based alloy with enhanced hydrogen-storage capacity and easy activation, making it a promising candidate for room-temperature hydrogen storage applications.

Acknowledgment

Funding for this research was provided by the Korea Institute of Science and Technology and the National Research Foundation of Korea.

References

[1] Reilly, J.J.; Wiswall, R.H. Formation and properties of iron titanium hydride. *Inorg. Chem.* 1974, **13**, 218–222.

[2] Jung, J.Y.; Lee, Y.S.; Suh, J.Y. ; Huh, J.Y.; Cho, Y.W. Tailoring the equilibrium hydrogen pressure of TiFe via vanadium substitution. *J. Alloys Compd.* 2021, **854**, 157263–157272.

[3] Faisal, M.; Suh, J.Y. ; Lee, Y.S. Understanding first cycle hydrogenation properties of Ti–Fe–Zr ternary alloys. *Int. J. Hydrogen Energy* 2021, **46**, 4241–4251.

[4] Leng, H.; Yu, Z.; Yin, J.; Li, Q.; Wu, Z.; Chou, K.-C. Effects of Ce on the hydrogen storage properties of TiFe0.9Mn0.1 alloy. *Int. J. Hydrogen Energy* 2017, **42**, 23731–23736.

Dr. Mohammad Faisal is a Senior Researcher at the Renewable and Sustainable Energy Research Center (RSERC), Technology Innovation Institute (TII), Abu Dhabi. He leads cutting-edge R&D in hydrogen storage materials and systems, driving innovation in clean energy and decarbonization technologies. Dr. Faisal earned his Ph.D. in Materials Science and Engineering from IIT Kanpur, India, and developed patented hydrogen storage hybrids. His postdoctoral work at KIST (South Korea) resulted in a US patent, and Brunel University London focused on advancing room-temperature metal hydrides and hydrogen-based thermal systems utilizing industrial waste heat.
Presentating author: Mohammad Faisal, e-mail: mohammad.faisal@tii.ae tel:+971-543091833

Development of Palladium based alloys for hydrogen separation membranes

Fatih Piskin [1,2] and Tayfur Öztürk [2,3]

1 Dept. of Metallurgical and Materials Engineering, Muğla Sıtkı Koçman University, Muğla,

2 ENDAM, Center for Energy Storage Materials and Devices, Middle East Technical University, Ankara

3Dept. of Metallurgical and Materials Engineering, Middle East Technical University, Ankara

The need for hydrogen separation membranes has augmented over the years and it appears that it will continue augmenting further in coming decades. Instead of classical approach of addressing the need for hydrogen separation in centralized syngas facilities, it appears that there will be widespread need of relatively small scale installments either for feeding the hydrogen into storage system or taking the hydrogen from it wherever it is needed. The storage system in question could cover a number of alternatives, the most important is the network of natural gas pipeline which appears to be the emerging storage medium for hydrogen. It is thus timely to have a look at cost reduction strategies that can be employed in fabrication of separation membranes. The basis is commonly used separation membrane with composition of Pd-23%Ag. Two strategies may be employed; one to follow the basic strategy reflected by Pd- 23 %Ag, i.e. f.c.c. membranes that are ductile and can be processed metallurgically into capillary tube or foil so that useful separation devices can be fabricated. Here there are two issues to be addressed; one how to reduce Pd content in order to make it cost effective, the second how to reduce the operating temperature which are traditionally targeted to syngas generation down to the much lower temperatures needed for the present or future needs. The second strategy would address the same but not via metallurgical processing of selected alloys but to direct fabrication of separation membranes via thin film deposition. In this paper, we investigate cost effective membranes in ternary alloys based on Pd-Ag-Ti, Pd-Ag-Ni, Pd-Ag-Mn and Pd-Nb-Ti using an efficient search methodology based on combinatorial material chemistry.

Fatih Pişkin is an Assoc. Professor in Department of Metallurgical and Materials Engineering at Muğla Sıtkı Koçman University. He received his BSc degree from Anadolu University in 2009, MSc and PhD degrees from Middle East Technical University in 2013 and 2018, respectively.

Corresponding author: Fatih Pişkin, e-mail: fatihpiskin@mu.edu.tr tel: +90 252 211 20 56

Hydrogen Processing of Ti6Al4V tuırnings for fabrication of fine powders for additive Manufacturing

Zeynep Ege Uysal[1,2], Sertaç Altıınok[2], Yunus Eren Kalay[1,3] and Tayfur Öztürk[1,3,4]

[1]Dept. of Metallurgical and Materials Engineering, Middle East Technical University(METU), Ankara
[2]Turkish Aerospace Industries Inc. Ankara
[3]ENDAM, Center for Energy Materials and Storage Devices, METU, Ankara
[4]INNOVASCOPE Materials Technologies Ltd Sti

Ti6Al4V is widely used in aerospace, biomedical, and other industries due to itshigh strength-to-weight ratio, corrosion resistance, and high-temperature performance. Additive manufacturing (AM) enables near-net-shape production with significantly reduced waste. Among AM techniques, selective laser melting (SLM) is the most widely used for Ti6Al4V, and it requires fine (15–53 µm) spherical powders.This study investigates a recycling route to produce such powders from

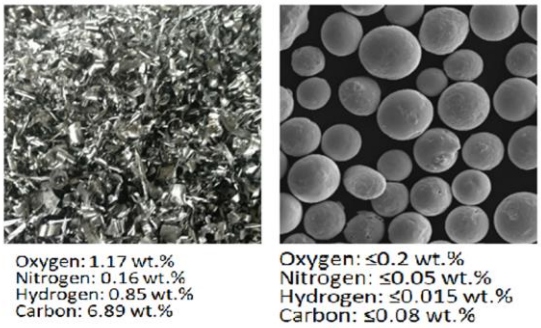

Motivation is to recycle contaminated turnings into fine Grade 3 spherical powders(<53 µm)

Ti6Al4V shavings. In this route, cleaned chips are hydrogenated, milled, and plasma spheroidized into spherical powders. To determine conditions of hydriding, chips were hydrided isothermally for a fixed duration at temperatures from 450 to 650 °C. This showed that the amount of hydrogen absorbed increased with increasing temperature. Then, pressure-controlled experiments were carried out. This was challenging since hydrogen absorption leads to an uncontrolled rise in temperature. Hydriding, therefore, was carried out with flow-controlled delivery. This showed that chips can be hydrided to 3.3 wt.% at 400 °C for a duration of 5 hours. The hydrided chips were milled with a tumbling ball-mill, which resulted in powders of irregular shape (<53µm) due to their brittleness.

Iregularly shaped fine powders were sphereoidized in RF thermal plasma 25 kW. The powders were fed into the torch from 15 to 5 g/min. 10 g/min provided the best balance between spheroidization and process efficiency.

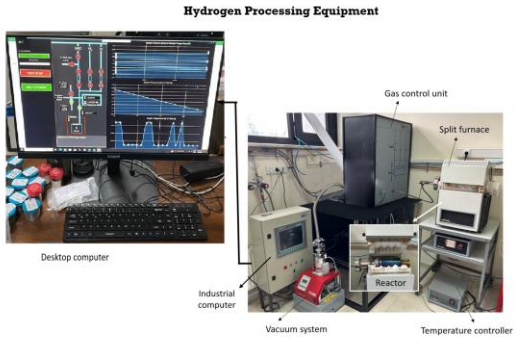

Equipment used for hydrogen processing of the turnings . The reactor where turnings are treated is inside the split furnace The equipment is a PCT apparatus (house built and impeoved over aperiod of 10 years).aapted for the purpose

It is concluded that direct spheroidization of hydrided powders in the plasma reactor results in desorption of hydrogen which adversely affact the temperature distribution in the reactor. Possible routes for succesful processing of plasma sphereoidization are discussed

Tayfur Oztürk is an adjuct professor in the Department of Metallurgical and Materials Engineering, Middle East Technical University. He earned his Ph.D. in Materials Science at Cambridge University in 1978 and his B.Sc. degree from Istanbul Technical University in 1973 . Before joining METU, he worked as a post-doc at Sheffield University and Istanbul Technical University. While faculty member at METU, he was a visiting scholar at McMaster University in 1989 and Los Alamos National Laboratory, 1990. His research interest focuses on rechargeable alkaline batteries, metal hydrides, nanopowder synthesis, thermal plasma processing of materials. He is the founder of ENDAM, i.e. Center for Energy Materials and Storage Devices He is the iniator of mESC-IS series of international symposia organized each year now as well as of the summer school, mESC-School orgainized biyearly in Türkiye
Corresponding author:Tayfur Öztürk, e-mail: ozturk@metu.edu.tr, Tel: +90(312)210 5935

FUEL CELLS AND ELECTROLYSERS

Performance and Evaluation of Synthesized Polybenzimidazole/Functionalized Boron Nitride Composite Membranes for High-Temperature PEM Fuel Cell Test System

Ali Hassen Ali[1], Ramiz Gultekin AKAY [1] Ebru Erünal[2]
[1]Department of Chemical Engineering, Kocaeli University, 41380 Kocaeli, Turkey.
[2] Department of Chemical Engineering, Gebze Technical University, Kocaeli 41400, Türkiye

Polybenzimidazole (PBI)-based membranes have emerged as promising candidates for high-temperature proton exchange membrane fuel cells due to their exceptional thermal and chemical stability, as well as their ability to maintain proton conductivity under anhydrous conditions. [1],[2] To improve the properties of PBI membranes, researchers have concentrated on incorporating inorganic nanofillers. Functionalized boron nitride (BN) nanosheets are particularly promising as reinforcing additives because of their high thermal conductivity, chemical inertness, and capacity to form additional proton transport pathways within the polymer matrix. [2],[6] The purpose of using functionalized boron nitride (BN) in proton exchange membranes is to increase the performance of PEM fuel cells and reduce material costs.[4],[5] The superior thermal and mechanical stability and high proton conductivity of boron nitride play an important role in improving the poor thermal and mechanical properties of Polybenzimidazole (PBI) membranes.[2],[3] The main aim to this study provide valuable insights into the evaluation and optimization of novel PBI-based composite membranes for high-temperature fuel cell system. In this context, the addition of BN provides a lower cost and environmentally friendly alternative compared to existing per fluorinated membranes, providing a wider potential for use in energy applications. In this study, polybenzimidazole was successfully synthesized via condensation polymerization in polyphosphoric acid (PPA) at a temperature range of 150–230°C and the functionalization of hexagonal boron nitride (h-BN) with amine groups (NH_2) was carried out to enhance its chemical properties and compatibility with various applications. A novel PBI membranes containing functionalized BN fillers were synthesized and systematically characterized to assess their potential for HT-PEMFC applications. FTIR

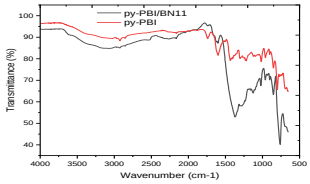

Fig:1 FTIR Result for composite membrane and Pure py-PBI

spectroscopy was performed to confirm the structural features of the polymers. The FTIR spectra show key differences confirming BN incorporation into the Py-PBI matrix. Pure Py-PBI exhibits peaks at 2924 and 2855 cm^{-1} (C–H stretching), 1738 and 1598 cm^{-1} (C=N, C=C stretching), and distinct bands between 1434–742 cm^{-1} (ring vibrations)

In the composite membrane, new peaks appear at 1266, 962, and 903 cm^{-1}, indicating B–N and B–N–H bonds. The shift from 2924 to 3062 cm^{-1} and enhanced intensity at 1372 cm^{-1} confirm strong interaction and successful composite formation.

The polymer exhibited an intrinsic viscosity of 1.51 dL/g and an average molecular weight of 70,999 Da

The XRD pattern of pyridine-PBI shows a broad peak around 25°, indicating its amorphous nature with low crystallinity

Electrochemical impedance spectroscopy (EIS) was performed using a Gamry Instrument 3000 Reference over a frequency range of 1 MHz to 1 Hz The proton conductivity was then calculated based on the following Equation.

$$\sigma(s/cm) = \frac{L}{R*w*t} \qquad [1]$$

Proton conductivity reached 0.224 S/cm at 180°C, and making py-PBI suitable for moderate-temperature applications, though its performance declined at higher temperatures due to dehydration and structural changes. Thermal stability was assessed in an air environment with a heating rate of 10 °C/min. Initial minor loss (65.93–118.23 °C) Major degradation begins at 385.73 °C and continues beyond 749.81 °C, indicating high thermal stability. The TGA results for the synthesized Py-PBI indicated a weight loss of 58% at 900 °C.

Overall, these studies provided insights into the structural integrity, of the synthesized PBI/functionalized membranes, supporting their suitability for high -temperature PEMFC fuel cell development.

Acknowledgment

This work was supported by Research Fund of the Kocaeli University project no. FDKB-2024-3674 and FKA-2024-3862

References

[1] N. Üregen, K. Int J Hydrogen Energy. 2017;42(4):2636
[2] Hussin DE, Budak Y, Int J Energy Res. 2022;46(4):4174
[3] Bhimanapati G, Kozuch D, Robinson J Nanoscale (2014) 6(20) 11671
[4] Haque, M.A International Journal of Hydrogen Energy, 2017,9156
[5] Nauman Javed, R.M. Renewable and Sustainable Energy Reviews, 16(August),2022 P. 112836.
[6] Berber M, Nakashima J.of Membrane Science (2019) 591(August) 117354

Dr. Ramiz Gültekin Akay is an associate professor at Kocaeli University He completed his B.Sc., M.Sc., and Ph.D. at Middle East Technical University. he has published extensively and edited the book *Direct Liquid Fuel Cells: Fundamentals, Advances and Future*. His research focuses on electrochemical technologies and fuel cell applications.

Microwave Assisted Synthesis of Graphene Supported PtCo Alloys as Efficient Cathode Electrocatalysts for PEM Fuel Cells

Çiğdem İyigün Karadağ[1]
[1]TÜBİTAK Marmara Research Center Hydrogen and Fuel Cell Technologies Research Group,
Barış Mah. Dr. Zeki Acar Cad. No:1, P.O Box 21, 41470 Gebze, Kocaeli/TÜRKİYE

Abstract

In this study, graphene supported PtCo electrocatalysts were synthesized via microwave assisted polyol reduction method with varying irradiation temperatures and their performance were evaluated as cathode electrodes in polymer electrolyte membrane fuel cells (PEMFCs). The impact of microwave irradiation temperature on the structural, morphological, and electrochemical properties of the catalysts was systematically investigated. Among the synthesized catalysts, the sample prepared at 170 °C (PtCo/G-170) exhibited the highest performance, acheiving a peak power density of approximately 520 mW/cm² and an ECSA value of 87.3 cm²/g. These results demonstrate that the microwave-assisted synthesis method yields a more effective nanoparticle dispersion compared to conventional heating method, significantly enhancing the electrocatalyst's efficiency.

1.Introduction

The important characteristics of polymer electrolyte membrane fuel cells (PEMFC) like high energy efficiency, low temperature operation and zero emission make them promising clean energy devices [1–3]. The problems that are encountered in their widespread commercialization is the high cost due to the use of precious metal electrocatalysts and limited durability, due to sluggish kinetics of oxygen reduction reaction (ORR) [4,5]. There are tremendous research on overcoming these limitations, i.e. alloying Pt with transition metals (Co, Ni, etc.) for enhancement of ORR characteristics and decreasing the cost with the reduction of noble metal amount [6–8]. PtCo alloys exhibit high catalytic activity and stability under acidic PEMFC conditions [9], where the activity and durability are affected not only by the morphology of the catalyst but also the nature of the support material.

Graphene is denoted as an ideal support for noble metal electrocatalysts with its large specific surface area, excellent electrical conductivity, mechanical strength, and chemical stability [10–12]. Due to increased metal-support interaction and uniform distribution, there is an enhancement in the catalytic activity where graphene is used as a support. Moreover, the catalyst preparation method has a significant impact on morphology and catalytic activity. Conventional synthesis methods, such as chemical reduction under reflux, often lead to particle aggregation, broad size distribution, and incomplete alloy formation, limiting the catalyst's efficiency. Microwave-assisted synthesis has recently gained attention as an efficient and sustainable alternative due to its rapid volumetric heating, reduced reaction times, and improved control over nanoparticle growth [13–15]. By providing homogeneous thermal energy, microwave irradiation promotes uniform nucleation and prevents excessive particle growth, enabling the formation of finely dispersed and well-alloyed nanoparticles on graphene supports.

In this study, we report the synthesis of PtCo/graphene composite electrocatalysts via a microwave-assisted polyol method and evaluate their performance as cathode catalysts in PEMFCs. The effects of synthesis temperature on the structural, morphological, and electrochemical properties of the catalysts are systematically investigated. The results demonstrate that the microwave-assisted approach not only enhances nanoparticle dispersion and alloy formation but also significantly improves fuel cell performance compared to conventional methods. This work highlights the potential of microwave-assisted synthesis in designing high-performance, graphene-supported electrocatalysts for next-generation PEMFC applications.

2.Experimental

Graphene samples were obtained from CealTech (Norway). Chloroplatinic acid hexahydrate ($H_2PtCl_6 \cdot 6H_2O$, ≥99.9%), cobalt(II) chloride hexahydrate ($CoCl_2 \cdot 6H_2O$, ≥98%), ethylene glycol (EG, ≥99%), Nafion® solution (5 wt%), and isopropanol (≥99.5%) were purchased from Sigma-Aldrich and used without further purification. Ultrapure water (resistivity 18.2 MΩ·cm) was used throughout all experiments.

Dr. Çiğdem İyigün Karadağ received her Ph.D degree from Middle East Technical University Department of Chemistry. She has been working as a Senior Chief Researcher at TÜBİTAK Marmara Research Center (MAM) Hydrogen and Fuel Cell Technologies Research Group since 2007. Her research focuses on proton exchange membrane fuel cells, electrocatalyst development, and hydrogen production technologies. She has led and contributed to numerous national and international projects on hydrogen technology and has authored multiple peer-reviewed publications and conference papers in the field of clean energy technologies.

Corresponding author: Çiğdem İyigün Karadağ, e-mail: cigdem.karadag@tubitak.gov.tr tel:+902626772721

2.1 Synthesis of PtCo/Graphene Catalysts

PtCo/graphene catalysts were synthesized using a microwave-assisted polyol reduction method. First, 160 mg of graphene was dispersed in 10 mL of ethylene glycol (EG) via ultrasonication for 1 h to ensure homogeneous suspension. In a separate container, 79 mg of $H_2PtCl_6 \cdot 6H_2O$ and 20 mg of $CoCl_2 \cdot 6H_2O$ were dissolved in 1 mL of EG under ultrasonication for 10 min. The metal precursor solution was then added dropwise to the graphene suspension under magnetic stirring. The resulting mixture was transferred into Monowave 400 microwave reactor (Anton Paar) and heated to 90 °C under continuous stirring. After the reaction, the product was cooled to room temperature, filtered, and washed thoroughly with ethanol and deionized water. The obtained black powder was dried under vacuum at 80 °C overnight. For comparison, additional samples were synthesized at 110 °C and 170 °C, and a control sample was prepared using a conventional reflux method at 170 °C for 8 hours.

The morphology and particle size of the catalysts were analyzed using transmission electron microscopy (TEM, JEOL JEM-2100F). X-ray diffraction (XRD) patterns were recorded on a Rigaku Miniflex 600 diffractometer using Cu Kα radiation (λ = 1.5406 Å) to confirm alloy formation. Elemental mapping and compositional analysis were performed using energy-dispersive X-ray spectroscopy (EDS) coupled with scanning electron microscopy (SEM, Phenom XL).

The electrochemical analysis was performed on the Fuel Cell Test Station (Scribner Associates). Cathode electrodes were prepared by spraying the catalyst ink onto the gas diffusion layer (GDL, Sigracet 29 BC) till 0,2 mg/cm^2 loading was achieved (Fig. 1). For the anode side, 0,6 mg/cm^2 of %20 Pt/C was coated on the gas diffusion layer (Sigracet 29 BC). The membrane electrode assembly was prepaed by hot pressing the anode and cathode electrodes with the membrane (Nafion XL).

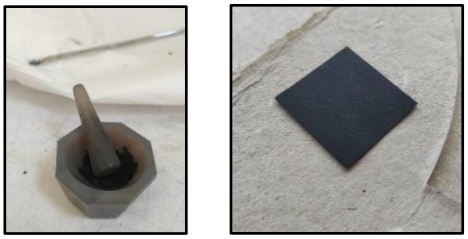

Fig 1. The prepared electrocatalyst and coated gas diffusion layer

3. Results and Discussion

The SEM and TEM images of the graphene support before catalyts preparation step is shown in Fig 2.

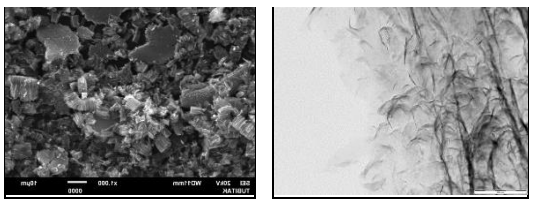

Fig 2. The SEM and TEM images of graphene support

Graphene-supported PtCo catalysts were synthesized via microwave-assisted processing at sequential temperatures of 90 °C, 110 °C, and 170 °C to investigate the effect of synthesis temperature on catalyst properties. Moreover, the polyol reduction with conventional reflux method was applied, to investigate the effect of microwave heating. The EDS analysis of the graphene-supported PtCo catalyst is presented in Fig. 3. The EDS spectrum confirms a Pt:Co atomic ratio of approximately 1:1 and a homogeneous distribution of both elements on the graphene support

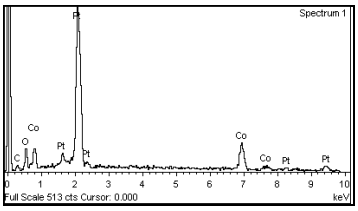

Fig 3. EDS sprectrum of graphene supported PtCo catalysts

The XRD patterns of the catalysts synthesized via conventional reflux and microwave-assisted polyol methods at different temperatures (90 °C, 110 °C, and 170 °C) shows that all samples exhibit diffraction peaks characteristic of face-centered cubic (fcc) Pt, indicating the formation of Pt-based alloy structures. Notably, samples synthesized at higher microwave irradiation temperatures (170 °C) demonstrate slight peak shifts compared to those produced under reflux conditions, suggesting lattice contraction due to cobalt incorporation into the Pt lattice. This structural modification, typically associated with PtCo alloy formation, was further supported by the calculated lattice parameters, which were lower than that of pure Pt (3.92 Å) and consistent with reported values for PtCo alloys (3.85–3.89 Å). These findings confirm that microwave-assisted synthesis at elevated temperatures promotes alloying and produces well-dispersed nanoparticles on the graphene support.

The TEM images of graphene supported catalysts prepared by microwave sysnthesis at 90, 110 and 170 °C and conventional reflux method are shown in Figure 5.

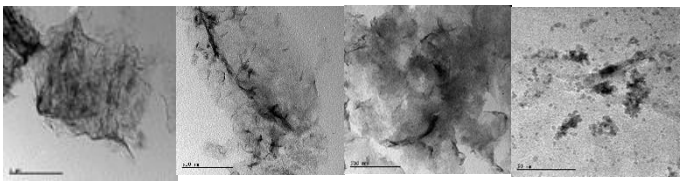

Fig 5. TEM images of the catalysts prepared at 90, 110. 170°C by microwave irradiation and conventional reflux, respectively.

The microstructural evidence indicates that microwave irradiation facilitates uniform nucleation and controlled growth kinetics, resulting in a homogeneous dispersion of catalyst nanoparticles on the support, whereas conventional reflux heating leads to non-uniform thermal gradients and pronounced particle agglomeration.

The electrochemical specific surface area (ESCA) of the prepared electrocatalysts by conventional reflux method and microwave assisted synthesis at 90, 110 and 170 °C are calculated from the cyclic voltammograms reported at 60 and 80 °C are listed in Table 1.

Table 1. The electrochemical specific surface area (ESCA) values of the electrocatalysts.

	ESCA (cm^2/g)	
Temperature	60 °C	80 °C
PtCo/G-Reflux	51,59	62,70
PtCo/G-90	49,20	42,85
PtCo/G-110	67,46	69,04
PtCo/G-170	80,95	87,30

Fuel cell performance tests of the prepared electrocatalysts were performed under H_2/O_2 gases with 1.2:2.0 stoichiometric ratio, under humidified conditions at 80 °C. Fig 6, represents the polarization curves of the catalyts prepared by microwave assisted synthesis at 90, 110, 170 °C and conventional reflux method.

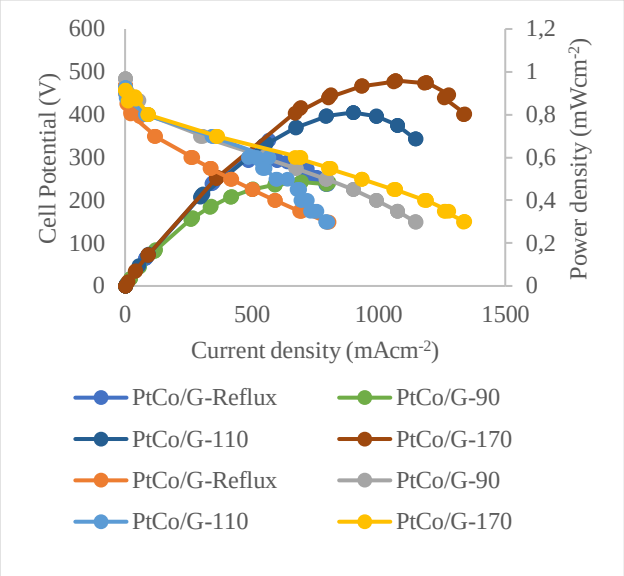

Fig 6. Polarization curves of graphene supported PtCo electrocatalysts

According to the polarization and power density curves, the **PtCo/G-170** catalyst exhibited the highest cell performance, delivering a peak power density of 520 mW cm^{-2}, while **PtCo/G-110** reached 410 mW cm^{-2}. In contrast, the **PtCo/G-90** and conventionally synthesized **PtCo/G-Reflux** catalysts exhibited significantly lower power densities of approximately 330 mW cm^{-2} and 230 mW cm^{-2}, respectively. A direct comparison between the Reflux-derived catalyst and the microwave-synthesized **PtCo/G-170** clearly indicates a substantial improvement (>500 mW cm^{-2}) in the latter, particularly in the mid-to-high current density region of the polarization curve. This demonstrates the superior catalytic activity and enhanced efficiency of the microwave-assisted PtCo/Graphene catalyst relative to its conventionally prepared counterpart.

In terms of high-current-density operation, PtCo/G-170 maintained a power density of approximately 520 mW cm^{-2} even at 1.3 A cm^{-2}, confirming its excellent electrochemical stability under heavy load conditions.

From an electrochemical perspective, the improved performance is attributed to the synergistic effects of the PtCo alloy and the graphene support. The incorporation of Co enhances oxygen reduction reaction (ORR) kinetics by modifying the Pt electronic structure, while the graphene support improves electron conductivity, suppresses nanoparticle agglomeration, and mitigates corrosion-related degradation. Consequently, the catalyst exhibits stable performance at high current densities, indicating homogeneous nanoparticle dispersion, strong structural integrity, and sustained catalytic activity over extended operation. These findings demonstrate that the microwave-assisted synthesis route yields a high-performance and durable PtCo/Graphene catalyst, outperforming conventionally synthesized materials in terms of power density, stability, and ORR activity.

4- Conclusions

This study has demonstrated that the production of PtCo/graphene-based cathode catalysts via a microwave-assisted synthesis method offers significant technical and economic advantages over conventional methods. Microwave irradiation enables rapid and uniform heating without the need for high temperatures or prolonged processing, thereby substantially reducing synthesis time, lowering energy consumption, and minimizing production costs. Furthermore, the catalysts produced using this method exhibit enhanced electrochemical performance due to characteristics such as smaller particle size, uniform metal dispersion, and well-defined crystal structure. However, for the widespread commercialization of such high-performance systems, cost-effective production processes must be scalable and applicable at the industrial level.

Acknowledgement

The work was supported by TÜBİTAK under Grant No. 122N064 which the author gratefully acknowledges. CealTech (Norway) and Fan Huang are kindly acknowledged for the graphene samples. The study is part of a collaborative project (LOCOMOTION) under MARTERA programme, where SINTEF is the coordinator. The project partners are kindly acknowledged.

References

[1] A. EG&G Technical Services, Inc., “Fuel Cell Handbook,” 7th ed., U.S. Department of Energy, Office of Fossil Energy, Morgantown, WV, 2004.
[2] B. C. H. Steele and A. Heinzel, “Materials for fuel-cell technologies,” Nature, vol. 414, no. 6861, pp. 345–352, Nov. 2001.
[3] O. Z. Sharaf and M. F. Orhan, “An overview of fuel cell technology: Fundamentals and applications,” Renewable and Sustainable Energy Reviews, vol. 32, pp. 810–853, Apr. 2014.

[4] J. Larminie and A. Dicks, Fuel Cell Systems Explained, 2nd ed. Chichester, U.K.: Wiley, 2003.
[5] M. H. Rashid, *Hydrogen Production, Storage and Applications*, 1st ed., Academic Press, 2015.
[6] N. Z. Muradov and T. N. Veziroglu, “Hydrogen energy

problems and perspectives," *International Journal of Hydrogen Energy*, vol. 33, no. 23, pp. 6804–6839, Dec. 2008.

[7] Z. Wang, G. Yin, and S. Zhang, "Pt-based electrocatalysts with high performance towards oxygen reduction reaction," *Journal of Power Sources*, vol. 171, no. 2, pp. 331–339, Oct. 2007.

[8] H. A. Gasteiger et al., "Activity benchmarks and requirements for Pt, Pt-alloy, and non-Pt oxygen reduction catalysts for PEMFCs," *Applied Catalysis B: Environmental*, vol. 56, no. 1–2, pp. 9–35, Mar. 2005.

[9] S. Gottesfeld and T. A. Zawodzinski, "Polymer electrolyte fuel cells," in *Advances in Electrochemical Science and Engineering*, vol. 5, Wiley-VCH, 1997, pp. 195–301.
2, pp. 9–35, Mar. 2005.

[10] V. R. Stamenkovic et al., "Improved oxygen reduction activity on Pt3Ni (111) via increased surface site availability," *Science*, vol. 315, no. 5811, pp. 493–497, Jan. 2007.

[11] M. Shao, "Electrocatalysis in fuel cells: A non- and low-Pt perspective," *ACS Catalysis*, vol. 1, no. 4, pp. 402–416, Apr. 2011.

[12]Jamil E, YararKaplan B, Sadhu V, AlkanGürsel S. "Argi nine-glycine-aspartate (RGD) peptide-modified graphene as efficient support material for Pt electrocatalyst in proton exchange membrane fuel cells". *Int J Energy Res*. 2022; 46(4): 4712-4725. doi: 10.1002/er.7467

[13] S. M. Haile, "Fuel cell materials and components," *Acta Materialia*, vol. 51, no. 19, pp. 5981–6000, Nov. 2003.

[14] R. Borup et al., "Scientific aspects of polymer electrolyte fuel cell durability and degradation," *Chemical Reviews*, vol. 107, no. 10, pp. 3904–3951, Oct. 2007.

[15] V. Mehta and J. S. Cooper, "Review and analysis of PEM fuel cell design and manufacturing," *Journal of Power Sources*, vol. 114, no. 1, pp. 32–53, Jan. 2003.

Fabrication and Characterization of SPEEK Proton Exchange Membranes (PEM) for Fuel Cells by Solution Casting Methods

Akbar Khoshnoudi[1], Sema Samatya Yılmaz[1], Ayşe Aytaç[1,] Ramiz Gültekin Akay[1]

Science Institute, Chemical Engineering Department Kocaeli University, Izmit Türkiy

Abstract

The intensive use of fossil fuels has led to serious environmental and political problems in the last century. Therefore, sustainable and efficient energy solutions are needed. While renewable energy sources offer solutions to this problem, Polymer Electrolyte Membrane Fuel Cells (PEMFCs), which convert chemical energy directly into electrical energy, stand out with their high efficiency and low emissions. However, perfluorinated sulfuric acid (PFSA)-based membranes commonly used in PEMFCs have been criticized for their high costs and environmental impacts. In this context, alternative fluorine-free hydrocarbon-based membranes are being investigated. This project aims to develop membranes based on sulfonated polyether ether ketone (SPEEK) derived from PEEK derivatives. SPEEK offers advantages such as tunable proton conductivity, high thermal stability, and low methanol permeability as a low-cost and environmentally friendly alternative.

1.Introduction

Global efforts to meet the increasing energy demand have prompted researchers to develop innovative technologies that ensure high reliability and low emissions [1]. In this regard, hydrogen energy has emerged as a promising and sustainable alternative to conventional energy sources. Among various conversion technologies, fuel cells represent one of the most efficient methods for transforming hydrogen energy into electricity [2][3]. In particular, proton exchange membranes (PEMs) have attracted significant attention in recent years due to their high energy efficiency, elevated power density, zero greenhouse gas emissions, and relatively low operating temperatures. [4]. Owing to these characteristics, PEMs have found widespread application in advanced technological fields, including stationary power generation, residential energy systems, the automotive industry, and portable electronic devices [5][6][7]. With an operational temperature range of 25–120 °C and an efficiency reaching up to 65%, PEMs stand out as a promising technology for future sustainable energy systems [8].

2.Expremental

In the experiments to be carried out at Kocaeli University, SPEEK will be synthesized by sulfonation at different PEEK/acid ratios, and the relationships between the degree of sulfonation, molecular weight, and proton conductivity will be investigated. The obtained SPEEK membranes will be produced by both methods, and their mechanical and chemical resistance be tested. The surface morphology of the membranes analyzed by SEM, and water uptake, swelling ratio, and ion exchange capacities will be evaluated. Proton conductivity will be measured by EIS and compared with commercial Nafion membranes. In addition, thermal stability will be analyzed by DSC and TGA, and chemical resistance in different media will be analyzed. FTIR spectra were used to confirm the chemical structures of SPEEK membranes. As shown in figure1.

3.Results and Discussion

FTIR spectroscopy FTIR spectrum of pure SPEEK membrane is shown in Figure 1 (Supplementary Information). The hydroxyl (–OH) groups are represented by a characteristic broad absorption band in the FTIR spectra, which appears around 3300–3500 cm^{-1}. Furthermore, the frequency ranges of 1050 cm^{-1}, 1250 cm^{-1}, and 1465 cm^{-1} exhibit three distinct absorption bands of the –SO3H groups. These absorption bands can be ascribed to the S = O stretching, the asymmetric O = S = O stretching, and the symmetric stretching vibration of O = S = O, respectively [9]. Table 1 shows the analysis data of SPEEK membrane samples. The data obtained reveal that the DS increases as the concentration decreases, while the molecular weight (Mw) decreases and the ionic conductivity (σ) increases significantly. It was observed that sulfonation conditions at low concentrations resulted in a deeper and more widespread sulfonic group insertion into the polymer chain, which increased the DS (%) and improved the proton conductivity.

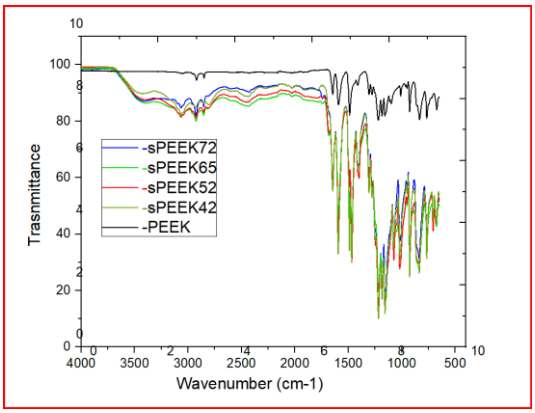

Fig. 1. FTIR of SPEEK sampales

Ph.D. Akbar KHOSHNOUDI is with the Department of Chemical Engineering, Science Institute, Kocaeli University, İzmit, Turkey. He graduated from Sahand University of Technology, Tabriz, in 2015, earned his M.Sc. in 2023 and began her Ph.D. studies in 2025. His research focuses hydrogen production and fuel-cell technologies. Email: akbarkhoshnoudi@gmail.com

Tel: +90 552 261 5215

However, the high degree of sulfonation also caused partial distortion of the polymer chain and a decrease in chain length, resulting in a decrease in molecular weight and increase in DS (%) and proton conductivity. According to the data obtained from the results of this study, it was reported that the sPPEK12 membrane with a low sulfonation degree and high molecular weight can be used instead of Nafion 115, and the sPPEK4 membrane with high DS and low Mw can be used instead of Nafion 212.

Table 1

Data obtained from some analysis results

Samples	(Mw) (g/mol)	DS (%)	IEC	Conductivity (δ) ms/cm
PEEK	29345.33		0.067	-
sPEEK38	25565.52	38.2	1.20	21.7
sPEEK40	22976.06	40.3	1.23	28.2
sPEEK45	20671.50	45.6	1.35	33.4
sPEEK66	16944.19	66.1	1.94	45.6
sPEEK73	15496.30	72.9	2.21	56.3
Nafion 115	-	21.3	0.70	21.5
Nafion 212	-	26.5	0.78	36.7

As DS increases in SPEEK, the SO_3H density and consequently the IEC increase; this increase generally enhances proton conductivity while also increasing water uptake and swelling. Therefore, DS is the main tuning parameter in the conductivity–dimensional stability trade-off. The literature shows that with very high DS (high hydrophilicity), mechanical weakening and the risk of excessive swelling/dissolution increase; whereas a more balanced performance is achieved in the medium DS range. Nafion-class PFSA membranes offer high hydrated conductivity due to distinct nano-phase separation and continuous hydrophilic channels, whereas in SPEEK, phase separation may be weaker, leading to a noticeable decrease in conductivity, especially at low relative humidity[10]. Table 2 shown Nafion™ NR212 is a commercially available PEM based on a chemically stabilized PFSA/PTFE copolymer, approximately 50.8 µm thick, in acid form. Manufacturer bulletins report typical values for NR212 of a total acid capacity in the range of 0.95–1.01 meq·g^{-1}; and tensile strength of ~32 MPa. In contrast, the IEC value for SPEEK membranes can be designed over a wide range depending on the DS; fuel permeability is reported to be lower than Nafion in most studies; however, proton conductivity and water management are strongly dependent on the DS and morphology[11].

Table 2

SPEEK and Nafion212 properties

Parameter	SPEEK	Nafion™ NR212
Thickness	20–100 µm	≈50.8 µm
Total acid capacity / IEC	≈1.0–2.5 meq·g^{-1} (tunable via DS)	0.95–1.01 meq·g^{-1}
Water uptake	≈20–70%	≈50% ±5 (100 °C, 1 h)
Proton conductivity 80 °C	≈0.03–0.12 S·cm^{-1} 80 °C / 100% RH	0.036 S·cm^{-1} under 80 °C / 100% RH
Methanol permeability	Generally, ~1–2 orders of magnitude lower than Nafion	Relatively high (disadvantage in DMFC)

Proton Conductivity, hydration and moisture dependence SPEEK's proton conductivity is fundamentally dependent on (i) –SO_3H density (IEC/DS), (ii) water content and water states (bound/free), (iii) continuity of the hydrophilic phase, and (iv) measurement geometry. Under fully hydrated conditions, it has been reported that SPEEK membranes can achieve conductivities approaching those of Nafion with appropriate DS selection. However, due to the limited morphological phase separation and stronger water binding, SPEEK may be more susceptible to conductivity loss at low relative humidity; this becomes particularly evident in the 40–100% RH range. Figure 2. Shown proton conductivities of membranes.

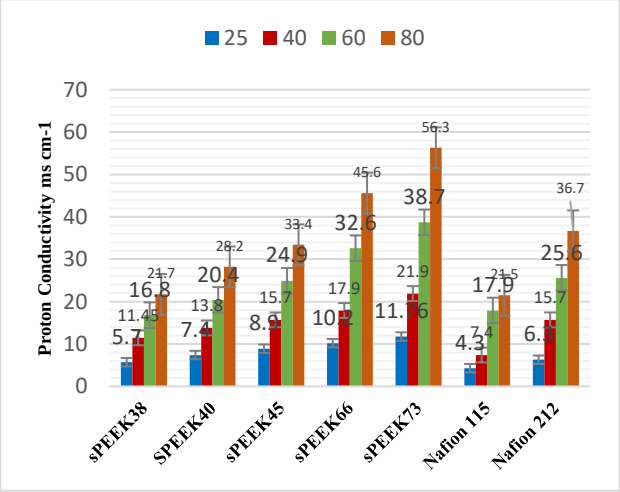

Fig.2. Proton conductivities of membranes at various temperatures.

Thermal Stability, SPEEK's PEEK-based aromatic backbone provides high Tg and thermal stability advantages in hydrocarbon-based PEMs. While TGA studies typically show two-step mass loss (–SO_3H decomposition and backbone

degradation), membranes in the medium DS range can remain dimensionally more stable up to 150–200 °C. Mechanically, as DS increases, a tendency toward decreased modulus/tensile values may be observed due to hydrophilization and plasticization. Nafion NR212, on the other hand, offers strong chemical resistance and industrial maturity thanks to its perfluorinated backbone; however, disadvantages such as cost and fuel transfer make fluorine-free alternatives like SPEEK attractive. Fig 3 shown TGA and DSC curve of SPEEK samples.

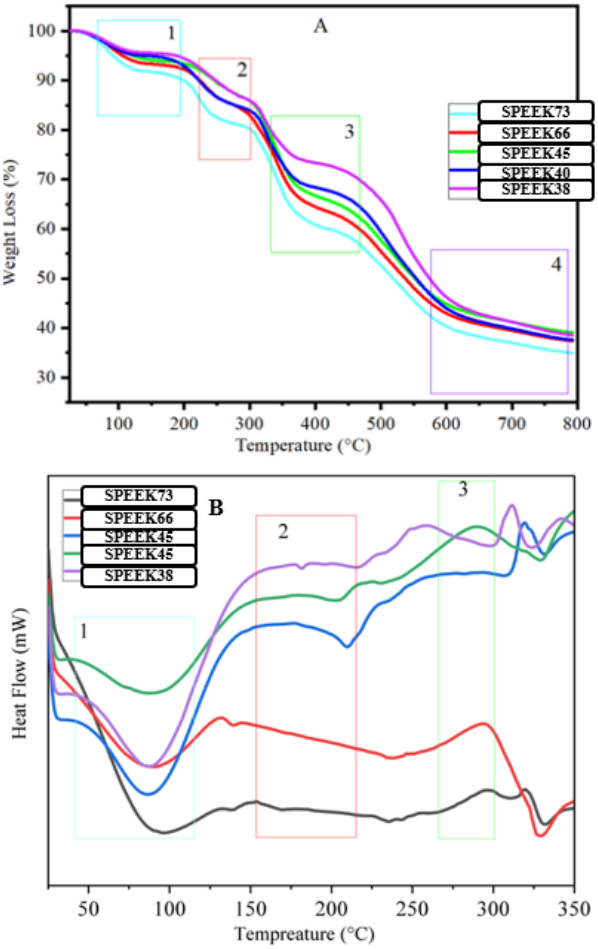

Fig. 3. TGA (A) and DSC (B) curves of the SPEEK membranes

In SPEEK, Tg increases with increasing sulfonation degree and water content, as clearly observed in Speek73 and sPEEK66 membranes [12]. In the 318–260 °C range (peak $T_{p3} \approx 330$ °C) a predominantly endothermic peak, occasionally exhibiting shoulders, is observed, corresponding to the initial pyrolytic steps of –SO_3H functional groups, including early desulfurization, dehydration, formation of SO_3-, H_2O-, or SO_2-related volatile species, and/or rearrangement of acidic groups; this region correlates with the second mass-loss band (180–350 °C) in TGA [13] [14].

4. Conclusions and Recommendations

SPEEK is a hydrocarbon PEM that can be synthesized relatively simply using a post-sulfonation approach with concentrated H_2SO_4 and whose properties can be widely adjusted via DS/IEC. The literature indicates that SPEEK offers a strong alternative to Nafion in DMFC applications, particularly due to its suppression of methanol permeability; however, its proton conductivity and low moisture performance may be more sensitive to morphology/hydration management. While Nafion™ NR212 is a strong reference in terms of industrial maturity and stability, limitations such as cost and fuel crossover continue to drive the search for alternative membranes. For future work, it is recommended to (i) ensure dimensional stability through DS/IEC optimization, (ii) develop design strategies that enhance phase separation, and (iii) report long-term durability using standardized metrics through accelerated aging tests (chemical/mechanical).

Reference

[1] "Advancements in proton exchange membranes for high-performance high-temperature proton exchange membrane fuel cells (HT-PEMFC)".

[2] A. KHOSHNOUDI and R. AKAY, "Simulation And Optimization Of Hydrogen Production By Steam Reforming Of Natural Gas," *Journal of the Turkish Chemical Society Section B: Chemical Engineering*, vol. 6, no. 2, pp. 123–136, Oct. 2023, doi: 10.58692/jotcsb.1346122.

[3] "Thermal Modeling of Solid Hydrogen Storage in a LaNi5 Metal Hydrid Tank".

[4] J. Liu, X. Peng, X. Wang, X. Zhong, and J. Wang, "Electrochemical ozone production: from fundamental mechanisms to advanced applications," Nov. 22, 2024, *Royal Society of Chemistry*. doi: 10.1039/d4ey00204k.

[5] T. Kocakulak and T. A. Arslan, "Investigation of the use of fuel cell hybrid systems for different purposes," *Engineering Perspective*, vol. 3, no. 1, pp. 1–8, 2023, doi: 10.29228/eng.pers.68466.

[6] D. Chen *et al.*, "Novel extraction method of working condition spectrum for the lifetime prediction and energy management strategy evaluation of automotive fuel cells," *Energy*, vol. 255, p. 124523, Sep. 2022, doi: 10.1016/j.energy.2022.124523.

[7] W. Zou, D. Froning, Y. Shi, and W. Lehnert, "An online adaptive model for the nonlinear dynamics of fuel cell voltage," *Appl. Energy*, vol. 288, p. 116561, Apr. 2021, doi: 10.1016/j.apenergy.2021.116561.

[8] Y. Pang and Y. Wang, "Water spatial distribution in polymer electrolyte membrane fuel cell: Convolutional neural network analysis of neutron radiography," *Energy and AI*, vol. 14, p. 100265, Oct. 2023, doi: 10.1016/j.egyai.2023.100265.

[9] A. Anis *et al.*, "Sulfonated poly(ether ether ketone)-Protic ionic Liquid-Based anhydrous Proton-Conducting composite polymer electrolyte membranes for High-Temperature fuel cell applications," *J. King Saud Univ. Sci.*, vol. 36, no. 6, Jul. 2024, doi: 10.1016/j.jksus.2024.103215.

[10] P. Xing, G. P. Robertson, M. D. Guiver, S. D. Mikhailenko, K. Wang, and S. Kaliaguine, "Synthesis and characterization of sulfonated poly (ether ether ketone) for proton exchange membranes," *J. Memb. Sci.*, vol. 229, no. 1–2, pp. 95–106, Feb. 2004, doi: 10.1016/j.memsci.2003.09.019.

[11] S. Xue and G. Yin, "Methanol permeability in sulfonated poly(etheretherketone) membranes: A comparison with Nafion membranes," *Eur. Polym. J.*, vol. 42, no. 4, pp. 776–785, Apr. 2006, doi: 10.1016/j.eurpolymj.2005.10.008.

[12] G. Li, J. Xie, H. Cai, and J. Qiao, "New highly proton-conducting membrane based on sulfonated poly(arylene ether sulfone)s containing fluorophenyl pendant groups, for low-temperature polymer electrolyte membrane fuel cells," *Int. J. Hydrogen Energy*, vol. 39, no. 6, pp. 2639–2648, Feb. 2014, doi: 10.1016/j.ijhydene.2013.11.049.

[13] M. M. Ali *et al.*, "Optimization of sPEEK/S-TiO2 nanocomposite membranes using response surface methodology for low-temperature fuel cell," *Results in Engineering*, vol. 24, p. 102862, Dec. 2024, doi: 10.1016/j.rineng.2024.102862.

[14] Y. Yagizatli, B. Ulas, A. Sahin, and I. Ar, "Preparation and Characterization of SPEEK–PVA Blend Membrane Additives with Colloidal Silica for Proton Exchange Membrane Fuel Cell," *J. Polym. Environ.*, vol. 32, no. 9, pp. 4699–4715, Sep. 2024, doi: 10.1007/s10924-024-03263-z.

Directions for Solving Design and Long-Term Operation Problems of Solid Oxide Fuel Cell Installations

Ramiz Hasanov, Riad Naghiyev , Saida Musevi

Azerbaijan State Oil And Industry University

Abstract

The thermo-mechanical analytical model proposed for different solid oxide fuel cell (SOFC) designs addresses the deformation behavior and mechanical stability of SOFCs at various thermal stresses, specifically the creep resistance and the long-term endurance beyond the elastic limit.

The model considers the deformation of multi-layer SOFC in the temperature range of 600–800°C and presents the combination of the correlated parameters for SOFC performance evaluation, stability and long-term endurance under realistic operating conditions and temperature gradients. The numerical analysis of the thermo-mechanical properties of the SOFC materials is presented in terms of mechanical behavior at failure conditions and the influence of rheological and structural properties on SOFC long-term endurance. The SOFC thermal behavior, creep parameters of the SOFC materials and long-term stability are analyzed in terms of stresses, deformations and displacements.

Keywords: modelling, materials, performances, operating temperature, design of compatibility, porous, plasticity, state of equilibrium, thermal strain stresses.

1.Introduction

Conventional energy sources such as gasoline (diesel), coal and hydro source are the main sources for power generation. However, these conventional energy sources are being depleted, and are also unfriendly to the environment. Alternative energy sources such as renewable energy (RE) systems are becoming more popular in power generation applications. RE sources include solar energy, wind energy, photovoltaic (PV) cell energy, fuel cell etc which are very effective in reducing the green house gas emissions. In the near future, large portions of increase in electrical energy demand will be met through widespread installation of distributed generation (DG). Many advantages are considered for application of DG, i.e., increased service reliability, reduction of the need for grid reinforcement, generation expansion and power factor correction. Furthermore, it is possible to improve voltage regulation and local power quality more precisely using DGs in comparison to conventional centralized generators. DG sources comprise of direct energy conversion sources producing DC voltages or currents such as fuel cells and photovoltaic sources, high-frequency sources such as micro turbines, and variable frequency sources such as wind energy. Power generation from solar energy sources and wind energy sources is unpredictable, because solar power depends on the availability of sun light and wind energy system depends on the wind. Since fuel cells have no geographical limitations, they are preferred for small scale power generation. Power generation in fuel cells depends on the hydrogen input which is available in abundance. Further, fuel cells are known for their low to zero emissions, high efficiency (35-60%) and high reliability because of the absence of moving parts. Fuel cells are static energy conversion devices that partially convert the chemical energy of fuels directly into electrical energy and produces water as its byproduct.

The successful utilization of materials requires that they satisfy a set of properties. These properties can be classified into thermal, optical, mechanical, physical, chemical, and nuclear,

promise of an efficient, low pollution technology for production of electricity and efficient use of waste heat including low and they are intimately connected to the structure of materials. The structure, in its turn, is the result of synthesis and processing. A schematic framework that explains the complex relationships in the field of the mechanical behavior of materials, shown in Figure 1, is Thomas's iterative tetrahedron, which contains four principal elements: mechanical properties, characterization, theory, and processing. Interrelationships among structure, properties, and processing methods, the most important theoretical approaches, and the most-used characterization techniques in materials science today.

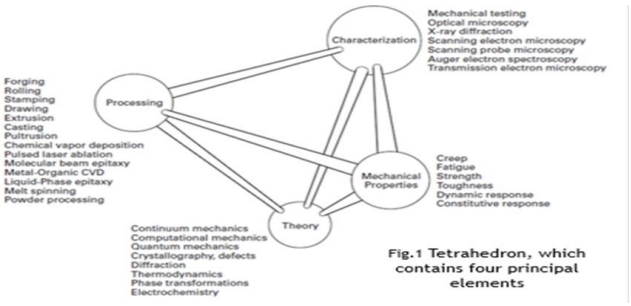

Fig.1 Tetrahedron, which contains four principle elements

Clean and sufficient energy is an important precondition for the continued growth in global wealth. Solutions must be found to utilize the remaining fossil fuels more efficiently and also to ensure that new environmentally friendly fuels can secure power production in the post-fossil fuel era. This is the essence of the global energy challenge. Fuel cells hold the promise of an efficient, low pollution technology for production of electricity. Because fuel cells rely on electrochemical rather than thermo-mechanical processes in the conversion of fuel into electricity, the fuel cell is not limited by the Carnot efficiency as is the case for conventional generators. High-temperature fuel cells hold the conversion of fuel to power. The only rotating parts in the system are a fuel pump and a small air blower. Accordingly, maintenance

transmission losses. Scalability, decentralization, and load following capabilities are major advantages that can play an effective role in future power grids and power supply.
Solid oxide fuel cells offer the potential of high volumetric power density, cost efficiency, and fuel flexibility, and significant progress has been made during the last 5 years in bringing SOFC technology closer to commercialization.
This entry will endeavor to answer the question whether SOFC technology is now ready for the market or perhaps put in another way: Is the market ready for SOFC technology and which challenges still need to be addressed? Requirements to SOFC design: There are six main types of fuel cell: alkaline fuel cell (AFC), phosphoric acid fuel cell (PAFC), molten carbonate fuel cell (MCFC), polymer electrolyte membrane fuel cell (PEMFC) and direct methanol fuel cell (DMFC), solid oxide fuel cell (SOFC). The entry will describe how SOFC technology can contribute to solving the energy challenges in the future. The current status of the SOFC technology and industry will be briefly discussed and the possible markets described. Three main challenges on the road to competiveness – life- time, reliability, and cost – are addressed. Techno-economic studies of the different market segments are used to define the threshold for market entry. The entry ends by looking ahead and concluding that the SOFC technology is ready for the market with respect to the projected cost and lifetimes, but that reliability under real-life conditions still remains to be demonstrated. The learning investments needed, however, do not appear to be prohibitive considering the benefits which this game - changing technology has to offer. Among different types and scale power generation systems, fuel cells have received more attention, because they can provide also both heat and power. Advantages of SOFC Fuel Cells are:

- Higher electrical efficiency. The SOFC technology will be able to provide an electrical efficiency of up to 60%. This efficiency is very high compared to worldwide power plants operating at average electric efficiencies of 30–35% and to existing decentralized, smaller power generation equipment (engines and generators) operating at as low as 5–10% for engines and 15–25% for generators. Application of SOFC units with higher electrical efficiency will result in substantial savings in fuel and money, and for operation on fossil fuels also in a proportional reduction in CO2 emissions;

- High efficiency for all capacities. The SOFC technology is scalable and can cover the complete range from 1 kW to 1 MW, or even higher, with almost no loss of efficiency. The technology offers a very competitive output per weight or volume compared to power plants. Because of this, the SOFC technology addresses a wide range of applications and finds use both in urban and remote areas and both for stationary and mobile purposes;

- Fuel flexibility. The SOFC technology is (together with MCFC) the only technology among the different fuel cell technologies which is able to effectively generate power directly based on the fossil fuels in use today, and at the same time, the technology has a clear path to renewables and CO2-neutral energy systems. This is due to the higher operating temperatures and the superior ability of the SOFC to convert hydrocarbon in the fuel cell stack. - Lower maintenance cost. The SOFC system provides a highly effective and direct electrochemical

costs are expected to be substantially lower, and operating periods between overhauls are substantially longer than conventional technologies.

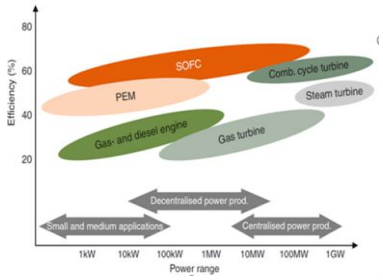

Fig. 2. SOFC compared with other power production technologies (illustrative figures)

2. Experimental

Materials and Methods:

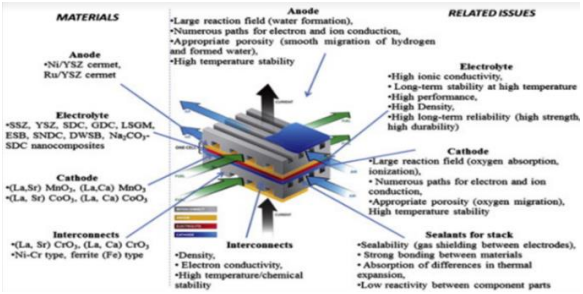

Fig. 3. Characterization of SOFC material support. (Yokokawa,H. 2003)

Structural strength of materials – a set of mechanical properties that ensure reliable and long-term operation of the material under operating conditions depend on a number of factors (fig.4)

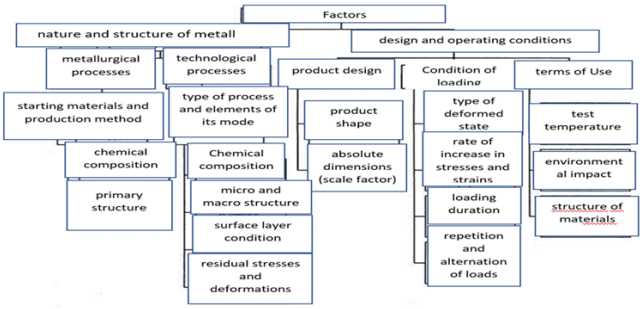

Fig 4. Factors define reliable and long-term operation of the material

According to the work is planned to study ma-terials of different structural content exposed to operating temperature during the operation of the facility, namely (Figure 5):

1. Dense structure, based on zirconium (Zr); 2. Porous structure, based on titanium (TI); 3. Materials based on transition metals, so-called Max Phase in different chemical composition.
Structural elements of operating process equipment in a deformable state especially for long-term operation that exist

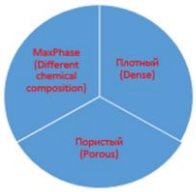

Fig.5. Used Material structure type

Creation of materials with given and desired properties to ensure a higher consumer quality of devices by synthesizing compatible combinations of the indicated disciplining factors and structural properties of materials [7, 8]

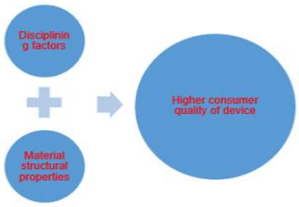

Figure 6. Creation of materials with given and desired properties

The structural properties of the materials used for SOFC elements (mainly their porosity) significantly affect their operational performance and are associated with their deformation behavior, which is accompanied by structural variability. These processes are also associated with the structural variants of the elements and the device in general. Thus, the study of the structural changes associated with the material supply of its elements (Fig. 7, 8) is an area of research that attracts attention, in which the operational processes of the structural operation of the device built on various elements are noted.

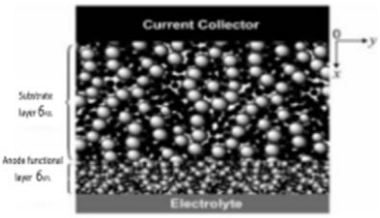

Fiq. 7. Schematic view of a two layer porous composite anode (Zenga, S., 2017)

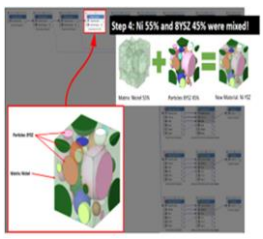

Fig.8. Sample of obtaining the porous structure

the Young's modulus of the skeleton and the medium that fills the pores under compression. During operation, the porous structure is also deformed under the influence of external factors. under high operating performances and in the course of activity are exposed to strong deformations. In the past, of these elements deformations, material of which characterized by a nonlinear character have been extensively investigated (Antman S.(2005) - Vasilev A.,1989). Importantly, these studies of various deformation processes in element's material allowed to predict the corresponding impacts of the deformation processes to the operating efficiency. In this regard, the numeric study of inelastic deformations under different conditions in porous structural elements during different stages of their exploitation and under non-equiaxial loading (Hasanov, 2011) has been performed. Furthermore, (Holm B., 2010) new experimental data has been generated on the strain hardening behavior in samples under operating conditions.

2.1 Influence of the elements surface

Influence of the elements surface on the stability of the SOFC design:

The third direction of work – to study of porous materials for use in the practice of designing a device as a whole and their elements. This issue has been discussed many times with project partners. With his great support and faith in the possibility of application in the practice of creating devices, the following task has been set and solved:

Development goal – the study of the deformation behavior of porous structure and the determination of an adequate deformation model for this behavior, taking into account mass transfer processes in a dynamic model for planning and effective implementation of various measures aimed at designing devices using of a similar material structure.

Task content:

1. The problem of determining a mathematical model of deformation behavior and studying, on this basis, the stress-strain state of porous structure under quasi-static and dynamic loading is being solved.
2. The presence of mass transfer during loading, etc. the dynamism of porous structure distinguishes and is decisive for choosing their equations of state.

Problem solution:

The mathematical model of deformation behavior for studying the stress-strain state of any medium with a porous structure includes 21 equations, of which:
- 9 equations of the form ε= ε(u) define geometric ratios;
- 9 equations of the form σ= σ(ε) define physical ratios;
- 3 equilibrium equations (or equations of motion if dynamic loading is considered).

Source dependencies:
1. A porous structure is considered, inclu ding a solid phase from the skeleton of the structure and a phase of the filling pore.
2. Reduced modulus of elasticity porous structure is defined as [1]

$$E_{pr}\frac{m_s E_s + m_g E_g}{m} \quad (1)$$

, where Epr is the reduced modulus of elasticity; m, ms, mg are, respectively describe both plastic and nonlinear elastic deformation of a body with a porous structure.

This contributes to the migration of the medium filling the pores in the direction of the pressure gradient - P in the pores, as a result of which the volume of the medium filling the pores changes, i.e. as a view from (1) Epr is a function of time and therefore:

$$E'_{pr} = \frac{m_s(E_g - E_s)}{(m_s - m_g)} m'_g \qquad (2)$$

Under quasi-static loading, which provokes a slow change in the stress state of the porous structure due to displacement, the mass of the medium filling the pores mg decreases (how many this is also question and must be defined!! This task is currently being studied)

Dependency analysis for Epr:

1. It is assumed that only mg changes with time, i.e. mg < 0;
2. For most porous structures Eg < Es;
3. Then from (2) due to the fact that ms(Eg − Es) < 0 and mg < 0, then Epr > 0, which means that over time the reduced modulus of elasticity for a porous structure, containing a certain medium in the pores increases, i.e. the tension diagram between the normal stress "σ" and the relative strain ε for uniaxial tension in various modes (see Figure 9) will have the form (see Figure 10).

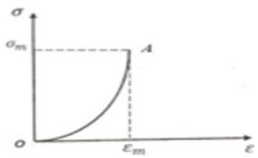

Figure 9. Tension diagram of a porous and non-porous structure, the pores of are filled with a medium, where σm, εm are the maximum values, respectively, of stress and strain.

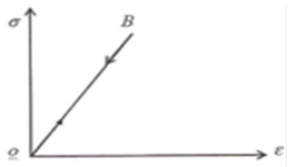

Figure 10. Tension diagram of a porous structure, the pores of which are filled with a medium (high-speed loading).

Thus, we can conclude that when the stress-strain state of a porous structure is studied, depending on the loading rate, different equations of state should be used, i.e.:

1. With dynamic processes, i.e. under impulse loads, the dependence σ = σ(ε) is represented by a straight curve, as a result of which the equation of state can be expressed by the Hook law.

2. Under quasi-static loading, i.e. for time-distributed loads, the application of the HUK law can lead to large inaccuracies (up to 80%). This is especially true for porous structures, in which the loading process is characterized by the presence of mass transfer and which have deformation characteristics that coincide with the characteristics for elastic-nonlinear bodies.

Thus, the equation σ = f(ε) of the load diagram branches can

Hence, to obtain the equation of state for porous body, the equation of state for structures with an elastic-plastic characteristic can be used.

Consequently, as a result of the analysis of the dependence that determines the change in one of the mechanical indicators - the reduced modulus of elasticity for the porous structure, two possible variants of its loading, different in terms of deformation behavior, have been established, namely:

1. Quasi-static (the reduced modulus of elasticity Epr increases);
2. Speed loading (the reduced modulus of elasticity Epr remains permanent).

As the initial equation, the functional dependence for elastic media in the form of the stress tensor σij on the components of the strain tensor εij , the components of the metric tensor gij and external disturbances (temperature, pressure and radiation dose) in various combinations is used, which is represented by the dependence below:

$$\sigma_{ij} = f_{ij}(\varepsilon_{\alpha\beta}, g_{\alpha\beta}, T - P, D), \quad i,j,\alpha,\beta = 1,2,3 \qquad (3)$$

To determine the equation of state for elastic and elastic-plastic structures in a general form, the method of expansion in a Taylor series of the original above equation was used to study the functional dependence σij and εij at T, P = constants, D = 0, which is presented both for stresses and for deformations:

$$\sigma_{ij} = Pg_{ij} + Q\varepsilon_{ij} + R\varepsilon_{ik}\varepsilon_{kj}, \quad i,j = 1,2,3$$
$$\varepsilon_{ij} = Ag_{ij} + B\sigma_{ij} + C\sigma_{ik}\sigma_{kj} \qquad (4)$$

where P, Q, R are functions of the invariants of the strain tensor and the stress tensor . In a particular case, it is assumed that P = lq, Q = 2m, R = 0, l, m – Lame coefficients; q = eij gij – relative volume change or the first strain invariant

To describe the deformation behavior of elastic-plastic structure, an analogy was used between the deformation characteristics of elastic and plastic structures in the processes of loading and unloading, which is based on the assumption that there are no constant values of the elastic modulus and yield strength for deformable porous structures.

After carrying out a number of mathematical calculations, the equations of state of porous structures were obtained for the variants of their loading, respectively, by quasi static and dynamic loads:

$$\varepsilon_{ij} = (1 - k_0)\left(\frac{1+\nu}{E_s}\sigma_{ij} - \frac{\nu I_1}{E_s} g_{ij}\right)$$
$$\varepsilon_{ij} = \frac{1+\nu}{E_r}\sigma_{ij} - \frac{3\nu}{E_r}\sigma_{ij}$$

Influence of the elements surface on the stability of the SOFC design:

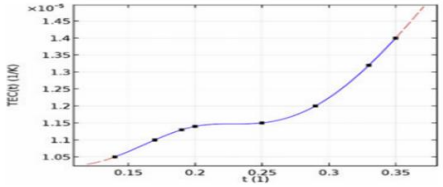

Figure 18. The relationship between porosity and TEC

5. At the initial stage of operation of a body made of a porous material, a decrease in pressure and saturation with environmental

Table 1

Layer	Young's Modulus[GPa]	Poisson's ratio	Coefficient thermal expansion (CTE) [10^{-6} K^{-1}]
Anod	220	0.3	12.5
Cathod	160	0.3	11.4
Electrolyte	205	0.3	10.3
Interconnect	205	0.28	12.3

In all models the most commonly used materials were studied to analyze the distribution of thermal stress. The mechanic properties of materials were listed in Table 1 taken from Refs. [8,23]. It should be noted that the material was assumed as linear elastic and isotropic. Fig. 18 showed the anode's coefficient of thermal expansion, which was a function of its porosity. Moreover, the Young's modulus (GPa) and shear modulus (GPa) was a function of porosity, which was the main point all of investigations and could be calculated from the used for that experimentally obtained equations.
The thermal strain stress was enhanced when the temperature increased, which resulted in a thermal expansion, which was different for each material (see table 1). The thermal stress was proportional to the coefficient of thermal expansion (a) and the difference of the temperature distribution (T) and the reference temperature (Tref). The reference temperature was the sintered temperature for the cell's materials and it was set as 800ºC, i.e., the thermal strain stress only emerged when the temperature was higher than 800ºC.

3. Results and Discussion

Basing on the received results it is possible to draw following results:

1. The relaxation time of the porosity of a porous medium in individual dimensional ratios has a different effect on its deformation behavior.

2. The most appreciable influence renders relaxation time on character of change of the porous body layers porosity. In bodies with it nonlinear elastic the deformable behavior porosity decreases more slowly than in mediums with pronounced relaxation character, and with increase in time of a relaxation rate of decrease in porosity is slows down.

3. In media with a high initial operating pressure, porosity can decrease in layers both in the nonlinear-elastically deformable mode and during relaxation and occurs faster than in media with a low initial pressure of the medium.

4. The pressure in the porous medium and their saturation with environmental products contribute to the relaxation process decreasing faster than in media with nonlinear elastic deformation behavior, and with increasing relaxation time the rate of their decrease intensifies.

products with a nonlinear-elastic deformable characteristic and with relaxation occurs under the same law, and subsequently, as the object is used, starting from a certain point in time in bodies with a nonlinear-elastic deformable medium and with relaxation there is a slower decrease in pressure and saturation than in bodies with a relaxation environment.

6. As the value of the initial pressure increases, the difference between the corresponding values of pressure and saturation in the case of a medium with relaxation and nonlinear elastic deformation behavior becomes more noticeable: an increase in the initial pressure increases the influence of relaxation processes on the determined values of body pressure and saturation.

7. To maintain stability the deformation behavior of a porous medium in bodies with a relaxation performances is greater than in media with a nonlinear elastic deformable characteristic, and the difference between their values is more significant in the case of media with a high initial saturation pressure.

8. It was found that increasing the operating (pressure) and design (decreasing the porosity and the tortuosity) conditions of the porous layers increase the cell performance.

The calculation results show that, taking into account relaxation processes in porous bodies, its highest values are observed in bodies with a high operating parameters. In other words, it is necessary to take into account the main parameters of the deformation behavior of porous bodies at high operating parameters, which confirms the high effect of relaxation of bodies.

Problems and requirements to fuel elements' production:

1.Two problems are of primary importance in the development of fuel cells, namely a. mechanical and materials science and b. electrochemical. Moreover, the main ones are studies in the field of "a" – MM.

2.It is necessary not to predict mechanical behavior during long-term operation, but to maintain such mechanical behavior that would support the duration of operation;

3.It is necessary not to develop analytical models of deformation and fractal behavior, but to study the deformation behavior of models of solid layered composite bodies with different creep cores and the structure of execution of similar SOFC elements and SOFC as a whole, taking into account the impact of factors in the processes of their production and operation and the oppressive factors accompanying these processes. This means that it is necessary to synthesize materials with structures that have the required creep core, i.e. to study the change in the creep core model during operation under the influence of operating temperatures. Namely, to study the kinetics of the change in the creep core (creep core) during operation (solve the inverse problem to achieve the required service life);

4.Ionic conductivity is good when the thickness is small and the temperature is low. Both of these factors limit the mechanical properties; A stable structure is:
a. High temperature – there is low porosity;
b. Low strength – there is high porosity.

References

v. The higher the temperature, the lower the porosity
d. The lower the porosity, the lower the strength
e. The higher the porosity, the higher the polarization.

5.To assess the influence of various factors on the deformation behavior of SOFC studies beyond the elastic limit of loading under the influence of operating temperatures, taking into account the design (porous substrate) and structural (pressure in pores) factors;

6.There is no need to predict the service life of the SOFC, but it is necessary to set the service life and solve the problem of reserving the design of the elements and the SOFC itself and increasing reliability;

7.There are two structural levels: Microstructure (grains and boundaries) and Macrostructure (SOFC elements themselves). Each macrostructure, presented as a laminated composite design, has structural and chemical homogeneity (SCH):

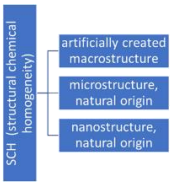

4. Conclusions

1. An algorithm has been developed for the synthesis of dense structure materials based on zirconium with properties that are compatible combinations with the operating temperature, shape and metric characteristics of devices from these materials;
2. It has been proven that porous structures are characterized by nonlinear elastic behavior under quasi-static loadings developing in time;
3. The equations of state are obtained and a mathematical model of the deformation behavior of porous structures is formulated to study their stress-strain state, taking into account the corresponding loading modes
4. It has been established that when Hooke's law is used as an equation of state to describe the deformation behavior of porous structures under quasi-static, i.e. loads distributed in time can contribute to 80% distortion of their stress-strain state.
5. The expansion in Taylor series of the original functional dependence was used, which determines the physical and geometric relationships in deformation behavior and, as a result, equations of state were obtained in general form for structure with elastic, elastic-plastic and nonlinear-elastic deformation character rustics.
6. The obtained dependences allow us to investigate various problems of studying the stress-strain state of porous structures under various loadings, determined taking into account implemented technological measures in the process of generating electricity by fuel cells on an anode substrate.

Acknowledgement

The author expresses your own sincere gratitued for this work, which was carried out with the financial support of the project G5949(Lightweight 600ºC solid oxide fuel cells for energy security (LW-SOFC) of the NATO Science for peace and Security Division during the period 2022-2025 years.

[1] Antman S.(2005).Nonlinear Problems of Elasticity.2nd edition, Springer,838 p.

[2] Baud P., Wong T. (2006). Shear-enhanced compaction and strain localization: inelastic deformation and constitutive modeling of four porous sandstones. Journal Geophysical Research, v. 111, is. B12, doi:10.1029/2005JB004101

[3] Guliyev A., Kazymov B. (2009). Deformation of rocks and its influence on their filtrations-capacitor properties and on processes of a filtration and development of oil and gas deposits. Baku: Elm, 88 p.

[4] Delin T., Zheng Ch. (2012). On A General Formula of Fourth Order Runge-Kutta Method. Journal of Mathematical Science & Mathematics Education, 7, (2), pp.1-10

[5] Chan, A. (1998). A unified finite element solution to static and dynamic geomechanics problems. Ph. D. Thesis C/Ph/106/88, University College of Swansea.

[6] Chai, Z., Shi, B., Lu, J., Guo, Z., (2010). Non-Darcy flow in disordered porous media: A lattice Boltzmann study. J. Computers & Fluids 39, pp.2069–2077

[7] Jeon D. (2009). A comprehensive CFD model of anode-supported solid oxide fuel cells, Electrochemical Acta, Vol. 54, no. 10, pp. 2727–2736

[8] Jones. R. (2009). Deformation theory of plasticity. Bull Ridge Corporation,622 p.

[9] Ju B. (2014). Mathematical model and numerical simulation of multiphase-flow in permeable rocks considering diverse deformation. Journal of Petroleum Science and Engineering, v.119, pp.149-155

[10] Hasanov R., Vasylyev O., Smirnova A., Gulgazli A., (2011).Modeling design and analysis of multi-layer solid oxide fuel cells. USA: Hydrogen Energy, Vol. 36, pp.1671-1682.

[11] Holm B., Ahuja R., Johansson B. (2001). Ab initio calculations of the mechanical properties of Ti3SiC2 Appl. Phys. Lett. 79:1450–52

[12] Pietzka M., Schuster J. (1994). Summary of constitution data of the system Al-C-Ti. J. Phase Equilib.15:392–400

[13] Vasilev A., Sotnik A. and Slis I. (1989) An influence of porosity of fracture toughness of brittle powder materials. Electron Microscopy and Strength of Materials, Institute for Problems of Materials, Kiyev

[14] Yokokawa,H. (2003) “Understanding materials compatibility,” Annual Review of Materials Research, vol. 33, pp. 581–610.

[15] Norouz Mohammad Nouri Amin Mirahmadi, Majid Kamvar (2010). A two-dimensional numerical model of a planar solid oxide fuel cell. J. Iran. Chemical. Research. 3, pp. 257-269

Synthesis of Metal/C electrocatalysts for seawater electrolysis

Dzhamal Uzun [1*], Ognian Dimitrov [1], Mariela Dimitrova[1], Adriana Gigova[1], Ivelina Tsacheva[2]

[1]Institute of Electrochemistry and Energy Systems "Academician Evgeni Budevski", Bulgarian Academy of Sciences, Acad. G. Bonchev Street., Sofia, 1113, Bulgaria

[2]Institute of Polymers, Bulgarian Academy of Sciences, Acad. G. Bonchev Street, Sofia, 1113, Bulgaria

The most important point for the production of hydrogen from seawater electrolysis was to find highly efficient and corrosion-resistant catalysts [1].

For the synthesis of transition metal catalysts such as manganese, cobalt, and their oxides supported on Vulcan XC-72 carbon black, the microwave technique was used in combination with thermal methods [2]. The aim of the study was to apply green synthesis, such as the microwave-assisted method, and to obtain spherical nanoparticles.

In this work, we considered the method and idea for green synthesis of electrocatalysts, improving the performance of Mn- and Co-based materials for OER stability in seawater, and focusing on their electrochemical characteristics. Mn- and Co-based electrocatalysts, which are cost-effective in terms of conductivity and corrosion resistance, are promising catalysts for industrial hydrogen production from seawater.

Table 1. The size of the crystallite.

Sample	Phase	Main direction		Crystallite size (nm)
		°2θ	hkl	
1	Mn_3O_4	36.09	(211)	14
2	$Co(OH)_2$	37.91	(101)	10
3	$MnCo_2O_4$	35.90°	(311)	8

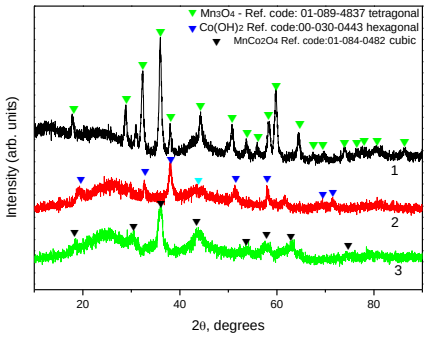

Fig. 1. XRD patern of catalysts synthesis of Carbon(/Vulcan XC-72R)/transition metal.

The electrocatalysts were characterized by X-ray diffraction, energy-dispersive X-ray spectroscopy with scanning electron microscopy, BET surface area, and pore size distribution.

Table 2. BET surface area of Metal oxide/Vulcan XC-72R nanocomposite.

Characteristics	1	2	3
Surface Area (BET), m^2/g	1128	553	856
Average Pore Diameter,(4V/S), nm	4.9	6.4	5.5

Mn and Co nanoparticles were uniformly dispersed on the surface of Vulcan XC-72R. From the newly obtained electrocatalysts, doubly coated electrodes on a nickel mesh were prepared by pressing and heating at 300°C. The fabricated electrodes had a geometric area of 2.5 cm^2.

Acknowledgments*:* The authors kindly acknowledge the financial support of the 8th Call of the Southeast Asia – Europe Joint Funding Scheme (JFS) 2023 for Technology, Research, and Innovation (*SEA-EU JFS* JFS23STI-186) and the National Science Fund at the Bulgarian Ministry of Education and Science of the project № KP-6-DO 02/3 -05.12.2024, "**Advanced Sea Water Electrolysis Technologies for Production of Green Hydrogen**" – **SeaWhy**

References

[1] Zhang, Han-Ming, et al. *Journal of Materials Science & Technology* 187 (2024): 123-140.

[2] Chen, Meng, et al. *EScience* 3.2 (2023): 100111.

Ph.D. DZHAMAL UZUN, Assist. Professor (Hydrogen Energy Systems-Electrocatalysis) at the Institute of Electrochemistry and Energy Systems" Academician Evgeni Budevski"- Bulgarian Academy of Sciences, Sofia, Bulgaria. Dzhamal Uzun graduated in 2005, obtained his M.Sc. in 2007, and Ph.D. in 2015. His research interests were electrochemical energy conversion: fuel cells, hydrogen, metal hydrides, electrochemical purification of organic pollutants, zinc-air systems, H2S and H2O (seawater) electrolysis, and synthesis of environmentally friendly electrocatalysts.

Presentating author: Dzhamal Uzun, e-mail:dzhamal.uzun@iees.bas.bg tel:+359 2 979 27 57

Design of Co/$BaTiO_3$@Vulcan XC-72 R with application in electrolysis of seawater

Ivelina Tsacheva[1], Mihaela Aleksandrova [2], Vladimir Petkov [2], Mariela Dimitrova [3], Adriana Gigova [3], Ognian Dimitrov [3], Shaban Uzun [2] and Dzhamal Uzun [3]

[1]Institute of Polymers, Bulgarian Academy of Sciences, Acad. G. Bonchev Street, Sofia, 1113, Bulgaria

[2]Bulgarian Academy of Sciences, Institute of Metal Science, Equipment and Technologies with Hydro- and Aerodynamics Centre "Acad. A. Balevski", 67 "Shipchenski Prohod" Blvd., Sofia, 1574, Bulgaria

[3]Institute of Electrochemistry and Energy Systems "Academician Evgeni Budevski", Bulgarian Academy of Sciences, Acad. G. Bonchev Street., Sofia, 1113, Bulgaria

The design of novel electrocatalysts for seawater electrolysis is an important milestone for the development of sustainable technologies through the integration of renewable energy sources. Here, we present the design of an electrocatalyst and the initial results of its application in seawater electrolysis.

The rapid rise in energy consumption in the last few years and low emission requirements have inspired many researchers to develop highly efficient, environment-friendly green energy sources. A high energy density system coupled with large energy efficiency is an effective way to store the energy produced from various renewable sources. $BaTiO_3$-based dielectric/ferroelectric materials have attracted much attention for energy storage applications in the past decade due to their improved dielectric, ferroelectric, and breakdown strength properties [1].

Barium titanate ($BaTiO_3$) (Figure 1) is the most successful ferroelectric material in the world in the production of thin films, ceramics, and composites. It was first discovered in 1944 during the Second World War in Japan, Russia, and the United States. First, it is chemically and mechanically very stable; second, it exhibits ferroelectric properties at room temperature and above; and third, it is easy to fabricate and apply in the form of polycrystalline ceramic samples. It is the world's first ferroelectric ceramic and a suitable candidate for several high-performance applications due to its excellent dielectric, ferroelectric, and piezoelectric properties. Because of its large dielectric constant and extremely low losses, barium titanate has been used in applications such as capacitors and actuators, transducers, and nanogenerators [2].

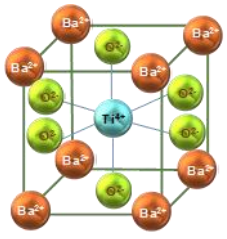

Figure 1. Structure of cubic $BaTiO_3$.

The nanocomposite of $BaTiO_3$ on Vulcan XC72R was obtained by microwave-assited technique. The use of microwave technique has a number of advantages related to better reaction control, improved reaction reproducibility, etc. With the addition of $Co(CH_3COO)_2$ to the obtained nanocomposites (Table 1), it is possible to investigate their application as alternative catalysts in the electrolysis of seawater.

Table 1. Content of the studied compound.

Sample code	Vulcan XC72R, g	$BaTiO_3$, g	$Co(CH_3COO)_2$, g
Co/$BaTiO_3$@ VulcanXC72R	1	2	2

The synthesized composite materials, using the microwave technique, could be candidates for cathode materials in seawater electrolysis, considering the electrochemical properties of Vulcan XC-72 R and transition metal (Co) in combination with the electric properties of $BaTiO_3$ they can be good electrocatalysts for the application of seawater splitting.

Acknowledgment

The authors kindly acknowledge the financial support of the National Science Fund at the Bulgarian Ministry of Education and Science of the project № KP-06-DO 02/3 _ 05.12.2024 and of Southeast Asia-Europe JFS Program 2023 STI (8th Call) JFS23STI-186/ SeaWHY, titled **"Advanced Sea Water Electrolysis Technologies for Production of Green Hydrogen".**

References

[1] A. Jain, Y.G. Wang, L.N. Shi, Journal of Alloys and Compounds, 928 (2022) 167066

[2] A. Bouhamed, S. Missaoui, A. Ben., A. Attaoui, D. Missaoui, K. Jeder, N. Guesmi, A. Njeh, H. Khemakhem, O. Kanoun, Energies 17 (2024) 4066

Associate Professor Ivelina Tsacheva is with the Institute of Polymers-Bulgarian Academy of Sciences, Department of "Polymers for Alternative Energy and Environmental Protection." She is a specialist in the synthesis of phosphorus-containing monomers and polymers with over 20 years of experience. Her research interests are related to the synthesis and characterization of new materials for energy.The results of her research have been published in 40 scientific papers in international and national journals and were also presented at more than 50 international scientific conferences.

Presentating author: Ivelina Tsacheva, e-mail: itsacheva@polymer.bas.bg tel: +359 2 979-66-32

Investigation of the Effect of Air Flow Rate on PEM Fuel Cell Performance and Comparison with an Alternative Membrane Prepared with Hygroscopic Additive to Reduce Drying Effect

Zeynep Dere[1],Ramiz Gültekin AKAY[2]
[1]Middle East Technical University, Chemical Engineering Department,06800, Ankara, Turkey
[2]Kocaeli University, Chemical Engineering Department, 41380, Kocaeli, Turkey

Due to the excessive consumption of fossil fuels worldwide and the accompanying environmental problems, research has increasingly focused on sustainable energy sources. Among these technologies, fuel cell systems have emerged as a prominent solution. Fuel cells are devices that convert chemical energy directly into electrical energy. In this study, one of the fuel cell types, the Proton Exchange Membrane Fuel Cell (PEMFC), was used. PEM fuel cells operate using hydrogen and oxygen/air as feed gases and produce only water as a byproduct. This study investigates the effect of air flow rate on the performance of a PEM fuel cell and aims to prevent membrane dehydration that may occur at low current densities.

To address this issue, performance tests were first conducted using a commercial Nafion membrane under various air flow rates. Subsequently, a composite membrane containing SPEEK/TiO_2 was fabricated in the laboratory and characterized. Performance tests were also carried out with this membrane, and a comparison was made between the results.

In parallel, a SPEEK membrane was prepared by dissolving 2 grams of PEEK in 40 mL of sulfuric acid under magnetic stirring at room temperature. After mixing, the solution was placed in an ice bath and stirred at room temperature for approximately 24 hours. The resulting sulfonated PEEK was then washed and dried in an oven at 50°C for 24 hours. The membrane was characterized through tests including water uptake, Degree of Sulfonation (DS%), Ion Exchange Capacity, and conductivity.

Following this, a SPEEK/TiO_2 composite membrane containing 1 wt% TiO_2 was prepared and subjected to the same characterization tests. Performance tests will also carried out on the composite membrane, and the results were compared to those of the pristine SPEEK membrane.

%DS value of the SPEEK was found with H-NMR at Middle East Technical University. According to H-NMR results, %DS value of SPEEK was found from the following equation.

$$\frac{n}{12-2n} = \frac{A_{H_E}}{\sum A_{H_{AA'BB'CD}}} \qquad (0 \le n \le 1)$$

$$DS = n \times 100\%$$

According to this equation, %DS value of SPEEK is calculated as %64.

Ion exchange capacity (IEC) was found by making titration. In titration, 0.01M NaOH and 2M NaCl was used. To calculate the IEC, following equation was used.

$$\mathrm{IEC} = \frac{C_{NaOH}(\frac{mol}{L}) \times V_{NaOH}(L)}{m_{dry\ membrane}(g)} \qquad [2]$$

According to this equation, IEC of SPEEK membrane and IEC of SPEEK/TiO_2 membrane was found 1.0295 m_{eqv}/g and 1.372 m_{eqv}/g, respectively.

Acknowledgment
This project supported by TÜBİTAK.
Project no: 1919B012328074

References

[1] R. Gültekin Akay, 'Development and Characterization of Composite Proton Exchange Membranes For Fuel Cell Applications Middle East Technical University, 2008.

[2] M. A. B. Ali, M. A. B. Moussa, S. U. Ilyas, R. Nasir, D. Ghorbel, and S. M. A. S. Keshk, vol. 14, no. 2, Aug. 2025, doi: 10.1007/s40243-025-00305-x.

Zeynep Dere is from Department of Chemical Engineering at Middle East Technical University. she is a fourth-year undergraduate student. Her research related with fuel cell technology and membrane development.

Corresponding author: Zeynep, e-mail: dere.zeynep@metu.edu.tr Tel: +90 545 606 30 85

Graphene derived materials as carbon component of composite supported platinum catalyst for polymer electrolyte membrane fuel cells (PEMFCs)

Ilgar Ayyubov[1], Emília Tálas[1], Irina Borbáth[1], Zoltán Pászti[1], László Trif[1], Ágnes Szegedi[1], Tamás Szabó[2], Erzsébet Dodony[3], András Tompos[1]

[1]Renewable Energy Research Group, Institute of Materials and Environmental Chemistry, HUN-REN Research Centre for Natural Sciences, Magyar Tudósok körútja 2, H-1117 Budapest, Hungary

[2]Department of Physical Chemistry and Materials Science, University of Szeged, Rerrich Béla tér 1, H-6720 Szeged, Hungary

[3]Institute for Technical Physics and Materials Science, HUN-REN Centre for Energy Research, Konkoly-Thege M. út 29-33, H-1121 Budapest, Hungary

The Polymer Electrolyte Membrane Fuel Cells (PEMFCs) are efficient, compact, and environmentally friendly energy conversion devices that generate electricity directly from hydrogen through electrochemical redox reactions. However, their widespread application is hindered by the high cost and limited durability of the platinum-based electrocatalysts, typically supported on carbon (Pt/C), which are prone to degradation and CO poisoning under operating conditions.

To address these challenges, recent research has focused on developing more stable and efficient catalyst supports. One promising approach involves composite materials that integrate the corrosion resistance and nanoparticle-stabilizing ability of TiO_2 with the co-catalytic properties of molybdenum and the high surface area and conductivity of carbon-based nanomaterials. Our previous studies demonstrated that Pt catalysts supported on $Ti_{(1-x)}Mo_xO_2$-C composite supports (C = carbonaceous materials) exhibit superior electrochemical stability and enhanced CO electrooxidation activity compared to commercial Pt/C catalysts [1].

Building on this concept, the current work explores the use of advanced carbon materials, graphite oxide (GO) and graphene nanoplatelets (GNP) mixtures, as the carbon component of the $Ti_{(1-x)}Mo_xO_2$-C composites. These materials are engineered *via* a sol-gel synthesis followed by high-temperature treatment to incorporate Mo into the rutile titania lattice and facilitate further crystallisation. By partially substituting costly GO with GNP, we also aim to reduce production costs while maintaining or improving conductivity and electrocatalytic performance. The resulting electrocatalysts are systematically characterized to assess their structural, electrical, and electrochemical properties, offering new insights into durable and cost-effective materials for PEMFC applications.

20wt%Pt/75wt%$Ti_{0.8}Mo_{0.2}O_2$-25wt%GNP_x-$GO_{(1-x)}$ (x= 0.25, 0.5, 0.75, 1) catalysts were produced either by use of GNP or GNP-GO carbon mixture with different GNP to GO ratios named as Pt/25GNP, Pt/50GNP, Pt/75GNP, Pt/100GNP. The electroconductivities of the GNP-GO mixed carbon containing catalysts increased as the GNP content increased. However, the GNP-only composite (Pt/100GNP) exhibited the lowest conductivity (see Figure 1A). Although GNPs possess high intrinsic conductivity, their strong tendency to agglomerate and restack in the absence of functional groups may lead to a poorly connected and discontinuous conductive network, resulting in significant electron transport resistance. In contrast, introducing GO into the GNP matrix improved the support morphology reducing GNP stacking, and providing better anchoring sites for the oxide particles [2]. The resulting composites show improved oxide dispersion, more effective carbon-oxide interfacial contact, and formation of continuous percolation networks, all of which contribute to higher overall conductivity. However, at high GO content the intrinsic resistivity of GO began to dominate, causing a drop in conductivity.

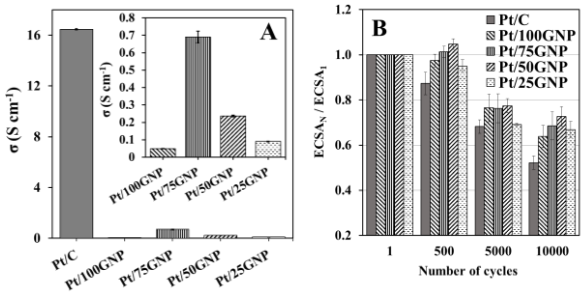

Figure 1. Electroconductivities (A) and electrochemical stabilities (B) of synthesized and reference (Pt/C) catalysts

In a long-term stability test of 10,000 polarization cycles, Pt/50GNP catalyst showed remarkable stability with an ECSA loss of 25.3%, while all synthesized electrocatalysts outperformed Pt/C (see Figure 1B). In addition, it possessed higher ECSA and ORR activity compared to its analogues.

Acknowledgment

Project no. RRF-2.3.1-21-2022-00009, titled the National Laboratory for Renewable Energy,
Hungarian innovation project VEKOP-2.3.3.15-2016-00002 (THEMIS microscope)

References

[1] Borbáth, I. et al. *Appl. Catal. A* 620 (2021) 118155.
[2] Mypati S., et al. *Carbon* 174 (2021) 581-593.

Ilgar Ayyubov is a PhD-level researcher in Research Centre for Natural Sciences, Budapest. He obtained his PhD at Budapest University of Technology and Economics in 2024. He is the MSc. graduate of Budapest University of Technology and Economics in 2020 and BSc. graduate of Baku Engineering University in 2018. His research focuses on hydrogen energy, PEM fuel cells, and advanced electrocatalytic materials. Currently, he is responsible for designing and testing of non-traditional carbon materials-containing composite supported electrocatalysts.

Ilgar Ayyubov, e-mail: ayyubovi@gmail.com tel: +36 20 2221258

A Comparative Study of A-site Deficient and Heterostructured $La_{0.6}Ca_{0.4}CoO_3$ Electrodes for Durable SOFCs

[1]Hatice Demirbas, [2]Onur Alp Aksan, [1]Seda Kol, [1,] *Mehmet Sezer

[1]Department of Materials Science and Engineering, Gebze Technical University, Kocaeli, Turkey
[2]Institute of Nanotechnology, Gebze Technical University, Kocaeli, Turkey

The development of economically viable solid oxide fuel cells (SOFCs) is critically dependent on improving the long-term performance stability of cathode components. While thin film $La_{0.6}Ca_{0.4}CoO_3$ (LCC) electrodes exhibit excellent initial electrochemical activity, they suffer from severe degradation at operating temperatures due to detrimental changes in surface chemistry, primarily cation segregation.

To address this critical stability issue, this study explores the strategic use of A-site deficient LCC (def-LCC) compositions. These materials are hypothesized to offer a dual benefit: (i) an abundance of oxygen vacancies to promote faster oxygen reduction kinetics, and (ii) slower cation diffusion to enhance surface chemical stability against segregation.

In this work, we aim to develop and systematically compare various electrode architectures to identify the optimal balance of performance and stability. The investigation will include def-LCC electrode and two distinct heterogeneous bilayer configurations: an LCC film with a def-LCC overlayer, and a def-LCC film with an LCC overlayer. All layers will be fabricated by spin coating at 3000 rpm to ensure morphological consistency.

The initial electrochemical performance and long-term stability of each electrode configuration will be thoroughly evaluated using Electrochemical Impedance Spectroscopy (EIS) on symmetrical half-cells at 700 °C. To uncover the underlying mechanisms responsible for any stability enhancements, X-ray Photoelectron Spectroscopy (XPS) will be employed to probe the surface chemistry. This comparative study is expected to reveal a viable materials engineering strategy for creating highly active and robust perovskite cathodes for next-generation SOFCs.

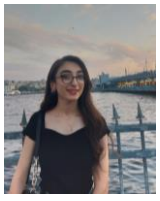

I am a senior undergraduate student in the Department of Materials Science and Engineering at Gebze Technical University. I conduct research on solid oxide fuel cells, with a focus on cathode materials, in Assoc. Prof. Dr. Aligül Büyükaksoy's laboratory.

Presentating author: Hatice Demirbaş, e-mail:h.demirbas2021@gtu.edu.tr tel: 5161634175

MgO-Doped CaO-Stabilized Zirconia: A Promising Earth-Abundant Electrolyte for Next-Generation Solid Oxide Cells

Canan Ekinci, Mehmet Sezer, Aligül Büyükaksoy

Department of Materials Science and Engineering, Gebze Technical University, Kocaeli, Türkiye

The advancement of solid oxide cells (SOCs) for clean energy applications relies heavily on the development of high-performance, durable, and sustainable electrolyte materials. While yttria-stabilized zirconia (YSZ) is the conventional choice, the supply risk and cost associated with yttrium necessitate the exploration of alternative compositions based on more abundant elements.

In this study, we systematically investigate the potential of a sustainable electrolyte system by synthesizing CaO-stabilized zirconia (CSZ) co-doped with varying concentrations of MgO (1, 2, 3, and 4 mol%). The primary objective was to enhance the ionic conductivity and thermochemical stability required for SOC operating conditions while eliminating the dependence on critical raw materials. The electrolyte powders were synthesized and subsequently characterized through a comprehensive suite of techniques. X-ray diffraction (XRD) was employed to analyze the crystal structure and phase purity, while scanning electron microscopy (SEM) was used to examine the microstructural morphology of the sintered pellets. The crucial electrical properties were determined via electrochemical impedance spectroscopy (EIS) to quantify the ionic conductivity. Finally, the practical viability of these materials as SOC electrolytes was validated by measuring the open circuit voltage (OCV) of fabricated cells.

Canan is an undergraduate student in Materials Science and Engineering at Gebze Technical University. She is currently working on electrolyte development for solid oxide fuel cells (SOFCs), specifically on MgO-doped CaO-stabilized zirconia systems, under the supervision of Assoc. Prof. Dr. Aligül Büyükaksoy. Her research focuses on enhancing ionic conductivity and reducing raw material supply risks in SOFC electrolytes.

Canan Ekinci , e-mail:c.ekinci2021@gtu.edu.tr tel:5510765112

Enhancing the Long-Term Stability of $La_{0.6}Ca_{0.4}CoO_3$ Cathodes for Solid Oxide Fuel Cells via Surface Modification with Constituent Cation Oxides

[1]Süleyman Enes Acar, [2]Onur Alp Aksan, [1]Seda Kol, [1,] *Mehmet Sezer

1Department of Materials Science and Engineering, Gebze Technical University, Kocaeli, Turkey
2Institute of Nanotechnology, Gebze Technical University, Kocaeli, Turkey

La0.6Ca0.4CoO3 (LCC) is a promising cathode material for Solid Oxide Fuel Cells (SOFCs), but its long-term stability is limited by performance degradation at high temperatures. This degradation stems from the surface segregation of secondary phases like CaO and La_2O_3.

In this work, we improved the stability of LCC cathodes by applying thin surface overlayers of their own constituent cation oxides (La_2O_3, CaO, and CoO_x). The goal was to suppress this detrimental segregation by stabilizing the electrode's surface chemistry. To ensure a direct comparison with our recent results, all cathodes were fabricated using an identical 3000 rpm spin-coating speed.

The long-term performance of the modified electrodes was evaluated at 700 °C using Electrochemical Impedance Spectroscopy (EIS), while X-ray Photoelectron Spectroscopy (XPS) was used to analyze the initial and post-operation surface chemistry. X-ray Diffraction (XRD) was employed to confirm the phase purity of the perovskite structure, while Scanning Electron Microscopy (SEM) was used to analyze the microstructure and surface morphology of the films before and after exposure to heat treatment for 100 hours in air. The results confirmed that the surface modification successfully mitigated degradation by preserving a more stable surface composition. This study demonstrates an effective strategy for engineering stable and high-performance perovskite cathodes for next-generation SOFCs.

Süleyman Enes Acar is a second-year student in the Materials Science and Engineering undergraduate programme at Gebze Technical University. During this period, he served as a member of the board of directors of the IEEE student club and also took on active roles in university teams related to rover and rocket technology. He is currently participating in research focused on solid oxide fuel cells at the same university.
Presentating author: Süleyman Enes Acar, e-mail: s.acar2022@gtu.edu.tr tel:5079018994

Lowering the Supply Risk of Raw Electrolyte Materials by Developing Ca and Mn Co-doped ZrO_2 Electrolytes for Solid Oxide Fuel Cells

Tuana Bal[1] , Mehmet Sezer[1] and Aligül Büyükaksoy[1]

[1] Department of Materials Science and Engineering, Gebze Technical University, Gebze, Kocaeli 41400, Turkey

Solid oxide fuel cells (SOFCs) are environmentally friendly electrochemical energy conversion devices that convert chemical energy directly into electricity using hydrogen as fuel. SOFCs work at high temperatures, between 500-800 ºC, to allow faster reaction kinetics and lower thermodynamic barriers to achieve high-efficiency rates (up to 90%) [1]. These systems are composed of porous, ionically and electronically conductive electrodes, and gas-tight and highly ionically conductive ceramic electrolyte membranes. The state-of-the-art electrolyte membrane is known as rare earth metal (Y, Sc, Gd, Ce) doped ZrO_2 [2]. Rare earth metal doping into zirconia-based electrolytes provides both high ionic conductivity with increased oxygen vacancies and thermal stability at operating temperatures for SOFCs. Although some rare earth elements are geologically abundant, their extraction is complex, and global supply chains are concentrated, leading to high supply risk and cost [3].

To address this problem, this study mostly focused on developing doped ZrO_2-based electrolytes without using high-supply risk raw materials. By finding an alternative material with a lower supply risk score, which shows similar ionic conductivity, chemical stability, and mechanical strength comparable to yttria-stabilized zirconia (YSZ) or scandia-stabilized zirconia (ScSZ), the sustainability can be enhanced.

One choice as an alternative material is CaO-stabilized ZrO_2 (CSZ) due to its high thermal stability. Using Ca^{2+} (0.99 Å) creates a larger difference in ionic radii between Zr^{4+} (0.79 Å) than Y^{3+} (0.93 Å). While this difference contributes to the thermal stability, retainment of the purely cubic phase at SOFC operating temperatures is doubtful and the achieved conductivities are somewhat lower than those achieved in YSZ. As a result, lowering the ionic conductivity of CSZ. To help stabilization, the effect of additives like MnO/MnO_2 or MgO has been researched [4].

Element	Supply risk	Element	Supply risk
Y	High	Mg	High
Sc	High	Ca	Medium
Gd	High	Mn	Medium

Table 1: Supply risk of related raw materials [3].

In this study, Ca and Mn co-doped ZrO_2 electrolytes were investigated by alternating Mn amount in $Zr_{0.83}Ca_{0.17-x}Mn_xO_2$ ($0.01 \leq x \leq 0.04$). CSZ powders doped with 1, 2, 3, and 4 mol% Mn were synthesized by the modified Pechini method and calcined at 800 ºC for 3 hours. Later, these powders were consolidated using uniaxial die pressing under ca. 50 MPa pressure and were further compacted using a cold isostatic press. Consolidated powders were sintered at 1400 ºC for 4 hours to obtain dense ceramic pellets.

Structural investigation of $Zr_{0.83}Ca_{0.17}O_2$ and $Zr_{0.83}Ca_{0.17-x}Mn_xO_2$ powders were carried out after calcination at 800 °C, using X-ray diffraction (XRD), which revealed that the desired crystal structure was successfully obtained. Electrical conductivity measurements of fabricated dense CSZ ceramics were carried out using electrochemical impedance spectroscopy (EIS), under stagnant air, by applying a silver current collector on both sides of the electrolyte membranes to provide electrical contact.

References

[1] Mendonça C, Ferreira A, Santos DM, *Fuels*, 2021, *2*, 393–419.
[2] Fergus JW. Electrolytes for solid oxide fuel cells. *J. Power Sources*. 2006;162(1):30–40.
[3] https://www.rsc.org/periodic-table (Last access: 28.06.2025)
[4] Kim S, Kim S, Lee H, Seo Y, Kim B, Lee H, Adv. Appl. Ceram., 2016, 115, 495–498.

Tuana is a senior undergraduate student in Materials Science and Engineering at Gebze Technical University. She completed an internship on electrode development for solid oxide fuel cells (SOFCs) at Boğaziçi University under the supervision of Assoc. Prof. Dr. Oktay Demircan. Currently, she is working on advancing electrolyte materials to minimize the supply risks of raw components and developing thin film air electrodes using a novel and facile polymeric precursor method under the supervision of Assoc. Prof. Dr. Aligül Büyükaksoy. She has a strong interest in electrochemistry and electrochemical interfaces.
Tuana Bal, e-mail: 0301tuana@gmail.com tel:

An Investigation into the Phase Formation, Ionic Conductivity, Surface Oxygen Exchange, and Long-Term Stability of Sr-Doped versus Undoped $LaFeO_3$ Composites with Gadolinium-Doped Ceria

Mehmet Sezer[1], Hayri Sezer[2], Ali Şems Ahsen[2] and Aligül Büyükaksoy[1]

[1]Department of Materials Science and Engineering, Gebze Technical University, Kocaeli, Turkey
[2]Department of mechanical engineering, Georgia Southern University, Statesboro, GA
[3]Department of Physics, Gebze Technical University, Kocaeli, Turkey

Mixed ionic-electronic conducting (MIEC) perovskites are critical materials for high-temperature applications such as oxygen separation membranes and cathodes for solid oxide fuel cells (SOFCs), operating between 700-900 °C. The long-term operational stability of these materials is often compromised by structural, microstructural, and chemical degradation. A primary failure mechanism in conventionally used perovskites like $La_xSr_{1-x}FeO_3$ (LSF) is the surface segregation of the A-site dopant, strontium (Sr). This phenomenon, driven by lattice strain and electrostatic attraction to surface oxygen vacancies, leads to the formation of an insulating $SrO/Sr(OH)_2$ layer, which passivates the electrocatalytically active surface and severely hinders oxygen exchange reactions, thus degrading performance.

This study re-evaluates the conventional approach of A-site doping by investigating a simplified, Sr-free material chemistry aimed at preventing surface segregation. While Sr-doping is known to create charge-compensating defects (V_o.. and h.) that initially boost performance, this work explores the potential for undoped perovskites to exhibit superior long-term stability. By maintaining a clean, active surface free from SrO passivation, the sustained performance of the Sr-free material could ultimately match or exceed that of the doped material.

In this work, Sr-doped and undoped $LaFeO_3$ powders, as well as their composites with Gadolinium-Doped Ceria (GDC), were synthesized using the Pechini method. The microstructure and phase composition were analyzed using Scanning Electron Microscopy (SEM) and X-ray Diffraction (XRD) on the as-prepared samples and after prolonged thermal exposure at 700°C. Furthermore, the evolution of ionic conductivity and the surface oxygen exchange coefficient was tracked by conducting Electrochemical Impedance Spectroscopy (EIS) and Electrical Conductivity Relaxation (ECR) measurements at 10-hour intervals throughout a 100-hour heat treatment at 700°C.

Dr. Mehmet Sezer completed his undergraduate studies in Metallurgical and Materials Engineering at Istanbul Technical University. Following his graduation, he worked as an engineer for five years in the iron & steel and plastics industries. He then pursued his graduate studies at Gebze Technical University, where he earned both his M.Sc. and Ph.D. degrees in the Department of Materials Science and Engineering. His doctoral research focused on solid oxide fuel cells and oxygen separation membranes. He currently continues his research at the same university on related topics.

Presentating author: Mehmet Sezer, e-mail:mehmetsezer@gtu.edu.tr tel:5556387090

High Proton-Conducting Electrospun Sulfonated-Silica-Based Composite Membranes for PEM Fuel Cell Applications

Naeimeh Rajabalizadeh Mojarrad[1], Selmiye Alkan Gürsel[1,2], Alp Yürüm[1,2], and Begüm Yarar Kaplan[3]

[1]Sabanci University SUNUM Nanotechnology Research Center, 34956, Istanbul, Turkey
[2]Sabanci University Faculty of Engineering and Natural Sciences, 34956, Istanbul, Turkey
[3]Departman of Industrial Engineering, University of Padova, 35122, Padova, Italy

PEM fuel cells are recognized as one of the cleanest energy conversion technologies, operating by combining hydrogen and oxygen to generate electricity, with water and heat as the only products. In recent years, they have become a practical and viable solution, particularly due to their successful integration into various sectors—most notably the automotive industry—where they contribute significantly to environmental sustainability and a cleaner future. Despite these advancements, PEM fuel cells still face challenges to widespread adoption and the replacement of conventional combustion engines, primarily due to the high cost of key components, especially membranes and electrodes, and concerns about their long-term durability. [1,2]

Nafion® is the mostly widely used membrane material in these systems which plays several critical roles in overall fuel cell performance, including proton conduction, gas separation, and water management. However, these costly membranes are suffering from several critical drawbacks such as highly water reliable conductivity and environmental concerns. Therefore, the development of new membrane materials has become a major research focus aiming to overcome their limitations.[3]

To this end, our approach involves designing either completely Nafion®-free composite membranes or tailoring membrane properties through the partial substitution of Nafion®, thereby creating more durable and cost-effective alternatives using electrospinning method.[3] This study presents the development of two types of electrospun composite membranes. In the first method, membranes were fabricated using P(VDF-TrFE) or PVDF as carrier polymers, incorporating synthesized sulfonated silica (S-SiO_2) nanoparticles known for their excellent water retention and ability to provide proton conductivity.[4] To assess the influence of S-SiO_2 content on membrane performance, samples were prepared with three different S-SiO_2/polymer ratios. As the second strategy, a dual electrospinning technique was used to produce Nafion®-based composite membranes composed of sulfonated silica, Nafion®, and either PVDF or P(VDF-TrFE) as the carrier polymers. This approach enabled the creation of dual-fiber structured mats.[5] As shown in Figure 1, a homogeneous and bead-free electrospun mat was obtained through this process. Following electrospinning, all fiber mats were converted into compact membranes through a hot-pressing process. Once the compact membranes were obtained, a comprehensive set of characterization techniques was employed to characterize their morphological, physical and electrochemical properties, including FTIR, XPS, SEM, TEM, and electrochemical impedance spectroscopy (EIS), along with measuring their exchange capacity (IEC), water uptake, and mechanical strength.

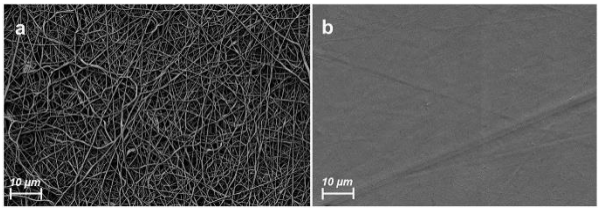

Figure 1. The SEM microgrph of SEM the electrospun mat (a) before and (b) after hotpressing pocess.

Finally, membrane-electrode assemblies (MEAs) were fabricated using these composite electrospun membranes, and fuel cell performance tests were conducted. The results demonstrated an improvement via incorporating sulfonated silica into the composite membranes, particularly under low-humidity conditions.

References

[1] Muthukumar M. et al. Materials Today: Proceedings, 45, 1181–1187 (2021).
[2] Mao J. et al. Energy and AI, 17, 100406 (2024).
[3] Shang Z. et al. Energies, 14 (20) (2021), 6709.
[4] Rajabalizadeh Mojarrad N. et al. Int J Hydrogen Energy, 46 (25), 13583-13593 (2021). [5] Rajabalizadeh Mojarrad N. et al. Solid State Ionics, 392, 11615

Naeimeh Rajabalizadeh Mojarrad holds a Ph.D. in Materials Science and Engineering from Sabancı University, where her research focused on developing electrospun sulfonated silica-based proton exchange membranes for PEM fuel cells. She also earned her M.Sc. from the same institution, working on radiation-grafted proton exchange membranes for high-temperature fuel cell applications. Her academic journey began with a B.Sc. in Materials Engineering–Ceramics from Tabriz University. She is currently working as a researcher at SUNUM (Sabancı University Nanotechnology Research and Application Center), focusing on advanced materials for energy applications..
Presentating author: Naeimeh Rajabalizadeh Mojarrad, email: nrajabalizadeh@alumni.sabanciuniv.edu, Tel: +905051305942

Synthesis and Characterization of Pyridine, Meta- and Para-Oriented Polybenzimidazole Membranes for High-Temperature PEM Fuel Cells: Thermal, Chemical, and Electrochemical Insights

Ali Hassen Ali[1], Ramiz Gultekin AKAY [1]
[1]Kocaeli University, Chemical Engineering Department

Abstract

Pyridine-, meta-, and para-polybenzimidazole membranes were synthesized via polyphosphoric acid-mediated condensation polymerization and evaluated for high-temperature proton exchange membrane fuel cells. Molecular weight analysis confirmed successful polymerization, with para-PBI exhibiting the highest chain length. Thermal and oxidative stability tests revealed superior durability for para-PBI, while meta- and pyridine-PBI showed higher proton conductivity due to greater phosphoric acid uptake. Electrochemical impedance spectroscopy indicated lower activation energy for para-PBI, reflecting more stable proton conduction pathways. The comparative results elucidate the influence of backbone orientation and heteroatom incorporation on membrane performance, providing valuable guidance for the rational design of advanced HT-PEM electrolytes.

1.Introduction

High-temperature proton exchange membrane fuel cells (HT-PEMFCs), typically operated in the 120–200 °C range, are attractive for stationary and mobility power systems because elevated temperature accelerates electrode kinetics, simplifies water/thermal management, and improves tolerance to fuel impurities such as CO relative to low-temperature PFSA-based PEMFCs. In this context, phosphoric-acid (PA) doped polybenzimidazole (PBI) membranes have become the benchmark electrolyte platform due to their intrinsic thermal/oxidative robustness, low gas permeability, and the ability to sustain high proton conductivity without external humidification.[1-3]

Despite their maturity, PA-doped PBI membranes still face well-recognized durability bottlenecks that directly constrain long-term HT-PEMFC performance: (i) phosphoric acid migration and leaching under load, (ii) mechanical creep/relaxation at high temperature (especially under compression in the membrane electrode assembly), and (iii) changes in acid speciation and distribution that couple conductivity to degradation. Recent literature therefore emphasizes that the “membrane problem” in HT-PEMFCs is not simply achieving high conductivity, but achieving conductivity together with acid retention and mechanical stability under realistic thermal and electrochemical stressors[4-6].

A central molecular-design lever for PBI electrolytes is the polymer backbone architecture, which governs chain packing, free volume, density of basic sites, and the hydrogen-bonding landscape available for PA coordination and proton transport. While “classic” AB-PBI-type backbones are widely used, contemporary work increasingly explores how structural isomerism and heteroatom incorporation can tune the balance among acid uptake (often expressed as acid doping level, ADL), segmental rigidity, and the formation of continuous proton-conducting pathways[7]. In particular, the comparison of meta- versus para-oriented PBI backbones (commonly derived from isophthalic versus terephthalic connectivity) is compelling because positional orientation influences chain linearity and packing efficiency: para-linked structures tend to promote more linear, tightly packed chains (often improving mechanical integrity but potentially limiting free volume for acid uptake), whereas meta-linked structures can introduce kinks that disrupt packing (often increasing acid uptake and mobility, but sometimes at the expense of dimensional stability). Studies leveraging meta-PBI specifically for mechanical integrity in PA-doped systems illustrate how backbone topology can be used as a structural scaffold while other components enhance conductivity[8]

In parallel, pyridine-containing PBI analogues (often denoted Py-PBI or related pyridine-bridged/oxypolybenzimidazole structures) introduce additional basic nitrogen sites and modified local polarity. The pyridine unit can strengthen acid–base interactions with PA, alter acid clustering, and increase the density of proton-accepting sites that participate in hydrogen-bond networks-mechanistic features that are frequently associated with improved high-temperature conductivity and/or improved acid utilization efficiency (i.e., higher conductivity at comparable or lower free-acid content). For example, pyridine-bridged PBI architectures have been investigated as promising HT-PEM candidates precisely because they couple high thermal stability with acid-mediated proton conduction, while offering an expanded chemical design space for controlling PA uptake and retention[9-10].

However, optimizing HT-PEM performance requires moving beyond a single-variable “maximize ADL” approach. Although increased ADL generally raises conductivity, excess free acid can plasticize the polymer, increase swelling, promote leaching, and accelerate mechanical creep-particularly under compression and thermal cycling. Recent assessments of PA-doped PBI systems therefore stress trade-offs among conductivity, dimensional stability, and durability, and motivate the need for membrane designs that immobilize acid or maintain a favorable acid distribution within mechanically resilient matrices.[1],[4,5]

Accordingly, the field has advanced several stabilization strategies-acid-base blending, inorganic/organic nanofillers, covalent or ionic crosslinking, and engineered polymer

Mr. Ali Hassen Ali is from the Department of Chemical Engineering at Kocaeli University. He graduated with a BSc from Bahir Dar University (Ethiopia) in 2013 and an MSc from Addis Ababa University (Ethiopia) in 2018. Currently, he is pursuing his PhD at Kocaeli University. His research interests include materials for energy storage, fuel cell technology, and membrane development.
Presenting Author: Ali Hassen, e-mail: alihassen131@gmail.com Tel: +90 546-826-96-64

morphologies-to mitigate acid loss and mechanical relaxation while maintaining fast proton transport. Acid-base blend membranes have demonstrated that it is possible to reach practical HT-PEMFC performance with substantially reduced acid uptake by engineering favorable acid-polymer interactions and transport pathways[7]

More recently, structural concepts such as gel-state and multi-crosslinked PBI networks have been reported to enable stable operation at temperatures approaching or exceeding 200 °C by suppressing membrane creep and limiting detrimental acid migration/evaporation phenomena[6].[11]

Within this broader landscape, a systematic comparison of pyridine-, meta-, and para-oriented PBI membranes evaluated under a common framework of thermal, chemical, and electrochemical characterization provides a direct route to linking molecular structure acid interaction/retention transport and stability.

.2.1 Experimental work

2.2.1 Synthesis of Polybenzimidazole Polymer

Under this study, three polybenzimidazoles have been synthesized, namely, meta-PBI, pyridine-, and para-PBI. The specific details of the synthesis procedure are as follows. For-meta-PBI, the technique was PPA 148.9 g and DAB (3.2650) added to a 2000-mL Pyrex® Resin reaction vessel, and the temperature was set between 150 and 168 °C during the course of 80 min. This temperature was then steadily increased to 230 °C. When the temperature reached 230 °C, 4.495 g, P2O5, 0.0587 g TPP, and 2.5300 g (0.015 mol) IPA were added to the flask, respectively. Polymerization was carried out at 230-238°C for 24 h. After polymerization, the mixture was placed into distilled water with vigorous stirring, and then the mixture was immersed in water for 3 days. The bulk was rinsed with distilled water three times, neutralized with NaHCO3, and immersed in a 5% NaHCO3 solution for more than 24 h. Then, the PBI resin was pulverized and dried on a hot plate for 4 h at 200 °C to obtain the PBI powder[12-13].

The procedure of para-PBI Membrane Preparation was the same as meta-PBI except the monomers molar concentration difference 4.08g of DAB, 3.1635 g of terephthalic acid (TA) and 200g of polyphosphoric acid (PPA) and 0.0587g of TPP were put in a 2000-mL Pyrex® Resin reaction vessel equipped with a nitrogen flow[13]

For the synthesis of Pyridine PBI, the polymerization conditions, covering monomer concentration, reaction temperature, reaction duration, and solvent type, were taken from the literature with some adjustments to the specific numerical values. [14][15]. Py-PBI was therefore synthesized by a condensation polymerization procedure at 200 °C in 300 g PPA solvent. Typically, in a 2000-mL Pyrex® Resin reaction vessel containing 300 g PPA, TAB was added. The solution was then stirred and heated at 157.2 to 164.6 °C under a N2 atmosphere for 2 h to eliminate the produced hydrochloric acid. A 5.0136 g amount of 2,5-Pyridinedicarboxylic acid was then added, and the mixture was agitated until a homogenous solution was obtained. The reaction temperature was then escalated to 166.5 °C to initiate the polymerization process, which proceeded for some hour, and then the temperature increased to 231.7°C with mechanical stirring. Next, the resulting polymer solution was put into a beaker containing water as a poor solvent to precipitate the Py-PBI polymer. The polymer was steeped in distilled water with slight agitation for 24 hours and then soaked in 2% NaHCO3 for 24 hours. The last phase was the same as the procedure of m-PBI synthesis.[14

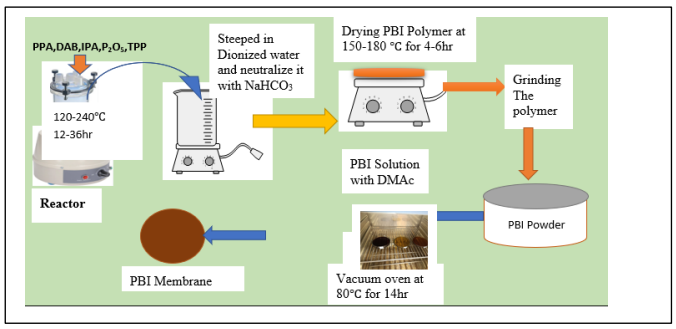

Figure 1: A simple PBI synthesis flow diagram on a laboratory scale

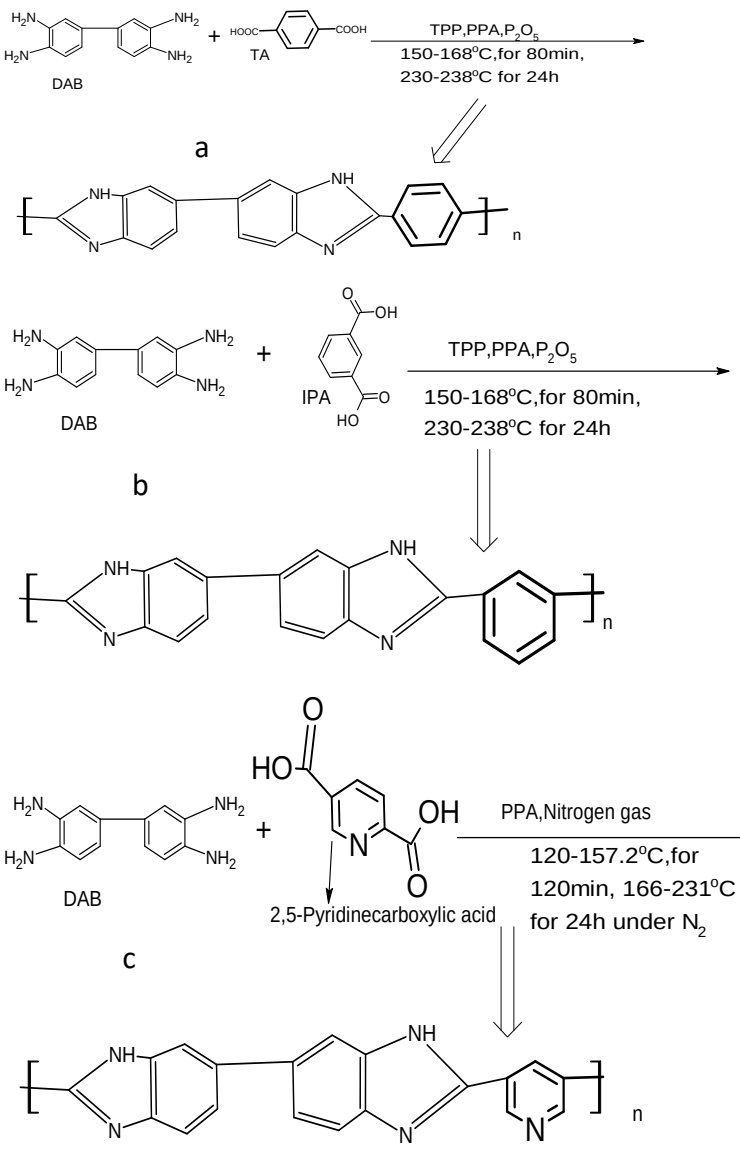

Figure 2: Synthesis of (a) p-PBI polymer and (b) m-PBI polymer and (c) py-PBI in PPA solvent

3.Results and Discussions

3.1 Molecular Weight and Inherent Viscosity Determination of the Synthesized PBI Polymer

To prepare a polybenzimidazole (PBI) polymer solution, the PBI polymer was dissolved in concentrated sulfuric acid (96 wt%) to achieve a concentration of 1.0 g/dL. Subsequently, four solutions were formulated at concentrations of 0.25 g/dL, 0.5 g/dL, 0.75 g/dL, and 1.0 g/dL. Each solution was then introduced into an Ubbelohde viscometer, where the flow time of the PBI polymer solution between the calibrated points of the viscometer was measured across three trials. The average flow time was calculated and utilized in the equation below to determine the reduced viscosity(η red).

The table illustrates the inherent viscosities (expressed in dL/g) and average molecular weights (MW, in Da) of each polymer. For the Bipy-PBI polymers with varied MWs that ranged from 48 to 141 kDa, corresponding to inherent viscosities of 1.05–2.85 dL/g, was reported by Harilal et al.[14] In fact, the monomer was 2,2′-bipyridine-4,4′-dicarboxylic acid (BPDCA), instead of 2,5'-Pyridinedicarboxylic acid and also the molar concentration was different from the one synthesized in this study, i.e., 30 mmol. Under this study, the Py-PBI exhibits an intrinsic viscosity of 1.51 dL/g and a molecular weight of 70,999 Da. M-PBI displays a slightly higher viscosity of 1.52 dL/g and a molecular weight of 71,510 Da. It was reported by Aili et al. the commercial m-PBI (Celazole®) revealed a low to medium molecular weight of 23,000–37,000 g /mol, leading to an IV in the range of 0.55–0.80 dL/g. but in this analysis the molecular weight is twice as high as the commercial.[16] In contrast, P-PBI possesses the highest inherent viscosity at 1.855 dL/g and the greatest molecular weight of 88,796 Da, indicating a longer polymer chain length or a higher degree of polymerization.

Table 1: Inherent Viscosity and Average molecular wight of py- PBI,p-PBI and m-PBI

Polymer	inherent viscosities $\eta\ dL/g$	Average Molecular Weight, MW (Da)
Py-PBI	1.51	70,999
M-PBI	1.52	71,510
P-PBI	1.855	88,796

3.2 Thermal stability

These tests were conducted under an air environment to evaluate the thermal stability of the synthesized PBI membranes, using a heating rate of 10 °C/min across a temperature range of 25–900 °C.

As the temperature increases, the weight loss continues, indicating thermal decomposition of the polymer backbones. At the final temperature (around 900 °C), the residual weights are approximately 55% for m-PBI, 58% for Py-PBI, and 61% for P-PBI. This shows that P-PBI exhibits the highest thermal stability, retaining the greatest amount of mass, while m-PBI shows the lowest, with the most degradation under high-temperature conditions. For the synthesized Py-PBI, the TGA result in this study showed a weight loss of 58%. However, in another study, the weight losses under inert gas and air were reported as 70% and 10%, respectively.[16] [15].

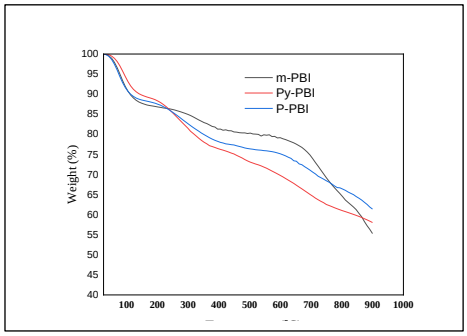

Figure 3 :TGA graph under an air environment for the synthesized PBI polymers.

3.3 EIS Analysis of PBI membranes

m-PBI membranes demonstrate good conductivity, ranging from approximately 202 to 214 mS/cm at temperatures between 180 and 200 °C.[23] However, their higher activation energy indicates the energy required for proton transport, which is often attributed to less organized acid channels.[24] The elevated acid leaching rate of approximately 66% is consistent with existing literature, which suggests that meta-linkages enhance acid uptake while lacking robust anchorage.[25] P-PBI demonstrates a more rigid structure, which restricts acid uptake to less than 15% and results in conductivity values of approximately 0.15–0.18 S/cm at temperatures ranging from 180 to 200°C. However, this rigidity leads to reduced activation energies, approximately 5 kJ/mol, attributed to the stability of the acid–polymer proton pathways.[24][23]

Table 2: Proton Conductivity, and Activation Energy Results

Polymer Membrane Types	Proton conductivity (mS/cm) 160℃	180℃	200℃	Activation Energy KJ/mol
P-PBI	145	163	180	4.98
m-PBI	183	202	214	7.26
Py-PBI	184	212	224	6.45

3.4 Chemical stability and Acid leaching

The fig.4 showed the oxidation stability of p-PBI, m-PBI, and py-PBI over 216 hours. p-PBI exhibits the highest stability, retaining about 82% of its weight. m-PBI shows moderate stability with around 77% remaining, while py-PBI has the lowest, retaining only 73%. The superior performance of p-PBI may result from its linear structure and strong chain interactions. or both p-PBI and m-PBI, the results were consistent with previous studies reported in the literature. Specifically, findings by Chen et al. and Rajab et al. indicated that the residual weight after exposure to the Fenton solution ranged from 93.5% to 72.5%.[26], [27] In contrast, py-PBI

degrades more rapidly, likely due to the electron-withdrawing effect of the pyridine ring.[28] It is also important to note that the current study was conducted over a duration of 216 hours, whereas Berber et al. reported the oxidation stability of py-PBI over a shorter period of 192 hours.

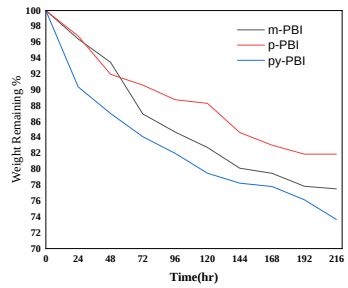

Figure 4 Oxidation Stability of the Synthesized PBI Membrane in Fenton's Reagent at 70 °C

4. Conclusion

Para-PBI exhibited the highest molecular weight, superior thermal stability, and excellent oxidative resistance, attributed to its linear and rigid backbone structure. Pyridne PBI and pyridine-PBI demonstrated higher proton conductivity due to enhanced phosphoric acid uptake; however, this benefit was accompanied by increased acid leaching and reduced chemical stability. Electrochemical analysis revealed lower activation energy for para-PBI, indicating more stable proton-transport pathways. Overall, the study establishes clear structure–property relationships and highlights backbone orientation as a critical design parameter for durable HT-PEM membranes.

Acknowledgement

This work was supported by Research Fund of the Kocaeli University project no. FKA-2024-3862 and FDKB-2024-3674

References

[1] R. R. R. Sulaiman, R. Walvekar, W. Y. Wong, M. Khalid and M. M. Pang, Membranes (Basel)., 12 (2022) 344.
[2] J. Escorihuela, J. Olvera-Mancilla, L. Alexandrova, L. F. del Castillo and V. Compañ, Polymers, 12 (2020) 1861.
[3] D. Aili et al., High Temp. Polym. Electrolyte Membr. Fuel Cells, 3 (2020) 4.
[4] Z. Xu et al., Molecules, 29 (2024) 4480.
[5] J. Müller-Hülstede et al., ChemSusChem, (2025) 202501575.
[6] L. Zhang et al., Nat. Commun., 15 (2024) 47627.
[7] F. Mack, K. Aniol, C. Ellwein, J. Kerres and R. Zeis, J. Mater. Chem. A, 3 (2015) 10864–10874.
[8] H. Cho et al., Eur. Polym. J., 58 (2014) 135–143.
[9] Harilal, A. Shukla, P. C. Ghosh and T. Jana, ACS Appl. Energy Mater., 4 (2021) 1644–1656.
[10] K. Lin, C. Wang, Z. Qiu and Y. Yan, Polymers, 14 (2022) 1283.
[11] T. Zhu, D. Zhu, J. Liang, L. Zhang, F. Huang and L. Xue, J. Energy Chem., 85 (2023) 91–101.
[12] J. Li et al., Energy Convers. Manag., 85 (2014) 323–327.
[13] S. Yu, H. Zhang, L. Xiao, E. W. Choe and B. C. Benicewicz, Fuel Cells, 9 (2009) 318–324.
[14] Harilal, A. Shukla, P. C. Ghosh and T. Jana, ACS Appl. Energy Mater., 4 (2021) 1644–1656.
[15] M. R. Berber and N. Nakashima, J. Membr. Sci., 591 (2019) 117354.
[16] D. Aili and R. He, High Temp. Polym. Electrolyte Membr. Fuel Cells, (2016) 151–167.
[17] L. Xiao et al., Fuel Cells, 5 (2005) 287–295.
[18] D. Ergun, Y. Devrim, N. Bac and I. Eroglu, J. Appl. Polym. Sci., 124 (2012) 36507.
[19] N. Üregen, K. Pehlivanoğlu, Y. Özdemir and Y. Devrim, Int. J. Hydrogen Energy, 42 (2017) 2636–2647.
[20] R. Nayak, T. Dey, P. C. Ghosh and A. R. Bhattacharyya, Polym. Eng. Sci., 56 (2016) 1366–1374.
[21] V. VijayaKumar, C. Ramesh Kumar, A. Suresh, S. Jayalakshmi, U. Kamachi Mudali and N. Sivaraman, R. Soc. Open Sci., 5 (2018) 171701.
[22] E. Qu et al., J. Mater. Chem. A, 11 (2023) 12885–12895.
[23] M. Malinowski, A. Iwan, G. Paściak, K. Parafiniuk and L. Gorecki, High Perform. Polym., 26 (2014) 436–444.
[24] Z. Zhou, O. Zholobko, X. F. Wu, T. Aulich, J. Thakare and J. Hurley, Energies, 14 (2021) 135.
[25] S. S. Araya et al., Int. J. Hydrogen Energy, 41 (2016) 21310–21344.
[26] P. Y. Chen, T. H. Chiu, F. J. Lin and J. C. Chen, J. Membr. Sci., 654 (2022) 120569.
[27] Z. Rajabi, M. Javanbakht, K. Hooshyari, M. Adibi and A. Badiei, Int. J. Hydrogen Energy, 46 (2021) 33241–33259.
[28] Y. J. Rathwa and N. P. Chikhaliya, High Perform. Polym., 35 (2023) 839–850.

Fabrication of LSC Cathodes for Intermediate-Temperature SOFCs via Spray Pyrolysis

Hakan Yüce and Gülhan Çakmak,

[1]Department of Metallurgical and Materials Engineering,Muğla Sıtkı Koçman University, Muğla, Türkiye

The increasing global demand for energy and the depletion of fossil fuel resources have intensified the pursuit of alternative, efficient energy conversion technologies. Solid oxide fuel cells (SOFCs) are highly promising candidates, offering direct chemical-to-electrical energy conversion with efficiencies reaching 40–50%, which can be further enhanced through cogeneration systems. These attributes make SOFCs particularly advantageous for stationary power applications.

A significant challenge in advancing SOFC technology lies in the development of cathode materials that exhibit low electrochemical resistance, particularly at intermediate operating temperatures (500–700°C). Traditional fabrication methods such as sol-gel synthesis and magnetron sputtering have shown some success but still present limitations in achieving optimal cathode performance. Notably, LSC-based cathodes produced by magnetron sputtering have demonstrated promising results, particularly when compositions such as LSC113 and LSC214 are strategically combined.

This study explores the spray pyrolysis technique as an alternative approach for the fabrication of LSC cathodes. Spray pyrolysis offers distinct advantages, including better control over composition, morphology, and scalability compared to conventional techniques. In this work, LSC cathodes were synthesized using spray pyrolysis, and their structural and electrochemical characteristics are being systematically evaluated. Emphasis is placed on assessing the morphological features and the electrochemical performance, specifically the area-specific resistance at intermediate temperatures.

Preliminary findings will be benchmarked against LSC cathodes fabricated by other methods, such as magnetron sputtering, to critically assess the potential of spray pyrolysis as a viable, cost-effective route for high-performance IT-SOFC cathodes. The outcomes of this study are expected to contribute to the advancement of scalable and efficient cathode production strategies for intermediate-temperature SOFC applications.

Acknowledgment

This research is supported by TÜBİTAK (The Scientific and Technological Research Council of Turkey) with project number 124M969 which the authors gratefully acknowledge.

References

[1] [1] Q. Liu, X. Dong, G. Xiao, F. Zhao, and F. Chen, “A novel electrode material for symmetrical SOFCs,” Advanced Materials, vol. 22, no. 48, pp. 5478–5482, Dec. 2010, doi: 10.1002/adma.201001044.

[2] D. Sari, F. Piskin, Z. C. Torunoglu, B. Yasar, Y. E. Kalay, and T. Ozturk, “Combinatorial development of nanocrystalline/amorphous (La,Sr)CoO3-(La,Sr)2CoO4 composite cathodes for IT-SOFCs,” Solid State Ionics, vol. 326, pp. 124–130, Nov. 2018, doi: 10.1016/j.ssi.2018.10.003.

Hakan Yüce is currently a Master’s student in Metallurgical and Materials Engineering at Muğla Sıtkı Koçman University. He is working at the Energy Materials Laboratory, and his research areas include Energy Storage Materials, Ni-MH Batteries, High Entropy Alloys, and Solid Oxide Fuel Cell cathode materials.

Presenting author: Hakan Yüce, e-mail: hakanyuce2@posta.mu.edu.tr tel: +90 531 526 4175

Development of MoS_2/ZIF-67 Hybrid Catalysts for Enhanced Cathodic Performance

Yaren Erdağ Maden[1], Ali Furkan Albora[2], Murat Efgan Kibar[3], Şahika Sena Bayazit[2], Özge Kerkez Kuyumcu[1]

[1] Marmara University, Faculty of Engineering, Chemical Engineering, Maltepe, İstanbul, Türkiye
[2] İstanbul University-Cerrahpaşa, Institute of Nanotechnology and Biotechnology, Büyükçekmece, İstanbul, Türkiye
[3] Kocaeli University, Faculty of Engineering, Chemical Engineering, İzmit, Kocaeli, Türkiye

Transition metal dichalcogenides (TMDs), especially molybdenum disulfide (MoS_2), are promising electrocatalysts for the hydrogen evolution reaction (HER) due to their abundant active sites and earth-abundant composition. However, their low conductivity and limited edge sites restrict performance. Combining MoS_2 with porous materials like metal–organic frameworks (MOFs) enhances charge transfer and exposure of active sites [1]. Among them, ZIF-67 offers high surface area, tunable porosity, and chemical stability. MoS_2/ZIF-67 composites show enhanced HER activity due to synergistic effects, though optimization of MoS_2 content and electrode design remains essential [2].

MoS_2/ZIF-67 hybrid catalysts containing 5, 8, 10, 12 and 20 wt% MoS_2 were synthesized via a hydrothermal method and processed into catalyst inks [1]. The inks were prepared by dispersing 20 mg of catalyst powder in 0.5 mL deionized water and adding 3 µL Nafion solution. Subsequently, 7 µL of the ink was drop-cast onto a 0.3 × 0.3 cm² area of carbon cloth substrate and dried at 120 °C for 30 minutes to form flexible electrodes for electrochemical measurement applications [3].

For comparison, electrodes coated with pristine MoS_2 was also prepared using the same procedure. Electrochemical measurements were performed in a three-electrode cell under N_2 atmosphere using a platinum wire as the counter electrode, a saturated calomel electrode (SCE) as the reference, and the prepared carbon cloth electrodes as working electrodes.

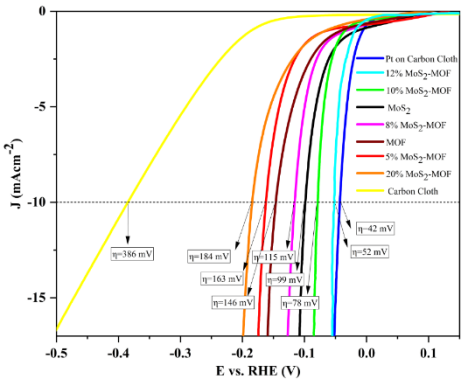

Fig.1. Polarization curves of catalysts

Linear sweep voltammetry (LSV) was conducted to evaluate the HER performance, and the resulting polarization curves (Fig. 1) illustrate the electrocatalytic behavior of MoS_2–MOF composites with varying MoS_2 loadings in comparison to pristine MoS_2, MOF, and carbon cloth electrodes. Among all samples, the 12 wt% MoS_2–MOF electrode exhibits the lowest overpotential (η = 78 mV at 10 mA cm^{-2}), demonstrating the highest catalytic activity toward the hydrogen evolution reaction. This enhancement can be attributed to the synergistic coupling between MoS_2 nanosheets and the porous ZIF-67 matrix, which provides efficient electron transport pathways and a higher density of exposed active edge sites, facilitating proton reduction.

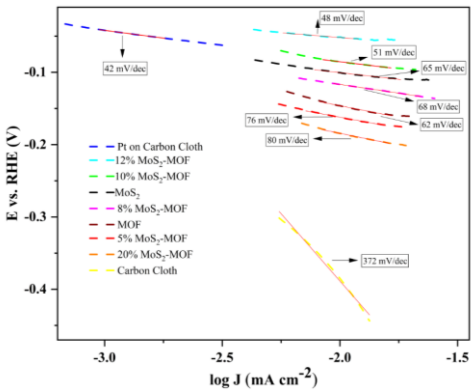

Fig.2. Tafel slopes of catalysts

The Tafel plots shown in Fig. 2 further confirm the improved reaction kinetics of the MoS_2–MOF composites. The optimized 12 wt% MoS_2–MOF sample delivers a Tafel slope of 48 mV dec^{-1}, approaching that of Pt/C (42 mV dec^{-1}), indicating a favorable Volmer–Heyrovsky mechanism for hydrogen evolution.

These findings demonstrate that proper integration and composition control of MoS_2 within the MOF framework significantly enhance the HER efficiency, providing a promising pathway for developing cost-effective and high-performance electrocatalysts.

References

[1] T.F. Jaramillo, K.P. Jørgensen, J. Bonde, J.H. Nielsen, S. Horch, I. Chorkendorff, *Science* 317 (2007) 100–102.
[2] K.S. Park, Z. Ni, A.P. Côté, J.Y. Choi, R. Huang, F.J. Uribe-Romo, H.K. Chae, M. O'Keeffe, O.M. Yaghi, *Proc. Natl. Acad. Sci. U.S.A.* 103 (2006) 10186–10191.
[3] L.-H. Qian, W.-W. Dong, M.-D. Xu, Y.-B. Cao, X. Wu, X.-J. Song, Y. Ding, X. Wang, *J. Solid State Chem.* 319 (2023) 123809.

Murat Efgan Kibar is currently working as associate professor at the Department of Chemical Engineering, Kocaeli University. In 2022 he became a deputy director of the Alternative Fuels Research and Development Center at Kocaeli University. His main research areas are catalysis and reaction engineering. He is currently working on the photocatalytic hydrogen and methanol production and designing photothermal reactors.
Murat Efgan KİBAR, e-mail: efgankibar@kocaeli.edu.tr tel: +90 (505) 451 07 11

Advancements in Direct Liquid Fuel Cells: A Comparative Study of Methanol, Ethanol, and Glycerol

Moussa Djibrine Ali[1] , Gültekin AKAY[1]
[1]Chemical Engineering department, Kocaeli university, Türkiye

Abstract

Direct Liquid Fuel Cells (DLFCs) represent a promising class of electrochemical energy conversion systems due to their ability to directly utilize liquid fuels, thereby avoiding the challenges associated with hydrogen storage and transportation. Among DLFC technologies, Direct Methanol Fuel Cells (DMFCs), Direct Ethanol Fuel Cells (DEFCs), and Direct Glycerol Fuel Cells (DGFCs) have attracted increasing attention for portable, stationary, and decentralized power applications because of their high theoretical energy densities and operational simplicity. This study provides a comparative assessment of recent advancements in DMFC, DEFC, and DGFC technologies, with particular emphasis on electrocatalyst development, membrane engineering, electrochemical performance, and fuel crossover behavior. DMFCs are the most mature DLFC technology and exhibit relatively fast oxidation kinetics; however, their performance is significantly limited by severe methanol crossover through proton exchange membranes, which leads to voltage losses and reduced fuel utilization efficiency. DEFCs offer advantages in terms of lower toxicity and the use of renewable bioethanol, but their electrooxidation is kinetically hindered by complex reaction pathways and incomplete carbon–carbon bond cleavage. DGFCs, utilizing glycerol as a fuel, demonstrate the highest theoretical energy density and significantly reduced fuel crossover due to the larger molecular size of glycerol, although their electrochemical oxidation involves multiple intermediates that require advanced catalyst formulations. Recent progress in nanostructured and alloy-based electrocatalysts, including platinum- and palladium-based systems combined with secondary metals and metal oxides, has resulted in improved catalytic activity, enhanced tolerance to poisoning species, and increased durability. Additionally, alternative membrane materials such as sulfonated aromatic polymers and alkaline anion exchange membranes have shown promise in mitigating fuel crossover and improving overall cell efficiency. The comparative analysis presented in this work highlights the current technological status, key limitations, and future research directions necessary to advance DLFC systems toward practical and commercial implementation.

1.Introduction

The transition toward sustainable and low-emission energy systems has intensified global interest in electrochemical energy conversion technologies capable of efficiently utilizing alternative fuels. Fuel cells are widely regarded as one of the most promising solutions, as they enable the direct conversion of chemical energy into electrical energy with high efficiency and minimal environmental impact [1,2]. In particular, low-temperature polymer electrolyte fuel cells have attracted significant attention for portable and decentralized power applications due to their compact design, rapid start-up, and flexible operational characteristics [3].

Conventional hydrogen fuel cells, despite their advanced technological maturity, continue to face practical challenges related to hydrogen production, storage, distribution, and safety. These limitations have motivated extensive research into Direct Liquid Fuel Cells (DLFCs), which operate using liquid fuels directly supplied to the anode, thereby eliminating the need for external fuel reforming [4]. Liquid fuels such as methanol, ethanol, and glycerol offer high volumetric energy density, simplified storage, and compatibility with existing fuel-handling infrastructure, making DLFCs attractive candidates for small-scale, mobile, and backup power systems [5].

Among DLFC technologies, Direct Methanol Fuel Cells (DMFCs), Direct Ethanol Fuel Cells (DEFCs), and Direct Glycerol Fuel Cells (DGFCs) have been widely investigated. DMFCs are the most established systems and exhibit relatively fast oxidation kinetics; however, their performance is significantly constrained by methanol crossover through polymer electrolyte membranes, which leads to reduced cell voltage, lower fuel utilization efficiency, and long-term durability issues [1,6]. DEFCs have gained increasing attention due to the renewable nature and lower toxicity of ethanol, yet their practical performance remains limited by

Ali Moussa Djibrine is a chemical engineer currently pursuing a Ph.D. at Kocaeli University, specializing in Direct Liquid Fuel Cells. He holds a Master's degree in Chemical Engineering and has experience as a business development specialist, production supervisor, and process engineer. His research focuses on advancements in fuel cell technology and bioreactor design. He has presented at international conferences and published in renowned scientific journals. Fluent in multiple languages, he is proficient in engineering software and has a strong academic and industrial background.

Presentating author: Moussa Djibrine Ali, e-mail: alidjibrine95@yahoo.com tel:+905369934094

sluggish electrooxidation kinetics and incomplete carbon–carbon bond cleavage, resulting in the formation of partially oxidized intermediates [7,8].

More recently, DGFCs have emerged as a promising alternative DLFC technology, driven by the availability of glycerol as a low-cost by-product of biodiesel production and its high theoretical energy density [9]. In addition, glycerol exhibits significantly lower crossover compared to methanol and ethanol due to its larger molecular size. Nevertheless, the complex multi-electron oxidation pathways of glycerol present substantial challenges in catalyst design and reaction selectivity, requiring advanced catalytic materials to achieve efficient and stable operation [10].

Recent research efforts have therefore focused on improving DLFC performance through the development of advanced electrocatalysts, including alloy and nanostructured systems, as well as membrane materials with reduced fuel permeability and enhanced stability [6–10]. Within this context, the present work provides a comparative overview of methanol-, ethanol-, and glycerol-based fuel cells, highlighting their current performance levels, key limitations, and future prospects. The objective of this study is to contribute to a clearer understanding of the relative advantages and challenges of each DLFC system and to support ongoing research toward their practical implementation.

2. Eperimental

The electrochemical performances of Direct Methanol Fuel Cell (DMFC), Direct Ethanol Fuel Cell (DEFC), and Direct Glycerol Fuel Cell (DGFC) systems were comparatively investigated under identical experimental conditions to ensure reliable performance evaluation. All experimental procedures were carried out in a chemical engineering laboratory in accordance with standard fuel cell fabrication and electrochemical testing protocols reported in the literature [1,2].

Platinum–ruthenium supported on carbon (PtRu/C, 50 wt.%) and platinum supported on carbon (Pt/C, 20 wt.%) catalysts were employed as the anode and cathode catalysts, respectively, due to their well-established activity for alcohol oxidation and oxygen reduction reactions [3,4]. Catalyst inks were prepared by dispersing the catalyst powders in a mixed solvent of 2-propanol and deionized water, with liquid Nafion solution used as the ionomer binder. The suspensions were first homogenized by magnetic stirring and subsequently ultrasonicated to achieve uniform dispersion and prevent agglomeration, following commonly adopted procedures for membrane–electrode assembly (MEA) preparation [5].

The prepared catalyst inks were deposited onto carbon-based gas diffusion layers (GDLs), cut to an active area of 2.5 × 2.5 cm^2, using an air-assisted spray-coating technique. A catalyst loading of 1 mg cm^{-2} was applied to both the anode and cathode electrodes. After deposition, the electrodes were dried at room temperature and subsequently heat-treated at 60 °C to ensure solvent removal and adhesion stability.

Sulfonated poly(ether ether ketone) (SPEEK) membranes were used as the electrolyte due to their favorable proton conductivity and reduced alcohol permeability compared to conventional Nafion membranes [6,7]. Prior to MEA fabrication, the membranes were pretreated in 1 M H_2SO_4, rinsed with deionized water until neutral pH was achieved, and dried at ambient temperature. The MEAs were fabricated by hot-pressing the anode and cathode electrodes onto opposite sides of the SPEEK membrane at 80 °C under approximately 500 bar for 15 minutes.

The assembled MEAs were integrated into single-cell fuel cell hardware equipped with graphite bipolar plates featuring serpentine flow channels. Silicone gaskets were used to ensure leak-tight sealing, and uniform compression was applied during cell assembly. Methanol (2 M), ethanol (2 M), and glycerol (1 M) aqueous solutions were supplied to the anode compartment for DMFC, DEFC, and DGFC systems, respectively, consistent with optimized concentrations reported in recent studies [8–10]. Compressed air was supplied to the cathode at a flow rate of 200 mL min^{-1} using a mass flow controller. No external humidification was applied, as ambient humidity was sufficient to maintain membrane hydration.

Electrochemical measurements were initiated after achieving steady-state operation. Polarization and power density curves were recorded to evaluate cell performance, while long-term stability tests under constant current conditions were conducted to assess MEA durability. The comparative evaluation focused on electrochemical performance, fuel utilization efficiency, operational stability, and practical applicability of the three direct liquid fuel cell systems.

Fig. 1. Fuel cell device

3- Results and Discussions

The performance of Direct Liquid Fuel Cells (DLFCs) is governed by the intrinsic physicochemical properties of the fuel, electrocatalyst activity, membrane transport characteristics, and operating conditions. In this section, the electrochemical behavior of Direct Methanol Fuel Cells (DMFCs), Direct Ethanol Fuel Cells (DEFCs), and Direct Glycerol Fuel Cells (DGFCs) is comparatively discussed based on polarization behavior, power density output, fuel crossover tendencies, and durability considerations, drawing on both the present experimental framework and recent literature data [1–3].

3.1 Performance Characteristics of DMFC, DEFC, and DGFC

Among the investigated systems, DMFCs generally exhibit the highest peak power densities, typically reported in the range of 60–120 mW cm^{-2} under operating temperatures between 60 and 90 °C, depending on catalyst loading and membrane type

[4,5]. The relatively simple molecular structure of methanol and its favorable electrooxidation kinetics on PtRu-based catalysts contribute to higher current densities and lower activation losses. However, polarization curves commonly show a pronounced voltage drop at elevated current densities, which is primarily attributed to methanol crossover through proton exchange membranes. Methanol crossover induces mixed potentials at the cathode, resulting in reduced open-circuit voltage (OCV) and lower overall fuel efficiency [6].

DEFCs typically deliver lower peak power densities, often reported between 20 and 60 mW cm^{-2} under comparable conditions [7]. The electrooxidation of ethanol involves a complex multi-electron reaction pathway requiring carbon–carbon bond cleavage, which significantly slows reaction kinetics and leads to the formation of intermediate products such as acetaldehyde and acetic acid. These intermediates partially block active sites on the catalyst surface, increasing activation and concentration overpotentials. Nevertheless, ethanol crossover rates are substantially lower than those of methanol, resulting in higher OCV values (commonly >0.75 V) and improved fuel utilization efficiency [8].

DGFCs represent an emerging class of DLFCs with distinctive performance characteristics. Although reported peak power densities are currently lower, typically below 20–40 mW cm^{-2}, DGFCs benefit from extremely low fuel crossover due to the larger molecular size and lower diffusivity of glycerol [9,10]. This reduced crossover translates into enhanced voltage stability during operation and higher theoretical fuel utilization. The primary performance limitation arises from the highly complex oxidation mechanism of glycerol, which involves multiple parallel reaction pathways and generates a wide range of intermediate products, necessitating advanced catalyst design for efficient and selective oxidation.

3.2 Effect of Catalyst Composition and Structure

Catalyst composition remains a critical determinant of DLFC performance. In DMFCs, PtRu/C catalysts continue to serve as the benchmark anode materials due to their superior tolerance to carbon monoxide poisoning and enhanced methanol oxidation activity via the bifunctional mechanism [4,11]. Reported studies indicate that PtRu catalysts can reduce CO adsorption energy by up to 30% compared to pure Pt, significantly improving sustained current output.

For DEFCs, catalyst modification through the incorporation of secondary metals such as Sn, Pd, or Ni has been shown to enhance ethanol oxidation activity by facilitating the oxidative removal of adsorbed intermediates [12]. PtSn- and Pd-based catalysts, in particular, promote partial C–C bond cleavage and improve reaction selectivity, leading to increased current densities and improved stability.

DGFC performance benefits from palladium-based and bimetallic catalysts, which demonstrate higher glycerol oxidation activity and improved resistance to surface poisoning [13]. Additionally, the use of nanostructured catalyst supports, such as carbon nanotubes and graphene-derived materials, increases the electrochemically active surface area and improves electron transport. These structural advancements have been shown to increase peak power density by 20–40% compared to conventional carbon black supports [14].

3.3 Membrane Effects and Durability Considerations

Membrane properties critically influence fuel crossover, ionic conductivity, and long-term durability. Nafion-based membranes, while offering high proton conductivity (>0.08 S cm^{-1} at 80 °C), exhibit significant permeability to methanol and ethanol, leading to efficiency losses in DMFCs and DEFCs [6]. In contrast, alternative membranes such as sulfonated aromatic polymers (e.g., SPEEK) and alkaline anion exchange membranes demonstrate reduced fuel crossover and improved chemical stability [15].

Durability studies reported in the literature indicate that fuel crossover-induced cathode degradation and catalyst poisoning remain the dominant degradation mechanisms during long-term operation. DMFCs are particularly susceptible to performance decay due to methanol-induced cathode flooding, whereas DEFCs and DGFCs show improved voltage retention over extended operation times exceeding 100 h under constant load conditions [16]. These findings highlight the importance of membrane–catalyst compatibility and optimized operating conditions for achieving stable and durable DLFC performance.

Table 1
Comparison of DLFC performance characteristics

Fuel Type	Power Density	Fuel Crossover	Technology Maturity
Methanol	High	High	Advanced
Ethanol	Moderate	Moderate	Devloping
Glycerol	Emerging	Low	Early-stage

3.4 Discussion and Comparative Assessment

Overall, DMFCs offer superior performance but suffer from efficiency losses due to crossover. DEFCs represent a balance between sustainability and performance, while DGFCs show strong long-term potential due to low crossover and high theoretical efficiency. Continued progress in catalyst design and membrane engineering is expected to further enhance the performance and applicability of DLFC technologies.

4- Conclusions

This work provided a comparative analysis of Direct Methanol, Direct Ethanol, and Direct Glycerol Fuel Cells with respect to electrochemical performance, fuel crossover, and operational stability. The results indicate that DMFCs deliver the highest power densities but suffer from significant efficiency losses due to methanol crossover and durability limitations. DEFCs exhibit moderate performance with improved open-circuit voltage and reduced crossover, though their practical efficiency remains constrained by slow oxidation kinetics and incomplete fuel utilization. DGFCs, while currently achieving lower power output, demonstrate superior fuel utilization, minimal crossover, and enhanced

voltage stability, highlighting their strong potential for long-term and sustainable energy applications. These findings emphasize the critical role of catalyst and membrane development in balancing power output, efficiency, and durability for the advancement of direct liquid fuel cell technologies.

Acknowledgement

The authors gratefully acknowledge the experimental facilities and technical support provided by the Kocaeli Hydrogen, Fuel Cells and Electrochemical Technologies Laboratory, Kocaeli University, where all membrane preparation, membrane–electrode assembly fabrication, and electrochemical performance measurements were carried out. The authors also thank the laboratory staff and colleagues for their valuable technical assistance and constructive scientific discussions throughout the course of this study.

References

[1] Y. E. Kalay, Y. Kuru, E. Unalan, Int. J. Hydrogen Energy, 12 (2015) 915–920.
[2] L. An, T. S. Zhao, Energy Environ. Sci., 15 (2022) 1723–1745.
[3] C. Coutanceau, S. Baranton, Wiley Interdiscip. Rev. Energy Environ., 11 (2022) e435.
[4] J. Zhang, Y. Tang, C. Wang, J. Power Sources, 520 (2022) 230870.
[5] H. Li, X. Liu, Fuel Cells, 24 (2024) 145–156.
[6] S. M. Jamil, M. H. D. Othman, Renew. Sustain. Energy Rev., 176 (2023) 113163.
[7] Y. Wang, Z. Liang, H. Yang, Renew. Sustain. Energy Rev., 176 (2023) 113169.
[8] A. Brouzgou, P. Tsiakaras, Appl. Catal. B, 291 (2021) 120054.
[9] P. K. Shen, Electrochim. Acta, 389 (2021) 138735.
[10] R. Silva, C. A. D. Rodrigues, J. Membr. Sci., 662 (2022) 120978.
[11] T. S. Zhao, Prog. Energy Combust. Sci., 89 (2022) 100980.
[12] S. Song, J. Catal., 404 (2021) 14–26.
[13] M. S. Ahmad, Electrochem. Energy Rev., 6 (2023) 100–123.
[14] X. Li, Carbon, 206 (2023) 214–226.
[15] H. Xu, J. Power Sources, 555 (2023) 232360.
[16] Y. Kim, Int. J. Hydrogen Energy, 48 (2023) 31245–31257.

Development of Biodegradable Membranes Functionalized with Reduced Graphene Oxide Reinforcement for Microbial Fuel Cell Applications

Necla ALTIN[1], Ayşe AYTAÇ[1,2]

[1]Department of Chemical Engineering, Faculty of Engineering, Kocaeli University, 41380, Kocaeli, Türkiye

[2]Polymer Science and Technology Department, Kocaeli University, 41380, Kocaeli, Türkiye

Microbial fuel cells (MFCs) are bio-electrochemical systems that can generate energy from organic waste [1]. MFCs are among the promising technologies for environmentally friendly and renewable energy production. In recent years, intensive research has been conducted in various areas, including the improvement of electrode materials, optimization of microbial consortia, selection of suitable substrates, and development of low-cost proton exchange membranes, to enhance the performance and economic viability of MFC systems.

Proton exchange membranes (PEMs), one of the critical components in these systems, directly affect system performance in terms of ion conduction and gas separation between compartments. While commercial PEMs offer high performance, they are disadvantageous in terms of sustainability due to their environmentally persistent nature and high cost. In this study, environmentally friendly composite membranes were developed by reinforcing reduced graphene oxide (rGO) into poly(3-hydroxybutyrate-co-4-hydroxybutyrate) (P34HB) matrix, a biodegradable polyester, and their use in microbial fuel cells was evaluated.

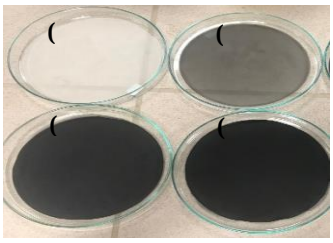

Figure 1. Pure P34HB (a) and P34HB reinforced with different ratios of rGO: 1wt.% rGO (b); 3wt.% rGO (c); 5wt.% rGO (d)

P34HB/rGO composite membranes were prepared by the solution casting method. Solutions containing pure P34HB and rGO at ratios of 1, 3, and 5% were dissolved in 95/5% chloroform/DMF solvent and homogenized in a magnetic stirrer, then poured into glass petri dishes and dried at room temperature. The resulting films were then placed in an oven at 60 °C to remove solvent residues. Three replicates were performed for each additive ratio, and membranes with homogeneous surfaces and a thickness of approximately 130 ± 5 µm were obtained. Figure 1 shows images of pure P34HB and its composites with rGO. The fabricated membranes were named according to the rGO ratio (e.g., 1 rGO; the membrane with 1wt.% additive).

The fabricated membranes were characterised in detail in terms of thermal properties, mechanical strength, hydrophilic properties, electrochemical performance, and fuel cell performance.

Proton conductivity measurements were performed using electrochemical impedance spectroscopy (EIS) at 100% relative humidity and the temperature range of 30-80 °C. The oxygen diffusion coefficient was calculated by measuring dissolved oxygen levels in the dual-chamber microbial fuel cell assemblies.

This study demonstrates that membranes developed with rGO reinforcement in biodegradable P34HB matrix can offer a sustainable and effective proton exchange membrane alternative in microbial fuel cell systems with their high proton conductivity, low oxygen permeability, and environmentally friendly structure. In addition, these membranes are considered to have a wide potential for use in energy generation applications from decentralized wastewater sources.

Acknowledgment

This study was supported by the Scientific and Technological Research Council of Turkey (TUBITAK) (Project 124C192-TUBITAK 2218).

References

[1] B. Das, S.S. Gaur, A.R. Katha, C.T. Wang, V. Katiyar, Crosslinked poly(vinyl alcohol) membrane as separator for domestic wastewater fed dual chambered microbial fuel cells, Int. J. Hydrogen Energy 46 (2021) 7073–7086. https://doi.org/10.1016/j.ijhydene.2020.11.213.

Ph.D. Necla Altın is a postdoctoral researcher at Kocaeli University. She graduated from Cumhuriyet University in 2015, received her master's degree in 2017 and PhD in 2024. Her research interests include microbial fuel cells, biofuels, algae technology, polymeric materials and composites, nanocomposites.,
Presentating author: Necla Altın e-mail: nejla_altin@hotmail.com tel: +90 (543) 976 13 23

MISCELLANEOUS

Photochemical properties of cobalt phthalocyanine pigment for the of solar cells

Khayit Turaev[1], Sherzod Kasimov[1], Dilmurod Shukurov[2], Panji Tojiyev[3], Olim Ruzimuradov[4]
[1]Termiz State University, Faculty of Chemistry, Termez, Uzbekistan
[2]Denau Institute of Entrepreneurship and Pedagogy, Denau, Uzbekistan
[3]Termiz State Pedagogical Institute, Termez, Uzbekistan
[4]Turin Polytechnic University in Tashkent, Tashkent, Uzbekistan

Solar energy is the most attractive way to obtain environmentally friendly energy. As you know, during the process of obtaining energy from silicon-based solar panels, silicon molecules are doped with atoms of elements of the third and fifth groups and are divided into the process of forming p-n junctions. This process is very complex and requires a lot of energy, so the use of semiconductor pigments sensitive to sunlight can significantly increase the efficiency of this process [1].

Research is often carried out in the field of synthesizing metal phthalocyanines as sensitizing dyes in semiconductor pigment materials. In particular, cobalt phthalocyanine ($C_{32}H_{16}CoN_8$) [2] is a semiconductor pigment material that has been studied as a potential semiconductor dye pigment for electron charge evolution in the process of obtaining solar cells. The voltammetric properties of $C_{32}H_{16}CoN_8$ semiconductor sunlight-sensitizing dyes in dye-sensitized solar cells have been investigated in several studies. These studies showed that $C_{32}H_{16}CoN_8$ exhibits good photochemical activity in the electron charge evolution reaction (DSSC). The researchers attributed this activity to the high conductivity and good stability of the $C_{32}H_{16}CoN_8$ film.

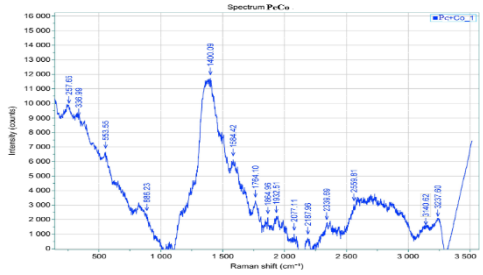

Fig.1 . Raman spectrum analysis of the PcCo pigment

In general, the electrocatalytic properties of PcMe semiconductor dye materials in solar cell production open up prospects for the development of efficient and stable anode materials by improving p and n junctions.

For the study of the photochemical properties a sensitive PcCo semiconductor pigment was synthesized by solid-phase deposition at high temperature in the presence of cobalt(II) sulfate, urea, phthalic anhydride, a catalyst, and concentrated sulfuric acid. The synthesized samples were deposited on a glass substrate with a size of 4×4 cm². The Raman spectrum analysis of the PcCo pigment is presented in Figure 1.

The following conclusions were drawn from the Raman spectroscopy analysis conducted to study the composition of the semiconductor pigment. The presence of an aromatic group in the benzene ring is determined by the absorption line at 3140.62 cm^{-1}. The valence vibration regions at 3237.60 cm^{-1} belong to O-H bonds. The valence and intensive vibration spectra are observed at 1864.96 cm^{-1} belong to C=O bonds, and the N-H bond spectra with differential vibrations are observed at 1584.42 cm^{-1}. The spectra in the 1400.09 cm^{-1} region belong to C-H bonds, and the differential bond spectra at 886.23 cm^{-1} belong to Me–N bonds. (EDX-8100 energy dispersive X-ray fluorescence spectrometer).

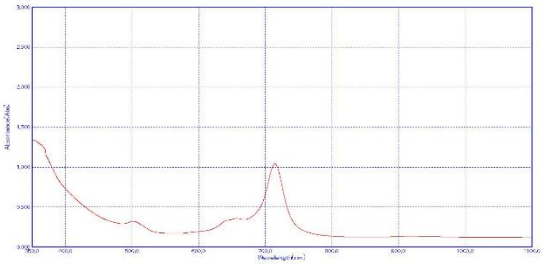

Fig.2 Optical absorption analysis of cobalt phthalocyanine pigment.

To study the photodynamic properties of cobalt-containing phthalocyanine dyes, it is necessary to analyze their spectral absorption characteristics. In particular, in the absorption spectrum of the cobalt phthalocyanine complex dissolved in N-methylpyrrolidone, a Q-band at 716 nm and B-bands in the range of 315–362 nm are observed. This makes them worthy of attention as a promising material for studying photovoltaic processes and for use in solar cells.

Acknowledgment

This study is financially supported by Termez State University within the framework of research programs in priority areas for 2024–2027.

References

[1] M. Gratzel. “Dye-sensitized solar cell”. Journal of Photochemistry & Photobiology C: Photochemistry Reviews pp. 145-153. (2003)

[2] M.G.Walter at all. Porphyrins and phthalocyanines in solar photovoltaic cells. J. Porphyr. Phthalocya., pp.759–792. (2010)

DSc., prof. Turaev Khayit Khudaynazarovich, works at the Termez State University, Faculty of Chemistry, Ministry of Higher Education, Science and Innovations of the Republic of Uzbekistan. He graduated from the Tashkent Polytechnic Institute in 1983. In 1990 he received the scientific title of Candidate of Chemical Sciences and in 1999 he received the scientific title of Doctor of Chemical Sciences. His research focuses on the synthesis of metal-phthalocyanine-based semiconductor materials for solar energy conversion, as well as the synthesis and research of ion- excheng sorbents containing donor atoms.
Khayit Turaev, e-mail: hhturaev@rambler.ru tel: +998 (91) 579 06 33

A New Perspective on the Liquid-Vapor, Liquid-Solid, and Solid-Vapor Critical Points of Hydrogen

Beycan Ibrahimoglu[1], Nushaba Kazimova[2]
[1]Plasma Technologies Development and Education Foundation, Gazi University (retired), Ankara, Turkiye
E-mail: beycanibrahimoglu@yahoo.com
[2]Department of Chemical Engineering, Middle East Technical University, Ankara, Turkiye
E-mail: nushaba.kazimova@metu.edu.tr

The critical point concept, in classical thermodynamics, was first defined along temperature, pressure, and density (T_{cr}, P_{cr}, ρ_{cr}) values, which belong to the end of the liquid-vapor equilibrium curve [1,2] and were supported by Van der Waals' theory [3]. However, this classical approach asserts that only temperature reaches the critical value while pressure and density change depending on it. This study aims to reevaluate critical parameters of pure substances by going beyond the limits of classical approaches [4].

The results of analyses with the method of thermo-axiomatic geometry and high-pressure experiments on benzene and benzonitrile derivatives show that the liquid-vapor critical pressure is much higher than the classical value. For instance, the experimental critical pressure of benzene was determined as $\mathbf{P_{cr} \approx 2229}$ bar, and this state was explained by the system's transition to the metastable region [5]. This condition can not be explained with classical theories.

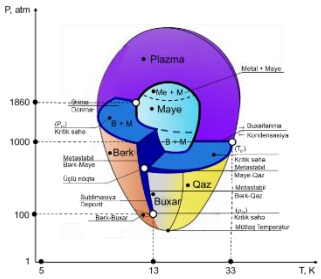

Figure 1 P-V-T Phase Diagram of Hydrogen

This study, at the same time, shows that the critical point concept is not limited to the liquid-vapor boundary curve, but also **liquid-solid** and **solid-vapor** transitions do have critical ending points [6]. Accordingly:

- At the end point of the liquid-vapor phase, the temperature,
- At the end of the liquid-solid boundary curve, the pressure,
- At the end of the solid-vapor boundary curve, the density is defined as a critical parameter.

With these, for a comprehensive understanding of phase transitions, a three-dimensional P-V-T phase diagram was created, and the plasma phase was also integrated into this structure as shown in Fig. 1. This new diagram, by going beyond two-dimensional P-T representations, facilitates multidimensional and topological analyses of energy systems, material technologies, and high-pressure environments. In this study, the determination of the critical pressure of hydrogen on the liquid-solid boundary curve and three-dimensional P-V-T phase diagram has been addressed [7].

References

[1] Bertrand Berche, M. Henkel, Ralph Kenna. Critical phenomena: 150 years since Cagniard de la Tour. Brasileira de Ensino de Física 13(3). DOI:10.1590/S1806-11172009000200015

[2] Allan A. Mills .The critical transition between the liquid and gaseous conditions of matter. Endeavour. Volume 19, Issue 2, 1995, Pages 69-75, https://doi.org/10.1016/0160-9327(95)93587-5

[3] Johannes Diderik van der Waals (23 November 1837 – 8 March 1923) equation of state for gases and liquids.

[4] Beycan Ibrahimoglu , Deniz Uner, Ayfer Veziroglu , Fuat Karakaya , Beycan Ibrahimoglu. Construction of phase diagrams to estimate phase transitions at high pressures: A critical point at the solid liquid transition for benzene. International Journal of Hydrogen Energy. Volume 46, Issue 29, 26 April 2021, Pages 15168- 15180 https://doi.org/10.1016/j.ijhydene.2021.02.010

[5] Beycan İbrahimoğlu. UNCERTAINTY OF A CRITICAL POINT ON THE FREEZING CURVE. German International Journal of Modern Science №53, 2023 79. DOI: 10.5281/zenodo.7796155

[6] Ibrahimoglu B., Sarikaya Y., Veziroglu A., ÖNAL M., Gokbel B.Supercritical phases of hydrogen. International Journal of Hydrogen Energy, cilt.46, sa.65, ss.32762-32767, 2021 (SCI-Expanded)

[7] Beycan ibrahimoğlu, Beycan Jr. İbrahimoğlu.Gritical States at Phase Transitions of Pure Substances. https//doi.org/10.1007/978-3-031-09966-3

Nushaba Kazimova is undergraduate student of Chemical Engineering at Middle East Technical University (METU), Ankara, Turkey. Her academic interests include critical parameters, phase transitions and thermodynamics.

Nushaba Kazimova, e-mail: nushaba.kazimova@metu.edu.tr tel: +905319601593

APPLICATIONS/INTEGRATIONS

Dynamic Analysis of Vanadium Redox Flow Cell System Integrated Into Solar Power Plant in Türkiye

Batuhan Mert LAÇİNKAYA[1], Mert TAŞ[2] ,Gülşah ELDEN[2]

[1]Graduate School of Natural and Applied Sciences of Energy Systems Engineering, Kayseri, Turkey

[2] Erciyes University, Engineering Faculty, Energy Systems Engineering Department, 383039, Kayseri Turkey

Countries increasingly favor renewable energy over conventional sources due to concerns about energy security, environmental sustainability, and zero-emission targets. However, the inherent variability and fluctuation of renewable energy source supply can cause grid power and frequency instabilities.To address this, battery energy storage systems are commonly integrated with renewable energy systems, and Vanadium Redox Flow Batteries (VRFB) stand out due to their long cycle life, deep discharge tolerance, and advanced controllability. Qazi et al. (2024) studied a VRFB system connected to an 11 kV grid stabilized frequency deviations from 50.1 Hz to nominal levels during load increases [1]. Similarly, Foles et al. (2022) demonstrated that VRFB can reduce sudden solar output drops with ±300 kW interventions and take down inverter ramp rates from 1 MW/min to 0.2 MW/min [2]. These findings highlight VRFBs' role in enhancing grid stability when integrated with renewable energy. Fares et al. (2014) demonstrated that a 1 MW/250 kWh VRFB system could respond within less than 0.5 seconds, successfully regulating frequency deviations within ±0.05 Hz under ERCOT grid simulations [3].

In this study, dynamic analysis of vanadium redox flow battery system integrated into solar power plant in Turkey was modeled and analyzed in MATLAB. The system parameters used in the model were obtained from commercial battery specifications and relevant literature. The open-circuit voltage (Voc) of the battery is calculated using the Nernst equation, based on the concentrations of the redox couples:

$$V_{oc} = E^0 + \frac{RT}{nF} ln\left(\frac{SoC}{1 - SoC}\right)$$

According to this equation, redox couple concentrations are determined based on the State of Charge (SOC) and incorporated into the model. At each step, the terminal voltage (Vt) is calculated iteratively by considering internal resistance and current.

$$V_T = V_{oc} - I.R_{int}$$

The State of Charge (SOC) is updated over time by considering the coulombic efficiency (η):

$$SoC_k = SoC_{k-1} + \frac{I.\Delta_t}{Q_{total}} \cdot \eta$$

To evaluate grid impact, a frequency response model was added. Deviations were calculated with and without VRFB using a sensitivity coefficient (K_{freq}).

Without VRFB: $\Delta_f = K_{freq} \cdot P_{net}$

With VRFB: $\Delta_{fVRFB} = K_{freq} \cdot (P_{net} - P_{battery})$

These deviations were added to the nominal grid frequency of 50 Hz to generate dynamic frequency profiles for both cases. The model evaluates the VRFB system's charge-discharge behavior, terminal voltage (Vt), SOC evolution, pump power consumption, and grid frequency response hourly, driven by the net power difference between solar generation and load. All system dynamics, including the effects of frequency stabilizing on the VRFB, are illustrated in detail in Figure 1.

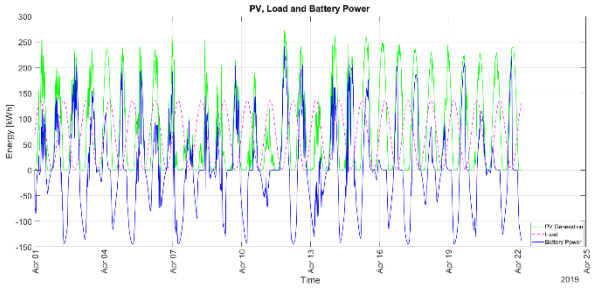

Figure 1. VRFB system impact: PV, load, and battery power

As shown in Figure 1, the VRFB system charges during generation surplus and discharges during deficits, effectively balancing the grid load. Battery current reached ±2000 A, and terminal voltage ranged between 500–560 V. The power difference between PV and load varied from +200 kWh to –150 kWh. Also, in this study, grid frequency remained near the nominal 50 Hz while with VRFB active. These findings confirm that the VRFB system enhances both energy balance and frequency stability in renewable-integrated grids.

References

[1] S. H. Qazi, D. V. Bozalakov, L. Vandevelde, Frequency and power shaving controller for grid-connected vanadium redox flow batteries for improved energy storage systems, Front. Energy Res., 12 (2024)

[2] A. Foles, L. Fialho, M. Collares-Pereira, P. Horta, An approach to implement photovoltaic self-consumption and ramp-rate control algorithm with a vanadium redox flow battery day-to-day forecast charging, Sustain. Energy Grids Netw., 30 (2022)

[3] R. L. Fares, J. P. Meyers, M. E. Webber, A dynamic model-based estimate of the value of a vanadium redox flow battery for frequency regulation in Texas, Appl. Energy, 113 (2014)

Batuhan Mert Laçinkaya is a graduate student in Energy Systems Engineering, focusing on sustainable energy technologies and applied research. He currently works as an R&D Project Engineer, managing TÜBİTAK-supported projects in autonomous robotics and photovoltaic systems. He has received recognition in national technology competitions and contributes to the development of innovative solutions in the energy sector. His background combines academic research with practical engineering experience across multidisciplinary teams.

Presentating author: Batuhan Mert Laçinkaya, e-mail: batuhanmertlacinkaya@outlook.com tel: +90 5536993599

Gel Polymer Electrolyte for Flexible Lithium-ion Batteries for Wearable Applications

Baidaa Alkhateab[1] and Serap Hayat Soytas[1]

[1]Sabanci University Nanotechnology Research and Application Center (SUNUM), Tuzla, 34956, Istanbul, Turkiye

Lithium-ion batteries (LIBs) are extensively used in portable electronic devices due to their high energy density and theoretical specific capacity. However, conventional LIBs employing liquid electrolytes pose safety risks – particularly leakage and flammability – limiting their suitability for wearable and flexible devices. Gel polymer electrolytes (GPEs) offer a promising alternative, providing enhanced electrochemical stability and safety. By blending acrylate monomers with diverse side chains and carefully tuning their stoichiometry, we tailor the polymer microstructure to enhance Li^+ mobility and mechanical elasticity.

While efforts focused on improving ionic conductivity of GPEs, achieving sufficient flexibility remains a challenge, especially for stretchable or wearable energy storage systems. In this study, we present a UV-curable GPE system that achieves both high conductivity and mechanical compliance. By blending acrylate monomers with diverse side chains and carefully tuning their stoichiometry, we tailor the polymer microstructure to enhance Li^+ mobility and mechanical elasticity. The GPEs were synthesized via UV curing of acrylate monomer blends mixed with $LiPF_6$ or LiTFSI. Key parameters, such as the Li^+: monomer ratio, curing time, and UV exposure distance, were systematically optimized. FTIR spectroscopy confirmed successful polymerization.

As shown in Figure 1, the FTIR spectrum of the monomer mixture exhibits peaks at 1620 cm^{-1} and 1635 cm^{-1}, corresponding to the stretching vibrations of the C=C bonds. After exposure to UV light these peaks disappeared, indicating successful photopolymerization and complete monomer consumption.

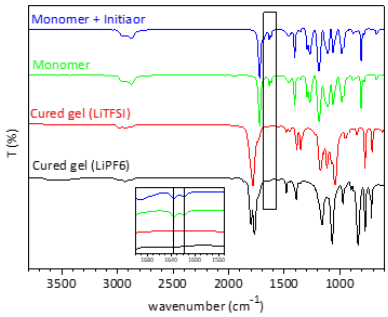

Figure 1. FTIR spectra of monomers and cured gels.

To measure compression strain of cured gels, specimens were prepared in a cylindrical shape with a diameter of 20 mm and a height of 5 mm, and tested in compression using a TA.XT Texture Analyzer at a rate of 0.02 mm/min. Figure 2a represents the compressive stress curves of two types of GPEs. Gel 2 exhibits excellent mechanical performance up to 0.27 MPa compressive stress at maximum load, which is almost 10 times higher than 0.028 MPa of Gel 1, with up to 30% strain at maximum load.

The ionic conductivity of GPEs was tested using electrochemical impedance spectroscopy (EIS) using a blocking symmetric steel//GPE//steel cell from 1 MHz to 100 mHz with an amplitude of 5 mV. In the EIS, the Z_0 intercept of the straight line on the real axis is related to the bulk resistance of GPEs. It can be seen from the inset of Figure 2b that Gel 2 exhibits much lower bulk resistance compared to Gel 1, meaning that its ionic conductivity is higher. Ionic conductivity was calculated by the following formula:
$\sigma = d / R_b \cdot S$, where d, S, and R_b are the thickness, area, and bulk resistance, respectively. The results of Gel 2 revealed that it has an impressive ionic conductivity of 4 $mS \cdot cm^{-1}$.

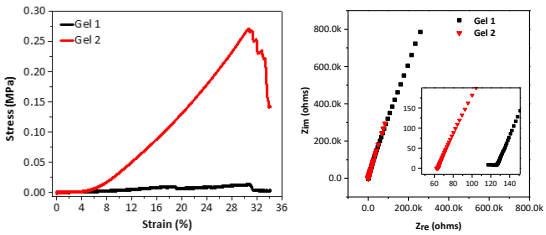

Figure 2. (a) Compression stress-strain curves, and (b) Nyquist plots for cured gels.

This work demonstrates a fast, scalable, and cost-effective approach to fabricating UV-curable GPEs with the dual advantage of high ionic conductivity and mechanical flexibility, paving the way for safer and more adaptable lithium-ion batteries in flexible electronics.

Acknowledgment

This study is financially supported by the Scientific and Technological Research Council of Turkey (TUBITAK) (Project No.123M050).

Dr. Baidaa Alkhateab is affiliated with the Nanotechnology Research and Application Center (SUNUM) of Sabanci University in Istanbul, Turkey. She received her M.Sc. in Electrochemistry from Istanbul Technical University in 2017 and her Ph.D. in Materials Science and Nanoengineering from Sabanci University in 2023. Her research focuses on two main areas: polymers for energy storage devices and structural composites for aerospace applications.

Presentating author: Baidaa Alkhateab, e-mail: baidaa.sharani@sabanciuniv.edu tel: +90 537 848 64 42

Development of a flexible lithium-ion battery and integration of a triboelectric nanogenerator for self-charging energy systems

Kaan YAPICI[1,2], Baidaa ALKHATEAB[2], Serap HAYAT SOYTAŞ[2]

[1]Faculty of Engineering and Natural Sciences, Sabanci University, Tuzla 34956 Istanbul, Turkiye

[2]SUNUM Nanotechnology Research Center, Sabanci University, Tuzla 34956 Istanbul, Turkiye

The growing demand for wearable electronics has highlighted the need for lightweight, flexible, and autonomous energy systems. Conventional lithium-ion batteries, though effective in energy density and stability, lack the mechanical adaptability and self-sufficiency required for next-generation wearable devices. To address these challenges, this study proposes the development of a self-charging energy platform that integrates a flexible lithium-ion battery with a triboelectric nanogenerator (TENG) into a unified, stretchable architecture. While TENGs and flexible batteries have been studied individually, their combination remains largely unexplored. The proposed system aims to achieve continuous energy harvesting, high cycling stability, and practical usability in wearable electronics.

The flexible battery is fabricated on elastomeric substrates, ensuring conformability and durability under motion. Nanostructured conductive coatings are used to enhance electrical conductivity while preserving stretchability. A custom-developed gel polymer electrolyte is used to replace conventional liquid electrolytes, offering improved safety, leakage resistance, and mechanical compatibility with flexible form factors. The electrolyte exhibits high ionic conductivity and strong interfacial adhesion to electrode layers, ensuring stable electrochemical performance under deformation. The battery design is optimized for stable operation under bending, stretching, and repetitive mechanical stress conditions typical of wearable applications.

Simultaneously, the TENG is fabricated using electrospun nanofiber layers with high triboelectric polarity. These high-surface-area membranes harvest biomechanical energy from movements like walking or fabric deformation. The system includes custom energy conditioning circuits to convert the pulsed AC output of the TENG into a regulated form suitable for real-time battery charging.

This study was financially supported by the Scientific and Technological Research Council of Turkey (TUBITAK) (Project No. 123M050).

Kaan Yapıcı is a master's student in Materials Science with a background in Physics Engineering. His academic focus includes nanomaterials, conductive inks, and additive manufacturing techniques. He has experience in national and international research projects, particularly in the field of printed and flexible electronics. Kaan is interested in developing sustainable, high-performance materials for next-generation electronic applications.

Presentating author: Kaan YAPICI, e-mail:kaan.yapici@sabanciuniv.edu tel:+905069795550


KOCAELİ ÜNİVERSİTESİ
1992

BOĞAZİÇİ ÜNİVERSİTESİ
1863

ENDAM

GEBZE
TEKNİK ÜNİVERSİTESİ



Sabancı
Üniversitesi

REFERANS
KİMYA

KOCAELİ
BÜYÜKŞEHİR
BELEDİYESİ

Tüpraş